AN INVESTIGATION INTO BIOLEACHING OF URANIUM AND RARE EARTH ELEMENTS FROM QUARTZ-PEBBLE CONGLOMERATE ORES FROM ELLIOT LAKE, ONTARIO

By

Aimee Lynn Williamson

A thesis submitted in partial fulfillment

of the requirements for the degree of

Doctor of Philosophy (PhD) in Material Sciences

The School of Graduate Studies

Laurentian University

Sudbury, Ontario, Canada

THESIS DEFENCE COMMITTEE/COMITÉ DE SOUTENANCE DE THÈSE
Laurentian Université/Université Laurentienne
School of Graduate Studies/École des études supérieures

Title of Thesis
Titre de la thèse AN INVESTIGATION INTO BIOLEACHING OF URANIUM AND RARE EARTH ELEMENTS FROM QUARTZ-PEBBLE CONGLOMERARE ORES FROM AT ELLIOT LAKE, ONTARIO

Name of Candidate
Nom du candidat Williamson, Aimee Lynn

Degree
Diplôme Doctor of Philosophy

Department/Program
Département/Programme Materials Science

Date of Defence
Date de la soutenance June 3, 2014

APPROVED/APPROUVÉ

Thesis Examiners/Examinateurs de thèse:

Dr. Graeme Spiers
(Supervisor/Directeur de thèse)

Dr. François Caron
(Committee member/Membre du comité)

Dr. Michael Schindler
(Committee member/Membre du comité)

Mr. Roger Payne
(Committee member/Membre du comité)

Mr. Randy Knapp
(Committee member/Membre du comité)

Dr. Thomas Kotzer
(External Examiner/Examinateur externe)

Dr. Douglas Boreham
(Internal Examiner/Examinateur interne)

Approved for the School of Graduate Studies
Approuvé pour l'École des études supérieures
Dr. David Lesbarrères
M. David Lesbarrères
Director, School of Graduate Studies
Directeur, École des études supérieures

ACCESSIBILITY CLAUSE AND PERMISSION TO USE

Abstract

Biogeochemical mineral dissolution, the microbial-assisted dissolution of minerals, is an effective method for economically promoting the release of metals of interest from ores and mine waste materials. As the low-grade ores of the Elliot Lake region may be suitable for development of a sustainable heap-leach method for the extraction of U and REEs from the low-grade host mineralization, this thesis is focused on the geochemical and biological process simulation monitoring of the biogeochemical release of elements to the leaching solutions. The response of the retired heap material to a variety of passive closure strategies is also addressed.

A series of biogeochemical mineral dissolution experiments have provided a detailed understanding of the biogeochemical mineral dissolution process, with the investigation of passive approaches to prepare for decommissioning to determine suitability to the ore materials from the study site. The chemical analyses of effluents collected throughout the experimentation, coupled with mineralogical and geochemical analyses of the feed and residual mineral material has enabled an understanding of the chemical controls of the overall biogeochemical mineral dissolution process for Fe, U, and Th, together with the preferential leaching release patterns for REEs, to be obtained. A mechanism describing U retention in secondary coatings has been proposed, with a passive approach to closure using inhibition and encapsulation methods being demonstrated, along with a determination of the potential for ongoing radionuclide release from a simulated heap upon decommissioning.

The laboratory research in this study has shown that biogeochemical mineral dissolution, followed by waste material encapsulation, can be successfully applied to heap-leach pads potentially, enabling the economic recovery of U, Th, and selected REEs to solution for subsequent metallurgical collection. The studies strongly support the concept of sustainable development for heap-leach operations in the Elliot Lake region.

Keywords: Acid mine drainage, *Acidithiobacillus ferrooxidans*, biogeochemical mineral dissolution, bioleaching, passive approaches to prepare for decommissioning, Elliot Lake, encapsulation, extraction

flasks, ferrous-sulphide minerals, geochemical dynamics, inhibition, leaching columns, mineralogical dynamics, radionuclide, radium, rare earth elements, uranium, thorium

Co-Authorship Statement

Recently published in the Journal of Environmental Radiochemistry, Chapter 9 is co-authored by Aimee Lynn Williamson, Francois Caron, and Graeme Spiers. Spiers contributed to the conception of the overall study, with Caron providing suggestions for leachate extraction and preparation for gamma measurements, calculating detector efficiency, and providing guidance on interpretation of gamma spectroscopic data. Williamson solely conducted all experiments and analysis, and conceived the interpretations and conclusions. The manuscript was prepared by Williamson, with editorial comment from Caron and Spiers.

Acknowledgments

Completing this thesis has been the most challenging task I have attempted in my journeys and it would not be achievable without the assistance and support of countless individuals throughout the last four years, eight months, and twenty-four days. First and foremost, I would like to thank my thesis supervisor, Dr. Graeme Spiers, who has encouraged me every step of the way. He has taught me to trust my scientific judgment and to never give up when times get difficult or science gets tough. His lessons have allowed me to grow into a confident scientist, albeit stubborn at times as I continued to practice patience, which Dr. Spiers exemplifies so well. I would also like to thank my thesis committee members: Dr. Francois Caron, Dr. Michael Schindler, Mr. Roger Payne, and Mr. Randy Knapp. I am grateful that such a diverse group of professionals have guided me through this process. I have learned something unique from each of you.

I have been grateful to have been supported by the folks at Pele Mountain Resources Inc. who entrusted me to find a solution for the company's research questions. Communications with PMR president, Mr. Alan Shefsky, have always been positive and encouraging and his excitement for the project has provided never-ending motivation. Roger Payne, PMR Executive Vice President, has always brought positivity to the project and was truly one of the best resources that I had during my studies, although there has never been enough time to take full advantage of everything that Roger could teach me from all of his extraordinary experiences. Also, thank you to Fergus Kerr, who provided great insight and experience to the early phase of the project. The opportunity to work directly with a company on this project has allowed me to witness the true meaning of my work and its consequences.

The body of experimental work could not have been completed without the assistance provide by the Geoscience Laboratories, the Elliot Lake Research Field Station, the Department of Chemistry at Laurentian University, and MIRARCO. Sample preparation and preliminary mineralogical studies were conducted at the Geoscience Laboratories, with special thanks to Sandra Clark and John Hechler for their continued guidance in this area. The great people at ELRFS have been available every step of the way, in

particular Troy Maki, who has supported the development of analytical methods and carried out some sample analysis. A special thank you goes out to former-ELRFS staff member and fellow graduate student Kendra Driscoll for her support in the laboratory and for always being available for a coffee break to discuss our research results and life in general. I would also like to acknowledge the Chemistry Department at Laurentian University for providing countless supplies and small instruments required to complete special analysis and to Dr. Joy Gray-Munro for the use of her laboratory for an IR study. MIRARCO and the EMR research group have provided administrative support to the project as well as a personal workspace and facilities that any grad student could appreciate. I am very thankful for the friendships I developed working with the old CEM group at MIRARCO, established during fieldwork excursions and strengthened during conference outings and holiday parties. Special thanks to Dr. Jennifer Hargreaves for her 'groovy' guidance and to John Waddell, Michael Folcher, and Widjdan Malik for their assistance in the construction of my experimental set up.

The support that I have received from friends and family has been so strong. Andrea and Josée, grad school would have been nowhere near as exciting without the two of you at my side. Sophia, you have been my rock and I thank you always being there at the other end of the phone line to provide encouragement and help me through the stressful times. Tony, you have been so patient and supportive while I worked through this chapter of my life and I am sure you know more about biogeochemical mineral dissolution then you have every cared to know. I am excited and look forward our next chapter and hope I can show just as much patience and support in return. I love you with everything I have and promise that I will never make you wear a blue safety suit ever again! My final acknowledgements go out to the very important people in my life who have been with me since the beginning, my parents. You have witnessed every step I have taken, supporting me through struggles and celebrating my successes. To my brothers, Shane and Chase, you have provided me with a strong, grounded foundation and remind me of the things in life that are truly important. There are not enough words to express how grateful I am to have such a loving and supportive family. I love you all with every piece of my heart.

Table of Contents

List of Tables

List of Figures

Acronyms and Abbreviations

ALARA	As low as reasonably achievable
AMD	Acid mine drainage
Ap	Apatite
ARD	Acid rock drainage
ATP	Adenosine triphosphate
BSE	Backscattered electron
CCV	Continuous calibration verification
CRM	Certified reference material
DDI	Distilled deionized
Eco Ridge	Eco Ridge Mine Rare Earths and Uranium Project
ECPM	Environmental Code of Practice for Mines
EDS	Energy dispersive spectroscopy
ELRFS	Elliot Lake Research Field Station
EMPA	Electron probe micro-analyzer
Eu	Europium
Fe	Iron
g	Gram
Gd	Gadolinium
IC	Ion chromatography
ICP-MS	Inductively coupled plasma mass spectrometry
IR	Infrared spectroscopy
IRM	Internal reference material
IS	Internal standard
K	Potassium
L	Litre
La	Lanthanum
LA-ICP-MS	Laser ablation inductively coupled plasma mass spectrometry
Lu	Lutetium
m	meter
MAC	Maximum authorized concentration
MIRARCO	Mining Innovation and Applied Research Corporation
MMER	Ming Metals Effluent Regulations
mol	Mole
Mz	Monazite
NADPH	Nicotinamide adenine dinucleotide phosphate
NIST	National Institute of Standards and Technology
Or	Orthoclase
ORP	Oxidation reduction potential
P	Phosphorus
PMR	Pele Mountain Resources Inc
ppb	Parts per billion (1000 ppb = 1 ppm)
ppm	Parts per million (1 ppm = 1 mg/kg)
Py	Pyrite, FeS_2
Qz	Quartz, SiO_2
REE	Rare earth element
RPM	Rotations per minuet
Rt	Rutile, TiO_2
Sc	Scandium
SD	Standard deviation
SEM	Scanning electron spectroscopy
SLS	Sodium lauryl sulphate
SOP	Standard operating procedure
SPT	Sodium polytungstate
Th	Thorium
Ti	Titanium
U	Uranium
Urn	Uraninite, UO_2
XRD	X-ray diffraction
XRD	X-ray diffraction
Y	Yttrium
Zm	Zircon, $ZrSiO_4$

CHAPTER 1

1 Introduction

Biogeochemical mineral dissolution a natural process responsible for the formation of acid rock drainage (ARD), which is a concern for the mining industry, having elevated dissolved metal concentrations and low pH (Kim, et al., 1999). This process can be controlled and utilized as an economic release method for metals of interest in low-grade ores under conditions having the proper mineralogical, microbiological, and chemical relationships (Rawlings, 2002). Waste material resulting from the application of this release method may have a lesser environmental affect as the processing conditions have been optimized to promote acid generation and metal dissolution, thus producing less reactive waste material (Rawlings, 2002). The application of biogeochemical mineral dissolution has been applied for the release of copper, gold, and uranium (U) (Rawlings, 2002; Rohwerder, et al., 2003), and may be successfully applied for the release of U from the low-grade, quartz pebble conglomerate beds of Elliot Lake, Ontario.

1.1 Regional History: Elliot Lake Ontario

In the late 1940s, U-bearing minerals were discovered near Elliot Lake, Ontario and within 10 years, a dozen operational mines were in place. The mines of Elliot Lake proved to be a superior source for U at the time and mine operators held contracts with organizations worldwide. By 1957, the Canadian government had contracts with the United States Atomic Energy Commission to provide more than $1.5 billion worth of uranium oxide, two thirds of which originated from Elliot Lake (Mawhiney & Pitblado, 1999). The discovery of higher grade deposits in Canada in the 1960s and 1970s, followed by development in the early 1980s, resulted in an oversupply of U at a decreased price, leading to the closure

of the now less economic Elliot Lake U mines (Mawhiney & Pitblado, 1999). Uranium extraction and production ceased in Elliot Lake in 1996.

Technical studies state that abundant reserves of low-grade U deposits are present in the Elliot Lake region, namely along the Quirke Syncline, providing opportunities for the redevelopment of the Elliot Lake mining camp (Cochrane, et al., 2007). The principal U-, thorium (Th)-, and rare earth element (REE)-bearing minerals in Elliot Lake area conglomerate are reported in Table 1.1. Biogeochemical mineral dissolution for the release of U, Th, and REEs is a potentially viable option for the exploitation of the low-grade ores located along the Quirke Syncline.

Table 1.1 Principal minerals carrying U, Th, and REEs is Elliot Lake area conglomerate identified by Sylvester (2007) and Sapsford (2012).

Mineral Phase	Chemical formula
Primary phases	
Thorium enriched uraninite	$(Th)UO_2$
Monazite (thorium rich)	$(Ce, La, Y)PO_4$
Thorite	$(Th, U)SiO_4$
Allanite	$(Ca, REE)Al_2Fe(SiO_4)(Si_2O_7)O(OH)$
Secondary alteration phases	
Coffinite	$U(SiO4)_{1-x}(OH)_{4x}$
Brannerite	UTi_2O_6
Pitchblende	$(Th, REE\ poor)UO_2$
Florencite	$(REE)A1_3(PO_4)(OH)_6$
Xenotime	YPO_4
Uraniferous rutile or ‘‘leucoxene’’	UO_2–Rutile
Silicified monazite	Mz-Silicate
Very fine-grained intergrowth of pitchblende, pyrite and aluminium-rich silicate phase	UO_2–Pyr–AlSi-mix
Uraniferous pyrite	UO_2–Pyrite

Study Site

Pele Mountain Resources, Incorporated (PMR) is a junior exploration and development company based in Toronto, Ontario. The company is focused on the sustainable development and potential operation of the

Eco Ridge Mine Rare Earth and Uranium Project (Eco Ridge), located east of Elliot Lake, Ontario, Figure 1.1.

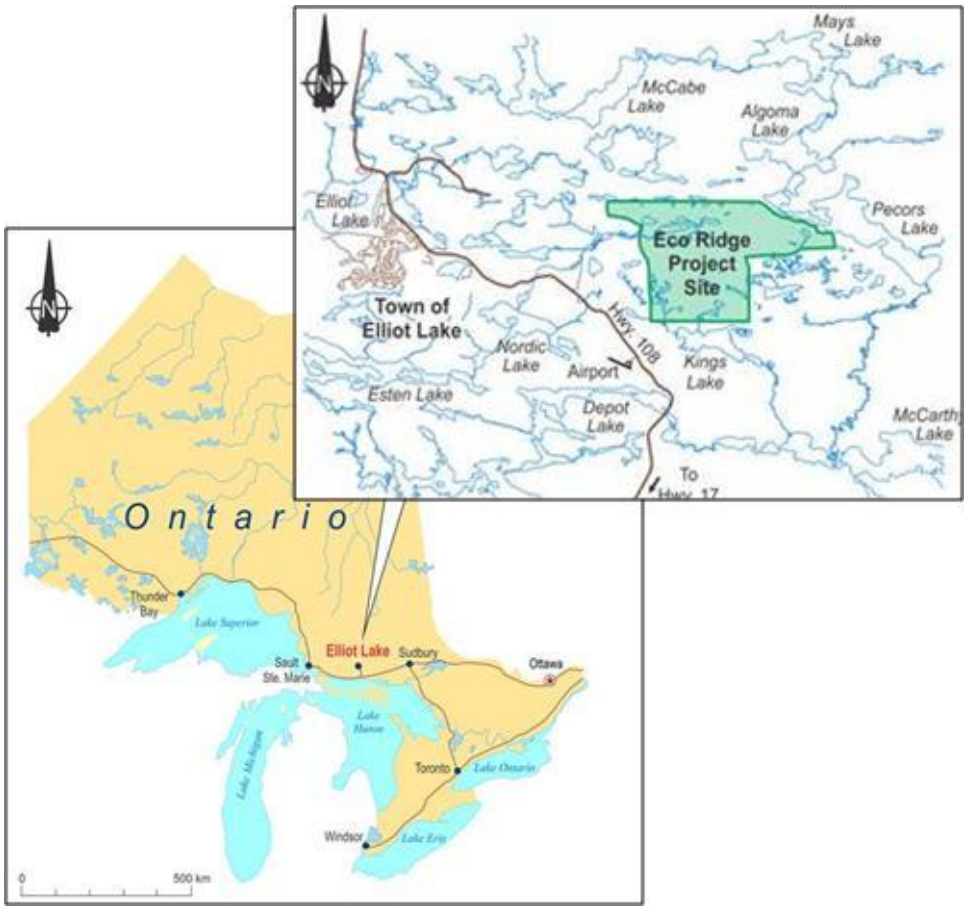

Figure 1.1 Location of Eco Ridge Mine Rare Earths and Uranium Project, east of Elliot Lake, Ontario (provided by PMR Ltd. 2013).

On the Eco Ridge site, U mineralization is located in three distinct quartz-pebble conglomerate beds: Upper, Main, and Basal Beds. The indicated and inferred uranium oxide and total rare earth oxide mineral resource at the Eco Ridge site are presented in Table 1.2 (Cox, et al., 2012). Indicated resources are quantified when the quality, density, shape, and physical characteristics of the resource are estimated based on detailed and reliable exploration and testing information, whereas inferred resources are estimated based on limited sampling and the assumed geological and grade continuity (Postle, et al., 2000).

Table 1.2 Eco Ridge mineral resource estimate (Cox, et al., 2012).

Classification	Uranium Oxide		Total Rare Earth Oxides	
	mg kg^{-1}	metric tonnes	mg kg^{-1}	metric tonnes
Indicated	260	12550	1157	56
Inferred	260	9870	1100	42

Ferrous sulphides content in the ore is important to the success of biogeochemical mineral dissolution. The pyrite content of the Main Bed is 10 to 15% (Sylvester, 2007), suggesting that biogeochemical mineral dissolution of ferrous sulphide minerals at the Eco Ridge site may be capable of promoting the dissolution of U from insoluble phases.

Previous investigations in the region document the existence of microbial populations appropriate for driving the biogeochemical mineral dissolution of ferrous sulphide minerals (Ferroni, et al., 1986; McCready, et al., 1986). Passive release methods proved successful for U extraction in investigations and applications at Agnew Lake Mines and Denison Mines (Campbell, et al., 1985; McCready & Gould, 1990).

1.2 Biogeochemical Mineral Dissolution & Passive Approach to Decommissioning

Biogeochemical mineral dissolute, the microbial-assisted dissolution of minerals, occurs when sulphidic minerals, such as pyrite, become oxidized, supplying the environment with elevated concentrations of metals and acidity (Lundgren & Silver, 1980; Leduc & Ferroni, 1994; Suzuki, 2001). The control of the biogeochemical mineral dissolution, including the potential application for an economic release method and the management of associated environmental liabilities, is based on the understanding of the existing and anticipated microbiological, chemical, and mineralogical relationships.

An approach for the extraction of U from low-grade ore driven by biogeochemical mineral dissolution may have a lesser environmental affect compared to traditional mineral processing methods, thus reducing decommissioning efforts and costs. Today, microbial leaching methods are practiced worldwide to accelerate the dissolution of copper (Cu)-, gold (Ag)-, and U-bearing minerals. Previous experimentation conducted at Denison Mines in Elliot Lake demonstrated that bioleaching technologies

were a potentially viable option to extract U and yttrium (Y) from the low-grade U ore in the region (Harrison, et al., 1965; McCready, 1986)

Passive approaches to decommissioning compliment the application of biogeochemical mineral dissolution extraction. In the absence of bacterial activity, biotic oxidation of ferrous-sulphide minerals no longer takes place (Kleinmann, 1987) and the spontaneous cycle of the bacterially mediated oxidation of ferrous iron coupled with pyrite oxidation stops when existing ferric iron is exhausted. The application of a bacterial inhibitor will decrease the biogeochemical mineral dissolution reaction rate, thus limiting acid production and subsequent metal dissolution. Passivation, on the other hand, aims to block oxidation of a reactive mineral by depositing a protective coating on the mineral surface (Evangelou, 2001). The formation of a barrier phase between the metal sulphide and the oxidizing environment would prevent oxidation of the sulphide and hinder the biogeochemical mineral dissolution process.

1.3 Objectives

The U and REE mine at PMR's Eco Ridge site, as initially proposed, requires a sustainable method for the extraction of U and REEs from the low-grade host mineralization. To plan for subsequent decommissioning, the geochemical and biological response of retired heap material to a variety of passive closure strategies requires detailed investigation. Biologically mediated heap-leach conditions, simulated using a series of extraction flasks and leaching columns experiments, are used to monitor the long-term mineralogical and geochemical dynamics of the extraction process and provide a detailed understanding of the biogeochemical mineral dissolution process controls. Passive approaches to prepare for decommissioning methods, applied to simulated waste material, determine the suitability of each application for the ore materials from the Eco Ridge site. Detailed chemical analyses of effluents, collected throughout experimental programs, provide critical information used to estimate the rate and quantity of release of selected elements to solution phases. Mineralogical and geochemical analyses of feed and residue mineral material has been applied to describe preferential leaching of U and REE as well

as document the morphology of the dissolution features on the mineral surfaces and the mineralogy and composition of the secondary phases formed. The objectives of this thesis are to:

- Demonstrate the application of biogeochemical mineral dissolution using and assess the chemical controls on U and Th dissolution;
- Complete a solid phase investigation to identify the REE-bearing mineral phases and examine the dissolved phase chemistry after biogeochemical mineral dissolution to provide an understanding of the mineralogical and chemical controls on dissolution of REE;
- Describe the retention mechanism of U in secondary precipitates formed on mineral surfaces during and after biogeochemical mineral dissolution;
- Demonstrate the application of pacification and inhibition treatments to previously leached mineral materials and assess the short-term capabilities of each treatment to resist further oxidation and subsequent mineral dissolution from the simulated waste rock; and
- Assess and monitor the decrease of radiological activity of uraniferous mineral material and determine the potential release of U and Radium-226 to the aqueous solution following biogeochemical mineral dissolution to provide models to guide decommissioning efforts.

1.4 Thesis Organization

This thesis contains ten chapters: Introduction, two literature reviews, Experimental Approach and Methods of Analysis, five detailed experimental reports, and a Summary. The literature reviews provide background information describing previous investigations on specific selected topics including biogeochemical mineral dissolution and passive approaches to prepare for decommissioning, as they pertain to both the study site and the objectives of this thesis. The Experimental Approach and Methods of Analysis section provides the protocol for each phase of leaching and decommissioning for simulated heap experiments, and also describes methods of analysis and interpretation of results for dissolved and solid phase studies. Each of the following five reports address the objectives identified above. The reports

are written as standalone documents, with dedicated introductions, methods, results, discussion, and conclusion sections, thus, some overlap exists among the individual reports and other chapters in this thesis. A summary of the major findings of the reports, in meeting the thesis objectives, is provided in the final chapter. A series of Appendices are provided, highlighting the experimental work and results not highlighted within the previous chapters. The appendix chapters document the dedicated methods, experimental data, and results, along with discussions and conclusions from microcosm and column studies. The data tables necessary to produces the summary figures presented in the chapters of the thesis body are in the final appendix.

CHAPTER 2

2 Biogeochemical Mineral Dissolution

2.1 Introduction

Biogeochemical mineral dissolution, the microbial-assisted dissolution of minerals, can produce reaction products to drive the dissolution of other non-target mineral phases from the host mineralization and/or mine waste material. Although biogeochemical mineral dissolution may be applied to a broad range of ore types, this review is primarily focused on the biogeochemical mineral dissolution of ferrous sulphides, pyrite in particular, and uranium (U)-bearing minerals. The application of biogeochemical mineral dissolution as a passive recovery method has been proposed for leach pads at Pele Mountain Resources, Incorporated's (PMR) Eco Ridge Mine Rare Earths and Uranium Project (Eco Ridge). The topics explored in this chapter include: the geochemistry of bioleaching, *Acidithiobacillus ferrooxidans* metabolic requirements, previous laboratory experimentation, and method application.

The oxidation of pyrite and other metal sulphides results in the release of other metals bound in the sulphide mineralization or elsewhere in the mineral complex (Baker & Banfield, 2003). The biogeochemically accelerated dissolution of sulphide minerals on undisturbed landscapes is slow and limited by the exposure of the sulphide mineral to the oxygen in air and water. This is a natural process, consequences of which are commonly termed acid rock drainage (ARD), or in the mining industry, acid mine drainage (AMD). Landscapes altered through the extraction processes of blasting, crushing, grinding, and processing significantly increase the exposed surface area of sulphide minerals exposed to air and water, thereby increasing the rate of ARD generation. Left untreated or uncontrolled, levels of acidity and sulphate in waters become elevated, often with associated elevated concentrations of metals of

economic value or environmental significance. A passive method for recovery of minerals of interest from low-grade or economically unfavorable deposits is sometimes achievable by way of the ARD processes.

Chemolithotrophic microorganisms accelerate the dissolution of sulphidic minerals, releasing sulphide to solution with a concomitant release of protons, which encourage the dissolution of other minerals (Lundgren & Silver, 1980; Leduc & Ferroni, 1994; Suzuki, 2001). Biogeochemical mineral dissolution of sulphidic minerals drives the dissolution of other minerals with the potential to release elements of economic value or environmental significance from the host mineralization or mine wastes materials. Microorganisms involved in this process are generally aerobic chemolithotrophic acidophiles. The mining industry has used this natural process as an extractive approach for some metals, termed bioleaching or biomining, because the microorganisms promote the conversion of insoluble metals to a soluble form for further processing and recovery (Rawlings, 2002).

The success of bioleaching depends on important interactions between the microbial population and the mineralogy, with iron-sulphide minerals being of fundamental importance to the bioleaching process. In the presence of iron oxidizing organisms, the rate of ferrous-sulphide mineral oxidation at low pH is increased by six orders of magnitude compared with abiotic oxidation (Singer & Stumm, 1970; Marchand & Silverstein, 2003; Johnson, 2010). *Acidithiobacillus ferrooxidans,* having a very high tolerance for acidity and low pH environments, dominates the bioleaching process having an ability to oxidize both iron and sulphur (Nemati, et al., 1997). The microbial bioleaching process is capable of dissolving all metal sulphides and some metal-containing minerals in slightly acidic to acidic sulphate solutions (Nemati, et al., 1997).

Unknowingly, the earliest miners applied bioleaching for the recovery of copper, although the exact process and microbial importance has not always been clear. Historical records indicate that the addition of metallic iron filings precipitated copper in some streams, which are now known to have high dissolved

copper contents because natural mineral dissolution takes place when the water flows through the copper-bearing mineralization. Evidence suggests that early applications of bioleaching for metal recovery by the Chinese date back as far as 100-200 BC (Ehrlich, 2001). The Romans used similar methods to recovery copper from river water in southern Spain at the current location of Rio Tinto mine, named for the colour of the water (Rawlings, 2004). Recently, an increased understanding of this natural process has allowed the commercialization of bioleaching facilities for the recovery of copper, gold, and U in controlled environments worldwide (Boseker, 1997; Rawlings, 2002; Rohwerder, et al., 2003).

2.2 Geochemistry

Acid generation occurs at mineral processing and mine tailing sites around the world where sulphide minerals exposed to air and water produce sulphuric acid (Baker & Banfield, 2003; Johnson, 2010). The oxidation of sulphide minerals contributes to acidification and release of metals to surface and ground waters, creating critical environmental challenges for the mining industry. The most abundant sulphide mineral in the earth's crust, pyrite (Johnson, 2010), is commonly associated with metal ore deposits (Evangelou & Zhang, 1995). Pyrite is commonly used to illustrate the biogeochemical processes of ARD generation and the biogeochemical leaching process. As pyrite is the major metal-sulphide mineral at the Eco Ridge site (Sylvester, 2007), the use of pyrite to illustrate the bioleaching process is appropriate. Table 2.1 lists common sulphide minerals identified by Silverman and Ehrlich (1964).

Table 2.1 Commonly sulphide minerals (Silverman & Ehrlich, 1964).

Mineral	Abbreviation	Chemical Formula
Arsenopyrite	Apy	$FeS_2 \cdot FeAs_2$
Bornite	Bn	Cu_3FeS_4
Chalcocite	Cc	Cu_2S
Chalcopyrite	Ccp	$CuFeS_2$
Covellite	Cv	CuS
Enargite	Ena	$Cu_2S \cdot As_2S_5$
Galena	Gn	PbS
Marcasite	Mrc	FeS_2
Millerite	Mlr	NiS
Molybdenite	Mol	MoS_2
Orpiment	Orp	As_2S_3
Pyrite	Py	FeS_2
Sphalerite	Sp	ZnS
Tetrahedrite	Ttr	$Cu_8Sb_2S_7$

Oxidation of Pyrite

The oxidation of pyrite and subsequent solubilization of U takes place through the series of reactions illustrated in Figure 2.1. In the presence of air and water, ferrous-sulphide minerals are chemically oxidized, liberating ferrous iron and acid to the environment (Reaction 2.1). The ferrous iron is oxidized by molecular oxygen (Reaction 2.2), liberating ferric iron, which oxidizes additional ferrous-sulphide minerals (Reaction 2.3). The continuous oxidation and reduction of iron is a cyclic, self-propagating process (Kleinmann, et al., 1981).

Reaction 2.1 $$FeS_2 + \frac{7}{2}O_2 + H_2O \rightarrow Fe^{2+} + 2{SO_4}^{2-} + 2\,H^+$$

Reaction 2.2 $$Fe^{2+} + \frac{1}{4}O_2 + H^+ \rightarrow Fe^{3+} + \frac{1}{2}H_2O$$

Reaction 2.3 $$FeS_2 + 14Fe^{3+} + 8H_2O \rightarrow 15Fe^{2+} + 2{SO_4}^{2-} + 16H^+$$

Reaction 2.4 $$UO_2 + 2Fe^{3+} \rightarrow UO_2^{2+} + 2Fe^{2+}$$

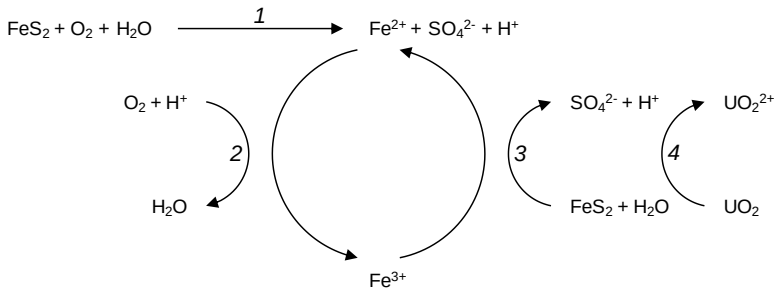

Figure 2.1 Schematic diagram illustrating the biogeochemical mineral dissolution processes for pyrite and the relationship with U (Guay, et al., 1976; Kleinmann, 1987; Evangelou & Zhang, 1995; Fernandes & Franklin, 2001; McIlwaine & Ridd, 2004)

The chemical oxidation of iron is slow, and is the rate determining step in this process. In the presence of iron-oxidizing bacterial cultures, this oxidation rate can be increased up to six orders of magnitude (Singer & Stumm, 1970; Evangelou & Zhang, 1995; Marchand & Silverstein, 2003; Johnson, 2010). When pH conditions increase with aeration and mixing of the waters, ferric hydroxide may precipitate (Reaction 2.5).

Reaction 2.5

$$Fe^{2+} + \frac{5}{2}H_2O + \frac{1}{4}O_2 \rightarrow Fe(OH)_3 + 2H^+$$

Many of the works by Kleinmann have focused on describing this process as a succession of three reaction stages based on an evaluation of various chemical indicators (pH, oxidizing potential, acidity, and ferric/ferrous ratio) and microbial activity (Kleinmann & Erickson, 1983; Kleinmann, 1987). Table 2.2 provides a summary of the stages of pyrite oxidation.

Table 2.2 The three reaction stages of pyrite oxidation (Kleinmann & Erickson, 1983; Kleinmann, 1987).

Indicator	Stage 1	Stage 2	Stage 3
Dominating chemical processes	Abiotic and biotic oxidation Reaction 2.1) Abiotic oxidation dominates (Reaction 2.5); Rate determining process rate slows as pH decreases	Abiotic and biotic oxidation (Reaction 2.1) Biotic oxidation dominates (Reaction 2.5); Rate determining process	Biotic oxidation dominates (Reaction 2.2); Rate determining process Abiotic reduction (Reaction 2.3)
pH	Greater than 4.5	Between 2.5 and 4.5	Lower than 2.5
Oxidation potential (E_H)	Steady (low)	Increasing	Steady (high)
Acidity	Little or no acidity	Acidity increasing	High acidity
Ferric/ferrous Ratio	Low iron concentration owing to precipitation of $Fe(OH)_3$	Low	High $Fe^{3+} >> Fe^{2+}$
Sulphate concentration	Low	High	High

The third stage of pyrite oxidation may continue in the absence of oxygen, although biotic oxidation rates will slow because the chemical oxidation of pyrite (Reaction 2.2) will continue as long as ferric iron is available (Evangelou & Zhang, 1995; Banks, et al., 1997; McIlwaine & Ridd, 2004). Ferric iron will then become the principal oxidant involved in pyrite oxidation. Therefore, in the absence of oxygen and biotic oxidation, Reaction 2.2 is the rate-limiting process (Singh & Bhatnagar, 1988; Evangelou & Zhang, 1995).

Biogeochemical Mineral Dissolution for Uranium Recovery

In nature, U exists most commonly in a tetravalent or hexavalent state in a range of uraniferous minerals (Lundgren & Silver, 1980). Even though U is not normally found structurally in sulphide minerals, experiments support the successful recovery of U using bioleaching methods in the presence of ferrous sulphides because the oxidation of pyrite, through the biogeochemical mineral dissolution process, creates the geochemical conditions suitable for the dissolution of the U-bearing minerals (Harrison, et al., 1965). The relatively insoluble U minerals are dissolved when they are found in close association with ferrous-sulphide minerals because biogeochemical mineral dissolution liberates ferric iron, which oxidizes uraninite according to Reaction 2.4. This oxidation process promotes the transition from insoluble U^{4+} minerals to soluble U^{6+} (Reaction 2.6) (Lundgren & Silver, 1980).

Reaction 2.6 $U(IV) + 2Fe(III) \rightarrow U(VI) + 2Fe(II)$

2.3 Microbiology

Parr and Powel (1919) suggested the involvement of bacterium in the ARD process after comparing the sulphate concentration of solutions from coal piles that were inoculated against sterile controls. Their research found that the inoculated piles had significantly elevated levels of soluble sulphur and iron in the leachate, and thus they concluded that the rate of the oxidizing reactions was increased in the presence of bacteria or some other catalyzing agent.

The research group of Colmer, Hinkle, and Temple published a series of papers eventually leading to the identification and classification of the bacterium responsible for iron oxidation, *A. ferrooxidans* (Colmer & Hinkle, 1947; Colmer, et al., 1950; Temple & Colmer, 1951; Colmer, 1962). In their earliest research, a known sulphur-oxidizer, *Thiobacillus thiooxidans*, and an unidentified iron oxidizer were isolated from water samples collected from a bituminous coal mine water sample (Colmer & Hinkle, 1947). Colmer, Temple, and Hinkle (1950) discussed the characteristics of the unidentified bacterium and described the ability to oxidize both thiosulphate and iron as alternative energy sources, finally categorizing the bacterium as *Thiobacillus ferrooxidans*. Further investigations by Temple and Colmer (1951) confirmed the previously suggested autotrophic characteristics of *T. ferrooxidans.* Nearly ten years later, Colmer conducted culture and biochemical tests to reinforce the accuracy of the assignment of genetic categorization (Colmer, 1962).

In 2000, eight species, including *T. ferrooxidans*, were reassigned to the new genus *Acidithiobacillus* based on physical characters and 16s rRNA sequencing. *T. ferrooxidans* appears in earlier literature and reports and the designation has been used interchangeably in this thesis with *A. ferrooxidans* to reflect the current classification of the bacterium to relate to historic and current research.

The ability to oxidize both sulphide and iron compounds, as well as tolerance of low pH and adaptation to elevated dissolved metal concentrations makes *A. ferrooxidans* very important in ARD production, and indicates the potential for use in commercial bioleaching processes.

Metabolism of Acidithiobacillus ferrooxidans

The growth and maintenance of *A. ferrooxidans* relies on energy harnessed from the oxidation of ferrous iron and/or reduced sulphur compounds in an acidic environment while maintaining an internal pH of 6.5 (Leduc & Ferroni, 1994). Fixed carbon dioxide provides the only carbon source (Leduc & Ferroni, 1994), with nitrogen and phosphorus being provided from external nutrient sources to support cellular growth and health (Nemati, et al., 1997). These bacteria use oxygen as an electron acceptor to drive cellular metabolism (Nemati, et al., 1997), but in the absence of oxygen *A. ferrooxidans* may use inorganic sulphur compounds or ferric iron as an electron acceptor to maintain the energy levels required for cell growth and well-being for a limited amount of time. The model for electron transport by *A. ferrooxidans* to support cellular metabolism describes three electron carriers linking the external environment with the internal cell through the cell envelope, Figure 2.2 (Nemati, et al., 1997).

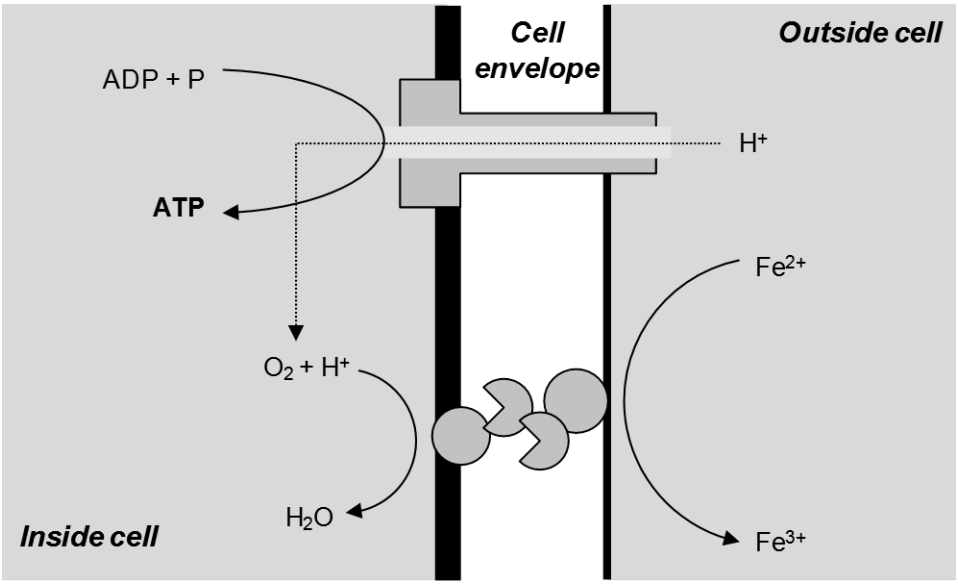

Figure 2.2: Model for A. ferrooxidans oxidizing and energy system, modified from Nemati et al. (1997).

The oxidation of ferrous iron (A similar electron transport model was proposed by Rohwerder a) provides electrons to transfer through the membrane proteins held in the cell wall. Rusticyanin, a 16.5 kilodalton

copper-containing protein, is very stable in acidic pH, allowing the cell to have a close interaction in an acidic environment without causing harm to the internal cell organelles (Lundgren & Silver, 1980). The electrons from the oxidation of ferrous iron are transferred through rusticyanin to cytochrome c. Cytochrome a1, positioned at the outer surface of the cell membranes, receives electrons from reduced cytochrome c, transferring them to molecular oxygen in the cell resulting in the spontaneous production of water (t the oxidation of ferrous iron by cytochrome Cyc2 at the cell) (Lundgren & Silver, 1980).

Reaction 2.7 $$Fe^{2+} \rightarrow Fe^{3+} + e^{-}$$

Reaction 2.8 $$\frac{1}{2}O_2 + 2e^{-} + 2H^{+} \rightarrow H_2O$$

The driving force for adenosine triphosphate (ATP) synthesis from ferrous iron oxidation is supported by chemiosmotic theory with a charge differentiation on either side of the cell membrane. When electrons are transferred from the external environment to the intracellular space, protons are essentially removed from the internal environment through the production of water, creating a proton gradient between the cell and environment. Proton channels existing throughout the cell membrane, coupled to ATPase class enzymes, allow controlled movement of protons into the cell. The passage through the protein-ATPase couple releases sufficient energy to synthesize ATP from adenosine diphosphate (ADP) and inorganic phosphate (Lundgren & Silver, 1980).

A similar electron transport model was proposed by Rohwerder and colleagues (2003) who suggest the oxidation of ferrous iron by cytochrome Cyc2 at the cell membrane is followed by a transfer of electrons through rusticyanin and/or a periplasmic cytochrome to a membrane anchored, aa3-type cytochrome oxidase. An assisted transfer of electrons from ferrous iron to rusticyanin is proposed because the predicted rate of electron transfer through rusticyanin alone is not capable of allowing iron oxidation fast enough to correspond to reported oxidation rates.

A. ferrooxidans synthesizes one molecule of ATP for every two electrons transferred to molecular oxygen across the cell membrane according to the model above. As a single cell needs to oxidize approximately 18.5 moles of ferrous iron to fix one mole of carbon; a cell operating at 100% efficiency would require 500 kilojoules to meet the basic demands to meet cellular metabolism requirements (Silverman & Lundgren, 1959). Complete efficiency is not expected, with reported efficiencies for iron oxidation of *A. ferrooxidans* varying between 3.2% (Temple & Colmer, 1951) and 30% (Lyalikova, 1958). Given this low efficiency, large quantities of ferrous iron are required to be oxidized in order to meet the energy demands of the bacterium.

Optimum Growth Conditions for Acidithiobacillus ferrooxidans

The ability of *A. ferrooxidans* to oxidize ferrous iron is dependent on the environmental pH, temperature, oxidizing potential, and oxygen availability. A range of optimum conditions are reported throughout literature reflecting differences between bacterial strains and environmental condition of the various studies, with reported optimum conditions further differing depending on the process indicator used in the study to describe the relative microbial activity; such as cell count, population growth measures, or chemical indicators, including ferrous iron concentration.

Laboratory experiments commonly include a nutrient-rich liquid media to maintain viable and active cell cultures. Organic compounds are not used to grow or maintain the bacteria cultures because most are found to impede the activity of *A. ferrooxidans* (Bryner & Jameson, 1958; Alexander, et al., 1987; Sasaki, et al., 1996). Tuovinen and Kelly (1973) demonstrated that *A. ferrooxidans* was not able to be cultured successfully on organic media such as agar and silica-based gels, leading to the development of a ferrous-iron rich growth media and liquid broth for culture maintenance. The liquid media, commonly termed TK media after the developers, has been widely used in experiments to grow and maintain *A. ferrooxidans* cultures. TK media is acidic and contains nutrient salts of potassium, magnesium, nitrogen, and ferrous iron (Table 2.3).

Table 2.3 Composition of TK growth media to grow and maintain *A. ferrooxidans* cultures (Tuovinen & Kelly, 1973)

Nutrient	Concentration
H_2SO_4	0.11 N
K_2HPO_4	0.4 g L^{-1}
$MgSO_4 \cdot 7H_2O$	0.4 g L^{-1}
$(NH_4)_2SO_4$	0.4 g L^{-1}
$FeSO_4 \cdot 7H_2O$	33.3 g L^{-1}
pH	1.3

Acidophiles are resistant to acidic pH because of the structure and composition of their cell wall giving the bacterium the ability to maintain a neutral pH within the cell whilst existing in acidic conditions (Nemati, et al., 1997). Increased rigidity and decreased permeability at low pH is provided by large quantities of fatty acids held in the cell membrane, which protect the internal components from the acidic environment. A disruption in the protective layer would allow seepage of the acid solutions into the cell, resulting in cell death. *A. ferrooxidans* survives between pH 1.5 and 6.0 (Drobner, et al., 1990) and optimum pH for maximum activity is reported to be between 2.0 and 2.3 (Smith, et al., 1959; Ingledew & Houston, 1986; Torma, 1977; Karamanev & Nikolov, 1988; Drobner, et al., 1990), with higher ranges of between 2.5 and 5.8 also being suggested (MacDonald & Clark, 1970). At pH greater than 3.5, the bacterium is not able to meet full metabolic demands because abiotic oxidation of ferrous iron dominates, and thus the activity and availability of ferrous iron is decreased (Dugan, 1987a).

Most strains of *A. ferrooxidans* are mesophilic, living in conditions between 20°C and 40°C (Nemati, et al., 1997). Optimum temperature is pH dependent, with a decrease in optimum temperature being reported when acidity increases (MacDonald & Clark, 1970; Ahonen & Tuovinen, 1989). Table 2.4 outlines reported optimum temperatures and the corresponding pH values as documented in a series of studies.

Table 2.4 Reported temperatures for maximum growth and activity of *A. ferrooxidans*.

Investigated Temperature (°C)	Investigated pH	Optimum Temperature (°C)	Reference
20 to 35	1.9 to 2.4	25-30	Smith, Luthy and Middleton (1959)
4 to 46	1.5	28	Ahonen and Tuovinen (1989)
10 to 30	2.4	30	Okereke and Stevens (1991)
20 to 31	2.0 to 2.3	31	Lacey and Lawson (1970)
20 to 40	2.5 to 3.5	33	MacDonald and Clark (1970)

The growth and metabolism of *A. ferrooxidans* is dependent on an ability to oxidize ferrous iron (Nemati, et al., 1997), the availability of which is related to the pH and oxidizing potential of the environment as highlighted in the Pourbaix diagram below (Figure 2.3). Below pH of 2.3, the soluble iron species is dependent on the oxidation potential of the solution. For instance, for a solution with an oxidation potential above 0.8 volts, reactions favouring ferric iron production will prevail whereas below 0.8 volts, reactions favouring ferrous iron production will dominate. When ferrous iron concentration is limited, iron-oxidizing organisms will not be able to meet energy demands for sustenance, resulting in a decrease in growth rate or activity (Silverman & Lundgren, 1959).

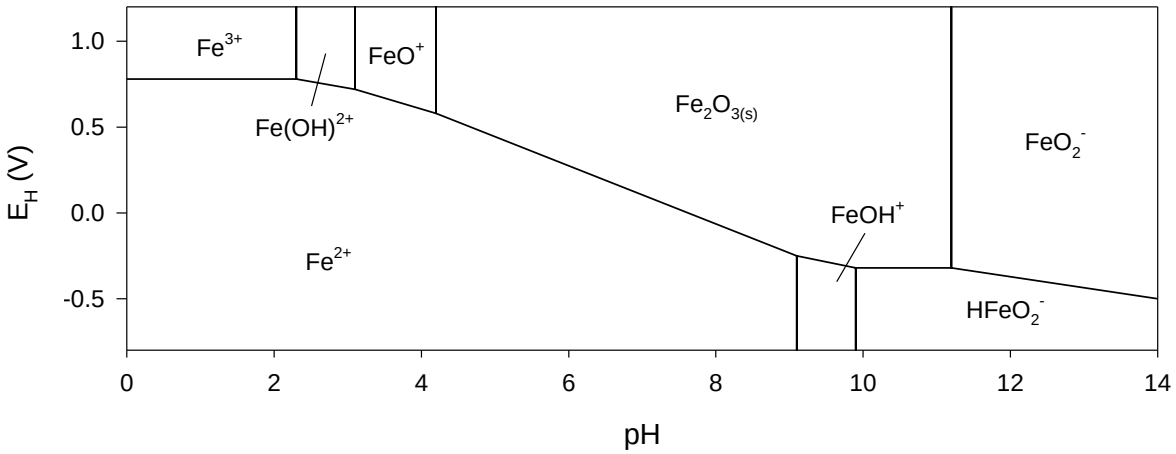

Figure 2.3 Pourbaix diagram for the Fe-H_2O system under standard conditions; modified from Takeno (2005).

Biogeochemical mineral dissolution increases the solubility of other minerals, releasing metals from the mineralized ore materials, some of which may be detrimental to *A. ferrooxidans*. The tolerable concentration range of metals differs among strains of *A. ferrooxidans.* For instance, a strain originating

from a copper ore body environment is more adaptive and tolerant to elevated levels of copper then a strain evolved outside of a copper-rich environment (Tuovinen, et al., 1971). Table 2.5 summarizes reported inhibitory concentration ranges for select metals for a range of *A. ferrooxidans* from a variety of sources and strain IDs.

Table 2.5 Concentrations of selected metals shown to be inhibitory to *A. ferrooxidans*.

Metal	Concentration (mg L^{-1})	Reference
Arsenic	110	Tuovinen, et al. (1971)
Copper	450	Imai, et al. (1975)
	1000 to 2000	Nemati, et al. 1997)
	4450	Tuovinen, et al. (1971)
	5100, natural strain	Brahmaprakash, et al. (1988)
	10100	Leduc & Ferroni (1994)
	29800, adapted strain	Brahmaprakash, et al. (1988)
Mercury	Quite sensitive	Kusano, et al. (1992)
	1	Norris & Kelly (1978)
	2	Imai, et al. (1975)
Nickel	6 to 60	Tuovinen, et al. (1971) and Imai, et al. (1975)
Uranium	700	Tuovinen, et al, (1971)
	100-10900	Huber & Setter (1975), Martin, et al.(1983), and Leduc & Ferroni (1994)

Leduc, Ferroni, and Trevors (1997) have investigated *A. ferrooxidans* strain D7, isolated from Denison Mines, Elliot Lake, Ontario, concluding that this particular strain is particularly resistant to several metals (Cu, Ni, U, and Th) at elevated levels. Inhibitory concentrations were defined for the following metals by Leduc and colleges (1997) for the D7 strain: Cu^{2+}, 635 mg L^{-1}; Ni^{2+}, 1175 mg L^{-1}; UO_2^{2+}, 2160 mg L^{-1}; and Th^{2+}, 465 mg L^{-1}. The study defined an inhibitory concentration as the concentration at which a significant decrease in ferrous iron oxidization took place compared with that for the metal-free control and they reported that the D7 strain is one of the most U-tolerant strains of *A. ferrooxidans*.

Unlike microbes existing in soil environments, the activity of *A. ferrooxidans* and related microbes are suppressed in the presence of organic acids, including humic, fulvic, tannic, and oxalic acid, resulting in limited cellular activity or cell death (Bryner & Jameson, 1958; Alexander, et al., 1987; Kleinmann &

Rastogi, 1996; Sasaki, et al., 1996). Saski and colleagues (1996) confirmed that the presence of naturally existing organic acid in the habitual environment of *A. ferrooxidans* suppressed biotic oxidation of ferrous iron (Figure 2.4). The group concluded that ferrous iron oxidation is limited in the presence of organic acids through a process of competitive reduction followed by the complexation of ferric iron ions with the acids, rendering the ferric iron unavailable to participate in the cyclic oxidation and reduction process (Sasaki, et al., 1996).

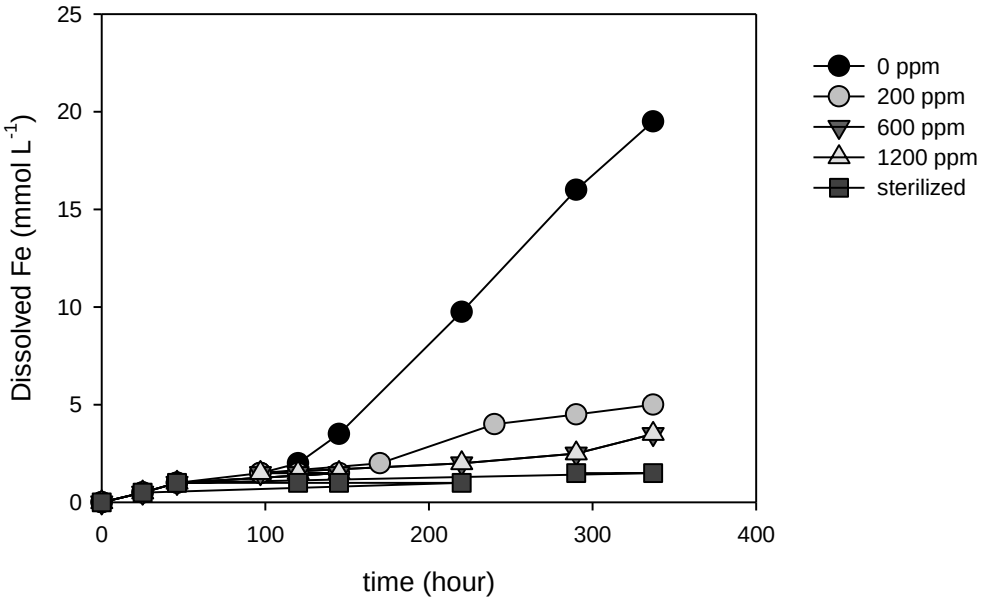

Figure 2.4 Inhibitory effects of fulvic acid on ferrous iron oxidation by *A. ferrooxidans*; modified from Sasaki et al. (1996).

2.4 Previous research

The success of bioleaching for the recovery of metals from mineralized material depends on the characteristics of the host rock mineralization, microbial population, and environmental conditions. At an industrial scale, many factors contributing to a successful bioleaching operation can be influenced or controlled. Experimental planning is based on the review of laboratory-scale bioleaching experiments to establish process parameters to guide bioleaching trials for an assessment of the conditions suitable for surface heap leaching at the proposed Eco Ridge site. Prior to field trials and full-scale operations, assessment studies must be conducted to confirm that the bioleaching methodology will be successful and the metals of interest are recoverable from the parent material. Parameters influencing bioleaching

operations were investigated through various experiments at the laboratory scale. Three assessment scales are common:

- Extraction flask and bench-top experiments to investigate the interactions between the selected microbial population and the mineralized material, either with ideal leaching conditions or altered conditions to determine threshold values (Munoz, et al., 1993);
- Column- or laboratory-scale assessments that provide details of particular leaching characteristics that may be controlled at the field level (Wadden & Gallant, 1985; Munoz, et al., 1993; Nemati, et al., 1997); and
- Field-scale testing to reinforce findings from the previous laboratory stages and to confirm the application of the selected methods at a close-to operational scale (Munoz, et al., 1993; Munoz, et al., 1995).

The influence of individual parameters can be controlled or manipulated in small laboratory experiments to determine the overall effect of the parameter on the leaching process. Experiments of this scale require minimal materials and can generally produce results over a relatively short timeframe while assessing many parameters in controlled environments, compared with more elaborate investigations. When basic parameters are established using bench-top experiments, researchers can then use leaching columns to gain greater insight of the leaching process using methods as they are more representative of a full-scale model. Essentially, the column represents one plug of the heap that can be monitored and studied as a representative sample of a large heap pile. Leaching columns also allow for a greater quantity of material to be evaluated, with leaching methods being applied to mimic the application of leaching solution across a large heap.

Variation of Bacterial Population

In natural environments, many species of indigenous bacteria exist together. In a laboratory setting, control of the bacterial consortia composition is achievable, allowing the investigation of a pure-strain or co-existing populations. Laboratory studies use purified bacteria strains to investigate details about the

particular bacterium, or to assess the response to new or altered conditions. The Denison Mines bioleaching project previously characterized the bacteria *A. ferrooxidans* through in-depth studies at Laurentian University and Dalhousie University (Ferroni, et al., 1986; McCready, et al., 1986). The studies documented the characteristics of the D7 strain of *A. ferrooxidans,* as well as its capabilities and response to stress.

The most heavily studied species is *A. ferrooxidans*, owing to its role in the oxidation of not only sulphur and sulphide compounds, but also ferrous iron, thus driving the cyclic oxidation of ferrous iron and ferrous-sulphide minerals. In contrast, *A. thiooxidans* has the ability to oxidize sulphur and metal sulphides but is incapable of oxidizing ferrous irons, thus having less impact on the overall ARD processes. Sand and colleagues (1992) investigated a mixture of *A. thiooxidans* and *Leptospirillum ferrooxidans*, a strict iron oxidizing bacteria, concluding complementary paring enhanced the leaching process. The sulphur oxidizer *A. caldus* is particularly efficient at oxidizing secondary sulphur compounds (McCready & Gould, 1990). The oxidizing abilities of these bacterial species are summarized in Table 2.6

Table 2.6 The oxidizing abilities of bacteria important to the biogeochemical mineral dissolution process.

Bacteria	Sulphide (S^{2-}) and sulphur (S^0)	Ferrous iron (Fe^{2+})
A. caldus	x	
A. ferrooxidans	x	x
A. thiooxidans	x	
L. ferrooxidans		x

In natural environments, mixed populations of microbes commonly exist having synergistic or complementary interactions. Investigations of natural or mixed bacterial populations have reinforced not only the individual importance of *A. ferrooxidans* to the oxidation of ferrous sulphides, but the significance of mixed populations. In controlled studies investigating mixtures of *A. ferrooxidans* and *A. thiooxidans*, the oxidation of pyrite was enhanced when a mixed culture was present compared with *A. ferrooxidans* alone, despite the fact that alone, *A. thiooxidans* is incapable of oxidizing ferrous iron and does not contribute to the cyclic oxidation of pyrite ferrous iron (Wakao, et al., 1983). In another

example, a mixed population of *A. caldus* and *A. ferrooxidans* enhanced the leaching rate of copper from chalcopyrite in reactors when compared with *A. ferrooxidans* alone. *A. caldus* has an enhanced ability to oxidize elemental sulphur and sulphur compounds which may form a secondary layer on the mineral grain, thus reducing the mineral surface area available for reaction sites (Zhou, et al., 2007). Thus, in the absence of *A. caldus*, the full potential of *A. ferrooxidans* may be limited because the surface exposure available for reaction may be decreased because of the formation of a sulphur layer. Mixed cultures have proven to be more robust, maintaining oxidation rates over a wider range of temperature and pH environments. McCready and Gould (1990) found that the use of indigenous sulphur- and iron-oxidizing bacteria originating from extreme environments, such as those having high concentrations of particular metals, have superior microbial activity in simulated extreme conditions whereas laboratory cultures or bacterial populations from other sources may not have the required tolerance to survive.

The completion of investigations under optimum growth conditions is useful in batch studies to assess the bioleaching capabilities of a consortium population or to determine the leaching capabilities of the indigenous bacteria from mineralization originating from a particular source. Natural consortia cultured from environmental samples may be more useful at providing an understanding at the laboratory scale of how the indigenous consortium at a specific site will perform under ideal leaching conditions. Conditions supplying the necessities for optimum bacterial growth should promote the maximum bioleaching activity.

Variation of Material Parameters

The major factor contributing to the success of bioleaching for industrial application is the existence of ferrous-sulphides (pyritic minerals) in the host mineralization. The accessibility of these sulphidic minerals is a key determining factor controlling the degree of bioleaching achieved. As the particle size is related to the amount of exposed mineral surface available for oxidation by the bacterial consortia, control of particle size of the ore minerals is critical. Although smaller particle sizes have a larger surface area, particles may be small enough to create a slurry or sludge which may be prone to compaction and thus

limit the movement of liquids through the material making the particle surfaces inaccessible to the microorganisms (Lundgren & Silver, 1980). A deconcentration effect may also arise with smaller particle sizes because the increase in surface area results in an overall increase in the non-reactive minerals compared with the reactive phases. Larger particle size, on the other hand, may be more susceptible to preferential flow patterns through a heap pile, thereby promoting the flushing of not only leached metals, but also essential bacteria from the reaction site, yet leaving some areas of the pile unaffected. Particle size is an important factor at each level of investigation, as well as at the operational level. Experiments using small particle sizes and greater amounts of liquid in flask-scale bioleaching experiments provide larger surface area and excess liquid, allowing reactions to take place at a faster rate, thus potentially providing details of the leaching results in a shorter time frame. Column experiments using larger particles, similar in size to that expected to exist at the operational level, obtain more accurate results to define a methodology which may be applied at the field scale. Laboratory assessments to determine the optimum particle size for maximum leaching and release of metals of economic and, perhaps, toxicological interests are crucial.

The nature of the material available and the timeline of investigation may determine the particle size. Reported particle sizes used in flask experiments range from 0.030 mm to 0.125 mm (Guay, et al., 1976). Guay, Silver, and Torma (1976), for example, reported higher U amounts extracted from 0.037 mm material compared with 0.125 mm in a series of parallel experiments. Wolf (1981) investigated the influence of particle size on the leaching efficiency of U ore in column experiments. Experimental conditions subjected four different particle sizes, ranging from 0.17 cm to 10.16 cm, to identical leaching conditions, with results indicating that extraction efficiency was greatest when the particle size was the smallest (Table 2.7). These results confirm that smaller particle size increases the reaction surface area, thus increasing extraction efficiency for selected elements of interest (Lundgren & Silver, 1980).

Table 2.7 Extraction efficiency from U ore for a range of ore sizes after 185 days of bioleaching, (Wolf, 1981).

Ore Size (cm)	Extraction Efficiency
10.16 to 15.24	18.0%
5.8 to 7.62	32.4%
1.35 to 2.54	68.2%
0.17 to 0.335	91.5%

Pulp density, expressed as the solid-to-liquid ratio of the mixture, plays a significant role in the leaching process because increasing the amount of solids provides additional substrate and can increase the concentration of solubilized metals, an observation confirmed by a study utilizing a series of flasks, ranging between 5 and 40% pulp density by Lundgren and Silver (1980). Guay and colleagues reported that a pulp density of 5% had the highest U extraction efficiency for both the 0.037 and 0.125 mm (400 and 120 mesh) materials, results illustrated in Figure 2.5 (Guay, et al., 1976).

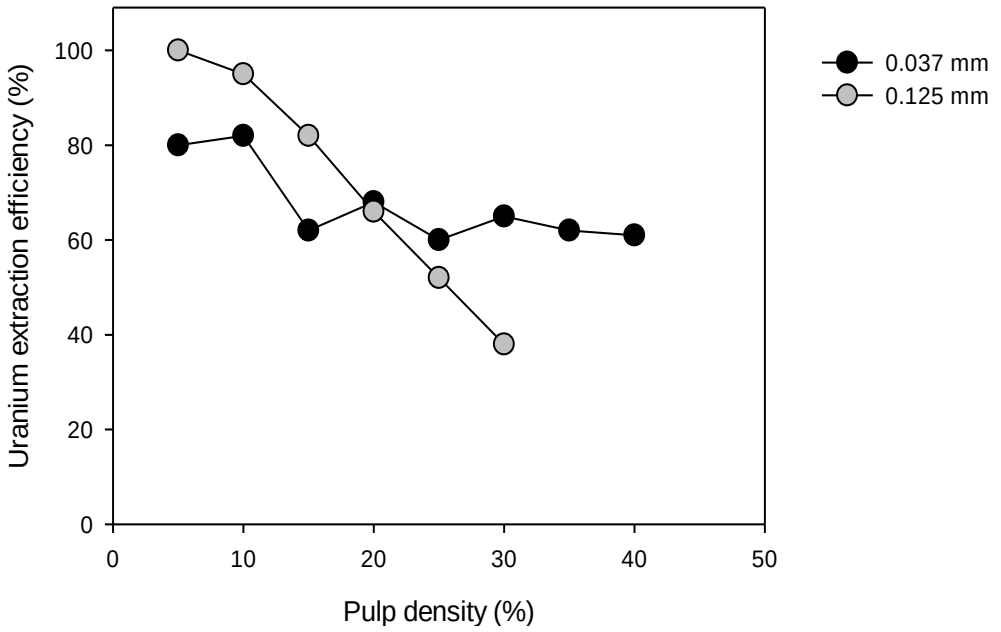

Figure 2.5 Relationship between pulp density and U leaching efficiency for two particles sizes; modified from Guay, Silver, and Torma (1976).

Experiments have shown that an extended duration of leaching increases extraction efficiency, with smaller particle sizes leached for a shorter time or larger particle sizes leached for a longer time producing similar extraction efficiencies (Bartlett, 1998). The generation of smaller particle sizes present challenges for larger scale initiatives because of the increased operational cost for excess crushing and preparation of

the material. Further, the permeability of the heap or pile becomes limited because of compaction, with smaller particle size ranges decreasing flow paths for solution percolation.

Small batch experiments are generally performed using 250-milliliter Erlenmeyer flasks with a tapered, conical shape, which allows the flasks to be swirled on a bench-top shaker without splashing or spilling the contents (Munoz, et al., 1993). Column experiments are not as standardized and consist of a wide array of sizes and materials, described in Table 2.8.

Table 2.8 Reported leaching column designs for biogeochemical mineral dissolution experiments.

Research Investigation	Material		Charge		Leaching method	
	Material	Length/ diameter (cm)	Particle size (cm)	Mass (g)	Flow Rate (mL min^{-1})	Wetting
Bioleaching of a copper-cobalt-zinc ore (Ahonen & Tuovinen, 1995)	glass	50/9		800		continuous
Bioleaching of gold ore with varying leaching parameters (Bouffard & Dixon, 2002)		170/25.4	1.25		0.42	continuous
		170/25.4	0.33		0.42	continuous
Bioleaching of U ore (Kleinmann & Erickson, 1983)			< 12			continuous
Bioleaching of U ore, small to large scale experiments (Harris & Lottermoser, 2006b)	glass	40/7.5	> 0.65	500		continuous
	concrete	300/300	> 25	2 700 kg		continuous
Bioleaching of U (Harrison, et al., 1965)	glass			400	percolated	continuous
Acid neutralization and metal mobility in tailings (Jurjovec, et al., 2002)	clear acrylic	10/9	tailings		percolated	flood
Sulphate reducing bacteria to prevent the generation of acid mine drainage from mine waste piles in situ (Kim, et al., 1999)	acrylic	17/3.2	mine waste	40	0.45	continuous
Effect of column size investigating sulphuric-acid rinsing (Li, et al., 1996)	Plexiglas	123/15.2	< 2.54	32 kg		continuous
	Plexiglas	173/16.2	< 2.54	60 kg		continuous
	heavy plastic	308/67	< 15	1400 kg		continuous
	heavy plastic	671/66	< 15	3338 kg		continuous
Bioleaching of U ore (McCready & Gould, 1990)	rubberized steel	300/61	broken ore	1500 kg		
Bioleaching of zinc ore (Mousavi, et al., 2006)	Plexiglas	220/30	0.05 to 0.30	410 kg	0.59	continuous
Bioleaching of U, comparing parameter relationships (Munoz, et al., 1993)	glass	70/7			30	continuous
	plastic	75/14			10	continuous
	PCV	275/24			16.7	continuous
Bioleaching of U, scaling from column to filed experiments (Munoz, et al., 1995)	glass	70/7	0.6 to 1.5		1.67 to 5.0	continuous
	methacrylate	70/14	3 to 5		1.67 to 5.0	continuous
	PCV	250/25	> 5		1.67 to 5.0	continuous

Table 2.8 continued

Research Investigation	Material		Charge		Leaching method	
	Material	Length/ diameter (cm)	Particle size (cm)	Mass (g)	Flow Rate (mL min^{-1})	Wetting
Bioleaching of copper ore concentrates (Petersen & Dixon, 2002)		50/10	40 µm	320	0.7	continuous
Comparison of cover techniques for tailings (Simms, et al., 2000)	Plexiglas	200/30			0.1	
Bioleaching of U ore (Wadden & Gallant, 1985)		610/61		2500 kg		continuous
		610/61		2500 kg		flood
Bioleaching of black schist using varying microbe populations and particle size (Wakeman, et al., 2008)	methacrylate	100	0.020 to 0.065	3 kg		
	methacrylate	100	0.065 to 0.12	3 kg		

The material used to construct a column also varies considerably, with high density polymer-plastic and glass being most common. Factors that must be considered when selecting column material include the strength, permeability, and reactivity of the material, which must be strong enough to withstand the loading of the crushed material and liquid, impermeable to prevent any loss of leaching fluid, and inert so as to not influence the leaching process. Uncoated metal columns, for example, would not be appropriate for metal leaching studies. The columns may be transparent to allow for visual monitoring of the leaching process in the column.

The internal diameter of the column is an important consideration because preferential flow patterns and/or wall affects may be observed if the column is too large or small compared with the material size, with the leaching solution draining down the wall of the column rather than through the mineral materials (Li, et al., 1996). The internal column diameter is also dependent on the particle size of the material, with an ideal particle-to-column diameter size ratio between four and 20 being reported (Munoz, et al., 1995). Figure 2.6 illustrates the relationship between internal diameter and particle size for the experiments reported in Table 2.8. With few exceptions, the column designs summarized in Table 2.8 meet the criteria of having a particle-to-column diameter size ratio between four and 20.

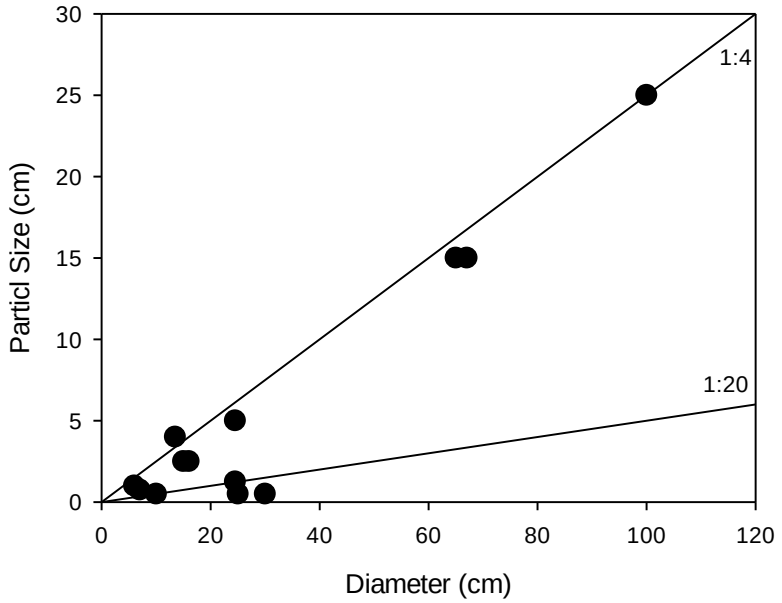

Figure 2.6 Variability between particle size and internal column diameter for various column leaching experiments in Table 2.8.

The height of the column depends on the amount of material to be studied, and may also mimic the actual height of a leaching pile proposed for site development. The column diameter and mean particle size will also influence of the mass of material in the column because smaller particles pack more closely than large particles of the same total mass, thus requiring less volume.

Variation of Environmental Conditions

The bioleaching capabilities of the selected bacteria population are measured using batch and column studies under controlled conditions. The conditions tested may deviate from optimum conditions for the growth of the bacterium in order to accurately represent the conditions expected at the operational phase. Comparison studies can also provide a means of evaluating the effects of different parameters and methods. For example, the capacities of a microbial population in optimal or extreme temperatures can be assed in a laboratory investigation by either controlling the operational temperatures or by promoting a varying range outside the optimal temperatures. Heap leach piles typically maintain a higher temperature than atmospheric conditions, influenced by the height of the heap, exothermic biotic oxidation processes, aeration, and feed solution application rate (Olson, et al., 2003). The temperature of leaching columns can

be controlled by maintaining solution temperature with the use of a temperature controlled recirculating system, or may be allowed to evolve naturally within a controlled room environment.

The pH of the leaching environment may be controlled or left to naturally evolve in experimental trials. The pH of a metal-sulphide leaching system decreases significantly in the early stages of leaching because *A. ferrooxidans* drives the oxidation of sulphur minerals. The natural accumulation of acidity from the biogeochemical reaction processes, combined with the buffering capacities of the host mineralization, maintains the pH of the column or heap system between 2.0 and 2.5 (Boseker, 1997). This pH range promotes the maximum activity levels for *A. ferrooxidans* (Nemati, et al., 1997). The pH of the leaching solution cycling through a column in a close circuit loop does not generally need to be adjusted, providing an optimum level to promote leaching. The pH of a fresh solution, or a combination of fresh and re-circulated solution, may be adjusted to maintain acidity and discourage the precipitation of secondary oxide minerals, which will occur if the pH of the aerobic solution is above 3.5. The solution pH should be monitored because with a decrease in pH to below two, the ferrous iron oxidation rate of *A. ferrooxidans* may also begin to decrease (Boseker, 1997).

Oxygen and carbon dioxide are critical inclusions for bioleaching investigations. Carbon dioxide is the only carbon source used by the *A. ferrooxidans* cells through carbon fixation and the absence of this carbon source reduces the ferrous iron oxidation rate (Lundgren & Silver, 1980). In the absence of oxygen, the oxidation of ferrous iron is retarded, and the cell cannot meet maintenance energy demands. The solubility of oxygen in water and other liquid media decreases when the temperature increases. At 35°C, the solubility of oxygen in water is 0.5 moles L^{-1} (Das, et al., 1999). As *A. ferrooxidans* requires one mole of oxygen for every four moles of iron oxidized, at 35°C the dissolved oxygen content in water simply does not meet the respiratory requirements of the bacteria. Batch experiments are commonly provided essential gas supplies by bubbling into the leaching solution or allowing natural diffusion from the atmosphere. Leaching columns are supplied oxygen and carbon dioxide in a manner that is possible to also implement easily in field conditions, such as air inflow at the base of the column. The introduction of

oxygen and carbon dioxide at the base of the column ensures adequate aeration throughout the length of the column. Air input at the top of the column may limit diffusion through the column length, especially if under near saturated flow conditions. The amount of air supplied should be enough to meet the needs of the bacteria yet not dry out the material.

To support microbial metabolism, the composition of the leaching medium may be supplemented with salts of ammonium, phosphate and magnesium to provide additional nutrients to the bacterial population (Boseker, 1997). Leaching liquids are typically limited in dissolved carbonate, organic acid, and surfactant content to prevent pH increase and exposure of the microorganisms to inhibitory compounds (Boseker, 1997). During the leaching process, the concentration of dissolved metals in the leaching liquid will increase, with adapted strains potentially being more tolerant to elevated metal contents.

In batch tests, the leaching solution quantity is typically held constant, whereas in column-type studies the solution may be either recycled or fresh. Using the a re-circulated solution has been shown to promote more effective leaching results in flask experiments because conditions appropriate for leaching and further mineral dissolution, including low pH and elevated and/or steady oxidizing conditions, are well maintained (Harrison, et al., 1965; Kleinmann & Erickson, 1983; Mousavi, et al., 2006). Application of a fresh solution requires the system to strive constantly to reach steady-state conditions appropriate for leaching. Fresh solution may be required once metal concentration in recycled solution approaches inhibitory concentrations. Column studies are more useful to assess the effectiveness between recycled or fresh solutions. Recycled solution is recommended in some instances because conditions that promote effective bioleaching are established in the leachate, with a low pH and stable oxidizing potential necessary for the third stage of pyrite oxidation. However, fresh solution at a pH greater than the exiting pregnant solution may result in the precipitation of secondary metal-rich salts, which may block or clog circulation system. Concentration of toxic elements can also be limited by using a mixture of fresh and recycled solutions to maintain leaching conditions.

Wetting protocol, usually involving either flood or trickle application methods, is a parameter that can be easily investigated using column experiments. Columns can be flooded by two methods, either top-down or bottom-up. Flooding from the bottom-up ensures that there are no air pockets remaining in the column a common consequence of the top down approach. The percolating, or trickling method requires the solution be sprayed or poured on the top of the pile using a defined flow rate with set time intervals.

A comparison between flood and trickle leaching methods using ore from Denison Mines was performed by the Hydrometallurgical Department of the British Columbia Research Corporation to compare the U extraction efficiency between the wetting methods (Wadden & Gallant, 1985). Identical columns, as described in Table 2.8, were charged with ore smaller than 10 cm in size and either flooded or supplied liquid by a trickle method. After 250 days, the overall U extraction from the trickle leach column was 76.8%, with 75.2% was extracted from the flooding column (Wadden & Gallant, 1985). The researchers evaluated the flooding technique further because this method would be simpler to implement and maintain in vacant stopes of an underground operation. The success of flood leaching depends on the duration of flood time, time between flood cycles, and an adequate supply of oxygen. Shorter flood times, with rest stages between flooding intervals, is recommended to provide sufficient oxygen for bioleaching to continue, with prolonged flooding potentially producing an oxygen-deficient environment which may inhibit the bacterial leaching process (Wadden & Gallant, 1985).

Methods simulating surface heap leaching using the trickle leaching approach are far more commonly used in laboratory studies. Trickle methods are also easily implemented using surface infrastructure such as pipelines and overhead sprayers. Injected under pressure at the base of a heap, atmospheric oxygen will efficiently migrate through a heap pile. Consideration of the rate of fluid application flow is important because a faster rate may percolate too quickly through the pile, having a washout effect, whereas slower application rates may result in evaporation, concentrating the pregnant solution (Munoz, et al., 1995).

Many parameters can be altered, controlled, or monitored in laboratory scale studies. Monitoring the pH and oxidizing conditions will indicate the stage of oxidation that has been reached, with the measurement of total iron or ferrous and ferric iron concentration reinforcing these conclusions. An estimation of the bacterial population provides an insight to the health and growth of the culture. The determination of levels of acidity and microbial population diversity may also be included in laboratory studies. Parameters including temperature, particle size, nutrient content, oxygen, and carbon dioxide supply and dissolved metal concentrations are also generally reported and monitored or manipulated in laboratory studies.

2.5 Applications

Discoveries in the twentieth century describe the involvement of microbes in the leaching process, although the economic application of bacterial oxidation has a historical legacy. Historic accounts suggest that cementation was used to precipitate copper from metal rich streams mediated with the addition of metallic iron to the solution, with copper being obtained through similar means across Europe and Asia Minor as early as the second century (Ehrlich, 2001). A significant site for copper extraction by cementation is at Rio Tinto Mines, Spain (Campbell, et al., 1985; Ehrlich, 2001). Historical accounts describe the Rio Tinto, or Red River, as being devoid of fish, not suitable for drinking or cooking, and red in colour (Rawlings, 2004). At present, the river is known to have a low pH and elevated concentrations of transition metals (Johnson, 2006). Biogeochemical mineral dissolution of iron- and copper-containing sulphide minerals is known to exist at the source of the river today, being accelerated by bacterial oxidation, providing the river with the trademark colour from the precipitation of ferric iron compounds. Downstream, the addition of metallic iron to the water results in the precipitation of copper minerals.

At the end of the 19th century, in situ bioleaching of copper ores was practiced at the Mynydd Parys mine of north Wales. The practice of leaching at this historical mine site included flooding underground holdings and pumping the liquid to the surface where copper was precipitated through a cementation process, namely by the addition of metallic iron to the solution (Johnson, 2010). The Kennecott Copper Corporation was the first mining company to obtain a global patent for the use of bacteria to extract

copper from waste rock dumps (Zimmerley, 1958). The technology described in US patent number 2829964 was developed at Bingham Canyon Mine, Utah, and later applied to Chino mine in New Mexico (Johnson, 2010). Both operations were owned and operated by Kennecott Copper Corporation.

Bioleaching metals other then copper was not practiced on a large scale until the 1980s (Brierley & Brierley, 2001). Gold commonly exists with ferrous ores, held in arsenopyrite and pyrite matrixes. In the presence of *A. ferrooxidans*, pyrite-based minerals are solubilized with biogeochemical mineral dissolution, whereas gold and gold-ferrous minerals remain insoluble and inaccessible for recovery (Agate, 1996). Fairview Mine, currently operated by PanAfrican Resources PLC, South Africa, was the first site to construct a commercial plant for the biological oxidation of gold-sulphide ores. Commencing operations in 1986, gold-bearing arsenopyrite-pyrite concentrates were mixed in a large stirred, continuous flow reactor (Brierley & Brierley, 2001). Gold is not solubilized in the bioleaching process and must be recovered subsequently though cyanidation. The prior removal of pyrite minerals is critical to the cyanidation process, with an excess of sulphide minerals resulting in excessive cyanide consumption, with a production of waste thiocyanate. At the same time, iron complexes with other base metals to produce cyanide complexes. Thiocyanate and metal-cyanide complexes pose environmental threats if they are not removed from the mine waste, requiring specialized treatment stages before tailings can be disposed. With the incorporation of a bioleach circuit to remove ferrous-sulphide minerals from gold ores, the waste products of the cyanidation process require little further treatment and thus pose a lesser environmental threat.

Bioleaching for other metals has also been investigated, and in some cases, commercial plants or technical methods are in place. A stirred tank reactor method has been used to liberate cobalt from a 30-year-old stockpile located at the former Kilembe Copper Mine in Uganda (Brierley & Brierley, 2001). Through a complex process, a reported cobalt recovery of 92% was achieved from the waste piles, which were assessed to contain 1.38% cobalt and have a pyrite content of 80% (Brierley & Brierley, 2001).

Commonly associated, the metals from zinc and lead sulphides may be economically recovered with the assistance of bioleaching (Agate, 1996).

Uranium Leaching

Agnew Lake Mines partook in a collaborative research project with the Canadian Centre for Mineral and Energy Technology (CANMET) to investigate bacterial leaching at Agnew Lake's U mine, located east of Elliot Lake, Ontario (Campbell, et al., 1985; McCready & Gould, 1990). Results of the study, initiated in the late 1960s, indicated that after one year of operation 70% of the U contained in the low-grade ore could be extracted and after two years, an 82% extraction efficiency was reported (McCready & Gould, 1990). After successful field trials, Agnew Lakes developed a U recovery process based solely on the underground bioleaching of broken ore and above ground heap leaching (Campbell, et al., 1987). During operations, an yttrium extraction plant was also operated alongside the U extraction facility, making the bio-dissolution process even more economic (Campbell, et al., 1985). In situ leaching was not as successful in the field situation as the studies indicated. Challenges relating to improper fragmentation, technical difficulties, declining grade, and dropping U prices could not be overcome, bringing an end to in situ leaching at Agnew Lake in the late 1970s (McCready, 1986; McCready & Gould, 1990). In 1983, all mining actives at Agnew Lake Mines ceased (Campbell, et al., 1985; Campbell, et al., 1987).

Through the 1960s, acidic mine water used to wash the walls and floors of spent stopes was collected at Denison Mines of Elliot Lake, with the dissolved U in the wash water being removed in the conventional extraction circuit (Campbell, et al., 1985). In the early 1980s, when the need to reduce costs was recognized, Denison Mines, with the support of the CANMET, investigated the application of bioleaching (McCready, 1986). Recovering U from wash water required no additional milling or pumping costs, so these methods could be applied to broken ore and the walls of spent stopes with minimal additional costs to implement a full scale bioleaching circuit. The research project addressed four objectives:

- Determine an appropriate underground blasting procedure for proper ore fragmentation for leaching;

- Compare leaching methods to determine the best application method for the supply of leaching liquid to fragmented ore, either trickling or flooding;
- Address concerns and develop methods to handle increased radon emissions because of a larger volume of broken ore in a smaller area; and
- Work with universities to perform bacteriological studies to better understand the bioleaching process and nutrient requirements of the indigenous bacteria (McCready, 1986; Campbell, et al., 1987; McCready & Gould, 1990).

Microbiological research at two Canadian universities supported the Denison Mines leaching project. McCready, Wadden, and Marchbank (1986) investigated the optimization of nutrient requirements for the indigenous bacteria at Dalhousie University in Halifax, with strain isolation and identification and effect of temperature on growth rate were studied by the research group of Ferroni, Leduc, and Todd (1986) at Laurentian University in Sudbury. The results from the Dalhousie study indicated that the nutrients required to support the leaching bacteria exists in excess amounts in standard laboratory nutrient solutions, with U solubilization being maximized with the use of a nutrient solution containing 0.1 mmol L^{-1} potassium hydrogen phosphate, 0.5 mmol L^{-1} magnesium sulphate, and 0.5 mmol L^{-1} ammonium sulphate dehydrate (McCready, et al., 1986). A review of the nutritional value of the local mine waters revealed that only sulphate content was lacking (McCready, 1986). Observations of the growth of *A. ferrooxidans* isolated from the Denison Mine environment over a temperature range of 6°C to 35°C revealed that optimum growth takes place between 25°C and 30°C, with growth rate decreasing on each side of the optimum range (Ferroni, et al., 1986). Compared to a purified lab strain, the strain isolated from Denison Mine, *A. ferrooxidans* ATCC 33020, was shown to have superior growth prospects in the lower temperature range and survive in extreme concentrations of U (Ferroni, et al., 1986; McCready, et al., 1986).

In 1987, the Denison Mines underground leaching demonstration, consisting of the intermittent flooding of blasted ore in a series of underground stopes (Olson, et al., 2003), was set up at a cost of $1.5 million,

having the full support from senior management owing to the potential for cost reduction (Campbell, et al., 1987). Preliminary results indicated that U recovery between 70 and 80% could be achieved through bioleaching in 12 to 18 months (McCready, 1986). Production of 453 metric tons of U was projected in 1988, although only 381 metric tons was actually generated through the leaching project (McCready, 1986; McCready & Gould, 1990). In the lifetime of the project, 3.6 million metric tons of low-grade ore was biologically leached in-situ, recovering U from mineralized material that may not have been processed by conventional milling and extraction methods (McCready & Gould, 1990). No tailings or waste material was left exposed through this process, leaving no environmental liabilities at the mine surface.

2.6 Conclusions

In the presence of *A. ferrooxidans*, ferrous sulphide minerals undergo biogeochemical mineral dissolution resulting in a decrease of pH, an accumulation of acidity, an increase in oxidizing potential, and liberation of ferric iron. Free ferric iron subsequently oxidizes insoluble uraninite, releasing uranyl compounds to solution which may be recovered through conventional processing methods. Experimental conditions, including bacterial population composition, mineral material parameters, and environmental conditions have been investigated at a laboratory scale, with optimization of parameters for the release of U being established. Full-scale mine-site demonstrations in the Elliot Lake region have shown that biogeochemical mineral dissolution-mediated release of U is achievable. Locations in close proximity to Eco Ridge, expected to be similar in geology and microbial population, have conducted successful full-scale studies and applications, indicating that the biogeochemical mineral dissolution-mediated release of U from above ground heap leach pads at the Eco Ridge site will be achievable. Previously optimized experimental parameters from the literature can be used to guide laboratory investigation to monitor the long-term mineralogical and geochemical dynamics of extraction flasks and leaching columns designed to simulate biologically mediated heap-leach conditions using mineral material and microbial populations from Eco Ridge. These former studies, however, paid little attention to the potential for a concomitant

release of rare earth elements from the low-grade uraniferous ores, which may present additional economic benefit if successful.

CHAPTER 3

3 Passive Approaches to Prepare for Decommissioning

3.1 Introduction

The Environmental Code of Practice for Mines describes the recommended industry best-practice pollution control measures during all stages of the mine life cycle. The Code advises that, with the exhaustion of resource extraction at a mine site, processed tailings, waste rock piles, and spent heap pads be treated to control and remove possible environmental liabilities (Environment Canada, 2009). Current literature documents the effects of the release of deleterious substances in mine effluent to the environment, and explores methods of control, suppression, and mitigation. This review focuses on the environmental concerns of potential effluent release from Pele Mountain Resources, Incorporated's (PMR) planned Eco Ridge Mine Rare Earths and Uranium Project (Eco Ridge). This review examines the utility of two passive approaches to prepare for decommissioning that may be applied to mitigate the production of potentially toxic effluent at the end of the mine life cycle. Passive approaches have been selected to complement the potential application of biogeochemical mineral dissolution to process the mineral material for uranium (U) recovery in support of PMR's approach to the sustainable development of Eco Ridge.

3.2 Environmental Concerns

The Metal Mining Effluent Regulation (MMER) applies to all Canadian metal mines with effluent release to natural waters exceeding 50 m^3 day^{-1}, defined under sections 34(2), 36(5), and 38(9) of the Fisheries Act, 1985 (Government of Canada, 1985; Government of Canada, 2002). The maximum authorized

concentrations (MAC) of deleterious substances under the MMER are provided in Table 3.1; cyanide is only required to be reported when it is used in the processing of ores.

Table 3.1 MACs for deleterious substances under the MMER (Government of Canada, 2002).

Deleterious Substance (mg L^{-1})	Monthly Mean	Composite Sample	Grab Sample
Arsenic (As)	0.5	0.75	1.0
Copper (Cu)	0.3	0.45	0.6
Cyanide (CN)	1.0	1.5	2.0
Lead (Pb)	0.2	0.3	0.4
Nickel (Ni)	0.5	0.75	1.0
Zinc (Zn)	0.5	0.75	1.0
Radium (^{226}Ra, Bq L^{-1})	0.37	0.74	1.11
Total suspended solids (TSS)	15	22.5	30
pH range	6.0 to 9.5	6.0 to 9.5	6.0 to 9.5

The Canadian Nuclear Safety Commission (CNSC) requires all license holders of U mine and milling operations to meet the discharge criteria defined in the MMER, which applies the as low as reasonably achievable (ALARA) principal with respect to total U concentration in treated effluents (Canadian Nuclear Safety Commission, 2012). The optimization screening objective (OSO) recognized by the CNSC for total dissolved U concentration in treated effluent is 0.1 mg L^{-1} (Canadian Nuclear Safety Commission and Environment Canada, 2012). Adherence to these release guidelines prevents any unreasonable risk to the environment, and ensures that operators will not have any violation of license conditions with effluent concentrations. Discharge of U concentrations greater than the OSO requires facilities optimization and/or upgrade of effluent treatment process. The CNSC's OSO is considerably lower than established regulatory limits for the maximum monthly average U concentration permissible in the United States, 2 mg L^{-1} (Enviromental Protection Agency, 2000) and Saskatchewan, 2.5 mg L^{-1} (Government of Saskatchewan, 1996). The U content held in the solid phase in waste piles and retired heap pad will also dictate the amount mitigation and protection that is required protect the environment. For instance, a waste pile with a U content less that 40 mg kg^{-1} (approximately equal to 1 Bq g^{-1}) no

longer be requires a CNSC license or institutional control and is acceptable permanent storage(International Atomic Energy Agency, 2004).

Acid Rock Drainage

The oxidation of pyrite and other metal sulphides results in a decrease of pH and the associated release of other metals (Baker & Banfield, 2003). This natural process of acid rock drainage (ARD) is slow on undisturbed landscapes, generally limited by the surface area of the sulphide mineral exposed to oxygen and water. Anthropogenically altered landscapes, including mine rock and tailings confinements, may significantly increase the surface area of exposed sulphide minerals to air and water, thereby facilitating an increase in the rate of ARD generation. ARD generated through influences of the mining industry is termed acid mine drainage (AMD). Left untreated or uncontrolled, AMD contributes to elevated levels of acidity, sulphate concentration, temperature, and concentrations of metals in the waste pile and receiving aquatic systems.

The geochemical process of ARD production is well understood. Occurring in the presence of air and water, ferrous-sulphide minerals are oxidized, liberating ferrous iron and acid to the environment (Reaction 3.1). Ferrous iron is oxidized by molecular oxygen (Reaction 3.2), liberating ferric iron which, in turn, oxidizes additional ferrous-sulphide minerals (Reaction 3.3). The continuous oxidation and reduction of iron is a cyclic, self-propagating process (Kleinmann, et al., 1981). The chemical oxidation of iron is a slow and rate determining step, but in the presence of iron-oxidizing bacterial cultures this dissolution rate can be increased up to six orders of magnitude (Singer & Stumm, 1970; Evangelou & Zhang, 1995; Marchand & Silverstein, 2003; Johnson, 2010).

Reaction 3.1 $$FeS_2 + \frac{7}{2}O_2 + H_2O \rightarrow Fe^{2+} + 2{SO_4}^{2-} + 2\,H^+$$

Reaction 3.2 $$Fe^{2+} + \frac{1}{4}O_2 + H^+ \rightarrow Fe^{3+} + \frac{1}{2}H_2O$$

Reaction 3.3 $$FeS_2 + 14Fe^{3+} + 8H_2O \rightarrow 15Fe^{2+} + 2{SO_4}^{2-} + 16H^+$$

Acid mine drainage has the potential to degrade both surface and subsurface water quality at a much faster rate than natural ARD, having direct effects on the rest of the ecosystem (Boorman & Watson, 1976; Blowes & Jambor, 1990; Yanful & St. Arnaud, 1992). The pH range for the wellbeing of a fish population and MAC for deleterious substances identified in the MMER should be considered at all stages of a mine's life, including decommissioning (Government of Canada, 2002).

Radionuclides

Procedures should exist to prevent or control the release of radionuclides from U mine sites. Alpha or beta particles are emitted when an unstable isotope decays into a more stable radioisotope. Gamma radiation may also accompany alpha or beta decays when energy is released from the radio nuclei. The natural occurring decay chains, 4n, 4n+2, and 4n+3, daughter radionuclides, and occurrence are listed in Table 3.2.

Table 3.2 Details of the nature radioactive decay chains.

Decay chain	Parent	Daughters	Occurrence
4n	^{232}Th	^{232}Th, ^{228}Ra, ^{228}Ac, ^{228}Th, ^{224}Ra, ^{220}Rn, ^{216}Po, ^{212}Pb, ^{212}Bi, ^{212}Po, ^{208}Tl, ^{208}Pb, ^{210}Bi, ^{210}Po, ^{206}Tl, ^{206}Pb	natural Th-containing sample, whether metal, compound, or mineral.
4n+2	^{238}U	^{238}U, ^{234}Th, ^{234m}Pa, ^{234}Pa, ^{234}U, ^{230}Th, ^{226}Ra, ^{222}Rn, ^{218}Po, ^{218}At, ^{218}Rn, ^{214}Pb, ^{214}Bi, ^{214}Po, ^{210T}l, ^{210}Pb, ^{210}Bi, ^{210}Po, ^{206}Tl, ^{206}Pb	U-containing sample, whether metal, compound, or mineral
4n+3	^{235}U	^{235}U, ^{231}Th, ^{231}Pa, ^{227}Ac, ^{227}Th, ^{223}Fr, ^{223}Ra, ^{219}At, ^{219}Rn, ^{215}Bi, ^{215}Po, ^{215}At, ^{211}Pb, ^{211}Bi, ^{211}Po, ^{207}Tl, ^{207}Pb, ^{206}Tl, ^{206}Pb	U-containing sample, whether metal, compound, or mineral

The mineral material at Eco Ridge contains natural U and thorium (Th), so the potential for release of radionuclides from waste material must be addressed in closure planning for the decommissioning of heap-leach pads. The MMER define allowable concentration limits for ^{226}Ra, a daughter radionuclide of the 4n+2 series. Given higher concentrations of U at the Eco Ridge site, there is potential for ^{226}Ra release. Radon gas release is also of particular concern for the worker's health and safety in the U mining industry with evidence showing that exposure to high concentrations of radon is linked to lung cancer (Office of Radiation and Indoor Air, 2003). Radon exists in a gaseous form and special precautions should be taken to prevent or control the release of the gas from the site.

3.3 Decommissioning

Two conditions may be met to fully decommission a site in terms of AMD production and metal and radionuclide release, according to Li and colleagues (1998). Firstly, because AMD is a consequence of the biogeochemical dissolution of sulphide minerals, the removal of these minerals and associated soluble acidity will inherently prevent the production of acid and further release of metals and radionuclides. This method, although ideal, may not be fully achievable on closure at many mine sites. A second option to achieve a fully decommissioned state is to demonstrate control and treatment of acidity. For example, soluble ions released by acid generating processes may be precipitated *in situ* in the form of metal hydroxides and oxides, with the fluid conditions being maintained at neutral pH after the addition of liming materials. In this method, further metal dissolution from sulphidic phases is limited, but there are associated draw backs. The continuous precipitation of metal hydroxides and oxides creates a metal-rich sludge, which must be maintained at a neutral pH or be subjected to further treatment. Modern AMD prevention technologies are designed to change the biological, chemical, or physical nature of the mine wastes and/or its surrounding environment (Harris & Lottermoser, 2006b). The goal of achieving one of these conditions may guide the development of specific decommissioning strategies.

Decommissioning efforts for bioleach heaps can be less difficult than those for waste rock piles or tailings confinements because ARD production has been controlled in order to maximize metal recovery, resulting in waste material that is may be less reactive (Rawlings, 2002) and the uranium content may be depleted below a critical value, allowing the solid waste material to be acceptable for permanent storage and removing the need for institutional licensing. The bioleaching process also produces stored acidity and precipitated secondary phases, which may not be stable in all environmental conditions. The following issues, identified by Zang and Evangelou (1998), should be considered in order to decommission bioleaching heaps: stored acidity must be neutralized, secondary phases should be removed or stabilized, and the oxidation of any remaining sulphidic minerals needs to be prevented.

Approaches to the prevention and control of AMD and associated liabilities are based on the current understanding of the existing and anticipated microbiological, chemical, and mineralogical relationships. Although highly impossible to completely remove sulphidic minerals, the interruption of the mechanism that allows oxidation of the sulphidic minerals may be feasible. The oxidation of sulphur and production of acidic conditions is driven by the oxidation of ferrous-sulphides, a process increased by six orders of magnitude in the presence of *Acidithiobacillus ferrooxidans* and related sulphur- and iron-oxidizing microorganisms (Singer & Stumm, 1970; Marchand & Silverstein, 2003; Johnson, 2010). Although abiotic oxidation will continue, it is a slow process and the rate of acid production and accumulation of acidity would be significantly reduced, allowing for greater opportunity for control of the process (Singh & Bhatnagar, 1988).

Environmental conditions can be altered to promote conditions unfavourable for biotic oxidation, which may produce conditions appropriate to apply passive approaches to prepare for decommissioning for the retired heap. For instance, at an elevated pH, acidophilic microorganisms such as *A. ferrooxidans* do not operate at their full potential (Smith, et al., 1959), with ferric iron becoming insoluble as a ferric hydroxide precipitate. In the absence of ferric iron and an increase in pH, the rate of biotic oxidation is reduced, decreasing oxidizing conditions and promoting consumption of stored acidity. Another approach to control biotic oxidation requires either process inhibition or microorganism destruction. Reports that iron-oxidizing bacteria responsible for driving the biogeochemical mineral dissolution process may be chemically inhibited *in situ*, resulting in an overall reduction of the formation of acid mine drainage have been documented (Dugan & Lundgren, 1964; Dugan, 1975; Tuttle & Dugan, 1976; Tuttle, et al., 1977). *A. ferrooxidans* activity is known to be inhibited by various organic substances, thereby directly affecting the rate of iron oxidation. Finally, the rate of biogeochemical mineral oxidation can be reduced by limiting the contact between the oxidizing agents and the reactive mineral surfaces. This reduction may be achieved by promoting the establishment of protective coatings on the mineral surface to obstruct oxidation.

An in-depth examination of bacterial inhibition and mineral pacification methods aims to provide passive approaches to prepare for decommissioning of the bioleaching pads at the Eco Ridge site. Laboratory studies allow the investigation of a variety of decommissioning approaches under differing conditions. Similar to leaching studies, the laboratory scale decommissioning investigations can be completed prior to full-scale field implementation. Ferrous iron concentration is an important indicator for biotic oxidation, and thus measurement can be utilized to identify the effect a treatment has on the overall rate of iron oxidation. Typically, when the bacterial population or activity decreases, the rate of iron oxidation slows and ferrous iron begins to accumulate in the leaching solutions. Previous laboratory investigations of bacterial inhibition and pacification approaches provide a foundation for on which to develop experimental designs to assess decommissioning strategies to potentially employ for the decommissioning of spent heap pads at Eco Ridge.

To investigate passive approaches to prepare for decommissioning, the main goal of laboratory studies is to determine if the substance or method being tested either retards or stops the bioleaching process, allowing for the use of basic materials and simpler methods of control. For instance, batch studies generally use a ferrous iron-based liquid growth media or fine ground pyrite-based mineral material and a bacterial culture that is similar or identical to populations existing at the application site. In transitioning from laboratory-based studies to field level studies, consideration for the rate of application of the inhibitor and the method of application is important because application in similar quantities to the laboratory trials may not be applicable on a large scale.

3.4 Bacterial Inhibition

In the absence of bacterial activity, biotic oxidation of iron no longer takes place (Kleinmann, 1987) and the slower process of abiotic oxidation of pyrite begins to take over. Bacterial inhibition can be achieved by a variety of means, including adsorption of particulate material to the mineral surface, limiting oxygen supply, increasing ultra-violet light intensity, and application of chemicals including metals, organic acids, and anionic surfactants (Kleinmann, 1987). Many research groups have suggested that iron and

sulphur oxidizing bacteria may be inhibited by these methods in the field, thus retarding the production of AMD and further accumulation of acidity (Dugan & Lundgren, 1964; Dugan, 1975; Tuttle & Dugan, 1976; Tuttle, et al., 1977).

A. ferrooxidans is negatively affected by the presence of organic compounds, with a series of publications confirming the inhibition of *A. ferrooxidans* and related bacteria by organic substances having been produced (Leathen, et al., 1956; Silverman & Lundgren, 1959; Dugan & Lundgren, 1964; Duncan, et al., 1964; Tuttle & Dugan, 1976; Kleinmann & Erickson, 1983; Dugan, 1987a). Many of the compounds that prove to be inhibitory to the genus *ferrooxidans* are innocuous to other heterotrophic microorganisms (Tuttle & Dugan, 1976). Such compounds include various alpha-keto acids, carboxylic acids, benzoic acid, and sulphated anionic detergents (Dugan, 1987a). The inhibitory effects of the organic compounds on *A. ferrooxidans* are postulated to be related to the relative lipid solubility of the compounds, which in some cases, promotes the uncontrolled passage of protons through the cell envelope, disrupting the cell membrane and jeopardizing the biochemistry of the cell (Tuttle & Dugan, 1976).

Following the selection of a suitable compound, a method of application must be determined to maximize the interaction between the compound and the microbe population. For instance, application onto overburden or topsoil will limit contact and interaction between the organic substance and the microbe population present in the waste material (Kleinmann & Erickson, 1983). The success of chemical treatment for the inhibition of *A. ferrooxidans* depends on the toxicity of the compound to other living organisms, the economic availability of commercial quantities, the longevity of the compound in the environment and the suitability of the application method (Dugan & Lundgren, 1964; Tuttle, et al., 1968; Dugan, 1975; Tuttle & Dugan, 1976; Kleinmann, et al., 1981; Dugan & Apel, 1983; Onysko, et al., 1984).

Organic Acids

The extent that organic acids inhibit the growth of bacteria or inhibit iron oxidation mechanisms depends on the nature of the organism and the acid itself. Organic acids with functional groups that draw electrons away from the carboxyl group, such as alpha-keto acids or acids with adjacent benzene groups, have been

shown to have inhibitory effects greater than the simple hydroxyl acid analogs (Tuttle & Dugan, 1976). The overall inhibitory action of organic acids is related directly to their influence on the iron oxidizing system and ability to promote a disruption in the cell envelope, both processes will jeopardize the cell integrity and impede iron oxidation (Tuttle & Dugan, 1976). Further, Alexander, Leach, and Ingledew (1987), reported that organic acids may cross the bacterial cell membrane and accumulate in the cell causing a disruption to the cell potential.

Common plant and soil acids inhibit *A. ferrooxidans* activity and iron oxidation ability. Sasaki and colleagues (1996) investigated the response of the bacteria to various concentrations of fulvic, tannic, and oxalic acids. Their research showed that fulvic acid adsorbed to pyrite grains preventing access to the reaction site by the bacteria, thereby contributing to an overall decrease in ferrous iron oxidation rate. Limited pyrite oxidation by *A. ferrooxidans* in the presence of all three acids is postulated to occurred for two reasons: adsorption of the acid on the mineral surface, blocking access to the reactive mineral, and the formation of acid-ferric iron complexes, which render ferric iron unavailable to further participate in the abiotic oxidation of pyrite (Sasaki, et al., 1996). This study suggests that naturally formed humic substances in soil covers supporting plant life naturally produce inhibitory acids that may be useful in remediation approaches. Organically complexed iron is not expected to be accessible to *A. ferrooxidans* and other iron oxidizing bacteria, so ferrous-competing organic acids or acids that may precipitate as ferric salts limit the availability of iron bacteria, slowing the rate of biotic iron oxidation (Singh & Bhatnagar, 1988).

Tuttle and Dugan (1976) used batch studies to examine the iron oxidation inhibition abilities of twenty-three organic compounds, including carboxylic acids, metabolites, biochemical acids, and acids existing in natural environments. This study concluded that carboxylic acids have the greatest inhibitory effect of the organic molecules tested, with four methods being proposed to explain how organic molecules inhibit bacterial oxidation of ferrous iron (Tuttle & Dugan, 1976):

- Cause a disruption in the biochemical electron transport system;
- Complex or react with ferrous iron, rendering it inaccessible to the organism;
- Interfere with required nutrients such as phosphate or sulphate; or
- Cause disruption in the cell membrane, jeopardizing the health of the cell.

A series of controlled laboratory investigations by Onysko, Kleinmann, and Erickson (1984) and Singh and Bhatnagar (1988) further concluded that solutions of 0.10% of each benzoic acid, sodium benzoate, and sorbic acid effectively inhibited biotic oxidation of iron. Benzoic acid, a simple aromatic carboxylic acid, is present naturally in plants as a free molecule or bound benzoic acid esters. Widely used as a preservative in processed foods because of fungicidal properties and an ability to inhibit the growth of some moulds, yeast, and bacteria, benzoic acid is available in commercial quantities. The sodium salt of benzoic acid, sodium benzoate, is used in food preservation and has fungicidal properties rendering it capable of bacterial inhibition in low pH environments. Reaction of benzoic acid in water with sodium hydroxide yields the salt, sodium benzoate. Although sorbic acid is useful in food preservation to prevent the growth of mold, yeast, and fungi, the salts of sorbic acid do not have the same biocidal qualities as the acid. In the natural environment, sorbic acid is rather unstable and degrades quickly.

Benzoic acid, sodium benzoate, and sorbic acid have been shown to be capable of reducing biotic iron oxidation at low pH, but the compounds have shown more promise when used as fungicidal additives in combination with other compounds in the treatment of acid generating waste (Dugan & Apel, 1983; Dugan, 1987a). More commonly, benzoates are included in a treatment plan to prevent fungicidal degradation of more effective organic inhibitors (Dugan, et al., 1970b; Tuttle, et al., 1977; Dugan & Apel, 1983). Neutralization of acid waters treated with these organic acids results in the accumulation of organic and inorganic precipitates, including the ferric salts of benzoate and sorbate as a sludge or slurry (Dugan & Apel, 1983; Onysko, et al., 1984). Upon the return of acidic conditions, the ferric salts dissolve, reintroducing benzoic and sorbic acids to the environment to continue to inhibit fungi and yeasts, which degraded other organic compounds (Onysko, et al., 1984; Singh & Bhatnagar, 1988).

Flask-scale studies allow for observation of the effects of many different organic molecules in a small time-frame with limited materials. Onysko, Kleinmann, and Erickson (1984) used flask studies to assess the inhibitory effects to *A. ferrooxidans* of several organic compounds. Supplements of 5, 10, 25, or 50 mg L^{-1} of benzoic and sorbic acid were added to a series of parallel control and inoculated sample flasks containing modified TK media and ferrous iron. The study included monitoring of pH and ferrous iron concentration in order to determine if the rate of iron oxidation was increasing, constant, or decreasing. All acids suppressed the rate of bacterial oxidation of ferrous iron and the study concluded that benzoic and sorbic acids at concentrations greater than 10 mg L^{-1} inhibited biotic ferrous iron oxidation (Onysko, et al., 1984).

Organic Surfactants

Surfactants, commonly used as surface cleansers, are shown to a have great ability to inhibit bacteria at low pH conditions (Kleinmann & Erickson, 1983). The inhibitory action of surfactants is attributed to inducing damage to the cell membrane, resulting in a disruption of the barrier that protects the cell organelles from the environment to promote a leakage of cellular material from the cell or cell lysis (Tuttle & Dugan, 1976; Kleinmann, et al., 1981; Dugan, 1987a; Dugan, 1987b). *A. ferrooxidans* has a multi-layered cell wall that allows the cell to maintain a neutral internal fluid pH while existing in low pH environments. In low concentrations, surfactants are thought to alter pH sensitive enzymes in the cell wall, allowing uncontrolled seepage of protons into the cell causing a disruption of the proton gradient force driving iron oxidation, Figure 3.1. In these circumstances, the cell may continue to maintain itself, but the rate of iron oxidation will decrease (Hotchkiss, 1946; Hugo, 1965; Lundgren, et al., 1974; Dugan, 1975; Kleinmann & Crerar, 1979). At higher concentrations of surfactants, irreversible damage to the cell membrane occurs, completely destroying the barrier protecting the internal cell from the external environment. The inflow of highly acidic solution into the cell results in cell death (Hotchkiss, 1946; Shafa & Salton, 1960; Lundgren, et al., 1974; Dugan, 1975; Kleinmann & Crerar, 1979).

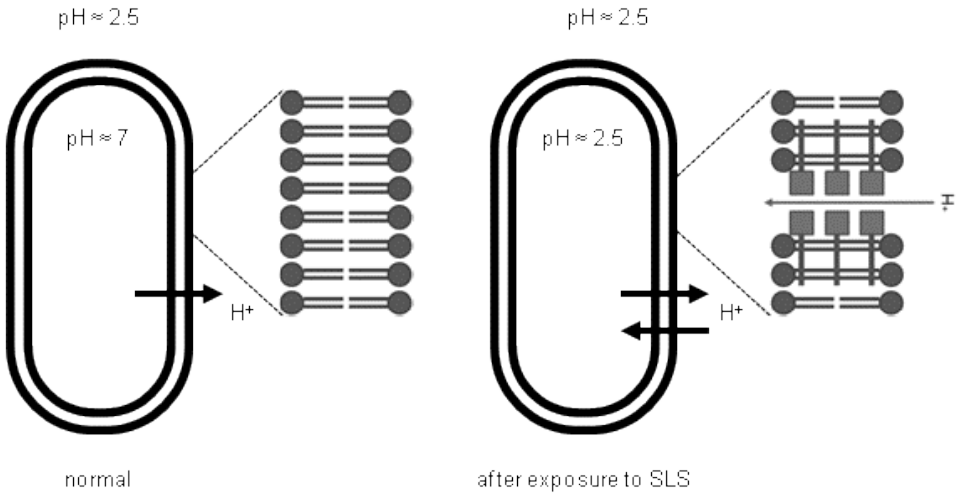

Figure 3.1 Normal cell (left) and disturbed cell after anionic surfactant treatment, allowing the uncontrolled passage of protons through the cell wall (right).

The most probable method of bacterial inhibition or loss of cellular integrity, as described previously, includes a disruption of the cellular membrane of the bacteria, resulting in the seepage of protons into the cell, creating hostile pH environments for the internal cell (Hotchkiss, 1946; Hugo, 1965). When cells lose their ability to oxidize iron, the biologically mediated generation of AMD slows and eventually stops. Surfactants are more aggressive at low pH, so in the event that significant concentrations of surfactants reach receiving waters, the elevated proton concentration of these waters will limit the bactericidal properties of the surfactant (Kleinmann & Erickson, 1983).

Organic surfactants that have bactericidal effects at concentrations as low as two mg L^{-1} at low pH include sodium lauryl sulphate (SLS), alkylbenzene sulphonate, and alpha olefin sulphonate (Dugan, 1975). Laboratory and pilot scale tests indicate that anionic surfactants have the potential to eliminate biotic pyrite oxidation by causing irreversible damage to the protective cell membranes of *A. ferrooxidans* (Kleinmann, et al., 1981; Kleinmann & Erickson, 1982). Organic surfactants are common ingredients employed in household cleansers to remove oils owing to their amphiphilic properties. Effective in low concentrations, SLS is a common ingredient for personal hygiene products, including shampoos, hand soaps, and body washes. SLS is biodegradable suggesting that, after a short time in the AMD environment, the surfactant will degrade before having any significant effect on the discharging water

(Kleinmann & Erickson, 1983). Biotic oxidation of iron contributing to the dissolution of sulphide minerals and AMD generation has been retarded or eliminated in the presence of SLS in both laboratory and field experiments (Dugan, 1975; Kleinmann & Crerar, 1979; Dugan & Apel, 1983). These properties make SLS a surfactant candidate worth further investigation of its bactericidal properties for AMD treatment and control.

Sodium lauryl sulphate was investigated as an inhibitor of biotic iron oxidation by Singh and Bhatnagar (1988) who applied concentrations up to 20 mg L^{-1}. An inhibitory effectiveness greater than 70% was reported when an application of greater than 10 mg L^{-1} was applied (Singh & Bhatnagar, 1988) and Onysko, Kleinmann, and Erikson (1984) reported that SLS efficiently inhibited biotic iron oxidation at concentrations as low at five mg L^{-1}. Although field studies have demonstrated the potential effectiveness of SLS at low concentrations (Kleinmann, 1980; Kleinmann & Erickson, 1982), the longevity of the treatment remains in question (Seidel, et al., 2000) as the biodegradable nature of the substance means that SLS does not remain in the environment for long periods of time. Various application methods have been considered to address the potential for the re-establishment of the bacterial population in the treated areas when SLS is eventually removed from the system, through either natural degradation or washout. Approaches include the periodic reapplication of SLS, sorption of the surfactant to the waste material surfaces, and incorporation of SLS into a slow release pellet (Kleinmann, 1980; Kleinmann, et al., 1981; Kleinmann & Erickson, 1982)

The longevity of SLS and other organic surfactants can be increased in the environment applied in combinations with organic acids that inhibit the growth of fungi, moulds, and yeasts, which may be actually responsible for the degradation of the surfactants (Dugan, et al., 1970a; Dugan, et al., 1970b; Tuttle, et al., 1977; Dugan & Apel, 1983). The combined application of surfactants and organic acids has been investigated by Dugan (1987a) who published findings linking increased longevity of SLS with the inclusion of sodium benzoate. Dugan (1987a) concluded that both substances are non-toxic to higher organisms, readily available, and rather inexpensive. With the combined application, biotic iron oxidation

in test waste piles was limited for a prolonged amount of time, warranting further investigation at a larger scale (Dugan, 1987a).

The method and frequency of application of inhibitor compounds is of significant interest. Kleinmann and Erikson (1983) identified that the application rate and method may differ between the experimental and field application phase. Compounds that inhibit bacterial oxidation at the laboratory level require special attention for use of the treatment in an uncontrolled environment. For example, rainfall events may wash out an inhibitory compound, or extreme environmental conditions may degrade the compound. The study by Kleinmann and Erikson (1983) assessed the application of SLS at a rate that would allow the compound to remain in the top 30 centimeters of the treatment area. The study provides the following reasons to support selection of the 30 cm treatment zone, with specific attention to application rate:

- Most oxidation takes place near the top of the waste pile and rates of oxidation will decrease with depth because penetration of the oxygen is depth limited;
- Compounds applied to the surface in small quantities at each application period would migrate further into the pile, but not far enough that they may completely percolate through; and
- Under-treatment, or application of quantities less than required, is preferred to prevent loss of compound to regional waterways.

For a duration of three to six months, a single application of 0.25% SLS applied at 5,000 L ha^{-1} was shown to effectively control the production of AMD after a single application, resulting in a reduction in acidity, sulphate, and iron concentration (Kleinmann, 1980; Kleinmann & Erickson, 1982). Bacterial inhibitors, such as SLS, provide a limited timescale in which oxidation by bacterial inhibition is successfully suppressed; continuous application is thus required to treat the waste material in the longer term (Evangelou, 1994; Harris & Lottermoser, 2006b).

To minimize the need for continual application, investigations of slow release inhibition materials are important because re-application would not be required. Testing at a pilot site-scale facility indicated that embedding SLS into a rubber pellet matrix allowed for a slower release of SLS to the treatment area, resulting in a prolonged suppression of bacterial activity and oxidation and successfully eliminated the need to reapply the treatment (Kleinmann, et al., 1981). Further, they demonstrated that the inclusion of SLS into a rubber pellet to promote the slow release of SLS with limited surfactant loss during rain fall, thereby potentially eliminating the need for reapplication following precipitation events. The initial field studies by Klinmann and colleagues (1981) found that acid production related to biotic oxidation of iron was inhibited for a time of only three to six months, thus requiring application a few times a year to ensure that biotic oxidation remained under control. Incorporation of SLS into slow release rubber pellets provided a reported 95% decrease in acid production after one year. A five year study by the same authors treated the area with slow-release SLS pellets in combination with a soil cover, reporting that the activity of *A. ferrooxidans* remained inhibited during the study period resulting from the combined effects of slow release SLS pellets with oxygen ingress limitation because of the soil cover (Kleinmann, et al., 1981). The establishment of vegetation of the cover further limited water flow to the underlying waste pile.

3.5 Passivation

A mineralogical approach to AMD control aims to prevent mineral dissolution and acid production at the source, either with the removal of the reactive mineral from the system or by rendering the reactive mineral inert. Only leaching to the point of complete dissolution or depletion will completely remove the reactive mineral. Chelating and precipitation methods to produce coatings on the surface of the reactive mineral can, however, effectively block oxygen transport to the mineral surface, thereby pacifying the reactive mineral and rendering it inaccessible to further oxidation (Evangelou, 1994). Natural pacification happens with the buildup of secondary mineral phases on the mineral surface. Organic or inorganic substances can also increase the extent of passivation. Although mineralogical-based approaches to AMD mitigation considers the future mineral dissolution and acid production, the current state of the site may

still require immediate or ongoing attention and additional treatments in the future to manage released acidity and dissolved elemental concentrations.

Exhaustion

Optimization of the bioleaching process with respect to particle size, aeration, moisture, and bacterial culture can leach all reactive sulphidic minerals from the material, theoretically. In reality, the ability to achieve and economically apply fully optimized leaching conditions also promotes the formation of natural coatings on the mineral surface, limiting the further oxidation of the material. Natural coatings that may form include elemental sulphur and metal hydroxides (Stott, et al., 2000). In practice, leaching rates decline over time, indicating that either the quantity or surface area of reactive minerals has decreased (Hackl, et al., 1995). The removal of natural coatings increases the reactive surface area, allowing further oxidation to take place.

Stott and colleges examined the potential for exhaustion of reactive chalcopyrite (Stott, et al., 2000). The rate of copper leaching slowed over time, owing to a buildup of secondary phase precipitation over the reactive mineral surface. The study employed a suite of iron-reducing microorganisms, *Sulfobacillus thermosulfidoxxidans*, *S. acidophilus*, and *Acidimicrobium ferrooxidans*, together with a consortia of iron-oxidizers to reduce insoluble precipitates. A cycle of microbial-driven oxidation-reduction reactions allowed the bio-oxidation of the minerals and bio-reduction of insoluble precipitates, which expose the mineral surface and allow continued bio-oxidation of the reactive mineral phases. The exhaustion of the reactive iron sulphide may not suitable for large-scale operation owing to the significant costs involved to provide fully segregated waste process materials.

Encapsulation

Encapsulation considers the hypothesis that the inhibition of biological oxidation of a reactive mineral surface, such as pyrite, can only by induced for the long-term by a surface coating directly on the reactive mineral (Evangelou, 2001). Whereas some approaches to prepare for site decommissioning aim to prevent oxidation of the reactive metal sulphide by providing a cover in an attempt to block oxygen diffusion to

the entire treatment area, encapsulation aims to treat each mineral grain, or waste rock particle, individually with the application of a coating directly on the mineral surface (Belzile, et al., 1997). Reactive metal sulphides may be encapsulated by forming thin coatings on the surface of the minerals preventing oxygen diffusion and subsequent mineral dissolution (Evangelou & Zhang, 1995; Chen, et al., 1999). Encapsulation of the sulphide mineral with an oxygen-impermeable ferric iron coating, either naturally produced or induced, provides long-term protection from chemical and microbiological oxidation (Harris & Lottermoser, 2006b). The use of ferric iron as a base for a pacifying coating has two beneficial outcomes: the formation of a pacifying coating and the removal of ferric iron from the cyclic oxidation reaction of the metal sulphide (Evangelou, 1994). Owing to the stable nature of induced coatings, Evangelou (2001) hypothesized that a coating on the reactive mineral surface is the only treatment that can be expected to completely control oxidation, acid generation, and mineral dissolution long term.

Natural Coatings

The deposition of natural encapsulating coatings on the mineral surface explains the decrease in dissolution rate over time as the surfaces of the reactive minerals become protected from oxidation (Hackl, et al., 1995). Secondary coatings resulting from the biogeochemical mineral dissolution of ferrous sulphide minerals are classified in three categories:

- Elemental sulphur deposition from the oxidation of sulphide;
- Polysulphidic layer generation; and
- Fe-(hydr)oxide secondary minerals, precipitation from the oxidation of iron.

These three layers can inhibit bacterial oxidation and elemental dissolution with coating thickness as little as 1 µm (Hackl, et al., 1995; Stott, et al., 2000). Environmental controls, such as pH, influence the formation of natural coatings. For instance, the deposition of iron-hydroxide coatings on pyrite mineral

surfaces takes place when materials are leached in a solution of near-neutral pH (Huminicki & Rimstidt, 2009).

Natural coatings engineered to encapsulate a reactive mineral may be more sensitive to change in pH and oxidizing potential, requiring long term site attention and effluent monitoring to ensure that the environmental conditions promoting stability of the coatings are maintained. A study completed by Huminicki and Rimstidt (2009) predicts, that to naturally encapsulate the reactive material in a waste pile in perpetuity, an alkaline source would need to be applied for several decades, similar to neutralization by alkali addition, to ensure that the encapsulation is stable enough to remain insoluble in local meteoric or percolating waters. Upon successful, stable encapsulation of the reactive phase, additional alkali input will not be further required.

Induced Inorganic Coatings

Leaching iron sulphides in the presence of an oxidant, buffer, and an inorganic salt can produce inorganic coatings on the reactive minerals (Evangelou, 2001; Harris & Lottermoser, 2006b). The presence of an oxidant is important because free ferric iron must be available to react with the inorganic compounds, with a buffer being required to maintain pH in the stability field of the coating (Evangelou, 2001). Waste material that has not been subjected to oxidation requires the addition of an oxidant, such as hydrogen peroxide, whereas material that has been oxidized naturally may have enough ferric iron liberated to establish the coating. Sulphide minerals with ferric (hydr)oxide coatings have been shown to be successfully protected from oxygen ingress and further oxidation (Fytas, et al., 1999; Evangelou, 2001).

The oxidation of pyrite in the presence of phosphate can induce the precipitation of an insoluble iron phosphate coating on the pyritic surface which is, in turn, capable of inhibiting further oxidation of the pyrite and associated acid generation and mineral dissolution (Evangelou, 1994; Fytas & Evangelou, 1998; Harris & Lottermoser, 2006b). Depending on the degree of saturation of the solution with respect to iron phosphate, either a discrete phase will precipitate, forming a porous coating network on the pyrite

surface. When the degree of saturation is low, iron phosphate may only form discrete islands, whereas a high degree of saturation results in a slower rate of pyritic oxidation and the deposition of an insoluble iron phosphate layer or film on the pyritic surfaces (Evangelou, 1994). Leaching pyrite in a phosphate solution in the presence of a strong oxidant promotes the formation of a ferric iron–rich surface, which will react with phosphate to form an insoluble ferric-phosphate coating rendering the pyrite below the mineral surface protected from further oxidation, described by Reaction 3.4 (Evangelou, 1994). Stabilization of phosphate coatings may be achieved by the use of a pH buffer, such as sodium acetate (Fytas & Evangelou, 1998; Evangelou, 2001; Harris & Lottermoser, 2006a; Harris & Lottermoser, 2006b).

Reaction 3.4 $$FeS_{2(s)} + H_2PO_4^- + \frac{15}{2}H_2O_2 \rightarrow FePO_{4(s)} + 2SO_4^{2-} + 3H^+ + 7H_2O$$

Laboratory studies more commonly investigate the process of coating deposition on a fresh, un-weathered mineral sample, free of any natural oxidation product coating. Strong acid sample preconditioning may even be used to remove oxidation coatings already existing on the mineral sample. Studies that do not employ a preconditioning phase, however, may better represent the coating application process on a more natural sample of the type expected for heap-leach pads. The addition of an oxidant may not be required in all cases because after bioleaching an abundance of ferric iron is already present in the environment.

The main component of a phosphate salt coating solution is typically potassium dihydrogen phosphate, KH_2PO_4, a soluble salt found in commercial fertilizer, food additives, and fungicides. A strong oxidizer and a buffer, typical hydrogen peroxide and sodium acetate, respectively, are used in laboratory testing to assist in the coating process. The concentration of the oxidant, phosphate salt, and buffer are dependent on the state of the sample, sample size, and experimental design. Evangelou (1994) demonstrated that a coating, 250 µm thick, could be established on pyrite shale samples, with a coating solution of 0.01 M KH_2PO_4 and 0.147 M H_2O_2, whereas more concentrated phosphate solutions were necessary to generate coatings for grain sizes between two and 10 mm (Harris & Lottermoser, 2006b). The coating solutions

may also contain background chemicals to mediate selected processes. Ethylenediaminetetraacetic acid (EDTA) has been used in control studies to complex free ferric iron to allow comparisons amongst uncoated samples, coated samples and samples which have had free iron complexed and unavailable for reaction with phosphates (Evangelou, 1994; Evangelou, 2001). A saturated solution of calcium hydroxide ($Ca(OH)_2$) may be percolated over the coated particles to form calcium phosphate complexes on pyrite or ferrous-phosphate surfaces, thus increasing the ability of the phosphate coating to protect form further oxidation (Evangelou & Zhang, 1995; Georgopoulou, et al., 1995). The four areas of the coating process, as applied in previous laboratory studies, include preconditioning, coating, background chemicals, and stabilizers, addressed in coating formation studies are summarized in Table 3.3.

Table 3.3 Compositions for investigated phosphate coatings including mineral precondition and coating stabilizing.

Preconditioning (M)		Coating (M)				Reference
HCl	HF	H_2O_2	KH_2PO_4	NaAc	NaCl	
	4	0.147			0.1	Evangelou (1994)
	4	0.147			0.1	
	4	0.147	0.01		0.1	
2		0.0 to 0.4	0.01 to 0.2	0.02 to 0.2		Georgopoulou et al. (1995)
2		0.01	0.2, 0.3	0.2		
1		0.01	0.2	0.2		Fytas and Evangelou (1998)
1		0.01	0.4	0.2		
1		0.1	0.4	0.2		
1		0.2	0.2	0.2		
2		0.106	0.001		0.01	Evangelou (2001)
2		0.106	0.001	0.01		
2		0.106			0.01	
2		0.106		0.01		
2		0.106		0.01		
		0.035	0.02	0.01		
1		0.01	0.2	0.2		Harris and Lottermoser (2006b)
1		0.01	0.4	0.2		
1		0.1	0.4	0.2		
1		0.2	0.2	0.2		
		0.01	0.2	0.2		
		0.01	0.4	0.2		
		0.1	0.4	0.2		
		0.2	0.2	0.2		

Many published studies follow or reference the methodology proposed by Evangaelou and Fytas (Evangelou, 1994; Fytas & Evangelou, 1998). In laboratory studies, mineral samples had been acid washed to remove any existing coatings. Leaching in the presence of the coating solution deposits the coating before the coating stabilization or maturation phase. To test the coating resistance to oxidation, coated samples are subjected to oxidizing conditions to predict long-term stability. Using two scales, small column and a large column, Georgopoulou investigated iron-phosphate coating deposition on pyrrhotite minerals, obtaining results consistent with previous studies investigating iron-phosphate

coatings on pyrite samples, and completing further experiments to assess the potential of applying the coating for long-term protection alone or in combination with other AMD mitigation methods (Georgopoulou, et al., 1995).

Fytas and Evangelou (1998) reported that a pH range between 5 and 6 produced the most stable coating on un-oxidized tailing samples. More recent studies from Evangelou used large columns and coarse grain pyrite mineral samples and samples of pyritic coal waste to evaluate the long-term ability of the coating to prevent acid production (Evangelou, 2001). The study compared the use of rock phosphate instead of K_2HPO_4 in coating solutions, but there were no clear differences in the nature of final coatings. The study also investigated the incorporation of limestone in the solutions because of the potentially beneficial acid consuming properties of limestone. This study hypothesized that limestone would increase the pH, aiding in the stabilization of the coating, but the release of excess sulphate from columns treated with limestone indicated that oxidation continued to take place. Iron-phosphate coatings on partly oxidized, polymineralic waste rocks have also been investigated by Harris and Lottermoser (2006b) using samples which may better represent the mineral state at a mine site. The coatings established on the polymineralic mine waste, successfully decreasing acid production. The study also found that the concentration of the oxidant, H_2O_2, was the most significant factor in controlling the development of iron-phosphate because, in the absence of a strong oxidant, ferric iron cannot be liberated to react with phosphate to form the coating. Although the studies varied in particle size, mineral source and purity, preconditioning and stabilization steps, and coating compositions, there is general agreement that the establishment of iron-phosphate coatings on the minerals when the coating solutions contain a strong oxidant, moderate amount of KH_2PO_4, and a buffer maintains a pH between 5 and 7.

Similar to phosphate coatings, the deposition of silicate coatings takes place in the presence of a strong oxidant and a buffer to control the pH level. Strong oxidants better oxidize exposed pyrite minerals, releasing ferrous iron, which is then oxidized to ferric iron, which will precipitate on the surface of the pyrite as ferric hydroxides at pH levels above four. In the presence of metal hydroxides, silica will

precipitate on the surface of the metal hydroxide and, in the case of pyrite minerals, once ferric iron is liberated a siliceous ferric hydroxide barrier has the potential to form across the surface of the mineral through oxidation, Reaction 3.5 (Evangelou, 1996). Since silica polymerization and precipitation is easily controllable by changing the silica concentration, temperature, and pH, silica coatings offer tunable application methods which are more acid resistant than phosphate coatings produced with similar methods (Zang & Evangelou, 1998; Fytas, et al., 1999; Bessho, et al., 2011). A ferric hydroxide-silica coating would be expected to reduce pyrite oxidation rates by preventing further oxidation of the pyrite and acting as a sink for free ferric iron (Vandiviere & Evangelou, 1998).

Reaction 3.5

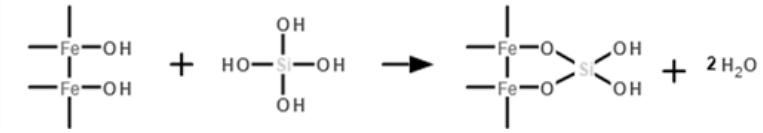

Evanglou (1996) patented a technology for an oxidation-proof silica surface coating on iron sulphides (US Patent 5494703). Pyrite was leached in the presence of a coating solution of water, an oxidizing agent (0.6% by weight), silica coating agent (sodium metasilicate, $1.8x10^{-3}$ mol L^{-1}), and a buffer to maintain a pH range between 4 and 6 (Evangelou, 1996). A strong oxidizer liberates ferric iron and a buffer controls the pH during the coating process. Research after the release of the patent investigated the significance of preconditioning the material, the use of different oxidants, and application of a coating at different concentrations of Na_2SiO_2 as well as a coating in the absence of a buffer.

The methods employed to apply silica coatings are quite similar to those for phosphate coatings. Preconditioning by leaching altered materials with a strong acid removes existing coatings and the incorporation of sand and limestone into the sample mixture increases hydraulic conductivity and pH to encourage ferric hydroxide precipitation (Zang & Evangelou, 1998; Fytas, et al., 1999). Silica and phosphate approaches to coating pyrite minerals consistently use hydrogen peroxide as a strong oxidant in coating experiments. Vandivere and Evangelou (1998) explored the application of calcium hypochlorite ($Ca(OCl)_2$) instead, noting that hydrogen peroxide may be too harsh to apply to actual environmental

sites, indicating that a different oxidant with less potential negative effects should be explored. Exploration of a milder oxidant for coating applications on pyritic material warrants exploration because the integrity of the coatings produced was not impacted with use of an alternative oxidant. The concentration of silicate is inconsistent throughout the reported literature, although higher concentrations were applied when mineral samples with a larger average grain sized was used (Fytas, et al., 1999), with lower concentrations being investigated for fine grained mineral samples (Zang & Evangelou, 1998; Kargbo & Chatterjee, 2005). A study carried out by Bessho et al. (2011) using 50 µm pyrite tailing samples established ferric hydroxide-silica coatings using solutions with silica concentrations between 2500 and 5000 mg L^{-1}, with coatings failing to form using solutions with silica concentrations below 2500 mg L^{-1}. The four areas of the coating process that are addressed in coating formation studies are summarized in Table 3.4. The use of background NaCl was limited in silica coating experiments and its involvement is negligible (Zang & Evangelou, 1998; Kargbo & Chatterjee, 2005).

Table 3.4 Compositions for investigated silicate coatings including mineral precondition and coating stabilizing.

Preconditioning (M)			Coating (M)				Reference
HCl	HF	Limestone (kg)	H_2O_2	$Ca(OCl)_2$	Na_2SiO_3	NaAc	
2	2		0.145		0.0018	0.01	Zang and Evangelou (1998)
2	2		0.145		0.0018		
2	2		0.145		0.0018	0.01	
			0.4375		0.02	0.1	Fyates and Bousquet (1999)
					0.1	0.01	
					0.1	0.01	
			0.01		0.11		
		0.03			0.11		
		0.01			0.11		
		0.01			0.11		
		0.01			0.125		
		0.01			0.125		
		0.01			0.14		
		0.01			0.14		
2			0.145		0.0018	0.01	Kargbo and Chatterjee (2005)
2			0.145		0	0	
2			0.145		0.018	0.01	

The parameters of coatings solutions mineral state and purity vary in the reported literature, but there is agreement that the formation of ferric hydroxide-silica barriers is a promising approach for the abatement of AMD generation by pyrite tailings or waste material (Fytas, et al., 1999; Kargbo & Chatterjee, 2005). There is consensus that further studies to evaluate the stability of silica coatings over time are required (Zang & Evangelou, 1998).

Laboratory studies subjecting coated mineral samples and uncoated controls to oxidative environments after coating deposition can assess the potential long-term stability of phosphate- and silica-based coatings. The extent of oxidation, or lack thereof, is determined by monitoring chemical parameters associated with the oxidation of ferrous sulphide minerals; pH, oxidation potential, total iron, and ferric and/or ferrous iron concentration. Previous studies employ an oxidation resistance testing procedure,

leaching coated and uncoated samples (either fresh mineral material or samples where the deposited coating has been removed) with 0.01 to 0.20 M hydrogen peroxide (Evangelou, 1994; Georgopoulou, et al., 1995; Fytas & Evangelou, 1998; Zang & Evangelou, 1998; Fytas, et al., 1999; Khummalai & Boonamnuayvitaya, 2005; Harris & Lottermoser, 2006b). Hydrogen peroxide is used for oxidation resistance tests because a strong chemical oxidant provides feedback information on the oxidation resistance of the material in a shorter timeframe when compared with natural chemical or biological oxidation. Only a few studies have incorporated an investigation of the resistance of the coatings to biological oxidation over a longer length of time (Vandiviere & Evangelou, 1998; Khummalai & Boonamnuayvitaya, 2005). The introduction of iron oxidizing bacteria to the coated particles under conditions ideal for maximum bacterial activity determines the potential resistance of the coating to biotic oxidation. Although there were no significant differences in the overall results of the studies that compared chemical and biological oxidation resistance of coatings, biological studies are important because these conditions mimic conditions at either active or abandoned coal, gold and/or base-metal mine sites.

Field scale testing has been limited for both phosphate and silica coatings. Vandiviere and Evangelou (1998) tested the durability of the phosphate and silicate coatings in natural environmental conditions using large leaching columns in a field-environment for four to seven months. For field application, $Ca(OCl)_2$ was used as the oxidant and limestone was applied to some columns to compare the effects of lime treatment alone and in combination on either phosphate or silica coatings, Table 3.5. The results of the study, including coating application and oxidation resistance testing (chemical and biological) showed that, after nineteen months in the field, the coating methods investigated successfully reduced further oxidation of pyritic mine wastes and that the best oxidation resistance was observed when the treatment included silica coatings (Vandiviere & Evangelou, 1998).

Table 3.5 Limestone treatment and silica and phosphate coatings on pyrite mine waste samples applied to outdoor leaching columns (Vandiviere & Evangelou, 1998).

Preconditioning (M)		Coating (M)		
Limestone (kg)	$Ca(OCl)_2$ (g)	KH_2PO_4	Na_2SiO_3	NaAc
.80				
.80	0.15			
.80	0.15			0.1
.80	0.15	0.01		0.1
.80	0.15		0.005	0.1
	0.15	0.001		0.1
	0.15	0.01		0.1
	0.15	0.1		0.1
	0.15		0.001	0.1
	0.15		0.005	0.1
	0.15		0.01	0.1

Research observations for formation and stability of inorganic coatings is generally limited to examination on fresh iron sulphides or iron sulphide wastes, indicating a critical knowledge gap exists understanding of the impacts of the application of these coatings to weathered waste materials. Surface oxidation with the use of a strong oxidation to produce ferric iron, such as hydrogen peroxide, is required to initiate the coating process on fresh or non-oxidized material (Elsetinow, et al., 2003; Khummalai & Boonamnuayvitaya, 2005). In reality, the application of hydrogen peroxide as part of a large scale decommissioning program may not be feasible, although not impossible (Elsetinow, et al., 2003).

3.6 Conclusions

The Environmental Code of Practice for Mines and the MMER outlines the best practices and effluent concentration controls required of the mining industry in Canada. Under these codes and regulations, the plans for the development of bioleaching pads at the Eco Ridge site, Elliot Lake, Ontario, also require development of a detailed decommissioning and closure plan which addresses the potential and management of AMD and associated metal and radionuclide release to environment. Development of a detailed understanding of the biogeochemical mineral dissolution process provides knowledge that may

be used to perturb, interrupt, prevent, or halt the bioleaching process, allowing a passive approached to be applied to prepare the site for full decommissioning,

The application of a bacterial inhibition solution by SLS application reportedly decreases the biogeochemical mineral dissolution reaction rates, thus limiting acid production and subsequently metal dissolution. Passivation by application of di-hydrogen orthophosphate or sodium metasilicate coating solutions has also been shown to promote the formation of a barrier phase between the metal sulphide and the oxidizing environment, which may prevent oxidation of the sulphide and hinder the ongoing biogeochemical mineral dissolution process. Investigations of varying scale, from laboratory to field application, may demonstrate the suitability of each method for the Eco Ridge site. Laboratory investigations based on the application of inorganic coatings using ferric iron generated by oxidation of ferrous sulphides through the biogeochemical mineral dissolution process requires further detailed investigation.

CHAPTER 4

4 Experimental Approach & Methods of Analysis

4.1 Material

The Eco Ridge Mine Rare Earths and Uranium Project site (Eco Ridge), owned by Pele Mountain Resources Incorporated (PMR), is located 11 km east of Elliot Lake, Ontario as shown in Figure 4.1. The region has a rich history in uranium (U) mining, with 12 mines operating between 1955 and 1996.

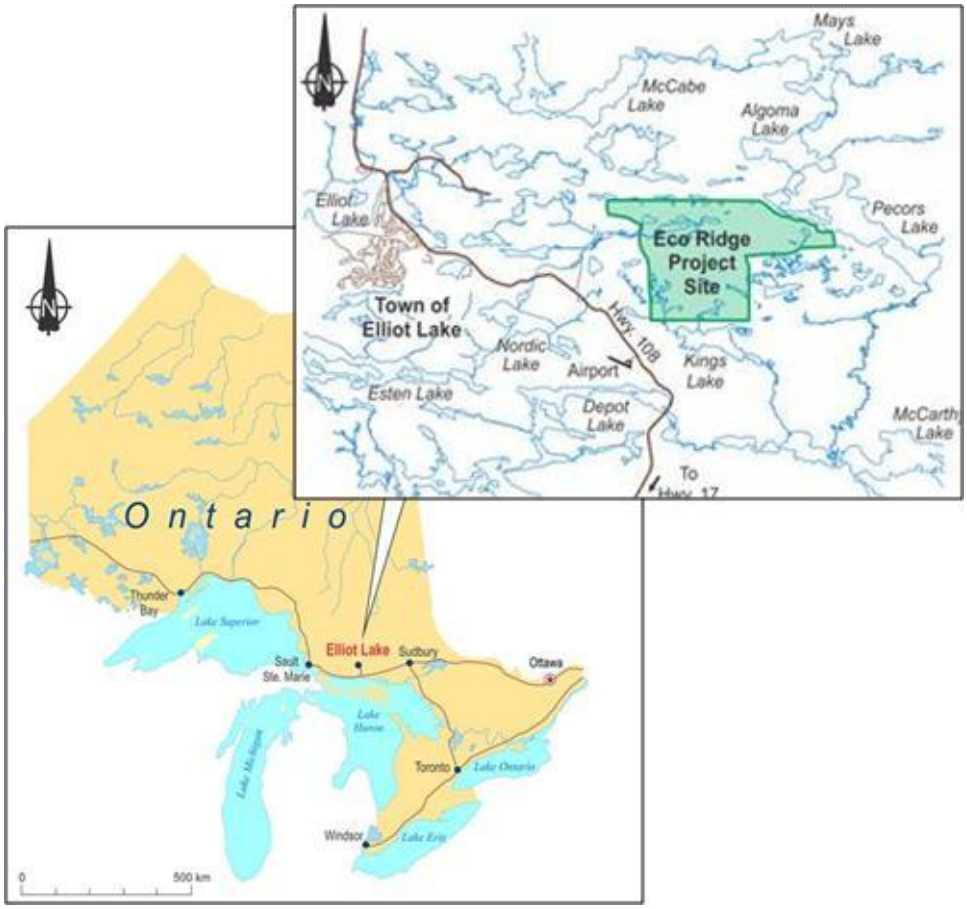

Figure 4.1 Location of Eco Ridge Mine Rare Earths and Uranium Project, east of Elliot Lake, Ontario (provided by PMR Ltd. 2013).

Drill core samples from Eco Ridge, approximately 500 kg, were collected by PMR in the spring of 2009 and provided to Laurentian University for the purpose of this thesis research. The outcrop of the quartz-pebble conglomerate bed at the EcoRidge sampling location is illustrated in Figure 4.2.

Figure 4.2 Quartz-pebble conglomerate outcrop, Eco Ridge Mine Rare Earths and Uranium Project site, Elliot Lake, Ontario.

The equipment used to crush, grind and subsample the mineral material is shown in Figure 4.3. The drill core was crushed with a large mouth jaw crusher (Patterson, a subsidiary of the Gorman-Rupp) to 2 to 4 cm and homogenized in a large tumbler. Approximately 15 kg was sub-sampled and crushed with a small crusher (RockLabs) to 1 to 2 mm , with a final sub-sample, approximately 5 kg, being ground to 74µm using an agate ball mill. The representative sub-samples were collected using a riffle splitter.

Figure 4.3 Drill core was crushed with a large mouth jaw crusher (a) to 2 to 4 cm (b), homogenized in a large tumbler (c), sub-sampled (d) and crushed with a small crusher (e) to 1 to 2 mm (e), sub-sample (g), and found ground using an agate ball mill (h) to 74µm (i).

The conglomerate beds at Eco Ridge are composed of 60 to 70% quartz, 10 to 20% orthoclase, 5 to 15% pyrite, 3 to 9% muscovite, and less than 1% U-, Thorium (Th)- and rare earth element (REE)-bearing minerals including Th-uraninite, monazite, and brannerite (Sylvester, 2007). The principal U, Th, and REE bearing minerals identified by electron probe micro-analyzer (EMPA) and optical mineralogy studies of mineral material collected from the same geological region of the study site by Sylvester (2007) and Spasford et al. (2012) are listed in Table 4.1.

Table 4.1 Principal minerals carrying U, Th, and REEs is Elliot Lake area conglomerate identified by Sylvester (2007) and Sapsford (2012).

Mineral Phase	Chemical Formula
Primary phases	
Th-enriched uraninite	UO_2
Monazite (Th rich)	(Ce, La, Y)PO_4
Thorite	(Th, U)SiO_4
Allanite	(Ca,REE)$Al_2Fe(SiO_4)(Si2O_7)O(OH)$
Secondary alteration phases	
Coffinite	$U(SiO_4)_{1-x}(OH)_{4x}$
Brannerite	UTi_2O_6
Uraninite	(Th, REE poor)UO_2
Florencite	$(REE)A1_3(PO_4)(OH)_6$
Xenotime	YPO_4
Uraniferous rutile or leucoxene	UO_2–Rutile
Silicified monazite	Mz-Silicate
Very fine-grained intergrowth of pitchblende, pyrite and aluminium-rich silicate phase	UO_2–Pyr–AlSi-mix
Uraniferous pyrite	UO_2–Pyrite

Solid Phase Analysis

Mineral characterization work by X-ray diffraction (XRD) of fresh, ground material (74 µm), presented in Figure 4.4, identifies quartz, feldspar, pyrite, and mica as the principal components of the mineral matrix of the ore material.

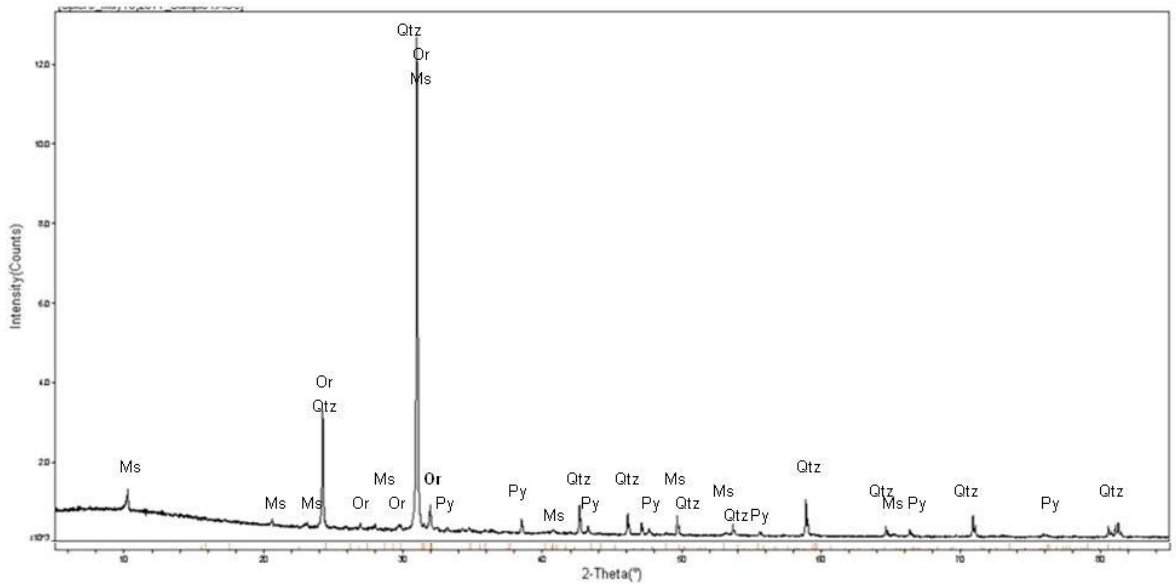

Figure 4.4 Powder x-ray diffraction pattern of the quartz-pebble conglomerate fresh material (74 µm) identifying (Qtz), feldspar (orthoclase, Or),pyrite (Py), and mica (muscovite, Ms) as the principal components.

The content of elements of economic interest and environmental significance was determined b-y ICP-MS analysis after multi-acid digestion, summarized in Table 4.2. Representative samples of the whole ore were obtained following tumbling to homogenize, with use of a riffle splitter. The large standard deviations obtained for the concentrations of some elements in the replicate samples suggest large variation in the distribution of heavy minerals within the ore material.

Table 4.2 Elemental composition of head grade quartz-pebble conglomerate ore ± standard deviations, in parenthesis (n=13).

Element	Concentration (mg kg^{-1})	
Economic Interest		
Sc	3	(0.5)
Y	50	(9)
La	300	(50)
Ce	590	(100)
Pr	53	(8)
Nd	180	(30)
Sm	30	(4)
Eu	1.79	(0.2)
Gd	30	(4)
Tb	2.7	(0.4)
Dy	11	(2)
Ho	1.8	(0.4)
Er	4.2	(0.9)
Tm	0.55	(0.1)
Yb	3.4	(0.7)
Lu	0.46	(0.09)
Th	340	(70)
U	310	(100)
Environmental Significance		
Ti	3400	(300)
Fe	23000	(9000)
Ni	20	(4)
Cu	78	(20)
Zn	24	(5)
As	13	(3)
Pb	68	(10)

4.2 Inoculum

The D7 strain of *Acidithiobacillus ferrooxidans* was provided by the laboratory of Dr. L. Leduc, Department of Biology, Laurentian University, Sudbury, Ontario in April 2009 (Leduc & Ferroni, 1994; Leduc & Ferroni, 2002). This strain is indigenous to the study area and was originally isolated by the Leduc research group from Denison Mines Ltd. in Elliot Lake, Ontario, as part of a study to characterize

the microbial population responsible for the biogeochemical mineral dissolution process at the mine site (Wadden & Gallant, 1985; Leduc & Ferroni, 1994). Within this thesis, the D7 strain of *A. ferrooxidans* is referred to as the 'pure strain'.

A modified TK nutrient solution was prepared by mixing four parts nutrient solution (Solution A) and one part ferrous iron solution (Solution B), with adjustment of pH to 2.5 using sulfuric acid, Table 4.3 (Tuovinen & Kelly, 1974). Solution A was sterilized by autoclave for 15 minutes at 121°C and Solution B was filtered under vacuum. Both solutions were prepared using distilled deionized water (DDI). A broth culture was prepared with a 1:40 inoculation with 200 mL of modified TK media in a 250 mL Erlenmeyer flask. The broth culture matured for two days at 30°C on an enclosed bench top shaker, with an agitation rate of 150 rotations per min (RPM) (McCready, 1988).

Table 4.3 Chemical composition of TK nutrient media solution (Tuovinen & Kelly, 1974).

Nutrient Salt	Concentration (g L^{-1})
Solution A	
KH_2PO_4	0.4
$MgSO_4$	0.4
$(NH_4)_2SO_4$	0.4
Solution B	
$Fe(SO_4)_2.7H_20$	167

A microbe population representative of that expected at Eco Ridge was cultured from water samples collected from the former tailings catchment area of Stanrock Mine and provided to the researchers by Pele Mountain Resources, April, 2010. The samples (5 ml each), collected from Dam A head pond and from the seepage from Dam A, were added to 200 mL of modified TK media in a 250 mL Erlenmeyer flask (Tuovinen & Kelly, 1974). A mature broth culture was successfully cultivated for each water source and used in a similar manner as the pure strain for the ensuing study. In this thesis the environmental sample of microbes is referred to as the 'environmental consortium'.

4.3 Experimental Approach

Prior to field trials and full-scale operations, assessment studies are carried out to confirm that the bioleaching methodology and approach to decommissioning may be successful and the elements of interest are recoverable from the parent material, with the potential to control and modify the leaching process when required. Thus, parameters influencing bioleaching and passive approaches to prepare for decommissioning are investigated through the following series of scaled experiments in the laboratory:

- Extraction flasks are used over short time frames to investigate many parameters using minimum amounts of materials;
- Small leaching column assessments investigate the application approach for the leaching and/or decommissioning options and provide details for particular leaching characteristics that may be controlled at the field level; and
- Large leaching columns in the laboratory or columns located on-site are used to reinforce findings from the previous stages and confirm the application of the selected methods at a close-to operational scale.

Simple schematics describing the extraction flasks and leaching column set up employed are shown in Figure 4.5.

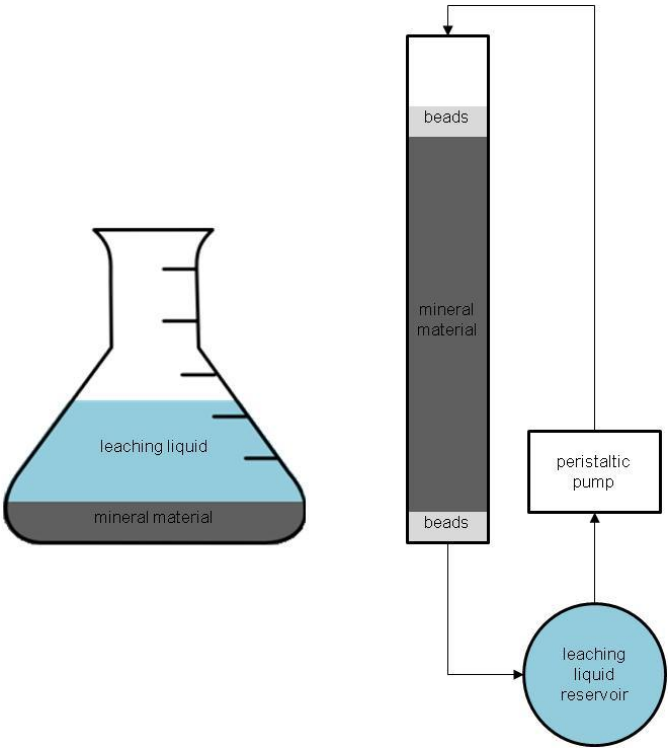

Figure 4.5 Model of extraction flasks (left) and leaching columns (right) used in all phases of the study.

The influence of individual parameters can be controlled or manipulated in small laboratory experiments to determine the overall affect of the parameter(s) on the leaching process. Experimental planning was based on the review of laboratory-scale experiments for bioleaching and passive approaches to prepare for decommissioning define a base of parameters to guide bioleaching trials for an assessment of the conditions suitable for surface heap leaching and decommissioning at Eco Ridge (see Chapters 2 and 3).

4.4 Leaching Methods

Leaching methods have been designed to investigate parameters known to encourage bacterial oxidation of ferrous sulphide minerals and to optimize the U extraction from ore samples from the Eco Ridge site. These methods may subsequently be applied to surface heap-leach pads. Reported optimum leaching conditions and methods have guided the experimental design for laboratory scale assessment except where noted otherwise.

Extraction Flasks

Homogenized mineral material was sterilized by heating 7.5 gram samples in 250 mL Erlenmeyer flasks to 200°C for 24 hours in a laboratory oven to allow for complete microbial control during the experiment (Trevors, 1996). Each sample flask was closed using aluminium caps to prevent contamination of the sample. After sterilization, 150 mL of sterile nutrient solution, TK solution A, was added to each flask. TK solution B is not added to extraction flasks because the iron source is already present in the mineral material. The ore-solution mixture was inoculated with 5 mL of prepared *A. ferrooxidans* broth culture, estimated to contain $2.4x10^{7}$ cells mL^{-1}. The flasks were agitated using an enclosed bench-top shaker at a rate of 150 RPM at 30°C under ambient lighting conditions for 10 weeks (Figure 4.6).

Figure 4.6 Laboratory set up for leaching experimental using extraction flasks with aluminium caps in an enclosed bench-top shaker.

Treatments were designed to compare controlled conditions with possible industrial application conditions. Variances of inoculum type, material sterilization, and leaching solution composition have been investigated. The D7 strain of *A. ferrooxidans* represented controlled conditions and a culture isolated from the Stanrock Dam in Elliot Lake represented industrial application conditions. Some mineral samples were not sterilized and various compositions of nutrient solutions were compared with

DDI water. Variation of inoculum type, material sterilization, and solution parameters were replicated in triplicate flasks to assess the effect of the parameters on the release of U, REEs, and other elements, which may affect decommissioning conditions from the mineralized material (Table 4.4). After the first 24 hours, extraction flasks were inoculated with 5 mL of the specified inoculum from prepared broth cultures. Non-inoculated controls are compared with each inoculated treatment depending on material treatment and solution selected.

Table 4.4 Extraction flask leaching treatments (n=3).

Parameter	1[a]	2	3[b]	4[a]	5[a]	6[a]	7[b]	8[b]
Inoculum								
Distilled deionized water	x	x	x					
Pure culture, A. ferrooxidans				x	x	x		
Environmental consortium								
Headwater source							x	
Dam seepage source								x
Mineral Sample								
Sterilized	x			x	x	x		
Not sterilized		x	x				x	x
Leaching Solution								
Nutrient media								
Acidic (pH = 3.5)	x	x		x				
Neutral (pH = 6.8)					x			
Solution B added (Fe^{2+} supplement)						x		
Distilled deionized water			x				x	x

[a] laboratory control conditions

[b] industrial application conditions

A sample (10 mL) was removed every two to fifteen days, with frequency decreasing over time and filtered (0.45µm). Sterile nutrient solution or water was added bi-weekly to compensate for volume loss from sampling and evaporation. The mass of the flasks was recorded before and after sampling and solution addition to allow for compensation of dilution. The extraction flask experiment was continued for approximately 80 days, a stage at which the cumulative elemental release rate from the mineralization

had reached an experimental maximum. Residue samples were collected from each flask for subsequent chemical and mineralogical analysis.

Small Columns

Lucite columns (1.27 cm internal diameter and 90 cm tall) were loaded from the bottom up with 2.5 mL of plastic beads (3 to 4 mm), 90 grams of mineral material, and another 2.5 mL of beads (Figure 4.7). The beads aid in the flow distribution through the column. The bottom of each column was covered with nylon mesh (0.5mm) to retain the charge before being connected to a reservoir filled with 760 mL of DDI water. Fresh air was supplied with an air pump at the base of each column to ensure aerobic conditions were maintained throughout the columns during the experimental period (Nemati, et al., 1997).

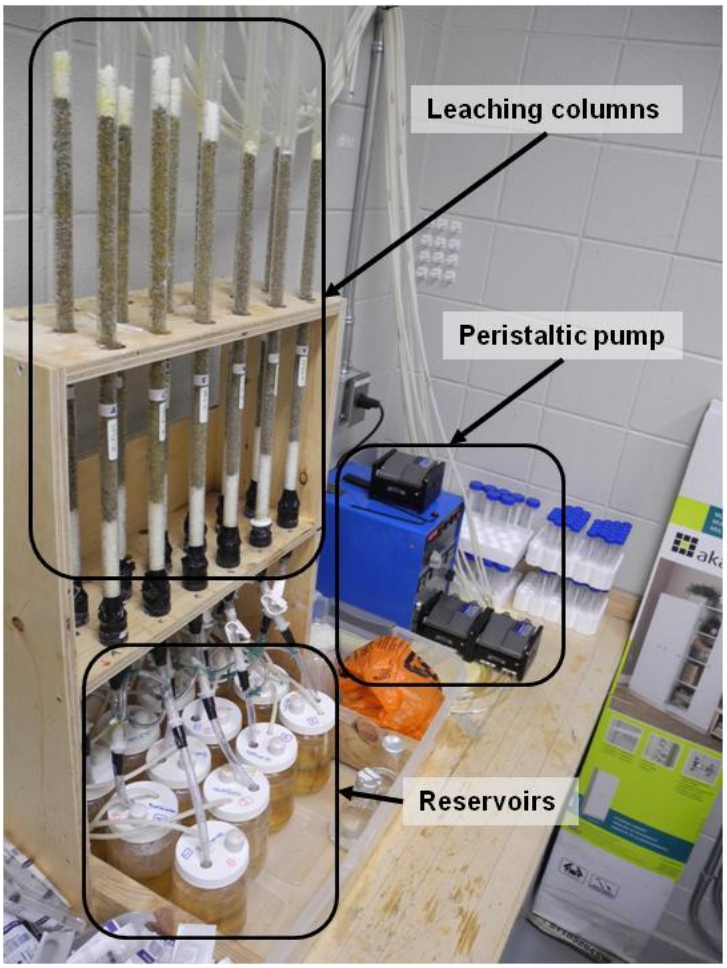

Figure 4.7 Laboratory set up for leaching experiments using small columns connected to reservoirs with solution supplied to the top of the column by peristaltic pump.

Treatments were designed to compare methods of leachate application that may be applicable at a pilot or field scales. Solutions were supplied using a closed-loop system by continuous irrigation (Munoz, et al., 1993) or flooding (Wadden & Gallant, 1985) (Table 4.5). The continuous irrigation simulations were fed with solution from a reservoir by peristaltic pump at 0.5 L hr^{-1}. The top-flooded columns were supplied 200 mL of solution by peristaltic pump, with the drainage valve closed and 50 mL of solution supplied to fully flood the mineralized material interstices in the column. The flood solution was released after 24 hours, with another 200 mL of solution being flushed through the column. After the first 24 hours of leachate application reservoirs were inoculated with 10 mL of the specified culture from prepared broth cultures.

Table 4.5 Small column leaching treatments (n=2).

Parameter	**1**	**2**	**3**	**4**	**5**	**6**
Inoculum						
water	x			x		
pure culture, *A. ferrooxidans*		x			x	
environmental consortium			x			x
Leaching solution						
recycled	x	x	x	x	x	x
Wetting Type						
continuous percolating	x	x	x			
periodic flooding				x	x	x

Leachate samples were collected using sterile syringes every two to fourteen days and filtered (0.45µm). The experiment was continued until the elemental cumulative release from the mineralized material reached a stead state, approximately 7 months. The research columns were disassembled and the residue material was stored for use in future decommissioning simulations. A subsample from each column was retained for subsequent chemical and mineralogical analysis.

Large Columns

Acrylic columns (11.5 cm internal diameter and 180 cm tall) were loaded from the bottom up with 500 mL of plastic beads (3 to 4 mm), 40 kg mineral material, and another 500 mL of beads (Figure 4.8). The

beads aid in the flow distribution through the column. Two columns were loaded with 20 kg of mineral material to represent shorter heap heights. The bottom of each column was covered with nylon mesh (0.5 mm) to retain the charge before being connected to a reservoir filled with 11 L of DDI water. Fresh air was supplied with an air pump at the base of each column to ensure aerobic conditions were maintained throughout the columns (Nemati, et al., 1997).

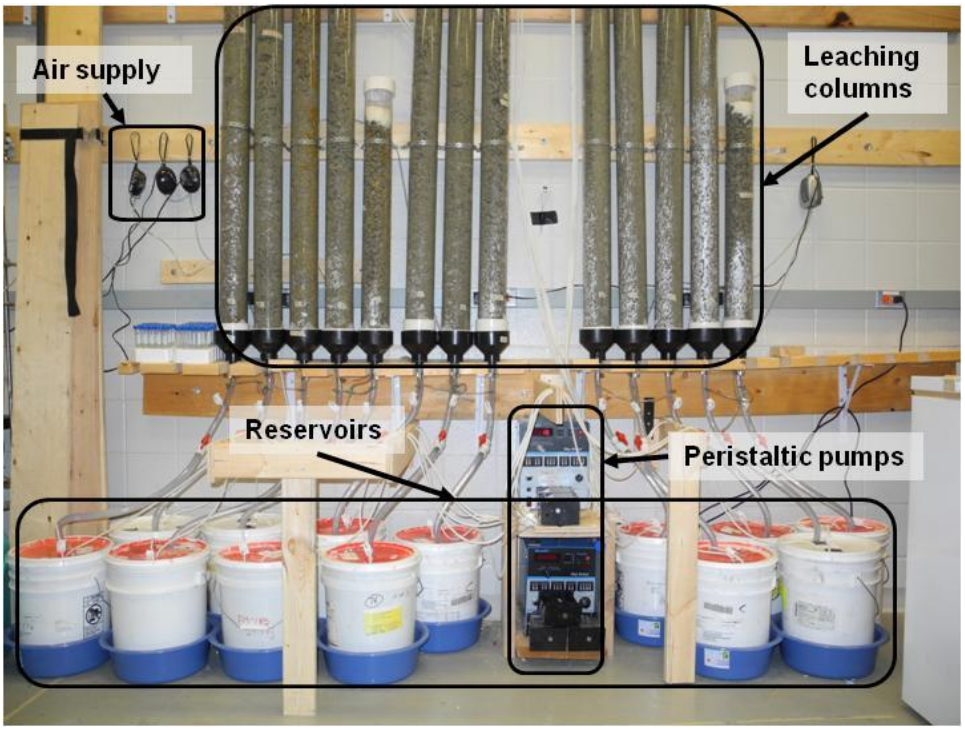

Figure 4.8 Laboratory set up for leaching experiment using large columns connected to reservoirs with solution supplied to the top of the column by peristaltic pump and air supplied at the base of the column using small air pumps.

Treatments were designed to demonstrate the leachate application using a closed-loop system by continuous irrigation (Table 4.6), the method deemed to be appropriate for large scale application after the completion of the small column leaching experiments (see Appendix B). Non-inoculated control columns were used to identify any natural leaching that may happen in the absence of intentional inoculation. Columns were stocked with varying amounts of mineral material to simulate different heights in the heap pile. All columns received leaching solution by the continuous irrigation at the top of a column, supplied from a reservoir by peristaltic pump at 1 L hr^{-1} (Munoz, et al., 1993; Munoz, et al.,

1995). After the first 24 hours of leachate application reservoirs were inoculated with 10 mL of the mature environmental broth culture.

Table 4.6 Large column leaching treatments (n1=3, n2=7, n3=2).

Parameter	1	2	3
Inoculum			
water	x		
environmental consortium		x	x
Amount of material			
20 kg			x
40 kg	x	x	

Leachate samples were collected using sterile syringes every two to fourteen days and filtered (0.45µm). The experiment was continued until the elemental cumulative release from the mineralized material reached a steady state after approximately 12 months. The peristaltic pumps were turned off and the research columns were allowed to dry and used as residue material to demonstrate the application of decommissioning strategies.

4.5 Decommissioning Methods

Decommissioning applications were designed to compare techniques known to limit bacterial activity and control acid production at a large scale to support the sustainable development and potential operation of the Eco Ridge site. Individual and combinations of organic acids and surfactants known to inhibit *A. ferrooxidans* activity and growth, as well as a lime neutralization method, have been investigated. Pacification methods have been investigated to render the surface area of reactive mineral inaccessible to oxidation.

Extraction flasks

Inhibition and passivation investigations using extraction flasks were conducted separately.

Inhibition Study

Five grams of homogenized residue material from the small column leaching phase was added to 250 mL Erlenmeyer flasks along with 125 mL of DDI water and inoculated with 5 mL of prepared environmental culture broth (Figure 4.9).

Figure 4.9 Inhibition study using extraction flasks with aluminium caps.

The flasks were agitated using an enclosed bench-top shaker at a rate of 150 RPM at 30°C under ambient lighting conditions for 4 weeks to reach biogeochemical equilibrium and an environment appropriate to further assess decommissioning options (Dugan & Apel, 1983). Once biogeochemical equilibrium was reached, various combinations of organic compounds known to inhibit the activity of *A. ferrooxidans* were added to the flasks (Table 4.7).

Table 4.7 Extraction flask inhibition treatments (n=3).

Inhibitor Concentration (mg L^{-1})		1	2	3	4	5	6	7	8	9
None		x								
Sodium Benzoate (SB)	10		x	x	x	x				
Sodium Lauryl Sulphate (SLS)	5		x	x			x	x		
Sorbic Acid (SA)	10			x	x		x		x	
Calcium-Magnesium Lime (lime)	0.15									x

After 4 four weeks from the time of treatment application, the contents of each flask was split three ways and conditions known to promote bacterial activity and/or acid production were introduced. The flasks

were either supplemented with an active bacterial culture and/or a ferrous iron solution to investigate the performance of the applied decommissioning treatment under conditions that promoted acid production.

Sample aliquots of 3 mL were collected from the flask using sterile pipette tips at predetermined intervals. The resistance testing was continued for 30 days. The mass of the flasks was recorded before sampling to monitor volume lost by sampling and evaporation.

Passivation Study

Passivation studies follow the methodology developed in the early works of Evangaelou and Fytas (Evangelou, 1994; Fytas & Evangelou, 1998). In these studies, the mineral samples to be coated are first washed with a strong acid, followed by DDI water, to remove any existing coatings. For the purpose of this study, the samples were not washed to remove existing coatings, as a strong acid wash would not be feasible at the field scale. Instead, the study was designed to test the application of pacification coatings on mineral grains with moderate secondary mineral formation present because these conditions effectively mimic oxidized, or weathered, mine waste material.

Ten grams of homogenized mineral material that had been subjected to oxidation under atmospheric conditions was added to 150 mL of the coating solution in a 250 mL Erlenmeyer flask (Figure 4.10).

Figure 4.10 Passivation study using extraction flasks with aluminium caps.

The coating solution is composed of an oxidant (5 g L^{-1} hydrogen peroxide, H_2O_2), a buffer (0.8 g L^{-1} sodium acetate, CH_3COONa), and an inorganic compound, either sodium silicate (Na_2SiO_3) or phosphate (KH_2PO_4) (Table 4.8). The pH of the solution was adjusted to between 5 and 6 using sodium hydroxide (NaOH) and hydrochloric acid (HCl). The flasks were agitated using an enclosed bench-top shaker at a rate of 240 RPM and 25°C under ambient lighting conditions for 24 hours.

Table 4.8 Extraction flask pacification treatments (n=1).

Coating treatment* (g L^{-1})	**1**	**2**	**3**	**4**	**5**	**6**	**7**
None	x						
KH_2PO_4							
0.14		x					
1.4			x				
14				x			
Na_2SiO_3							
0.12					x		
0.61						x	
1.2							x

*All treatments also contain 5 g L^{-1} H_2O_2 and 0.8 g L^{-1} CH_3COONa

After 24 hours, the residual material was air dried, with subsamples from each treatment being collected for oxidation resistance testing to evaluate the coating's effectiveness to prevent further abiotic and biotic oxidation and/or acid generation. Approximately 3 grams of dried sample from each treatment was added to a 250 mL Erlenmeyer flask along with the either oxidizer or DDI water alone. The flasks were shaken on a bench top shaker at 240 RPM and 25°C under ambient lighting conditions. The oxidation resistance testing was carried out over 6 days with frequent sampling.

Small Columns

Lucite columns (1.27 cm internal diameter and 90 cm tall) were loaded from the bottom up with 2.5 mL of plastic beads (3 to 4 mm), 60 grams of previously leached mineral material from the small column leaching phase, and another 2.5 mL of beads (Figure 4.11). The beads aid in the flow distribution through the column. The bottom of each column was covered with nylon mesh (0.5 mm) to retain the biogeochemically weathered mineral charge before being connected to a reservoir filled with 500 mL of

the inhibitor or coating treatment. Fresh air was supplied with an air pump at the base of each column to ensure aerobic conditions were maintained throughout the columns (Nemati, et al., 1997).

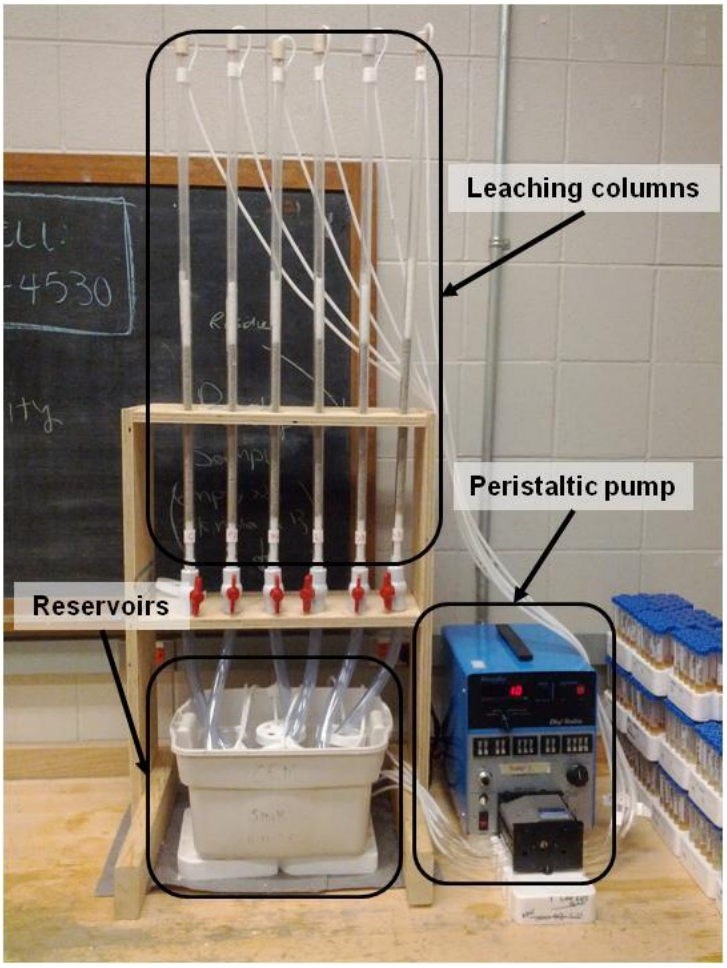

Figure 4.11 Laboratory set up for inhibition and passivation experiments using small columns connected to reservoirs with solution supplied to the top of the column by peristaltic pump.

The passivation methods followed in this laboratory study are based on the publications of Evangaelou and Fytas (Evangelou, 1994; Fytas & Evangelou, 1998), with the inhibition methods followed being similar to those described by (Dugan & Apel, 1983). The inhibition or coating solution was supplied to the columns using the same delivery methods as the continuously irrigated small columns using a closed-loop system with a peristaltic pump at a rate of 0.5 L hr^{-1} (Table 4.9). Coating treatments also included an oxidant (5 L^{-1} hydrogen peroxide, H_2O_2) and a buffer (0.8 g L^{-1} sodium acetate, CH_3COONa) with the pH of all reservoirs adjusted to between 5 and 6 with NaOH and HCl.

Table 4.9 Small column inhibition and pacification treatments (n=3).

Treatment (g L^{-1})	1	2	3	4	5	6
None	x					
*Passivation**						
KH_2PO_4						
1.4		x				
14			x			
Na_2SiO_3						
0.61				x		
1.2					x	
Inhibition						
SLS						*x*
0.010						

*coating solution also include 5 g L^{-1} H_2O_2 and 0.8 g L^{-1} CH_3COONa

Samples were collected from the reservoirs using sterile syringes every two days, filtered (0.45µm). Treatment application lasted for 12 days, after which the columns were deconstructed and the residues were aid dried.

The residual material from each treatment was split three ways and subjected to abiotic and biotic oxidation resistance testing by supplying 0.20 M hydrogen peroxide or bacteria culture, respectively. The flasks were agitated using an enclosed bench-top shaker at a rate of 240 RPM and 25°C under ambient lighting conditions. The oxidation resistance testing was carried out over 12 days with frequent sampling.

Large Columns

Acrylic columns (11.5 cm internal diameter and 180 cm tall) were loaded from the bottom up with 500 mL of plastic beads (3 to 4 mm), 40 kg mineral material, and another 500 mL of beads. These columns remained intact after the biogeochemical mineral dissolution demonstration phase, with only the reservoir contents being changed. These columns are expected to represent biogeochemically leached mineral material immediately prior to the decommissioning phase

The passivation methods followed in this laboratory study are based on the studies documented by Evangaelou and Fytas (Evangelou, 1994; Fytas & Evangelou, 1998), with the inhibition methods similar to those described by Dugan and Apel (1983). Two pacifying coating treatments and one inhibition treatment were applied to the columns using the same delivery methods as the large column leaching phase using a closed-loop system with a peristaltic pump at a rate of 1 L hr^{-1} (Table 4.10). Coating treatments also included an oxidant (5 g L^{-1} hydrogen peroxide, H_2O_2) and a buffer (0.8 g L^{-1} sodium acetate, CH_3COONa) with the pH of all reservoirs adjusted between 5 and 6 with sodium hydroxide and hydrochloric acid. The solution was supplied to the column using the same closed-loop system as the leaching study with a peristaltic pump at a rate of 1 L hr^{-1}.

Table 4.10 Large column inhibition and pacification treatments (n1=1, n2=3, n3=3, n4=3).

Treatment (g L^{-1})	**1**	**2**	**3**	**4**
None	x			
*Passivation**				
KH_2PO_4				
14		x		
Na_2SiO_3				
1.2			x	
Inhibition				
SLS				
0.010				x

Samples were collected from the reservoirs using sterile syringes every two days, filtered (0.45µm). Treatment application lasted for 10 days, after which the columns were left intact and allowed to air dry for one month.

Oxidation resistance testing was carried in the columns using the same closed-loop system with a peristaltic pump at a rate of 1 L hr^{-1}. The reservoirs were replaced with 11 L of fresh DDI water and an oxidizing solution containing either 0.20 M hydrogen peroxide or inoculated with 10 mL of mature bacteria culture. Both abiotic and biotic oxidation was individually investigated using 0.20 M hydrogen peroxide or bacteria culture, respectively. Samples were collected from the reservoirs using sterile

syringes every two to fourteen days and filtered (0.45µm). Oxidation resistance testing was carried out for 50 days.

4.6 Radionuclide Extraction Tests

Extraction tests, based on Standard Practice for Shake Extraction of Solid Waste with Water ASTM D3987−12 (ASTM International, 2013), were performed to estimate radionuclide release from simulated waste material. A 5 g sample was added to an Erlenmeyer flask, filled with 200 mL of de-ionized water, and agitated using an enclosed bench-top shaker for 72 hours at 30°C, with leachate collection by vacuum filtration through a 0.0.45 µm filter. A parallel extraction test was carried out using a tailings standard with a known U concentration (UTS-2, CANMET, Ottawa, ON). The leachate samples were evaporated on a polyethylene sheet in a dish placed on a low-heat plate under IR lamps overnight (Caron & Mankarios, 2004; Caron, et al., 2007). The sheet was folded and pressed to make a disk (2 cm by 0.5 cm) which was then laid into a 4.5 cm x 4.5 cm clear polystyrene jar (Qorpak) for gamma spectroscopic analysis. The dried residual solid materials were weighed (approx. 8 g) and placed in the same type of plastic jar for analysis.

4.7 Sample Analysis & Analytical Parameters

pH and Oxidation Potential (E_H)

The pH and oxidation potential (E_H), corrected to the standard hydrogen electrode, were measured using combination glass-calomel electrode (Orion 8165BNWP ROSS Sure-Flow Epoxy Bodied Combination pH Electrode) and platinum electrode (Accumet 13-620-115 Platinum Pin Indicating Half-Cell Electrode) coupled with the calomel electrode (Accumet 13-620-52 Glass Body Calomel Reference Electrode) respectively, connected to a Thermo Orion 370 PerpHecT Ion Selective Benchtop Meter. The pH electrodes were calibrated with pH 4 and pH 7 standard buffer solutions (Fisher Chemical), and E_H was calibrated using an Orion 967901 ORP Calibration Standard.

Inductively Coupled Plasma Mass Spectrometry (ICP-MS)

Inductively coupled plasma mass spectrometry (ICP-MS) was used to analyze all liquid samples collected from leaching and decommissioning phases and full chemical digests. The instrument (Varian 810) was tuned, optimized, and calibrated to operate under normal sensitivity mode. The instrument is equipped with a Varian SPS3 auto-sampler, controlled by the operator through the use of the supplied software. The complete method and instrument parameters are summarized in Table 4.11. The instrument is controlled by ICP-MS Expert software (Bruker, v2.3 b301). This analytical software has minimal data manipulation capabilities and all data is exported to spreadsheets (Microsoft 2007 Excel), with a commercially available graphing and statistical program (SigmaPlot 12.5) being employed for subsequent manipulation.

Table 4.11 Method summary and optimization conditions for ICP-MS analysis operating under normal sensitivity mode.

Parameter	Method settings		
Analysis Mode			
Quantitative, steady state, peak hopping			
Sampling			
Aerosol generation	Nebulizer		
Source	Autosampler		
Scans/Replicate	30		
Replicates/Sample	3		
Internal Standards (2)	*Analyte (81)*		
^{101}Ru	^{7}Li, ^{9}Be, ^{11}B, ^{23}Na, ^{27}Al, ^{43}Ca, ^{44}Ca, ^{47}Ti, ^{49}Ti, ^{51}V, ^{52}Cr, ^{55}Mn, ^{54}Fe, ^{57}Fe, ^{59}Co, ^{60}Ni, ^{62}Ni, ^{63}Cu, ^{65}Cu, ^{66}Zn, ^{68}Zn, ^{69}Ga, ^{72}Ge, ^{75}As, ^{77}Se, ^{78}Se, ^{82}Se, ^{85}Rb, ^{88}Sr, ^{89}Y, ^{90}Zr, ^{93}Nb, ^{95}Mo, ^{103}Rh, ^{104}Pd, ^{105}Pd, ^{107}Ag, ^{109}Ag, ^{110}Cd, ^{112}Cd, ^{115}In, ^{118}Sn, ^{121}Sb, ^{133}Cs, ^{137}Ba		
^{185}Re	^{139}La, ^{140}Ce, ^{141}Pr, ^{146}Nd, ^{147}Sm, ^{149}Sm, ^{153}Eu, ^{155}Gd, ^{157}Gd, ^{159}Tb, ^{161}Dy, ^{163}Dy, ^{165}Ho, ^{166}Er, ^{167}Er, ^{169}Tm, ^{171}Yb, ^{172}Yb, ^{173}Yb, ^{175}Lu, ^{178}Hf, ^{181}Ta, ^{182}W, ^{183}W, ^{193}Ir, ^{194}Pt, ^{195}Pt, ^{197}Au, ^{200}Hg, ^{202}Hg, ^{205}Tl, ^{207}Pb, ^{208}Pb, ^{232}Th, ^{235}U, ^{238}U		
Flow Parameters (L min^{-1})			
Plasma Flow	16.5		
Auxiliary Flow	1.65		
Sheath Gas	0.23		
Nebulizer Flow	1.00		
Torch Alignment (mm)			
Sampling Depth	6.0		
Other			
RF Power (kW)	1.35		
Pump Rate (RPM)	4		
Stabilization delay (s)	60		
Ion Optics (volts)			
First Extraction Lens	-1		
Second Extraction Lens	-265	Mirror Lens Bottom	32
Third Extraction Lens	-218	Entrance Lens	0
Corner Lens	-291	Fringe Bias	-2.6
Mirror Lens Left	16	Entrance Plate	-31
Mirror Lens Right	26	Pole bias	0.0

The ICP-MS analysis was completed using the CFI funded research instrument following the protocols of the ISO 17025 accredited facility, Elliot Lake Research Field Station (ELRFS) at Laurentian University.

The quality control program for ICP-MS analysis included the calibration, analysis of duplicates, certified reference material (CRM), internal reference material (IRM), and blanks. Internal standards (Ru and Re) were used to correct for any mass bias and calibration standards were used to provide for continuous calibration verification (CCV), with the instrument being recalibrated after every 60 samples. The calibration standard solutions (blank, 10 ppb, 100 ppb, and 1000 ppb) were prepared from multi-element stock solution, DDI water and acidified to 1% nitric acid. The multielement solutions are prepared from 100 ppm stock solutions from Inorganic Ventures, Inc. (Lakewood, NJ, USA), listed in Table 4.12. The stock solutions are in a matrix of 1% (by volume) trace metal grade nitric acid. A CCV solution was used as a quality control method to monitor and verify the reliability of the calibration throughout a sample run. The CCV should have little deviation from the value of the calibration standard. The 10 ppb calibration standard and a 100 ppb REE check solution, prepared with only CCS-1, were used for the CCV samples.

Table 4.12: Inorganic Ventures, Inc. 100 ppm stock solutions used in the preparation of multi-element standards.

Stock Solution ID	Element
CCS-1	Ce, Dy, Er, Eu, Gd, Ho, La, Lu, Nd, Dr, Sc, Sm, Tb, Th, Tm, U, Y, Yb
CCS-2	Au, Ir, Pd, Pt, Rh, Ru
CCS-4	Al, As, Ba, Be, Bi, Ca, Cs, Ga, In, K, Li, Mg, Na, Rb, Sc, Sn
CCS-5	B, Ge, Hf, Mo, Nb, P, Re, S, Sb, Si, Sh, Ta, Ti, W, Zr
CCS-6	Ag, Cd, Co, Cr, Cu, Fe, Hg, Mn, Ni, Pb, Ti, V, Zn

The CRM was used as quality control samples to evaluate any bias or variability between sample runs. The CRM (TMDA 51.3) was obtained from the National Water Research Institute and consists of filtered and diluted Lake Ontario water in a 0.2% HNO_3 matrix. The CRM does not contain all elements in concentrations in the same range of the experimental samples so an IRM stock solution, composed of actual experimental samples, was also included in the quality control program to identify the variation between critical elements of interest between analytical runs using matrix and elemental concentrations more representative of the leachate samples. Through the entire analysis, an internal standard (IS) of 100 ppb Re and Ru was continuously introduced to the sample and mixed with the sample using a Y

connection mixer prior to entering the nebulizer. The conditions under which the internal standard is added must remain constant to avoid unwanted interruptions or fluctuations in the flow of the IS. Prior to analysis, experimental samples were filtered (0.45 µm) and diluted (1:10) with DDI water and multi-acid digest samples were diluted (1:10) with DDI water. Every set of 60 samples included:

- Instrument calibration sequence with reagent blank, 10, 100, and 1000 ppb multielement solutions;
- Three CCV samples, including reagent blank, 10 ppb calibration sample, 100 ppb REE check solution;
- One CRM and one IRM sample; and
- Continuous addition of 100 ppb Ru and Re internal standard.

The method to report the actual concentration of the sample varied depending on the experimental phase. Samples collected from leaching studies and multi acid digests are reported as mg kg^{-1}, allowing the dissolution efficiency to be calculated by Equation 4.1. Concentrations reported in decommissioning studies are reported as dissolved elemental concentration, ppb.

Equation 4.1

$$\text{Dissolution Efficiency (\%)} = \frac{\text{Concentration dissolved } \left(\frac{\text{mg}}{\text{kg}}\right)}{\text{Solid phase concentration } \left(\frac{\text{mg}}{\text{kg}}\right)} \times 100\%$$

Ion Chromatography (IC)

Sulphate (SO_4^{2-}) concentration was determined by ion chromatography (IC) by ELRFS following Standard Operating Procedure (SOP) 3010 (Wang, 2001). Owing to increasing sulphate concentrations when leaching progressed, samples required up to 10,000 times dilution, after which all other anions in the leachates were below the detection limit.

Multi-Acid Digest

Total elemental concentration of the mineral material before and after leaching was measured by ICP-MS analysis after acid digestion of the material. To ensure selection of an accurate sub-sample of the material, a riffle splitter was used to produce representative subsamples. After grinding to 74 µm using an agate

ball mill, a 0.5 g sample was digested in an open 50 mL Teflon™ centrifuge tube using a programmable digestion block (Questron Q-Block 4200) according to the following steps:

- 10 mL of HF/HCl (1:1) and evaporated dryness at 110 ℃ for 3.5 hours;
- 14 mL HCl/HNO_3 (1:1) and evaporated dryness at 110 ℃ for 4 hours; and
- 12.5 mL of $HF/HCl/HNO_3$ (1:4:20) and heated to 110 ℃ to reduce sample volume to 8 to 10 mL.

After digestion, ultrapure water was added to bring the total volume in each tube to 50 mL for subsequent analysis. The samples were then diluted (1:10) and analyzed by ICP-MS. All concentrations were calculated in mass per mass dry mineral basis.

Gamma Counting

Uranium (^{235}U) and radium-226 (^{226}Ra) were analyzed by gamma spectrometry using a Canberra Model GC1020 high-purity germanium detector housed in a Canberra lead castle controlled by a DSA-1000 digital processor and Genie 2000 software. Jars containing the solid samples and the pressed polyethylene sheets were placed directly on the detector and counted for 12 and 24 hours respectively. Detector calibration and efficiencies (Table 4.13) were calculated by interpolation for the pressed polyethylene sheet using a National Institute of Standards and Technology (NIST) traceable multi-gamma standard (QCY-48, AEA Technologies). The detector efficiencies for equivalent masses for the solid material were obtained directly using a tailings standard (UTS-2, CANMET, Ottawa, ON) (Table 4.13). A background reading, counted for 24 hours, was used for spectral correction in the regions of the peaks of interest.

Table 4.13 High-purity germanium detector efficiency for gamma spectroscopy.

Sample type	Energy	
	143 keV	186 keV
Pressed polyethylene film	8.4%	7.3%
Solid material	38%	8.9%

The gamma spectra for U containing samples are complex, with ^{235}U having two prominent peaks at 143.8 keV (10.5% intensity) and 185.6 keV (54.0% intensity), respectively. The ^{235}U peak, overlapping

the ^{226}Ra peak at 186.2 keV (3.3% intensity), can be employed to correct for ^{235}U contribution in the composite peak at ~186 keV. The calculated contribution from ^{235}U at 185.6 keV is 5.14 times the peak intensity at 143.8 keV with deconvolution for the 186 keV peak allowing quantification of the ^{235}U and ^{226}Ra intensity contribution. The UTS-2 listed values were used to estimate the amounts of ^{235}U and ^{226}Ra, based on the source report (NUTP-2E). The above ratio of 5.14 was used to remove the ^{235}U counts at 186 keV in samples, based on the number of disintegrations expected for ^{235}U at 143 keV. The total number of disintegrations for ^{235}U and ^{226}Ra at 186 keV was calculated using Equation 4.2 and Equation 4.3 respectively, where C is the number of observed counts at indicated energy and ε is the detector efficiency that the indicated energy.

Equation 4.2
$$C_{U-235@186} = \frac{C_{U-235@143}}{\varepsilon_{143}} \times 5.14 \times \varepsilon_{186}$$

Equation 4.3
$$C_{Ra-226@186} = C_{total@186} - C_{U-235@186}$$

The specific activity, A_{Ei}, of each radionuclide i was calculated (Equation 4.4), where E is the energy, C_{Ei} net peak area of a peak at energy E, ε_E is the detection efficiency at energy E, t is the analysis time, and γ is the number of gammas per disintegration of this nuclide at energy E (Tzortzis et al., 2003).

Equation 4.4
$$A_{Ei} = \frac{C_{Ei}}{\varepsilon_E \cdot t \cdot \gamma}$$

Using these corrections, the comparison can be made for the crushed sample cores before and after leaching. The comparison between total U concentration (by digestion-ICP-MS analysis) and ^{235}U activity concentration (by gamma counting) is relative; hence back-calculating to total U is unnecessary.

Powder X-ray Diffraction (XRD)

Powdered samples (74 µm) were prepared from fresh mineral using the agate ball mill. Powder X-ray diffraction (XRD) was completed using a Philips PW 1729 X-ray diffractometer at an accelerating voltage of 40kV and current of 30 mA using Co Kα (0.179 nm) radiation. Diffraction patterns from powder samples were collected over a scan range of 5–75° 2θ with a step size of 0.02° 2θ and dwell times

of 4 to 10 seconds. Mineral identification was completed using X'Pert HighScore Plus (PANalytical, version 2.2).

Gravity Separation

Gravity separation using sodium polytungstate solution (SPT) (Carver, 1971; Callahan, 1987) was used to separate powdered mineral samples (74 µm) based on specific gravity (SG) by separating lighter minerals phases facilitate the identification of the heavy U, Th, and REE-bearing mineral phases by XRD. Ten (10) mL of SPT solution, adjusted to SG of 2.90 g cm^{-3} with distilled water (Sahin, et al., 2009), was added to 5 grams of the mineral sample in centrifuge tubes which were vortexed for three minutes to ensure sufficient dispersion of the mineral sample in the SPT solution prior to centrifugation for 6 min at 3,000 RPM (Morrow & Webster, 1989). After resting for at least 48 hours, separation of the phases was evident (Figure 4.12). The bottom of the centrifuge tube was frozen using liquid nitrogen and the top, unfrozen part was decanted and filtered to collect the light mineral fraction. After thawing, the bottom part was decanted and filtered to collect the heavy fraction (Morrow & Webster, 1989). Both fractions were washed with DDI water, followed with an acetone rinse to dry the mineral sample.

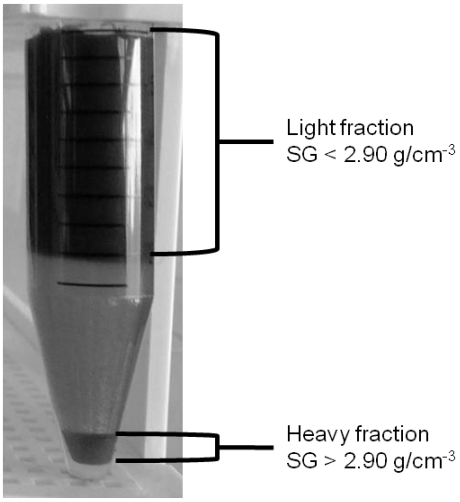

Figure 4.12 Separation of heavy and light mineral phases from powdered mineral sample (74 µm) using SPT solution (SG of 2.90 g cm^{-3}).

Scanning Electron Microscopy with Energy Dispersive Spectroscopy (SEM-EDS)

Electronoptical and microchemical examination of the mineral samples was completed using a SEM (JEOL 6400) with an operating voltage of 20 kV and a beam current of 1 nA using backscattered electron (BSE) and secondary electron microscopy. Phase identification was accomplished using energy dispersive spectroscopy (EDS) for quantitative chemical analysis (Oxford Instruments). Data analysis and image manipulation was completed using INCA software (v. 4.15) by Oxford Instruments Analytical Limited.

Two methods of sample preparation were used to obtain the desired information. Fine samples (74 µm) were placed on carbon tape and gold coated to visualize morphological features on the mineral surfaces of samples collected before and after the biogeochemical leaching experiments. Chemical phase analysis and microstructural examination was also performed on fresh and leached samples (2 mm top size) which were mounted in an epoxy resin prior to coarse polishing with 400, 600, and 1000 grit silicon carbide grinding powder (Buehler) in polishing oil on a smooth glass surface. The final polish was completed with aluminum oxide powder (Buehler) suspended in oil on a polishing pad.

Laser Ablation Inductively Coupled Plasma Mass Spectrometry (LA-ICP-MS)

Trace element distributions and concentrations in coatings on the surface of pyrite grains after biogeochemical dissolution were quantified by laser ablation inductively coupled plasma spectrometry (LA-ICP-MS) using a New Wave Nd:YAG 213 nm laser coupled to a Thermo X II series ICP-MS. Multiple areas of interest on each grain were analyzed using line scans with 19 µm spot sizes, a repetition rate of 5 Hz and an energy density of 7 J cm^{-2}. The sample ablation was done in a He atmosphere, with Ar being mixed as the carrier gas before introduction into the plasma. The data output line scans were recorded and used to generate region maps. The synthetic glass standard NIST610, which contains a nominal trace element abundance of about 400 mg $kg^{-1,}$ was used as the external calibration standard. At the beginning of each analytical run, intermittently during acquisition, and at the end of each sample, the standard was ablated under the same operating conditions. Detection limits for elements depend on the

experimental setting of the laser scan and are identified for a similar experimental setting in Durocher and Schindler (2011).

Total Sulphur

Total sulfur content was estimated by infrared detection of released SO_x upon sample combustion in an oxygen gas stream using Leco^{TM} instrumentation at the Ontario Geoscience Laboratories.

Ferrous Iron

Soluble ferrous iron concentration in selected leachate solutions was determined following the 1,10-phenanthroline method, which forms a complex with soluble ferrous iron, forming an orange-coloured complex measurable at 510 nm on a UV spectrophotometer (Marchand & Silverstein, 2003).

Geochemical calculations

Phreeqc v.3.0.6 (Parkhurst & Appelo, 2013) was used to calculate saturation indices (SI) for mineral phases and dissolved species molality using the pH, E_H, and chemical composition of the leachate sample collected during the final leaching cycle. Phreeqc was coupled with the Minteq thermodynamic database (Allison, et al., 1991).

Microbial Population density

The rate of ferrous iron oxidation is dependent on the activity of the iron-oxidizing microbe community, allowing relative populations to be compared based on the extent of iron oxidation. Centrifuge tubes holding 10 mL of TK media (made up of 5 parts solution A and 1 part solution B) were supplemented with 1 mL of unfiltered sample collected from extraction flasks or leaching column reservoirs. After 1 month, samples containing viable bacterium will have oxidized the ferrous iron available in the growth medium producing a yellow-orange colour, the intensity of which was measured by spectrophotometer at 610 nm; the larger or more active the population, the more intense the colour.

CHAPTER 5

5 Chemical Controls on Biogeochemically Mediated Dissolution of Uranium and Thorium

5.1 Introduction

The biogeochemical mineral dissolution processes drives the solubilization of rock forming minerals, some of which may contain elements of economic interest. The rate of ferrous-sulphide mineral oxidation is significantly increased in the presence of iron (Fe) oxidizing microorganisms making this reaction of fundamental importance to the biochemical mineral dissolution processes (Singer & Stumm, 1970; Marchand & Silverstein, 2003; Johnson, 2010). The oxidation of pyrite in ore materials containing uraniferous minerals promotes the subsequent solubilization of Uranium (U) through a series of reactions described in Figure 5.1 (Kleinmann, 1987; Garcia, 1993; Evangelou & Zhang, 1995; Fernandes & Franklin, 2001; McIlwaine & Ridd, 2004).

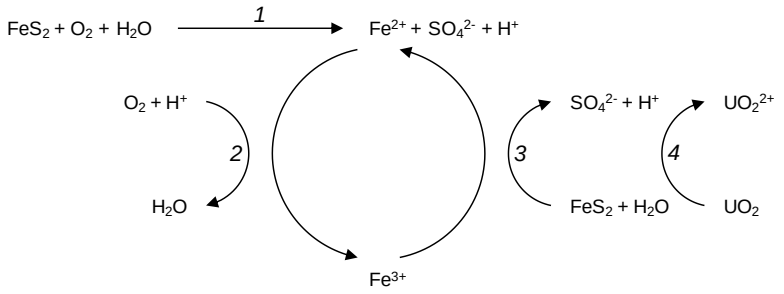

Figure 5.1 Schematic diagram illustrating the biogeochemical mineral dissolution processes for pyrite and the relationship with U (Guay, et al., 1976; Kleinmann, 1987; Evangelou & Zhang, 1995; Fernandes & Franklin, 2001; McIlwaine & Ridd, 2004)

In the presence of air and water, ferrous-sulphide minerals are oxidized, liberating ferrous iron (Fe^{2+}) and acid to solution phases, with possible release to the environment (Reaction 5.1). Ferrous iron is oxidized by molecular oxygen (Reaction 5.2), liberating ferric iron (Fe^{3+}) which, in turn, oxidizes additional

ferrous-sulphide minerals (Reaction 5.3). The continuous oxidation and reduction of Fe is a cyclic, self-propagating process (Kleinmann, et al., 1981).

Reaction 5.1 $$FeS_2 + \frac{7}{2}O_2 + H_2O \rightarrow Fe^{2+} + 2SO_4{}^{2-} + 2\,H^+$$

Reaction 5.2 $$Fe^{2+} + \frac{1}{4}O_2 + H^+ \rightarrow Fe^{3+} + \frac{1}{2}H_2O$$

Reaction 5.3 $$FeS_2 + 14Fe^{3+} + 8H_2O \rightarrow 15Fe^{2+} + 2SO_4{}^{2-} + 16H^+$$

.

The chemical oxidation of Fe is slow and the rate determining step of this process. In the presence of Fe-oxidizing bacterial cultures, this oxidation rate can be increased up to six orders of magnitude (Singer & Stumm, 1970; Evangelou & Zhang, 1995; Marchand & Silverstein, 2003; Johnson, 2010). *Acidithiobacillus ferrooxidans*, the most notable bacterial species driving the bioleaching process, is capable of oxidizing both Fe and sulphur compounds (Singer & Stumm, 1970; Evangelou & Zhang, 1995; Marchand & Silverstein, 2003). This bacterium is an aerobic mesophile and thrives in acidic conditions. When the rate of the reaction is increased significantly, acidity begins to accumulate and the oxidizing potential of the environment increases greatly (Baker & Banfield, 2003; Johnson, 2010). The concentration of dissolved Fe increases at a much faster rate with microbiologically mediated dissolution processes, than with chemical oxidation alone.

Uranium in its common mineral form uraninite is in a tetravalent oxidation state and relatively insoluble, making it challenging to recover from the mineral host (Lundgren & Silver, 1980). When a strong oxidizing agent is present, such as Fe^{3+}, U hosted in the uraninite mineral becomes oxidized to the hexavalent oxidation state to form a soluble uranyl compound, enabling dissolution from the mineral ().

Reaction 5.4 $$UO_2 + 2Fe^{3+} \rightarrow UO_2^{2+} + 2Fe^{2+}$$

Biogeochemical mineral dissolution for the solubilization of U has been documented at sites in the Elliot Lake area (Campbell, et al., 1985; McCready, 1986; Campbell, et al., 1987; McCready & Gould, 1990;

Olson, et al., 2003), with a renewed attention in both U and rare earth elements (REE) promoting interest in the former U-mining camp. In an effort to compete economically with higher-grade deposits elsewhere in Canada and in Australia, biogeochemical mineral dissolution in engineered heap leach piles in the Elliot Lake region may be a promising passive technology for the recovery of U and potentially REEs from low-grade mineralization.

Comprehensive electron probe micro-analyzer (EMPA) and optical mineralogy studies by Sylvester (2007) and Spasford et al. (2012) have identified the principal U-, thorium (Th)-, and REE-bearing minerals in Elliot Lake area conglomerate, with pitchblende (Th, REE-poor UO_2) and brannerite (UTi_2O_6) being the principal host minerals for U in the region (Sylvester, 2007). Uranium- and Th-bearing minerals identified in the host material by these studies are reported in Table 5.1.

Table 5.1 Principal minerals carrying U and Th is Elliot Lake area conglomerate identified by Sylvester (2007) and Sapsford (2012).

Mineral Phase	Chemical Formula
Primary phases	
Th enriched uraninite	(Th)UO_2
Thorite	(Th, U)SiO_4
Secondary alteration phases	
Coffinite	$U(SiO_4)_{1-x}(OH)_{4x}$
Brannerite	UTi_2O_6
Pitchblende	(Th, REE poor)UO_2
Uraniferous rutile or ‘‘leucoxene’’	UO_2–Rutile
Very fine-grained intergrowth of pitchblende, pyrite and aluminium-rich silicate phase	UO_2–Pyr–AlSi-mix
Uraniferous pyrite	UO_2–Pyrite

An understanding of the biogeochemical mineral dissolution process and chemical controls for the dissolution of U developed at the laboratory scale can be used to assess the potential for success of bioleaching in the Elliot Lake region. Earlier studies have determined the appropriateness for the use of an environmentally-sourced inoculum (Appendix A) and the optimum leachate delivery method (Appendix B). The purpose of this current investigation is to demonstrate the application of

biogeochemical mineral dissolution using large leaching columns to assess the chemical controls on U and Th leaching. Variation of the amount of material used to charge the column allowed simulation of different heap heights, with leachate solution chemical composition monitoring providing an understanding of the biogeochemical controls of leaching behavior.

5.2 Experimental Methods

Material

Fresh drill core was collected from the study site, Eco Ridge Mine Rare Earths and Uranium Project site (Eco Ridge), owned by Pele Mountain Resources Incorporated (PMR), approximately 11 km east of Elliot Lake, Ontario (Figure 5.2). The ore minerals are hosted in a quartz-pebble conglomerate bed with a matrix of fine-grained quartz, feldspar and up to 15% pyrite (Sylvester, 2007). Uranium, Th, and REE-bearing primary and secondary minerals exist in the matrix, being concentrated in halos around the quartz pebbles.

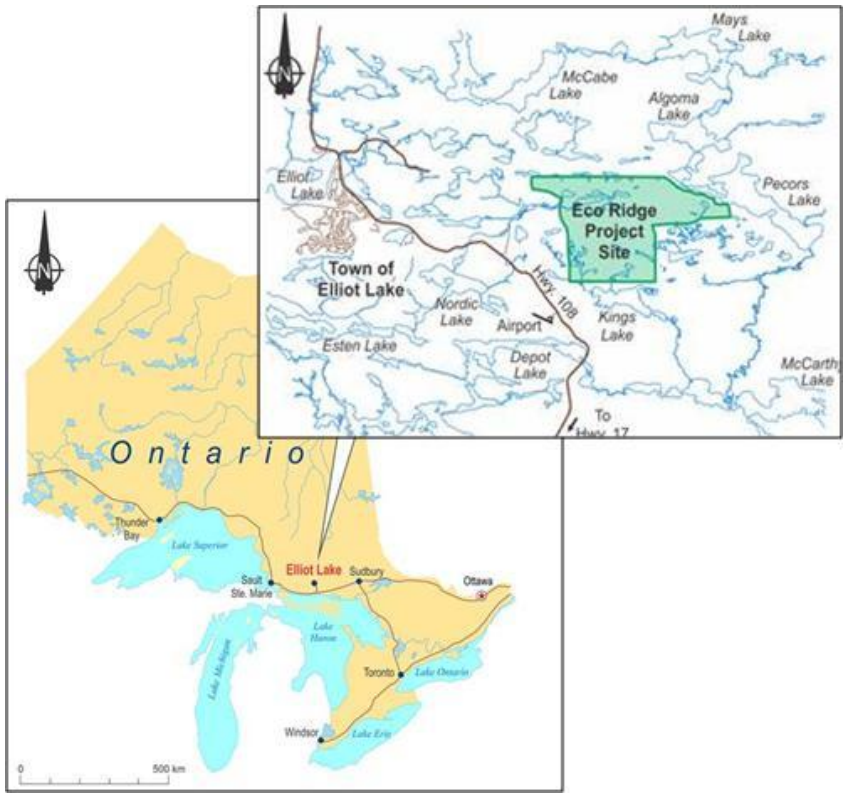

Figure 5.2 Location of Eco Ridge Mine Rare Earths and Uranium Project, east of Elliot Lake, Ontario (image provided by PMR Ltd. 2013).

A sub-sample of the material was crushed to 2 to 4 cm in size using a large mouth jaw crusher, a head size with 65% passing < 5 cm sieve being similar in size to that used in earlier bioleaching studies conducted at Denison Mines (Campbell, et al., 1987). A representative sub-sample of homogenized material was examined by X-ray diffraction (XRD), with the elemental composition being determined by spectroscopic analysis after acid digestion.

Inoculum

A microbial population representative of the study site was cultured from water samples collected from the former tailings catchment area of Stanrock Mine. A mature broth culture was successfully cultivated with the addition of five mL of the collected sample to 200 mL of modified TK media in a 250 mL Erlenmeyer flask (Tuovinen & Kelly, 1974). The environmental culture performed just as well, if not better, in regards to U and Fe extraction efficiency as pure *A. ferrooxidans* in the earlier extraction flask and small column leaching experiments (Appendix A and B). These results support the findings of Berthelot and colleagues who reported that cultures isolated from mine waters in close proximity to the study site were greatly diverse, being composed of autotrophs and heterotrophs, including *A. ferrooxidans* and other members from the genus *Acidiphilium* (Berthelot, et al., 1997). Johnson (2010), also supporting these conclusions, stated that consortia of microorganisms tend to show superior leaching kinetics compared with pure strains because they have synergistic metabolic physiologies.

Experimental Approach

Acrylic columns (11.5 cm internal diameter and 180 cm tall) were loaded from the bottom up with 500 mL of plastic beads (3 to 4 mm), either 20 or 40 kg mineral material, and another 500 mL of beads. The beads aid in the leachate flow distribution through the column. The smaller columns simulated shorter heap heights, with the bottom of each column being covered with nylon mesh (0.5 mm) to retain the charge before being connected to a reservoir filled with 11 L of DDI water. A fresh air flow was supplied with an air pump at the base of each column to ensure maintenance of aerobic conditions throughout the columns (Belzile, et al., 1997).

Treatments were designed to demonstrate the leachate application using a closed-loop system by continuous irrigation, a method deemed appropriate for large scale application after the completion of the small column leaching experiments (Table 5.2). All columns received leaching solution by the continuous irrigation at the top of a column, supplied from a reservoir by peristaltic pump at 1 L hr^{-1}(Munoz, et al., 1993; Munoz, et al., 1995). After the first 24 hours of leachate application reservoirs were inoculated with 10 mL of the mature environmental broth culture.

Table 5.2 Large column experimental leaching treatments (n1=3, n2=7, n3=2).

Parameter	1	2	3
Inoculum			
water	x		
environmental consortium		x	x
Amount of material			
20 kg			x
40 kg	x	x	

Leachate samples were collected from reservoirs connected to the base of the columns using sterile syringes every two to fourteen days, filtered (0.45µm), and analyzed for pH, E_H, and dissolved metal concentration by ICP-MS. The bioleaching experiment was continued for approximately 12 months until the elemental cumulative release from the mineralized material reached a steady state, with the leachate recirculation being discontinued, and the columns allowed to dry for subsequent use of the residual material to examine the application of selected decommissioning strategies.

Sample Analysis & Analytical Parameters

The pH was measured with a Thermo Orion 370 PerpHecT Ion Selective Benchtop Meter equipped with a glass electrode (Orion 8165BNWP ROSS Sure-Flow Epoxy Bodied Combination pH Electrode) and calibrated with pH 4 and pH 7 standard buffer solutions. The oxidation potential (E_H), corrected to the standard hydrogen electrode, was measured using a platinum combination electrode (Accumet 13-620-115 Platinum Pin Indicating Half-Cell Electrode) coupled with the calomel electrode (Accumet 13-620-52

Glass Body Calomel Reference Electrode) and calibrated with an oxidation-reduction potential standard (Orion 967901 ORP Calibration Standard).

Inductively coupled plasma mass spectrometry (ICP-MS), tuned, optimized and calibrated to operate under normal sensitivity mode, was used to analyze all leachate samples (Varian 810). The analysis was completed in an ISO 17025 accredited facility, Elliot Lake Research Field Station at Laurentian University. The quality control program included the analysis of duplicates, certified reference materials (CRM), internal reference material (IRM), and water blanks. Internal standards (Re and Ru) were used to correct for any mass bias and provide for continuous calibration verification (CCV). Prior to analysis, all experimental samples were filtered (0.45 µm) and diluted (1:10) with DDI. Samples collected from multi acid digests and leaching studies are reported as mg kg^{-1}, allowing the dissolution efficiency to be calculated by Reaction 5.1.

Equation 5.1
$$\text{Dissolution Efficiency (\%)} = \frac{\text{Concentration dissolved } \left(\frac{\text{mg}}{\text{kg}}\right)}{\text{Solid phase concentration } \left(\frac{\text{mg}}{\text{kg}}\right)} \times 100\%$$

Sulphate (SO_4^{2-}) concentration, determined by ion chromatography (Wang, 2001) required a high dilution factor, thus preventing the quantification of other anions. Total elemental concentration of the mineral material before and after leaching was measured by ICP-MS analysis after acid digestion of the material. To ensure samples used represented an accurate sub-sample of the material, a riffle splitter was used to produce subsamples. After grinding to 74 µm using an agate ball mill, a 0.5 g sample was digested in an open 50 mL Teflon™ centrifuge tube using a programmable digestion block (Questron Q-Block 4200) according to the following steps:

- 10 mL of HF/HCl (1:1) and evaporated dryness at 110 ℃ for 3.5 hours;
- 14 mL HCl/HNO3 (1:1) and evaporated dryness at 110 ℃ for 4 hours; and
- 12.5 mL of HF/HCl/HNO3 (1:4:20) and heated to 110 ℃ to reduce sample volume to 8 to 10 mL.

After digestion, ultrapure water was added to bring the total volume in each tube to 50 mL for subsequent analysis. The samples were then diluted (1:10) and analyzed by ICP-MS. All concentrations were calculated in mass per mass dry mineral basis.

Powdered samples (74 μm), were prepared from fresh mineral. Powder X-ray diffraction (XRD) was completed using a Philips PW 1729 X-ray diffractometer at an accelerating voltage of 40kV and current of 30 mA using Co Kα (0.179 nm) radiation. Diffraction patterns from powder samples were collected over a scan range of 5–75° 2θ with a step size of 0.02° 2θ and dwell times of 4 to 10 seconds. Mineral identification was completed using X'Pert HighScore Plus (PANalytical, version 2.2).

Electronoptical and microchemical examination of the mineral samples was completed using a SEM, (JEOL 6400) with an operating voltage of 20 kV and a beam current of 1 nA using backscattered electron (BSE) and secondary electron microscopy. Fine samples (74 μm) were placed on carbon tape and gold coated to visualize morphological features on the mineral surfaces of samples collected before and after the biogeochemical leaching experiments. Phase identification was accomplished using energy dispersive spectrometry (EDS) for quantitative chemical analysis (Oxford Instruments Analytical Limited). Data analysis and image manipulation was completed using INCA software (v. 4.15) by Oxford Instruments Analytical Limited.

5.3 Results

Solid Phase Analysis

The elemental composition of the ore material is summarized in Table 5.3. As samples collected were considered representative of the whole ore given the care taken in preparation (tumble mixer, riffle, splitter), the large standard deviations (SD) for some elements suggest considerable variation in the distribution of heavy mineral in the ore.

Table 5.3 Elemental composition of head grade quartz-pebble conglomerate ore ± standard deviations, in parenthesis (n=13).

Element	Head grade (mg kg^{-1})	
Sc	3	(0.5)
Fe	23,000	(9000)
Y	45	(9)
La	300	(50)
Ce	590	(100)
Pr	53	(8)
Nd	180	(30)
Sm	30	(4)
Eu	2	(0.2)
Gd	25	(4)
Tb	3	(0.4)
Dy	11	(2)
Ho	2	(0.4)
Er	4	(0.9)
Tm	1	(0.1)
Yb	3	(0.7)
Lu	0	(0.1)
Th	340	(70)
U	310	(100)

The conglomerate beds at EcoRidge are composed of 60 to 70% detrital quartz, 10 to 20% orthoclase, 5 to 15% pyrite, and 3 to 9% secondary muscovite, with less than one percent of the mineral material hosting U, Th, and REE-bearing minerals, including Th-rich, uraninite, monazite and brannerite (Munoz, et al., 1993). Mineral characterization work by X-ray diffraction (XRD) of fresh, ground material (74 µm), presented in Figure 5.3 identifies quartz, feldspar, pyrite, and mica as the principal components of the mineral matrix of the ore material.

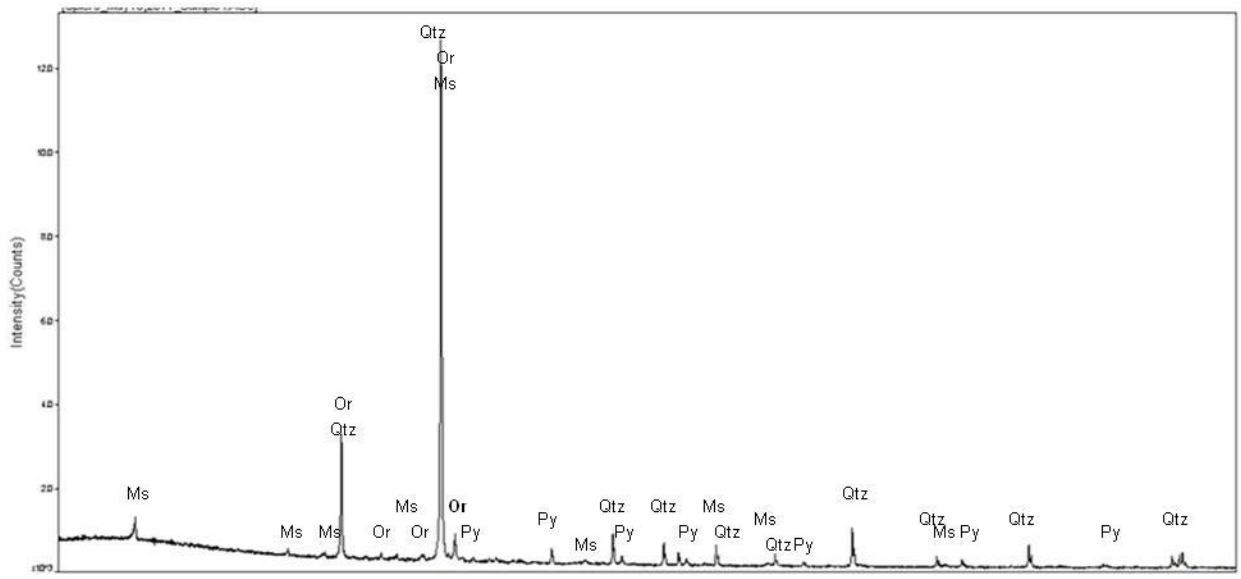

Figure 5.3 Powder x-ray diffraction pattern of the quartz-pebble conglomerate fresh material (74 µm) identifying (Qtz), feldspar (orthoclase, Or), pyrite (Py), and mica (muscovite, Ms) as the principal components.

The SEM images in Figure 5.4 show the surface of pyrite prior to leaching, leaching with non-inoculum bearing solution, and leaching in the presence of an inoculum bearing solution. Prior to leaching, the pyrite surface is relatively smooth (Figure 5.4a), with both leached grains having rough surfaces (Figure 5.4b and c). Many dissolution pits are evident in the sample leached with the inoculum (Figure 5.4c). These dissolution pits are not observed on mineral grains leached with a sterile leaching solution (Figure 5.4b).

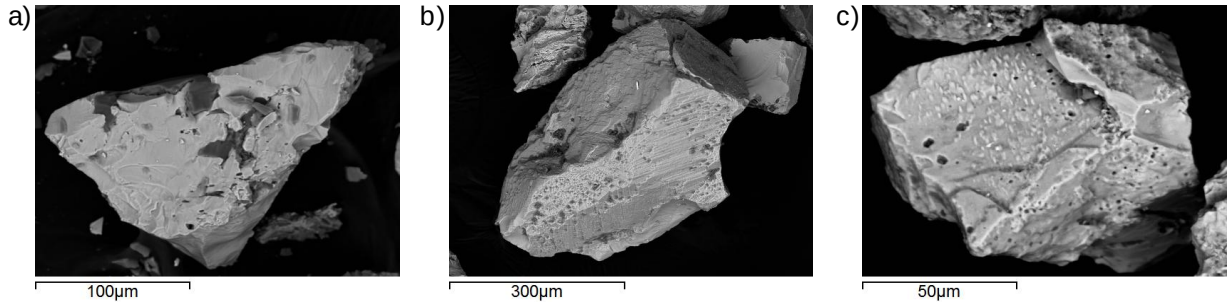

Figure 5.4 Electronoptical images of pyrite grains: (a) before leaching, (b) after leaching and not inoculated, and (c) after leaching and inoculated.

Dissolved Phases Analysis

The pH, oxidation potential (E_H), sulphate concentration, and Fe dissolution efficiency for all treatments are shown in Figure 5.5. The pH of all columns rapidly decreases from 5.4±0.1 to 4.0±0.1 after one day of

leaching, confirming the dissolution of protons by the dissolution process (Figure 5.5a). After this initial decrease, the pH in the inoculated columns continues to decrease steadily over the first two months, to pH 2.7 and 2.6 respectively, with the non-inoculated column decreasing to pH 3.1. The decrease of pH continues for the inoculated columns, although less rapidly, to a low of pH 1.8 after 10 months of leaching. The pH of the non inoculated column declined sharply between months 2 and 4 from 3.5 to 2.4, continuing to decline to a low of 1.8 after 10 months of leaching. The leachates for all columns were at pH of 1.9 after 12 months, regardless of inoculum or amount of mineral material.

Oxidation potential of 0.98V for de-ionized water at pH 5 prior to leaching immediately decreased to 0.70 V for all columns on initiation of the leaching process, and continued to decrease to less 0.60 V. After 3 weeks of leaching, E_H of the inoculated columns (Treatments 2 and 3) began to increase steadily, reaching 0.75 V after 2.5 months of leaching (Figure 5.5b). Oxidizing potential for the non-inoculated treatment remained in the range of 0.60 V until after the third month of the leaching process. For the remainder of the experiment, E_H for all three treatments fluctuated between 0.73 and 0.87 V, with an average of 0.80 V.

The sulphate concentration for the non-inoculated column (Treatment 1) and the inoculated columns (Treatment 2) provided initial differentiation, with the sulphate concentration in the inoculated column at 3.5 g L^{-1} after 1 day of leaching. This sulphate concentration level was reached by the non-inoculated column after 1.5 months of leaching, with both columns having a concentration of 6.0 g L^{-1} after 2 months. The concentration of sulphate in the leaching solution increased both the non-inoculated column and the inoculated columns to final concentrations of 170 and 187 g L^{-1}, respectively (Figure 5.5c).

The release of Fe followed a pattern similar to that of sulphate, with Fe dissolution initially occurring more slowly in the non-inoculated columns and all columns reaching similar concentrations after 12 months of leaching, approximately 8% of the total Fe in the ore (Figure 5.5d). Of note, the treatment designed to represent a shorter heap promoted greater Fe dissolution rates, being 9% after 12 months.

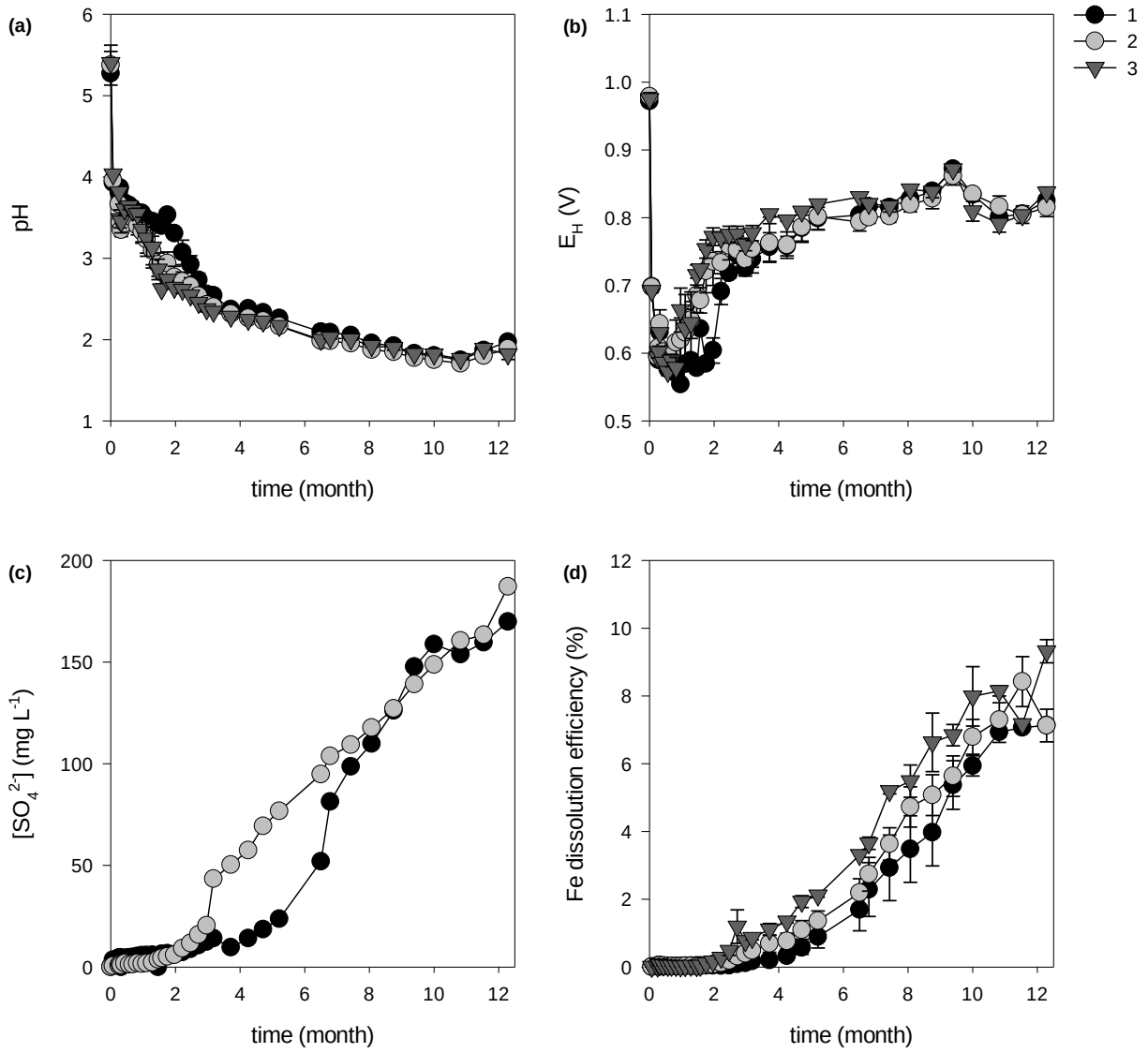

Figure 5.5 Time profiles for Treatments 1, 2 and 3 during one year of leaching displaying the changes in measured parameters resulting from the simulated ore leaching process: (a) pH, (b) EH, (c) sulphate concentration, and (d) Fe dissolution efficiency.

The cumulative release from the ore materials over one year for each treatment for U, Th, Sc, Y, and REEs, expressed as dissolution efficiency, is shown in Figure 5.6. There is a distinct release pattern displayed for each treatment between the light REEs (La, Ce, Pr, Nd, Sm, and Eu) and heavy REEs (Gd, Tb, Dy, Ho, Lu, Er, Tm, and Yb). The dissolution efficiency of scandium (Sc) during the experimental period is minimal, with the dissolution pattern of yttrium (Y) and Th being similar to that obtained for the heavy REEs. Uranium exhibits the highest dissolution efficiency in all treatments, producing a leaching pattern unlike any of the other elements listed. The amount of released element and the individual

dissolution pattern is probably controlled by a combination of the composition of host mineral phases, the chemical nature of the element and the actual leachate solution compositional chemistry.

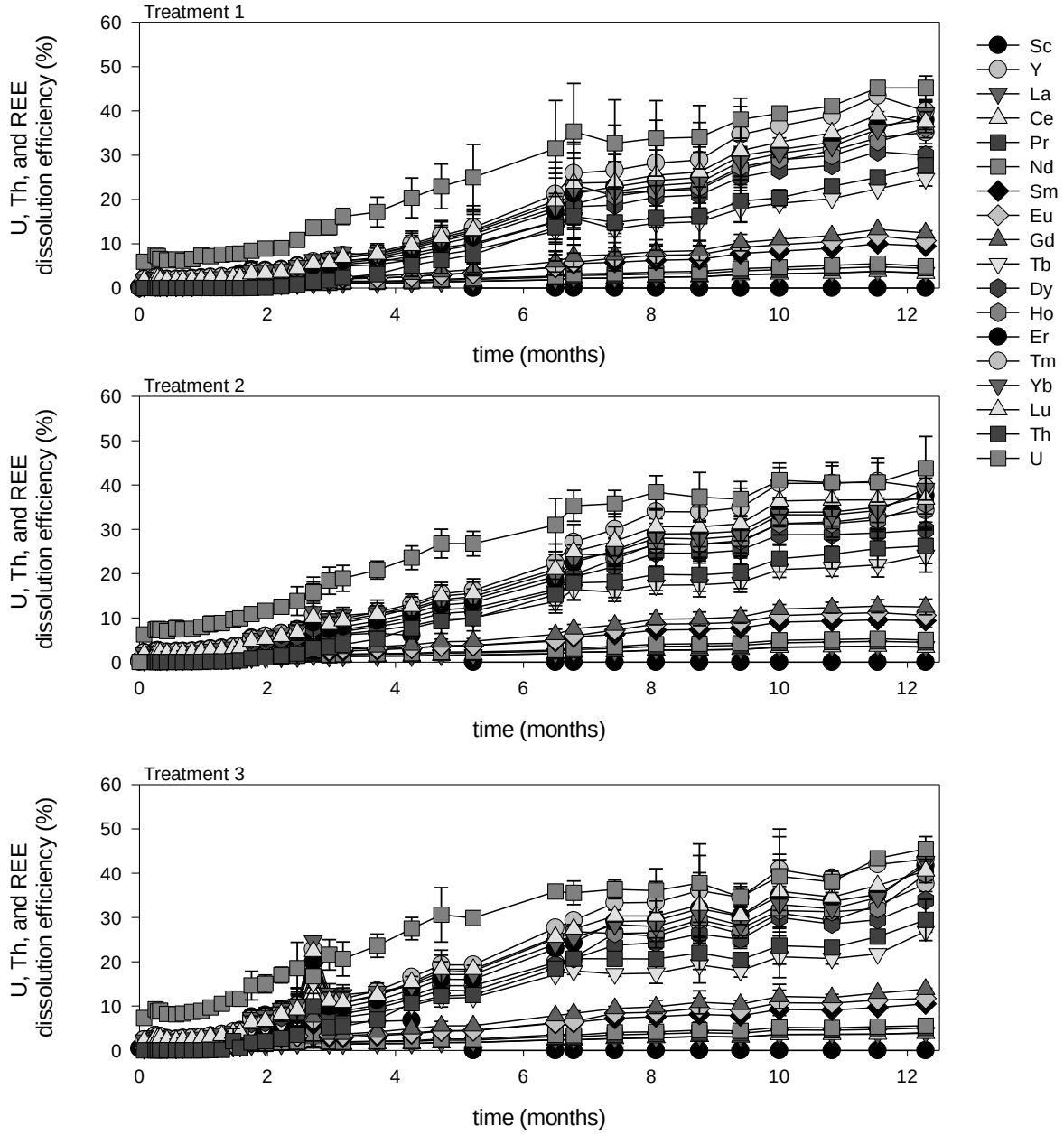

Figure 5.6 Elemental dissolution efficiency-time profiles for Sc, Y, REEs, U, and Th for Treatment 1 (top), 2 (middle), and 3 (bottom) during one year of leaching.

5.4 Discussion

Effect of Inoculation

The results from the solution phase analysis over 12 months of leaching inoculated and non-inoculated columns indicate that Treatment 1 may have become inoculated through self-inoculation because the mineral material was not sterilized prior to initiation of the experiments. Indigenous microbial communities may have existed within the material itself. Inoculation by contamination, because of the close proximity of all three treatments in the laboratory space, is also possible but not suspected as the prime driver. Minimal changes in pH and E_H during the first two months of leaching were observed for Treatment 1 in comparison to the treatments that were supplied with mature culture inoculum. The measured leachate pH decreased from 3.9 to 3.5, whereas for the other treatments pH decreased to 2.8 over the same period, and E_H was steady at ~0.60 V whereas E_H increased to 0.75 V for the same time interval for the inoculated treatments. However, after three months leaching, the pH of the non-inoculated treatment reached a value similar to the inoculated columns, with a similar trend being observed for the E_H in the treatments. The elemental release profiles for Fe, Sc, Y, U, Th, and the REEs for Treatment 1 are also quite similar to the other treatments, providing further evidence for inoculation by a similar microbiological consortium.

These results suggest that, in the absence of direct inoculation, indigenous microbial communities, which may take more time to develop, have the same leaching potential over the timescale of the experiment. The initial investigations of this thesis did use extraction flask microcosms to investigate the effects of inoculation (Appendix A), with experimental results illustrating benefits in terms of Fe and U dissolution from inoculation (up to 60% and 97%, respectively) when compared with sterile, non-inoculated microcosms (up to 1% and 25%, respectively).

It may be more realistic to, rather than consider a comparison between non-inoculated and inoculated columns, consider a comparison in the amount of inoculum supplied and method of inoculation with an unknown and uncontrolled indigenous amount introduced to Treatment 1 and a laboratory cultured,

mature broth population being supplied to Treatments 2 and 3. The dissolution and release patterns of sulphate and Fe indicate that similar micro-environments are created in the experimental microcosms after nine months of leaching, suggestive of the establishment of a viable microbial community.

Effect of Heap Height

Two heap heights were simulated using identical columns, with one series having twice the amount of crushed ore material as the other (Treatments 2 and 3, respectively). The total mass released from the simulated shorter heap (Treatment 3) is less than the simulated tall heap release (Treatment 2); however, the treatment representing a shorter heap has greater dissolution efficiency for all elements investigated in this study. This observed extraction efficiency improvement may have been achieved in shorter columns because of more efficient oxygen diffusion (Wadden & Gallant, 1985) and/or lower concentrations of metals in the leaching liquid. Increased levels of metals in the extraction leachate fluids, as present in Treatment 2, may limit microbial activity (Leduc, et al., 1997).

Dissolution Efficiency

The total dissolution masses, together with the calculated dissolution efficiencies, for Sc, Y, U, Th, and REEs after one year of experimental bioleaching are summarized in Table 5.4. The total U and Th dissolution efficiency is similar for all three treatments, being between 44 and 45% for U and 26 and 29% for Th, a much lower efficiency than obtained with small column leaching experiments containing finer ore materials (Appendix B). The decrease in U dissolution efficiency is suspected to be associated with an increase in mean particles size and, therefore, a decrease in the surface area of the mineral in contact with the leaching solution. For all treatments, the dissolution efficiency for the REEs increases with atomic mass, with up to 12% dissolution for the light REE compared with 41% for the heavy REEs and Y, and will be further explored in Chapter 6. The results obtained for Treatments 1 and 2 are very similar, with treatment 3, representing a shorter heap, promoting greater dissolution efficiency for the heavy REEs. Although the dissolution efficiency is greater for the heavy REEs, the greater abundance of light REES in the ore materials means the total mass of lighter REEs released to solution is greater than that of the

heavy REEs. However, a significant amount of the light REEs remain in the residual ore in the columns after the 12 month leaching period.

Table 5.4 Total elemental dissolution (mg kg^{-1}) and dissolution efficiency (%) for Sc, Y, REEs, U, and Th after one year of leaching.

Element	Treatment 1		Treatment 2		Treatment 3	
	(mg kg^{-1})	(%)	(mg kg^{-1})	(%)	(mg kg^{-1})	(%)
Sc	0.18	6	0.18	6	0.19	7
Y	16	35	16	34	17	38
La	10	3	10	3	12	4
Ce	20	3	20	3	23	4
Pr	2.4	5	2.4	5	2.6	5
Nd	8.7	5	8.8	5	9.7	6
Sm	2.9	10	2.9	9	3.2	10
Eu	0.2	11	0.2	11	0.2	12
Gd	3.1	12	3.1	12	3.5	14
Tb	0.7	25	0.7	24	0.7	27
Dy	3.4	30	3.4	30	3.8	34
Ho	0.6	36	0.6	36	0.7	40
Er	1.6	38	1.6	38	1.8	42
Tm	0.2	40	0.2	39	0.2	43
Yb	1.3	40	1.3	39	1.5	43
Lu	0.2	37	0.2	37	0.2	41
Th	95	28	90	26	101	29
U	140	45	140	44	140	45

Controls on the Dissolution of Uranium and Thorium

The composition of the leachate solutions plays a significant role in the release of elements from the mineral phase. Pourbaix diagrams (E_H-pH diagrams) are useful to describe the expected solubility and the chemical nature (oxidation state, physical state) of the element under different environmental conditions.

The fluctuation in measured E_H during this experimental study of between 0.73 and 0.87 V is significant because the conditions cover the transition region between the Fe^{3+}/Fe^{2+} redox couple at pH less than 2.3. Abiotic oxidation of pyrite generally takes place in the environment at a very slow rate, whereas biotic oxidation by chemolithotrophic acidophilic bacteria, such as *A. ferrooxidans*, can accelerate the rate of

Fe^{2+} oxidation by up to six orders of magnitude under ideal conditions (Evangelou & Zhang, 1995). Through inoculation, as in this experimental study, the rate of Fe oxidation is increased, thus driving the cyclic oxidation of Fe^{2+} and ferrous-sulphide minerals to ultimately generate stabilizing oxidizing conditions around 0.80 V. With the exception of the earliest samples, all samples lie along the border of the Fe^{3+}/Fe^{2+} species as pH decreases (Figure 5.7).

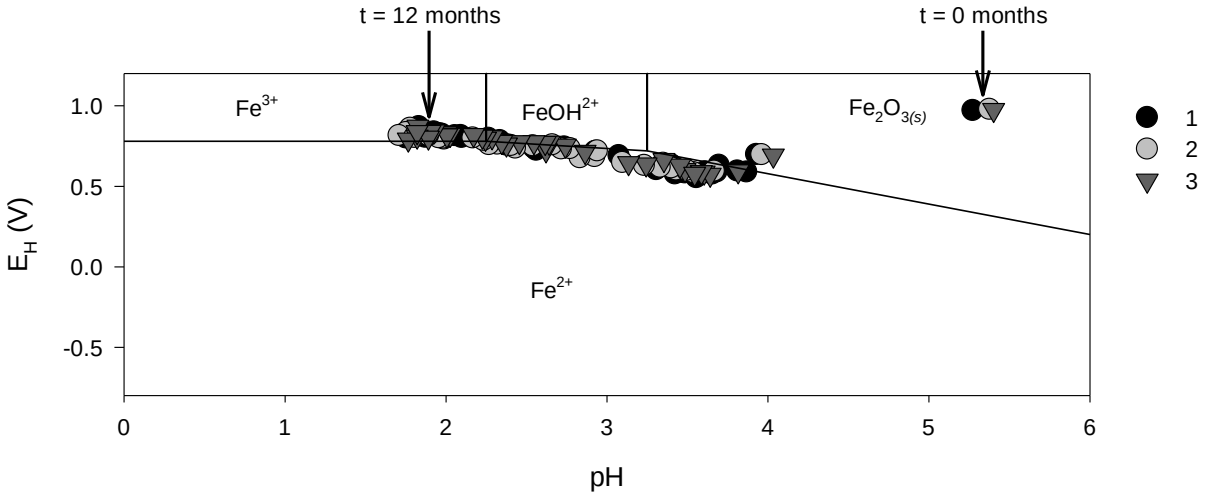

Figure 5.7 Pourbaix diagram for the Fe-O-H system under standard condition, modified from Tankeno (2005); experimental samples indicated (2005).

The solubility of U is not dependent on pH, but rather on the oxidizing potential of the environment, as illustrated in Figure 5.8 (Takeno, 2005). Under initial experimental potential and pH conditions, 0.98 V and 5.4, respectively, U^{4+} is not soluble. The oxidation of Fe increases the E_H of the leaching solutions, which, in turn, facilitates the oxidation and solubilization of U from the host mineral, uraninite. The Pourbaix diagram represented in Figure 5.8 predicts that the dissolved U exists as the uranyl ion, UO_2^{2+}.

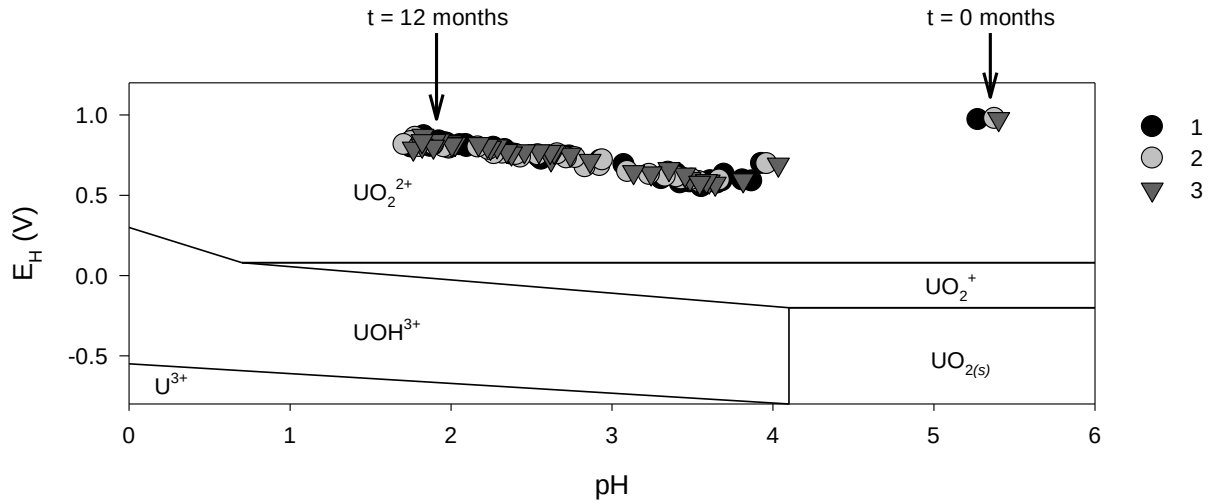

Figure 5.8 Pourbaix diagram for the U-H_2O system under standard condition, modified from Tankeno (2005); experimental samples indicated.

The pH of the leachate potentially enhances the Th dissolution processes because the E_H does not control solubility of Th above -1.8 volts (Kim & Osseo-Asare, 2012). Although Th as ThO_2 is predicted to be soluble below pH 1 in an aquatic system, the Pourbaix diagram (Figure 5.9) predicts that Th^{4+} species should exist in the aqueous phase under the experimental conditions; the results obtained in this study, with 26 to 29% Th dissolution efficiency, suggest otherwise (Kim & Osseo-Asare, 2012).

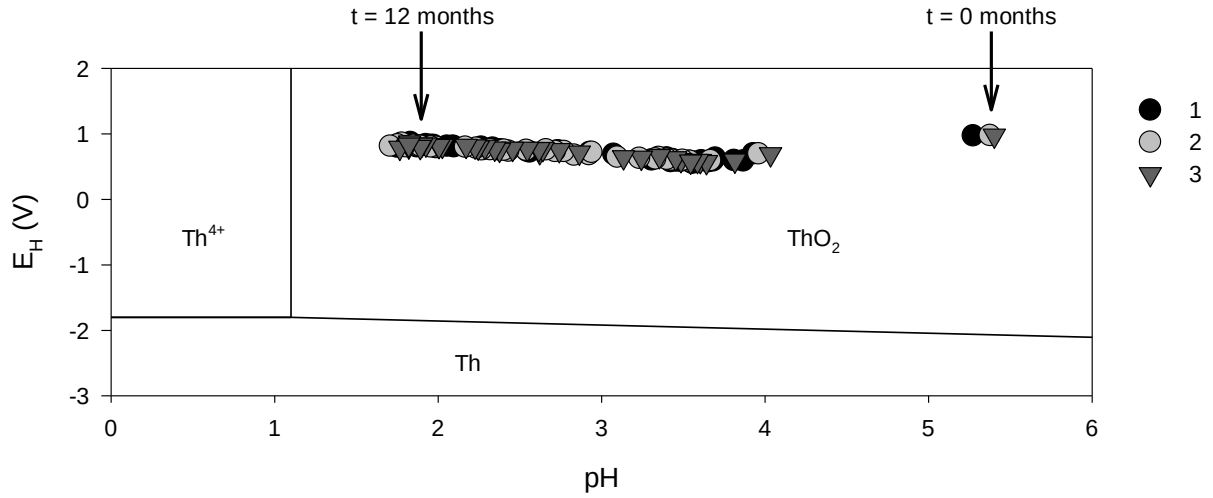

Figure 5.9 Pourbaix diagram for Th-H_2O system under standard condition, modified from Kim and Osseo-Asare (2012); experimental samples indicated.

Examination of the Pourbaix diagram for the Th-SO_4^{2-}-H_2O system in Figure 5.10 indicates that the solubility of Th is expected to be influenced by the concentration of sulphate, rather than the oxidation

potential at low pH.. As the concentration of sulphate increases with a concomitant pH decrease below 2.7, Th is expected to exist in the form of a soluble $Th(SO_4)_2$ phase in the leaching solutions.

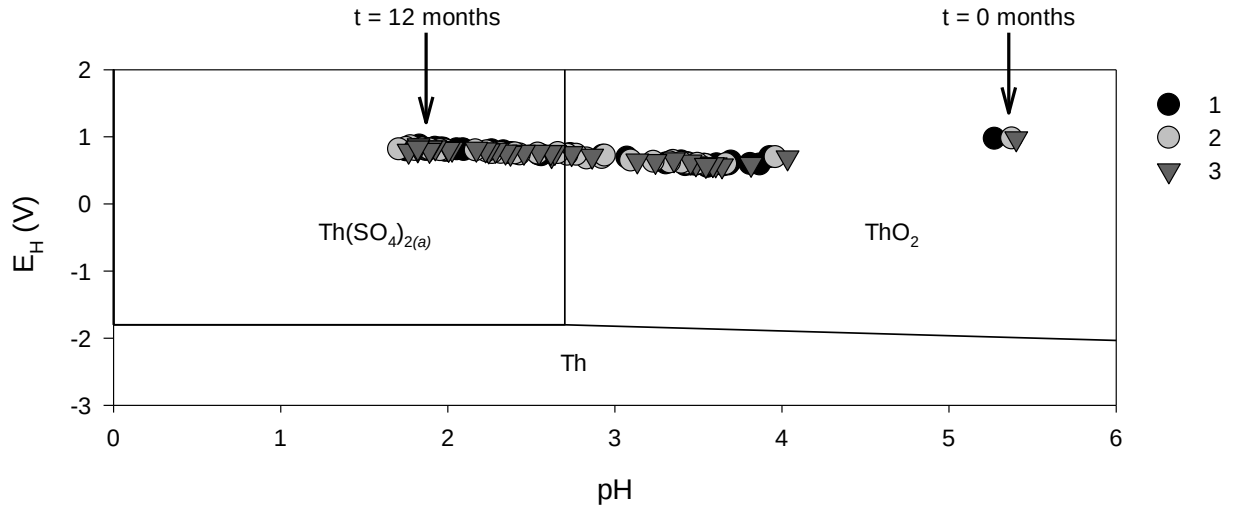

Figure 5.10 Pourbaix diagram for Th-SO_4^{2-}-H_2O system under standard condition, modified from Kim and Osseo-Asare (2012); experimental samples indicated.

Existing as inclusions in major mineral phases or as discreet minerals, the solubility of REEs is controlled by a combination of the existing chemical environment and the host mineralogical species. A detailed mineralogical and microchemical study has been conducted to investigate patterns in the preferential solubilization of U, Th, and REEs using the ore residues collected from the small column leaching investigation (Chapter 6).

5.5 Conclusion

The results obtained using large leaching columns (11.5 cm internal diameter) packed with ore material (2 to 4 cm diameter) demonstrate the biogeochemical controls on the leaching process, providing guidance for the potential development of large scale systems on a mine site. The experiments in this study demonstrated that the application of percolating liquids using a closed-circuit loop operated by peristaltic pump with air injection at the base of the column allowed the biogeochemical mineral dissolution processes to be monitored in columns inoculated with a microbial population representative of that to be expected at the potential mine site. The results obtained suggest that columns that were not intentionally inoculated at the initiation of the project became self-inoculated, with lower dissolution efficiency for Fe

and U being obtained by the end of the study as treatments inoculated with a mature culture. This critical observation suggests that the initial size, or maturity, of the microbial population may not be related to the success of the biogeochemical mineral dissolution process.

The design of engineered heaps must be optimized for elemental extraction efficiency to provide the greatest net return from the mine. This detailed study demonstrated that shorter heaps, as simulated by columns with less mineral material, have reported a better dissolution efficiency for elements such as U and REEs from the host ore. This observation must, naturally, be balanced with the total quantity extracted as a component of mine economics calculations given the construction costs of leach piles and associated recirculation equipment.

The study confirmed that the release of U from the host uraninite minerals is controlled by oxidation potential, an increase of which allows the transition from the tetravalent to the hexavalent oxidation state to form a soluble uranyl compound. The rate limiting chemical control on the oxidizing potential in the biogeochemical mineral dissolution process is the Fe^{3+}/Fe^{2+} redox couple, with dissolved Fe species and ratios being directly related to the activity of the Fe-oxidizing microbial community.

As a change in oxidation state is not required for the dissolution of Th, the solubility of Th is not dependent on the percolating fluid E_H, with the fluid pH and concentration of dissolved polyatomic ions, such as SO_4^{2-}, having a greater effect on the Th solubility. In this experimental system, Th is not expected to be solubilized except in the presence of dissolved anionic species, as an increase in sulphate concentration may promoted the formation of soluble Th-sulphate when pH decreased below 2.5.

The study, overall, demonstrates the importance of chemical, mineralogical, and microbiological optimization for the success of a biogeochemical mineral dissolution process for the recovery of U, Th, and REEs from heap-leach pads on mine sites in the Elliot Lake region. This study suggests that the parameters affecting the in-heap leaching environment may be optimized to promote microbial activity in

the absence of direct inoculation with a mature culture to promote the initiation of environmental leaching conditions appropriate for the release of U, Th, and REE from the host ore-bearing mineral material.

CHAPTER 6

6 Mineralogical Controls on Biogeochemically Mediated Dissolution of Rare Earth Elements

6.1 Introduction

The economic viability of mining low-grade ores using a biogeochemical mineral dissolution approach is dependent on the leaching efficiency for the elements of economic interest. Although rare earth elements (REEs) are rather abundant in the earth's crust, most deposits are low-grade with REE recovery often being as a by-product of the extraction of another target metal (Hayes-Labruto, et al., 2013; Wubbeke, 2013). The REEs include scandium (Sc), yttrium (Y), and elements of the lanthanide series. The lanthanide series is divided into two sub groups: light REEs, lanthanum (La) to europium (Eu), and heavy REEs, gadolinium (Gd) to lutetium (Lu). Based on ionic radius and chemical property trends, Y is commonly categorized with the heavy REEs, while Sc may not be included either group (Jordens, et al., 2013).

Rare earth elements have unique physical and chemical properties, making them essential raw materials in their pure forms for many high-tech, clean-tech, and precision applications. Currently, there are no accepted alternatives that provide comparable performance for electrical, optical, magnetic, and catalytic applications (Du & Graedel, 2013; Hayes-Labruto, et al., 2013). Technological advancements have also increased the demand for REE in electronic sectors, contributing to increased energy efficiency and miniaturization, thus decreasing environmental affects (Hayes-Labruto, et al., 2013). Table 6.1 identifies the end of use application for many REEs.

Table 6.1 End of use application of REEs for electrical, optical, magnetic, and catalytic applications (Du & Graedel, 2013).

End Use	Rare Earth Elements
Magnets	Pr, Nd, Gd, Dy
Battery alloys	La, Ce, Pr, Nd, Sm
Metallurgy	La, Ce, Pr, Nd
Automobile catalysts	La, Ce, Pr, Nd
Fluid cracking catalysts	La, Ce
Polishing powders	La, Ce, Pr
Glass additives	La, Ce, Pr, Nd, Y
Phosphors	La, Ce, Eu, Gd, Tb, Y
Ceramics	Pr, Nd, Y

The REEs do not exist as pure metals in nature, but are found in a variety of mineral types including silicates, carbonates, phosphates, and halides (Jordens, et al., 2013). Bastnasite (REE $(CO_3)F$), monazite ((REE, Th)(PO_4)), and xenotime (YPO_4) are the most commonly mined REE-bearing minerals (Wubbeke, 2013).

In 2008, China announced that REEs would no longer be exported to the global market because the demand for REEs in China was approaching the predicted internal supply potential (Du & Graedel, 2013). At present, China controls close to 95 to 97% of the global REE market (Hayes-Labruto, et al., 2013), and has placed heavy restrictions on the export of REEs in an effort to enhance China's position in the REE market. With over half of the world's current estimated REE resources located in China (Wubbeke, 2013), this embargo has created worldwide attention to the assessment of available REE reserves globally. A combination of increasing global demand for REE supply and lengthy processes for new REE developments has effectively formed a gap in the supply and demand chain (Du & Graedel, 2013).

While REE are not currently produced in Canada, over 200 exploration projects are underway targeting REE developments in efforts to establish Canadian REE suppliers to support economic and industrial development demands. Historically, Y was recovered as a by-product of uranium (U) mining at Denison Mines Ltd., Elliot Lake, Ontario, with a Y extraction plant being operated alongside the U extraction facility (Campbell, et al., 1985). Uranium mining in the region ended in the mid-1990s because higher

grade U deposits had been discovered and developed, resulting in an oversupply of U with a concomitant decrease in price, which prompted the closure of the still active Elliot Lake U mines in 1996 (Mawhiney & Pitblado, 1999). Opportunities to resume U mining in the Elliot Lake region exist because new technologies have developed which may allow the low-grade ore to be more economically recovered. Attention to techniques to optimize REE extraction as a by-product of the U extraction will be beneficial.

Comprehensive electron probe micro-analyzer (EMPA) and optical mineralogy studies by Sylvester (2007) and Spasford et al. (2012) have identified the principal U-, Thorium (Th)-, and REE-bearing minerals in the Elliot Lake area conglomerates. Pitchblende (Th, REE-poor UO_2) and brannerite (UTi_2O_6) have been identified as the principal host minerals for U in the region (Sylvester, 2007), with the REEs-bearing minerals identified in the host material by these studies being listed in Table 6.2.

Table 6.2 Principal minerals carrying REE in Elliot Lake area conglomerate identified by Sylvester (2007) and Sapsford (2012).

Mineral Phase	Chemical formula
Primary phases	
Monazite (Th rich)	(Ce, La, Y)PO_4
Allanite	(Ca,REE)$Al_2Fe(SiO_4)(Si_2O_7)O(OH)$
Secondary alteration phases	
Pitchblende	(Th, REE poor)UO_2
Florencite	(REE)$A1_3(PO_4)(OH)_6$
Xenotime	YPO_4
Silicified monazite	Mz-Silicate

A proposed approach for the recovery of low-grade U and the REEs from the ferrous sulphide-containing quartz pebble conglomerate beds in the Elliot Lake region is by biogeochemical mineral dissolution. This natural process drives the solubilization of minerals which may contain other elements of interest from the mineralization zones, including U, Th, and REEs. The oxidation of pyrite is a cyclic, self-propagating process, described in Figure 6.1, taking place through a series of well-known reactions, beginning with the oxidation of ferrous sulphide minerals (Kleinmann, 1987; Evangelou & Zhang, 1995; Fernandes & Franklin, 2001; McIlwaine & Ridd, 2004).

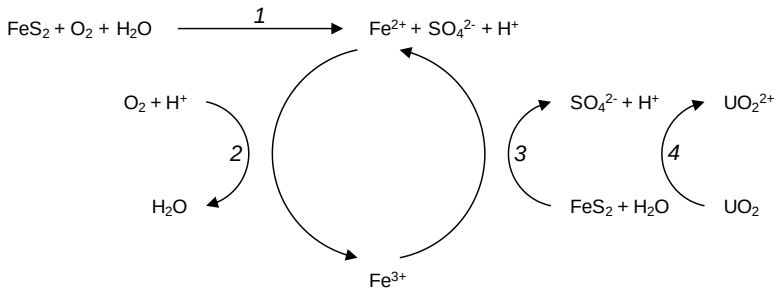

Figure 6.1 Schematic diagram illustrating the biogeochemical mineral dissolution processes for pyrite and the relationship with U (Guay, et al., 1976; Kleinmann, 1987; Evangelou & Zhang, 1995; Fernandes & Franklin, 2001; McIlwaine & Ridd, 2004).

The process by which the elements U, Th, and the REEs also become soluble varies depending on both the chemistry of the leachate and on the chemical nature of the individual element. For example, U commonly exists as insoluble tetravalent U in mineral such as uraninite (UO_2). The oxidation of pyrite through the biogeochemical mineral dissolution process is known to create the geochemical conditions suitable for the dissolution of the associated U minerals by promoting the oxidation of U to the more soluble hexavalent state. In an effort to compete economically with higher-grade U deposits in Canada and Australia, biogeochemical mineral dissolution, applied to engineered heap leach piles in the Elliot Lake region, may be considered a promising passive technology for the recovery of U from the low-grade mineralization. Understanding the controls influencing the dissolution of REEs in a biogeochemical dissolution process can maximize the potential for a successful resumption of U mining in the Elliot Lake region by employing processes tailored to optimize REE recovery. The purpose of this current investigation is to complete a solid phase investigation to identify the REE-bearing mineral phases and to examine the dissolved phase chemistry after a biogeochemical leaching process to provide an understanding of the mineralogical and chemical controls on REE dissolution from the solid phase to provide an explanation of the selective release of REEs identified in Chapter 5. The development of an understanding of the controls on the dissolution of the REE from the solid phase at the laboratory scale has potential to contribute to the successful application of biogeochemical mineral dissolution as an extractive technology for application in the Elliot Lake region of Ontario.

6.2 Experimental Methods

Material

Fresh drill core was collected from the study site, Eco Ridge Mine Rare Earths and Uranium Project site, owned by Pele Mountain Resources Inc. (PMR), approximately 11 km east of Elliot Lake, Ontario (Figure 6.2). The ore minerals are hosted in a quartz-pebble conglomerate bed with a matrix of fine-grained quartz, feldspar and up to 15% pyrite (Sylvester, 2007). Uranium, Th, and REE-bearing primary and secondary minerals exist in the matrix, being concentrated in halos around the quartz pebbles.

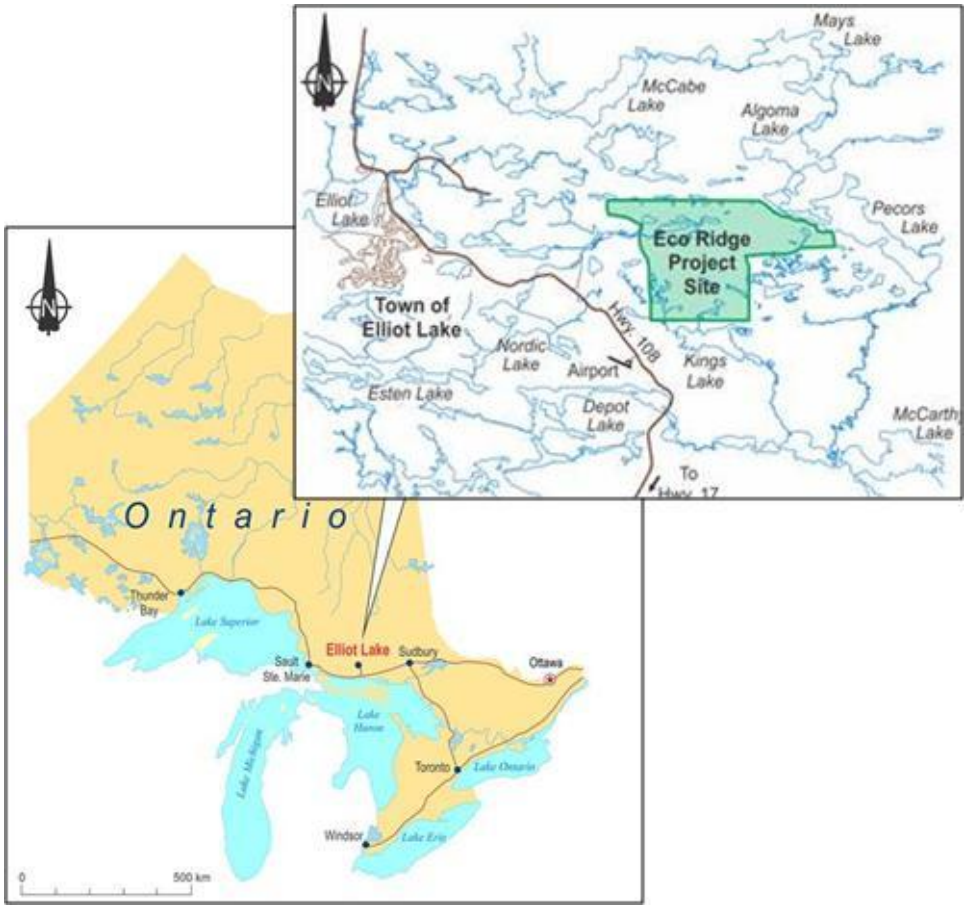

Figure 6.2 Location of Eco Ridge Mine Rare Earths and Uranium Project, east of Elliot Lake, Ontario (provided by PMR Ltd. 2013).

A sub-sample of the material was crushed to 2 to 4 cm in size using a large mouth jaw crusher, a head size with 65% passing < 5 cm, from which approximately 1 kg was further crushed to a head size with 53% passing < 2 mm (Figure 6.3). A representative sub-sample of homogenized material was examined

by X-ray diffraction (XRD), with the elemental composition being determined by spectroscopic analysis after acid digestion.

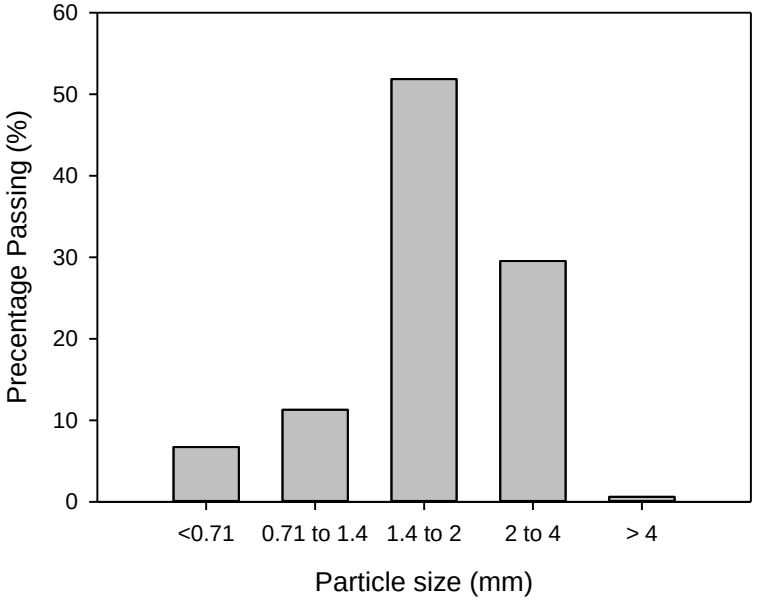

Figure 6.3. Particle size distribution of crushed mineral material used in small leaching columns.

Experimental Approach

Lucite columns (1.27 cm internal diameter), 90 cm tall were loaded from the bottom up with 2.5 mL of plastic beads (3 to 4 mm), 90 grams of mineral material, and another 2.5 mL of beads to mediate leachate flow distribution into the column. The bottom of each column was covered with nylon mesh (0.5mm) to retain the charge before being connected to a reservoir filled with 760 mL of DDI water. Fresh air was supplied with an air pump at the base of each column to ensure aerobic conditions were maintained throughout the columns (Nemati, et al., 1997). The treatment was designed to demonstrate a method of leachate application, which may be applicable for field scale. Solutions were supplied using a closed-loop system by continuous irrigation (Wadden & Gallant, 1985; Munoz, et al., 1993). The continuous irrigation simulations were fed with solution from a reservoir by peristaltic pump at 0.5 L hr^{-1}. After the first 24 hours of leachate application, reservoirs were inoculated with 10 mL of a microbe population representative of that expected at Eco Ridge previously cultured from the former tailings catchment area of Stanrock Mine, Elliot Lake.

Leachate samples were collected from reservoirs connected to the base of the columns using sterile syringes every two to fourteen days and filtered (0.45µm), and analyzed for pH, E_H, and dissolved metal concentration by ICP-MS. The bioleaching experiment was continued for approximately 7 months until the elemental cumulative release from the mineralized material reached a steady state. On completion of the leaching experiments the columns were carefully disassembled, with the residual material being air-dried and stored for future elemental and mineralogical analyses, and for decommissioning simulations.

Sample Analysis & Analytical Parameters

The pH was measured with a Thermo Orion 370 PerpHecT Ion Selective Benchtop Meter equipped with a glass electrode (Orion 8165BNWP ROSS Sure-Flow Epoxy Bodied Combination pH Electrode) and calibrated with pH 4 and pH 7 standard buffer solutions. The oxidation potential (E_H), corrected to the standard hydrogen electrode, was measured using a platinum combination electrode (Accumet 13-620-115 Platinum Pin Indicating Half-Cell Electrode) coupled with the calomel electrode (Accumet 13-620-52 Glass Body Calomel Reference Electrode) and calibrated with an oxidation-reduction potential standard (Orion 967901 ORP Calibration Standard).

Inductively coupled plasma mass spectrometry (ICP-MS), tuned, optimized and calibrated to operate under normal sensitivity mode, was used to analyze all leachate samples (Varian 810). The analysis was completed in an ISO 17025 accredited facility, Elliot Lake Research Field Station at Laurentian University. The quality control program included the analysis of duplicates, certified reference materials (CRM), internal reference material (IRM), and water blanks. Internal standards (Re and Ru) were used to correct for any mass bias and provide for continuous calibration verification (CCV). Prior to analysis, all experimental samples were filtered (0.45 µm) and diluted (1:10) with DDI. Samples collected from multi acid digests and leaching studies are reported as mg kg^{-1}, allowing the dissolution efficiency to be calculated by Equation 6.1.

Equation 6.1 $$\text{Dissolution Efficiency (\%)} = \frac{\text{Concentration dissolved } \left(\frac{\text{mg}}{\text{kg}}\right)}{\text{Solid phase concentration } \left(\frac{\text{mg}}{\text{kg}}\right)} \times 100\%$$

Sulphate (SO_4^{2-}) concentration, determined by ion chromatography (Wang, 2001) required a high dilution factor, thus preventing the quantification of other anions. Total elemental concentration of the mineral material before and after leaching was measured by ICP-MS analysis after acid digestion of the material. To ensure samples used represented an accurate sub-sample of the material, a riffle splitter was used to produce subsamples. After grinding to 74 µm using an agate ball mill, a 0.5 g sample was digested in an open 50 mL Teflon™ centrifuge tube using a programmable digestion block (Questron Q-Block 4200) according to the following steps:

- 10 mL of HF/HCl (1:1) and evaporated dryness at 110 ℃ for 3.5 hours;
- 14 mL HCl/HNO3 (1:1) and evaporated dryness at 110 ℃ for 4 hours; and
- 12.5 mL of HF/HCl/HNO3 (1:4:20) and heated to 110 ℃ to reduce sample volume to 8 to 10 mL.

After digestion, ultrapure water was added to bring the total volume in each tube to 50 mL for subsequent analysis. The samples were then diluted (1:10) and analyzed by ICP-MS. All concentrations were calculated in mass per mass dry mineral basis.

Powdered samples (74 µm), were prepared from fresh mineral. Powder X-ray diffraction (XRD) was completed using a Philips PW 1729 X-ray diffractometer at an accelerating voltage of 40kV and current of 30 mA using Co Kα (0.179 nm) radiation. Diffraction patterns from powder samples were collected over a scan range of 5 to 75° 2θ with a step size of 0.02° 2θ and dwell times of 4 to 10 seconds. Mineral identification was completed using X'Pert HighScore Plus (PANalytical, version 2.2.).

Gravity separation using sodium polytungstate solution (SPT) (Carver, 1971; Callahan, 1987) was used to separate powdered mineral samples (74 µm) based on specific gravity (SG) to separate lighter minerals phases, including quartz, to facilitate identification of the U, Th, and REE-bearing mineral phases by

XRD. Ten (10) mL of SPT solution, adjusted to SG of 2.90 g cm^{-3} (Sahin, et al., 2009) with distilled water, was added to 5 grams of the mineral sample in centrifuge tubes which were vortexed for three minutes to ensure sufficient dispersion of the mineral sample in the SPT solution prior to centrifugation for 6 min at 3,000 RPM (Morrow & Webster, 1989). After resting for at least 48 hours, the bottom of the centrifuge tube was frozen using liquid nitrogen and the top, unfrozen part was decanted and filtered to collect the light mineral fraction. After thawing, the bottom part was decanted and filtered to collect the heavy fraction (Morrow & Webster, 1989). Both fractions were washed with DDI water, followed with an acetone rinse to dry the mineral sample.. The heavy mineral phase was analyzed by XRD to enable mineralogical identification.

Electronoptical and microchemical examination of the mineral samples was completed using a SEM, (JEOL 6400) with an operating voltage of 20 kV and a beam current of 1 nA using backscattered electron (BSE) and secondary electron microscopy. Both fresh and leached samples (2 mm top size) were mounted in an epoxy resin prior to coarse polishing with 400, 600, and 1000 grit grinding powder (Buehler) in polishing oil on a smooth glass surface. The final polish being completed with aluminum oxide powder (Buehler) suspended in oil on a polishing pad. Phase identification was accomplished using X-ray spectrometry (EDS) for quantitative chemical analysis (Oxford Instruments Analytical Limited). Data analysis and image manipulation was completed using INCA software (v. 4.15) by Oxford Instruments Analytical Limited.

6.3 Results

Solid Phase Analysis

The content of the elements of economic and environmental interest in this study, namely iron (Fe), U, Th, Sc, Y, and REEs, is shown in Table 6.3. As the samples were carefully homogenized and split with a riffle splitter prior to sub-sampling for analysis the large standard deviations (SD) documented for some elements suggest a large variation in the distribution of the host heavy minerals in the ore.

Table 6.3 Elemental composition of head grade quartz-pebble conglomerate ore ± standard deviations, in parenthesis (n=13).

Element	Head grade (mg kg^{-1})	
Sc	3	(0.5)
Ti	3,400	(300)
Fe	23,000	(9000)
Y	45	(9)
La	300	(50)
Ce	590	(100)
Pr	53	(8)
Nd	180	(30)
Sm	30	(4)
Eu	2	(0.2)
Gd	25	(4)
Tb	3	(0.4)
Dy	11	(2)
Ho	2	(0.4)
Er	4	(0.9)
Tm	1	(0.1)
Yb	3	(0.7)
Lu	0	(0.1)
Th	340	(70)
U	310	(100)

The diffractogram obtained for the light mineral separate (SG < 2.90 g cm^{-3}) of the fresh ore material displayed in Figure 6.5 indicates the fraction is dominated, in order of relative abundance, by quartz, feldspar, and mica.

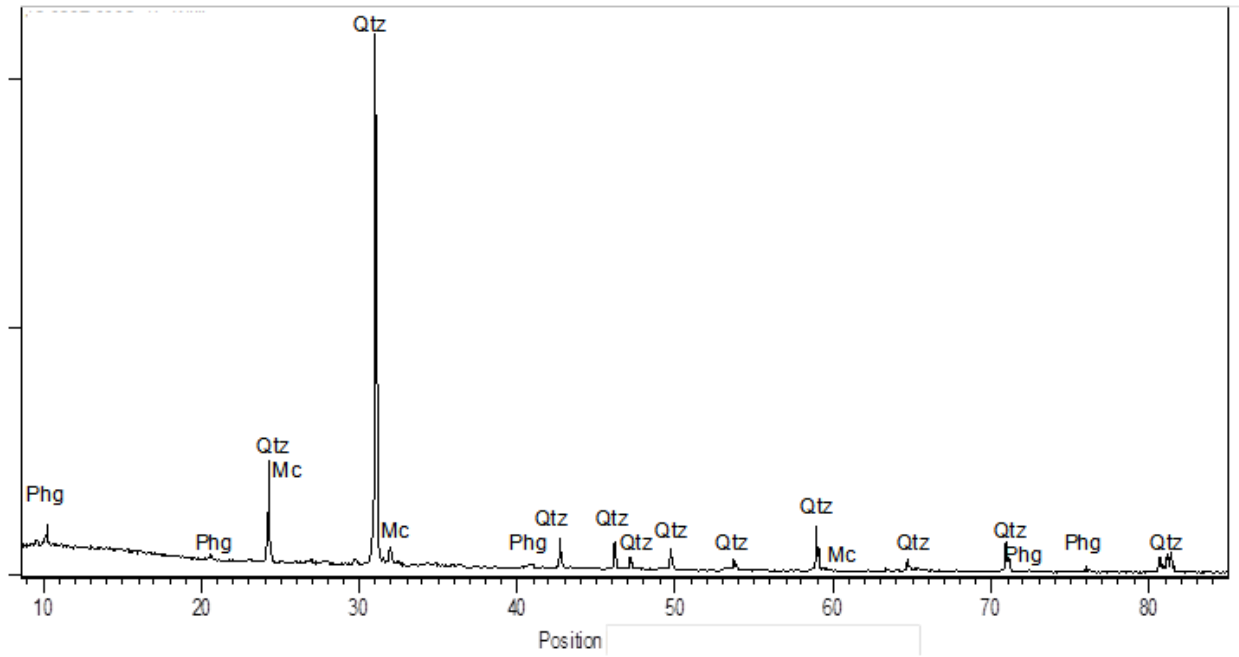

Figure 6.4 Powder x-ray diffraction pattern for the light fraction (SG < 2.90 g cm^{-3}) of fresh ground material (<74 µm) suggesting quartz (Qtz), microcline (Mc), and phengite (Phg).

The diffractogram of the heavy mineral separates (SG > 2.9 g cm^{-3}) shown in Figure 6.5 confirms the presence of pyrite, rutile, monazite, and uraninite in the mineral sample.

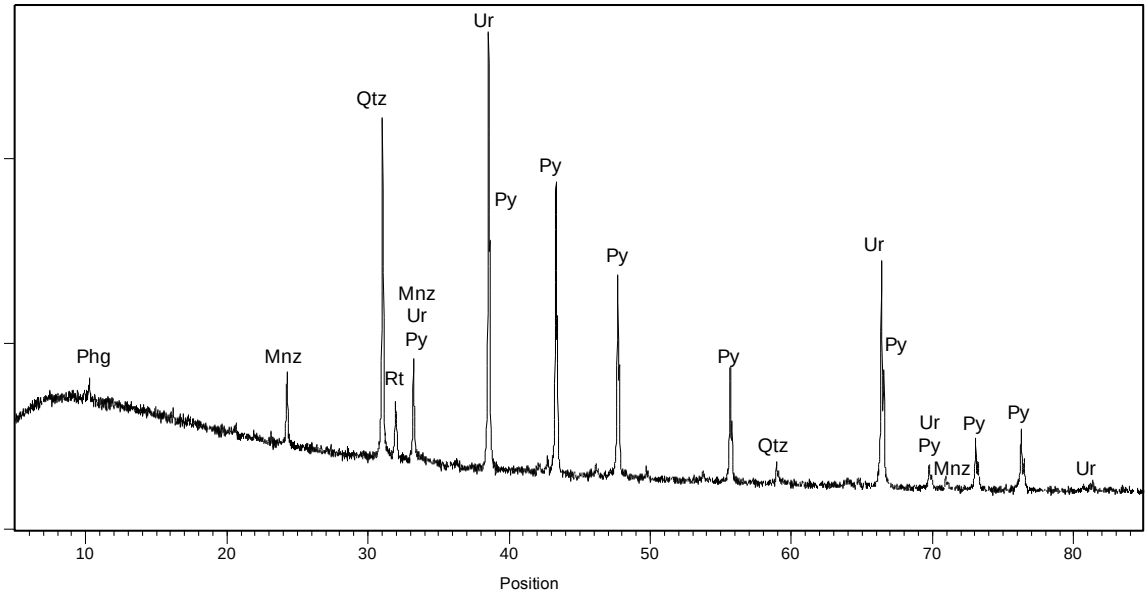

Figure 6.5 Powder x-ray diffraction pattern for the heavy fraction (SG > 2.90 g cm-3) of fresh ground material (<74 µm) suggesting pyrite (Py), rutile (Rt), monazite (Mnz), and uraninite (Urn).

Interestingly, the uraninite and monazite are the only phases identified in the current powder diffraction analysis of the heavy mineral fraction of the ore sample also identified in the EMPA and optical

mineralogy studies by Sylvester (2007) and Spasford et al. (2012). The absence of other detrital and secondary phases listed by these authors may reflect their very low abundance in the heavy separates as XRD best quantifies crystalline material to approximately >5% of sample.

The mineral phase analysis of the polished mineral materials by SEM-EDS further confirmed the presence of the mineral phases identified by XRD analysis, with indications of associations of REE's with other detrital phases such as rutile and pyrite. Elemental distribution maps highlight the distribution of selected elements through the mineral phases and assist in identifying phase boundaries. The BSE images of U-, Th and REE- bearing minerals, together with the associated elemental distribution maps and EDS spectra are shown in Figure 6.7 to Figure 6.13.

The BSE image and elemental distribution maps Figure 6.6 suggest that the bright grain, approximately 240 µm long and 100 µm wide, is a Th-enriched uraninite (Th-Urn) with cerium phosphate (monazite) intergrowth and as well as other REE mineral phases suggested by the elemental distribution maps. Other primary mineral phases indicated by the relative elemental concentrations are quartz, pyrite, and feldspar.

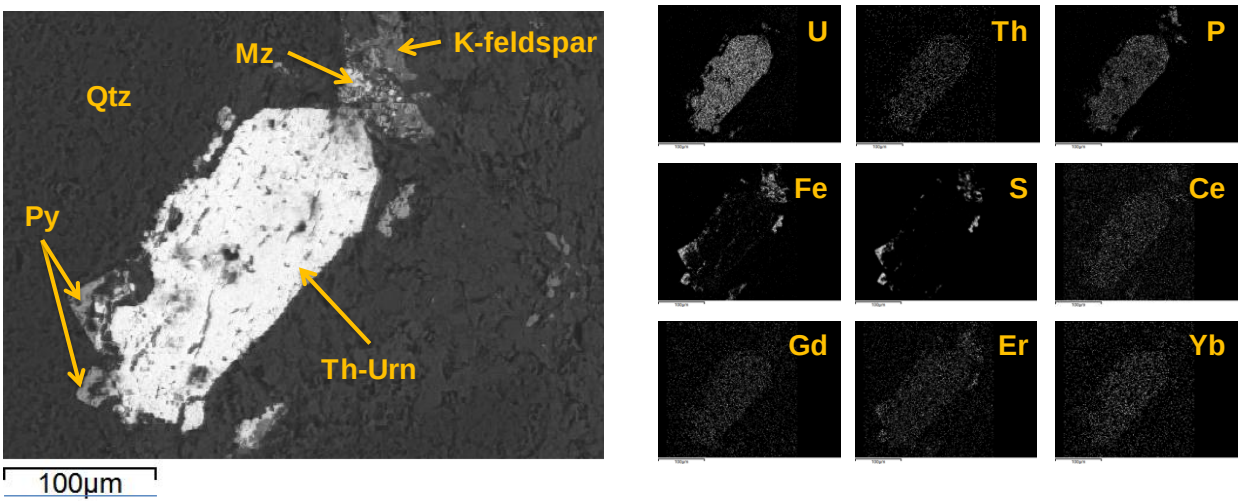

Figure 6.6 BSE images and EDS distribution maps indicating thorium-enriched uraninite with cerium phosphate (monazite) intergrowth BSE image from a fresh mineral sample (2-4 mm) with elemental distribution maps suggesting Th enriched-uraninite, feldspar, quartz, and pyrite.

The corresponding EDS spectra support these suggestions, with trace mineral phases being identified by the microchemical analysis including a Ce-monazite phase and K-feldspar (Figure 6.7).

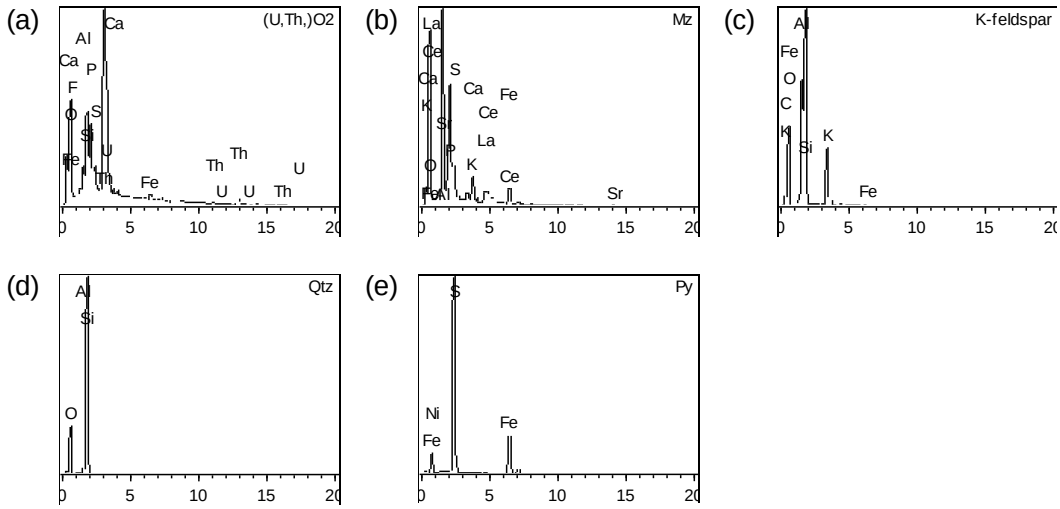

Figure 6.7 EDS spectra corresponding to the BSE image in Figure 6.6 indicating: (a) Th enriched-uraninite, (b) monazite, (c) K-feldspar, (d) quartz, and (e) pyrite.

The elemental distributional maps suggest that the bright grain in the BSE image in Figure 6.8 is a monazite, rich in Ce, La, and Nd, with zones of elevated U content being also evident, which s surrounded by quartz.

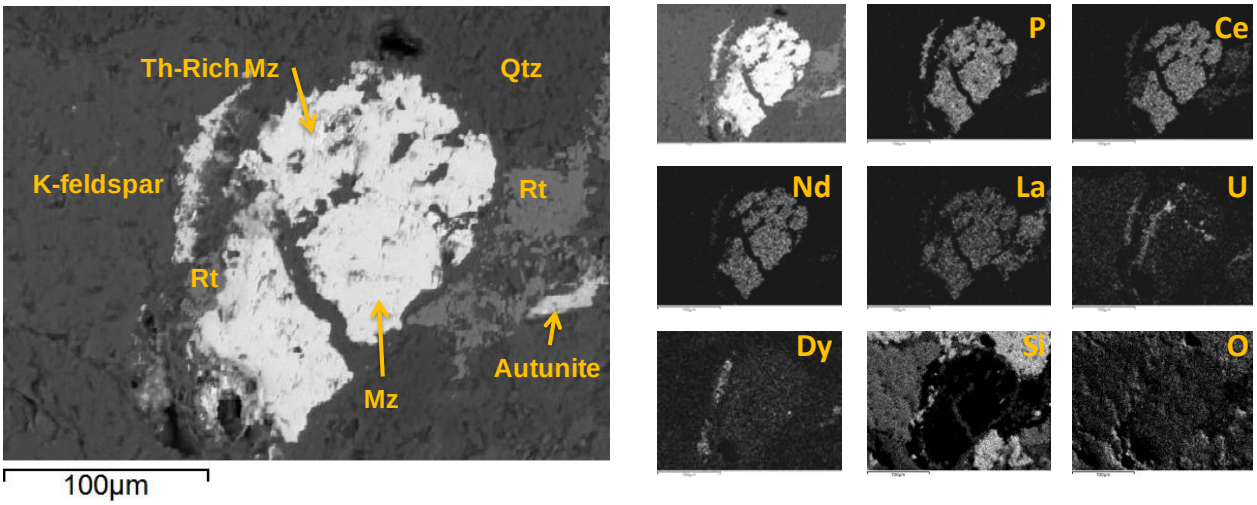

Figure 6.8 BSE image from a fresh mineral sample (2-4 mm) with elemental distribution maps suggesting monazite, quartz, and U-enriched monazite.

The corresponding EDS spectra support the identification of monazite, U-enriched monazite, and quartz (Figure 6.9a-c) in the ore material. Also identified by the EDS spectra is the titanium (Ti) mineral rutile (Figure 6.9d), the light grey phase, spanning 30 µm by 130 µm at the widest points, located to the right of the monazite grain, which shows association with La in the elemental distribution maps (Figure 6.8). The groundmass matrix surrounding the main monazite grain is mainly quartz, with a K-feldspar grain being

identified (Figure 6.9e), located on the right hand side of the BES image (Figure 6.8). Finally, a calcium (Ca) uranyl-phosphate phase of approximately 35µm in length, observed as a brighter phase further right of the rutile phase (Figure 6.8), is possibly autunite, being indicated by the EDS spectrum (Figure 6.9f) together with the calculated elemental ratio of U:Ca: P.

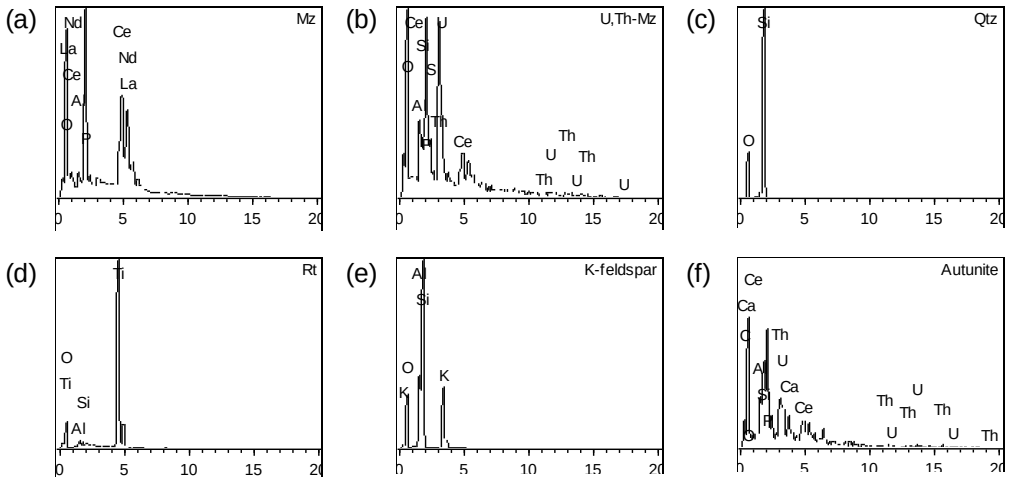

Figure 6.9 EDS spectra corresponding to the BSE image in Figure 6.8 indicating: (a) monazite, (b) U- and Th-enriched monazite, (c) quartz, (d) rutile, (e) K-feldspar, and (f) autunite.

Monazite exists in the samples as either individual grains, as described above (Figure 6.8), or as halos separating two distinct phases The elemental distribution maps show the separation of quartz and apatite, a Ca phosphate mineral, by a band of monazite approximately 5 µm in width (Figure 6.10).

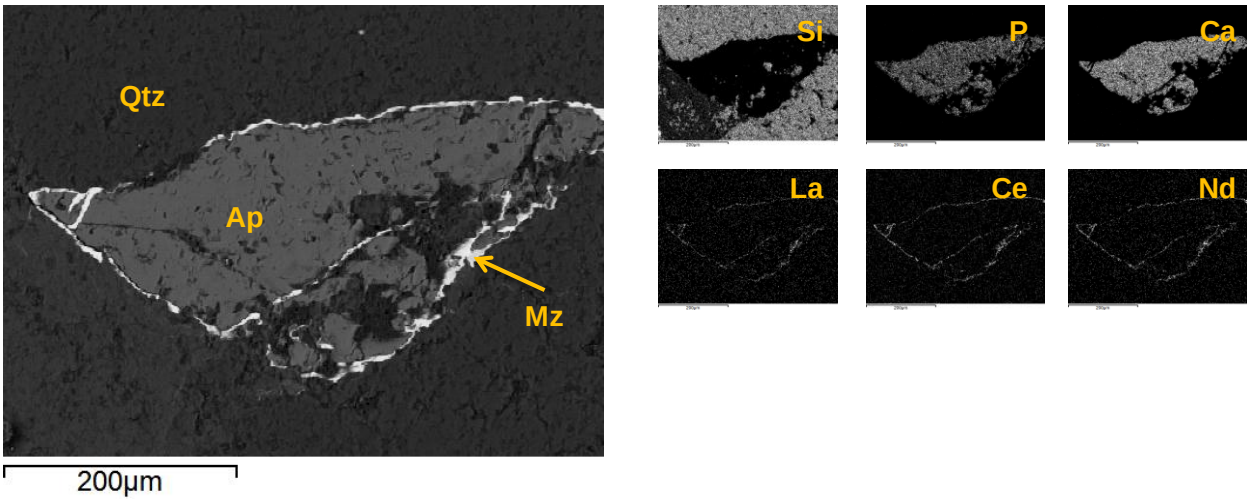

Figure 6.10 BSE image from a fresh mineral sample (2-4 mm) with elemental distribution maps suggesting apatite, monazite, and quartz.

EDS spectra collection at points in each phase indicated in the BSE image above provides quantitative support for the mineral phase identifications of apatite, monazite, and quartz (Figure 6.11).

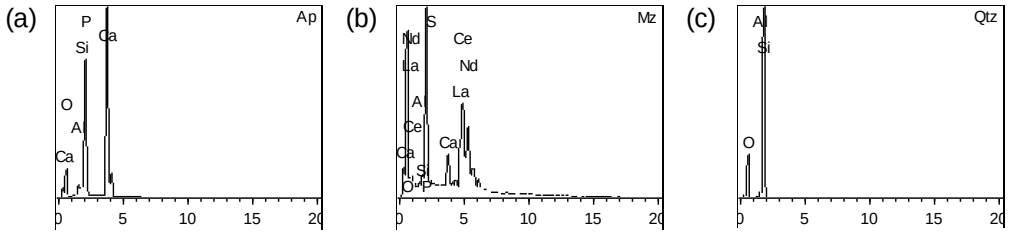

Figure 6.11 EDS spectra corresponding to the BSE image in Figure 6.10 indicating: (a) apatite, (b) monazite, and (c) quartz.

The BSE image, together with the elemental distribution maps in Figure 6.12, shows the association of specific REEs with rutile or pyrite. The elemental distribution maps indicate the light REEs (La, Ce, and Pr) are associated with the rutile phase, the darker grey phase in the middle of the frame which measures approximately 280 by 320 µm at the widest points. The heavy REEs (Tb, Dy, and Er) appear to be associated with pyrite, the lighter grey phase on either side of rutile. Feldspar phases are highlighted in the matrix, with epoxy below the lower feldspar in the BSE image.

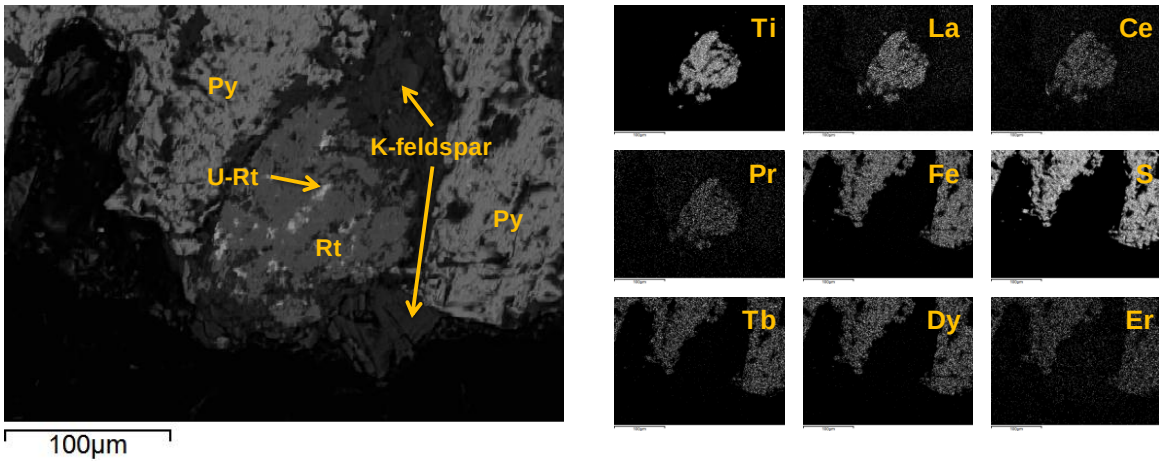

Figure 6.12 BSE image from a fresh mineral sample (2-4 mm) with elemental distribution maps suggesting rutile and pyrite.

The EDS spectra for the complex rutile grain provide evidence of a U-enriched rutile phase within the main grain (Figure 6.13a and b). The EDS spectra confirm the presence of pyrite and K-feldspar phases. (Figure 6.13c and d). The concentrations of REEs mapped in association with both rutile and pyrite are low, as their presence is not strongly evident in the qualitative EDS spectra.

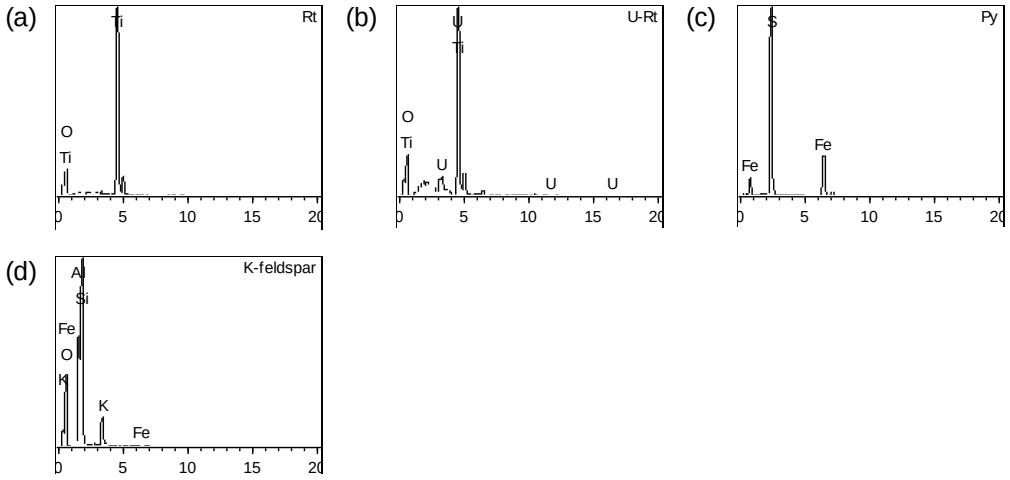

Figure 6.13 EDS spectra corresponding to the BSE image in Figure 6.12 indicating: (a) rutile, (b) uraniferous-rutile, (c) pyrite, and (d) K-feldspar.

Dissolved Phase Characterization

As the leaching process continued, the pH of the leachate decreased and the E_H increased (Figure 6.14). The pH dropped to 1.5 after 4 months of leaching and then increasing to 2.7 with the addition of fresh solution to the reservoirs to replace losses from sampling or evaporation. After 7 months of leaching, the leachate pH had dropped to 1.9. The oxidizing potential increased immediately in the first week of experimental leaching, from 0.6 V to 0.8 V, with fluctuations between 0.81 and 0.88 V for the remainder of the experimental period, with a slight decrease on fluid replacement after 4 months of leaching, with the range of fluctuation in E_H decreasing.

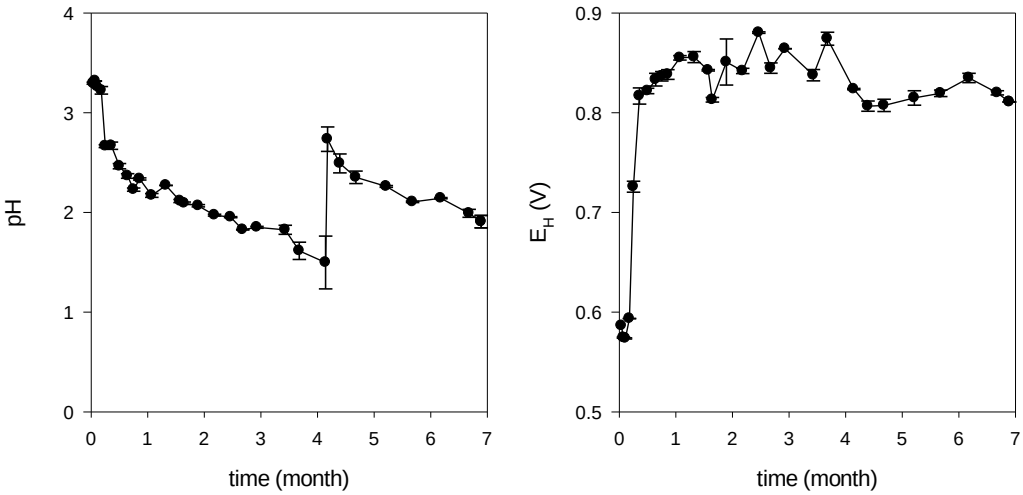

Figure 6.14 Time profiles during 7 months of leaching displaying the changes in pH (left) and E_H (right) from the simulated ore leaching process.

Under the environmental conditions generated during the biogeochemical mineral dissolution of pyrite in the columns, the entrained U^{6+} species becomes oxidized, which results in the subsequent dissolution of the soluble, U^{4+} species. The total dissolution of U from the ore materials was achieved in the inoculated columns (Figure 6.15), a result suggesting that the conditions generated by the experimental biogeochemical dissolution of pyrite promoted the oxidation of U in the uraninite structure, with release as uranyl ions to the leachate solutions. A dissolution efficiency over 100% is has been reported for U, calculated according to Equation 6.1. As a large variation exists for the concentration of U in the solid phase has been reported (310±100 mg kg^{-1}), the sample a dissolution efficiency over 100% may be reported for samples that contain a higher concentration of U mineral phases.

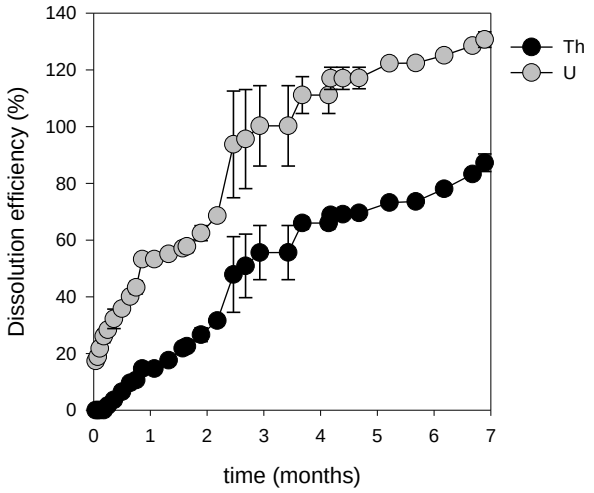

Figure 6.15 Time profiles during 7 months of leaching displaying the dissolution efficiency of Th and U from the simulated ore leaching process.

The cumulative dissolution of Fe and Ti during the biogeochemical leaching experiments is shown in Figure 6.16. The major potential source of these elements in the original ore material is in the minerals pyrite (Fe) and rutile (Ti), shown above to have distinctive REE association patterns. The biogeochemical mineral dissolution of pyrite contributes to the decrease in leachate pH and to the stabilization of E_H around 0.8 V, which together results in an increase in the concentration of dissolved Fe in the liquid phase. Under the described experimental conditions, the cumulative dissolution of Fe was 78%. The cumulative dissolution of Ti, however, was 0%, further confirming the resistance of rutile dissolution under the oxic low pH conditions common to near-surface biogeochemical mineral dissolution processes.

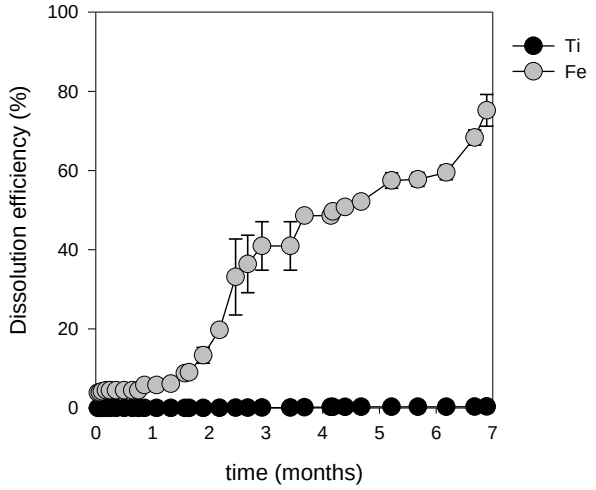

Figure 6.16 Time profiles during 7 months of leaching displaying the dissolution efficiency of Ti and Fe from the simulated ore leaching process.

The cumulative dissolution efficiency for the heavy REEs (35 to 95%) is much greater than for the light REEs (12 to 25%), illustrated in Figure 6.17. The dissolution pattern for Sc is similar to the light REEs (Figure 6.17a), while the dissolution pattern for Y corresponds to the heavy REEs, as expected (Figure 6.17b).

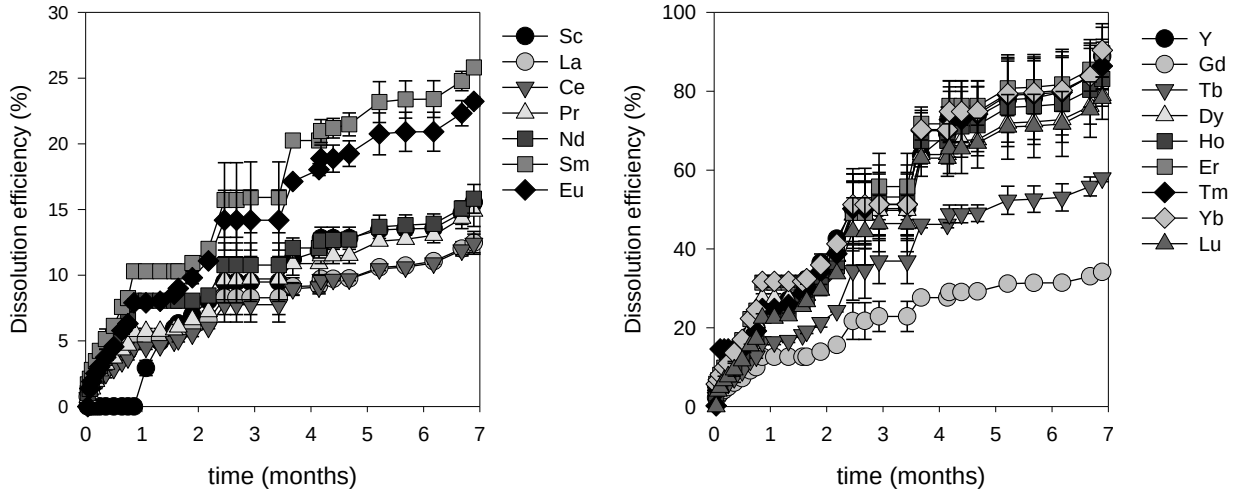

Figure 6.17 Time profiles during 7 months of leaching displaying the dissolution efficiency of Sc and light REEs (left) and Y and heavy REEs (right) from the simulated ore leaching process.

6.4 Discussion

The principal U-bearing mineral phases identified in the low-grade ore materials examined in this biogeochemical dissolution study are uraninite, Th-rich uraninite, uraniferous rutile, and autinite. With the exception of the autinite phase, each of these phases has been identified in previous regional

mineralogical investigations (Sylvester, 2007; Sapsford, et al., 2012). Rare earth element mineral phases are commonly associated with uraninite-based phase, as such, they are expected to become available to solution under the influence of the biogeochemical mineral dissolution process. Monazite is a major host mineral for the light REEs, although REE phases have been observed with rutile minerals as well. As the lack of Ti in the recirculating solutions in this study confirmed the relative insolubility of the rutile, the dissolution of monazite is obviously the major contributor of light REEs into the dissolved phase. Heavy REEs-bearing mineral phases associated with pyrite, the mineral phase responsible for driving the biogeochemical mineral dissolution process in many geological materials, are expected to be released to the leaching solution following the oxidation of pyrite. The presence of monazite and pyrite in the conglomerate beds from the Elliot Lake region has been identified in previous investigations (Sylvester, 2007; Sapsford, et al., 2012).

The chemical composition of the leachate solutions plays a major role in controlling the solubility of many mineral species in contact with the solutions. The biogeochemical mineral dissolution of pyrite generates acidic, sulphate-rich solutions which are known to control the dissolution of U, Th, Y, and REEs (Sapsford, et al., 2012). The controls on the dissolution of U and Th are discussed in Chapter 5.

The association of heavy REE-bearing minerals and pyrite was described above, with the observations suggesting that the dissolution of pyrite will contribute to the dissolution of the pyrite-associated heavy REEs-bearing phases. The light REEs-bearing minerals were found to be in association with the Ti-mineral, rutile, and monazite, a soluble light REE-containing phosphate mineral. Kim and Osseo-Asare (2012) explain the dissociation of REE phosphates as a two-step process in a strong sulphuric acid media, with a transition first from a REE-phosphate to a REE-sulphate (Reaction 6.1), which dissolves to release the metal ions to the solution phase (Reaction 6.2).

Reaction 6.1 $$2(REE)(PO_4)_{(s)} + 3SO_4^{2-} \rightarrow (REE)_2(SO_4)_{3(s)} + 2PO_4^{3-}$$

Reaction 6.2 $$(REE)_2(SO_4)_{3(s)} \cdot nH_2O \rightarrow 2\mathrm{REE}^{3+} + 3SO_4^{2-} + nH_2O$$

The dissolution of monazite, a REE phosphate mineral, may be best described by examination of the predicted aqueous stability of the REE ions using a pH-E_H diagram for the REE-phosphate-water system (Kim & Osseo-Asare, 2012). The dissolution of La, Ce, and Nd is expected in the phosphate-sulphate system in acidic conditions (Figure 6.18a-c). The leaching efficiency of Ti, contained in the mineral rutile, was effectively zero, indicating that (bio)geochemical mineral dissolution of rutile, and REEs within the mineral structure, did not take place under the experimental conditions.

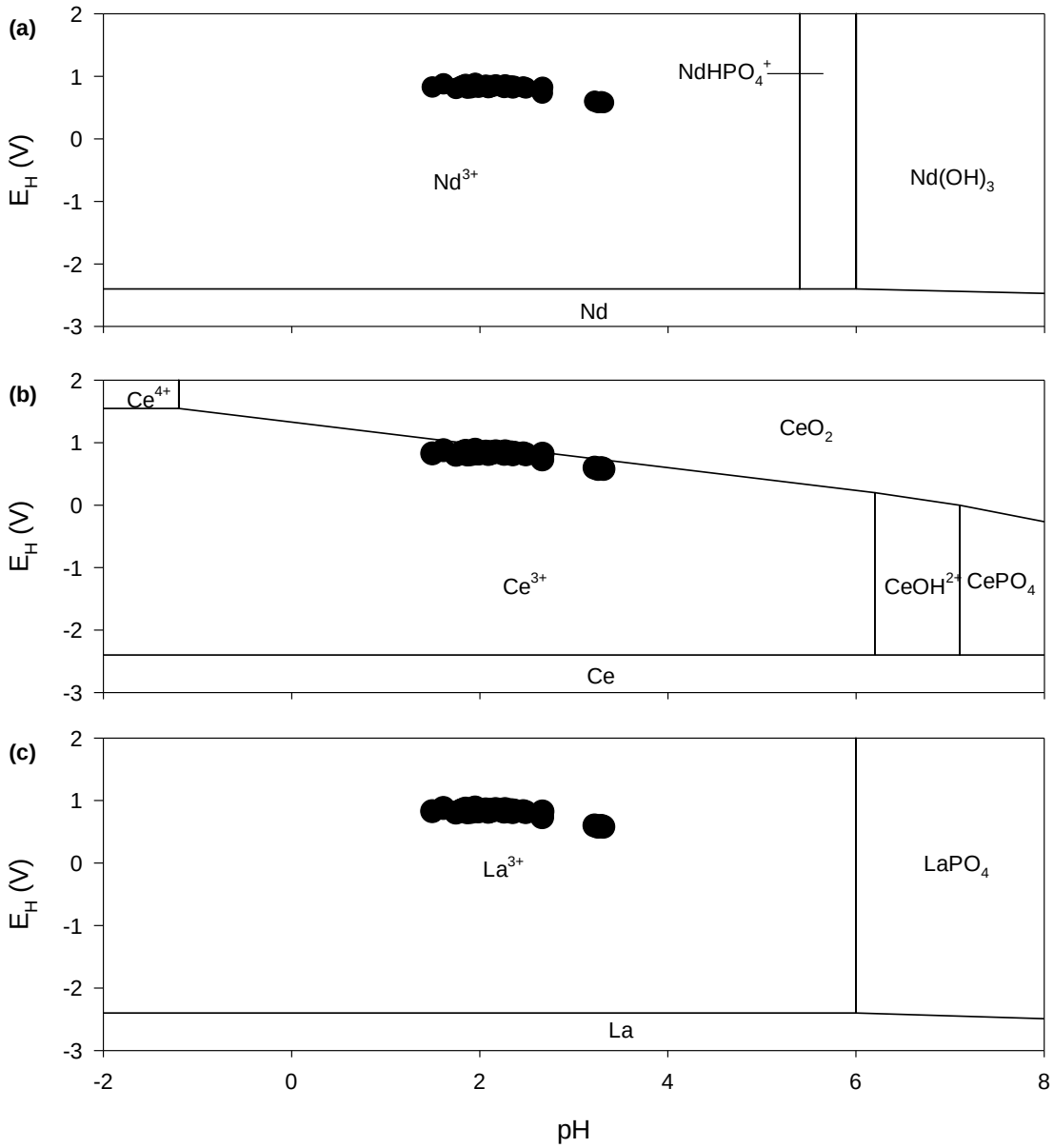

Figure 6.18 Pourbaix diagram for: (a) Nd-PO_4-H_2O, (b) Ce-PO_4^{2-}-H_2O, and (c) La-PO_4^{2-}-H_2O systems under standard condition, modified from Kim and Osseo-Asare (2012); experimental samples indicated.

The relationships of the REEs and major mineral phases may be further investigated by examining the leaching rates for each individual element and compared with the release rates of the major elements contained in the examined the mineral phases (Figure 6.19). Leaching rate, calculated as the mass of the element released per mass of sample per day, is reported to decrease for all elements over time. This observation suggests that a critical point in time exists, beyond which, at an industrial scale, continuation of the leaching process to release critical elements may not be economically beneficial. For example, after four months the change in leaching rate of Fe is effectively zero, a rate representative of a system with

equilibrium between the solid and liquid phases. The REEs have very similar leaching rate profiles, beginning with a very high leaching rate that decreases exponentially for the first two months of the leaching process. Beyond this time, the leaching release rate for all the REEs is low and continues to decrease.

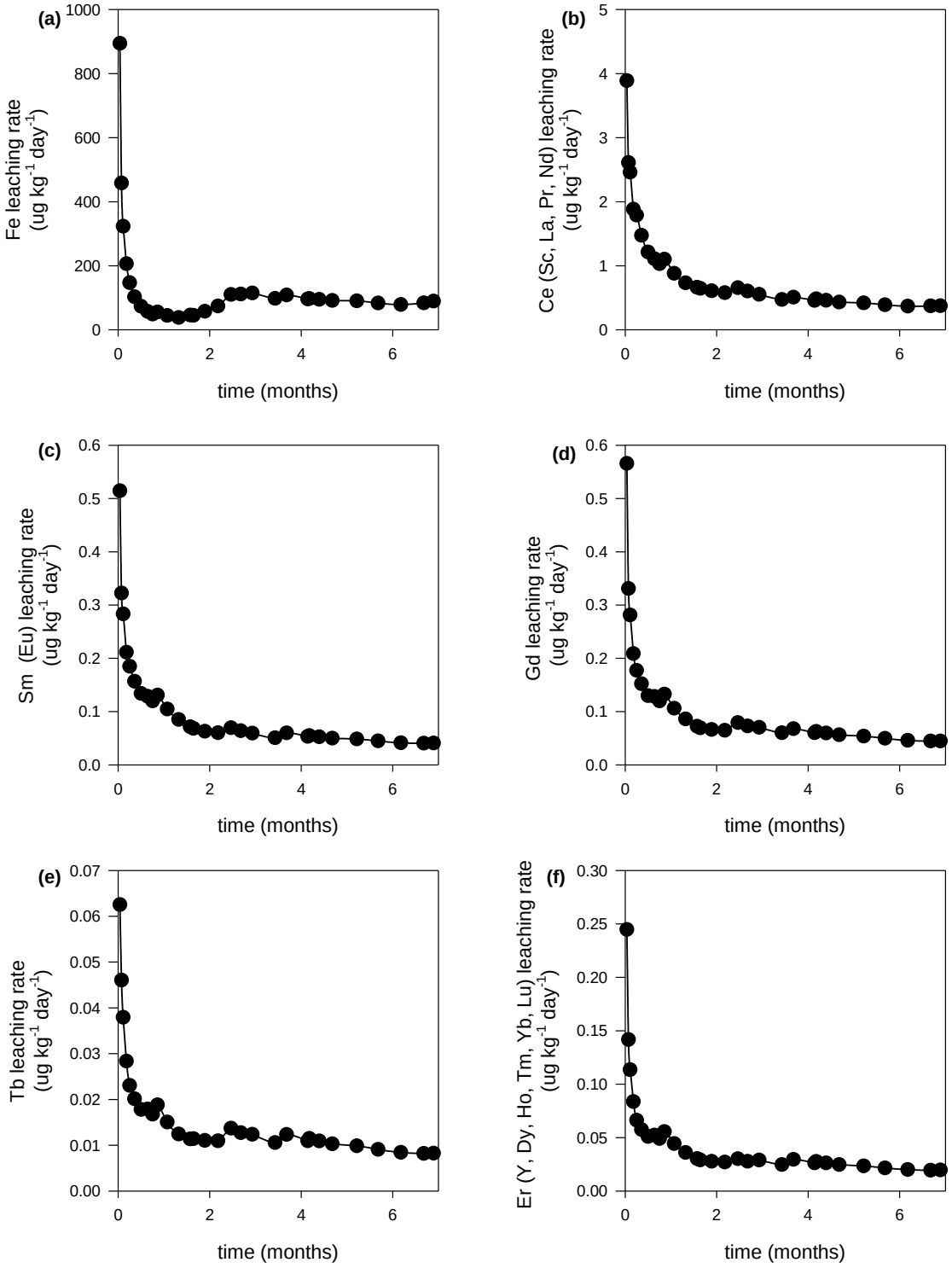

Figure 6.19 Time profiles during 7 months of leaching displaying the leaching rates from the simulated ore leaching process: (a) Fe, (b) Ce, (c) Sm, (d) Gd, (e) Tb, and (f) Er; elements with similar rates are noted in parenthesis.

6.5 Conclusion

The U-bearing mineral phases identified in the samples collected from the quartz-pebble conglomerate beds for this study are uraninite, Th-rich uraninite, uraniferous rutile, and autinite. Under the environmental conditions established by the biogeochemical mineral dissolution process, it is expected that REE-bearing mineral phases associate with uraninite-based mineral phases will be available to the leaching liquid. Monazite, also present in the quartz-pebble conglomerate bed, is the major host mineral to release the light REEs to the dissolved phase in the conditions of this study, with light REEs-mineral phases associated with the insoluble rutile phase not likely to become dissolve in the leaching solution. The heavy REEs are associated with pyrite, the mineral responsible for driving the biogeochemical mineral dissolution process with the associated production of acidity and release of sulphate ions to the percolating solutions.

As the biogeochemical mineral dissolution process continues, E_H increases to create chemical conditions favorable for the oxidation of tetravalent U in the solid phase. This well understood process provides the chemical processes to supply an economic foundation when considering the return of U mining activities to the Elliot Lake region. Accumulation of sulphate ions in the percolating solutions contributes to a decrease of pH, leading to the dissolution of monazite which, in turn, releases light REEs into the dissolved phase. The biogeochemical dissolution of pyrite releases associated heavy REEs into the dissolved phase, reflecting the association of the heavy REEs micro-zones with the ferrous sulphide mineralization. Rutile, on the other hand, is stable under the oxidizing, low pH leaching conditions, with release of the entrained REEs by leaching from this mineral phase not expected to contribute greatly.

The results of this biogeochemical, mineralogical, and microchemical study provide the critical information to demonstrate that the natural biogeochemical processes induced in the leaching system itself are sufficient to promote the dissolution of U and most REEs contained in the mineral phases of the quartz-pebble conglomerate beds of the Elliot Lake region. Increased recovery of the heavy REEs from the ore may be attained on further investigation of the geochemical controls of the rutile dissolution

processes. At the operational scale, identification of the critical point in time beyond which leaching rates slow to a point that any further dissolution of REE is insignificant will be critical for the potential economic viability of the operations. Conversely, the possibility of designing a leaching protocol to further optimize the dissolution of REEs to support the return to mining in Elliot Lake, the former U capital of Canada, may be feasible.

CHAPTER 7

7 Retention Mechanism of Uranium in (Hydr)oxide Coatings after Biogeochemical Dissolution

7.1 Introduction

The biogeochemical leaching of target minerals results in reaction products that promote the dissolution of other minerals from the host minerals. Biogeochemical dissolution for the recovery of uranium (U) has previously been assessed at sites in Elliot Lake, Ontario (McCready, 1986; Campbell, et al., 1987; McCready & Gould, 1990; Olson, et al., 2003), with a recent renewed interest in U and rare earth elements (REEs) bringing a focus back to the former U-mining camp. In an effort to compete economically with higher-grade deposits, the potential to apply biogeochemical mineral dissolution processes to engineered heap leach piles in the Elliot Lake region may be considered as a promising passive technology for the recovery of U from the low-grade mineralization. Williamson et al. (2014) reported an U extraction efficiency of 84% using biogeochemical dissolution methods applied to samples collected from the Elliot Lake region, indicating that 16% of the total U remains insoluble or is retained in secondary phases which may or may not remain stable.

Iron (Fe)-sulphide minerals are of fundamental importance to the bioleaching process as their oxidation controls the pH and oxidizing potential of the solution. The rate of the oxidation process is significantly increased in the presence of iron oxidizing microorganisms (Singer & Stumm, 1970; Marchand & Silverstein, 2003; Johnson, 2010). Under oxidizing conditions, ferrous sulphide minerals are oxidized, liberating ferrous iron (Fe^{2+}) and sulphuric acid to the immediate environment (Reaction 7.1). Ferrous iron is, in turn, oxidized by molecular oxygen (Reaction 7.2) to liberating ferric iron (Fe^{3+}) which then

oxidizes additional ferrous-sulphide minerals (Reaction 7.3). The continuous oxidation and reduction of iron is a cyclic, self-propagating process (Kleinmann, et al., 1981).

Reaction 7.1 $$FeS_2 + \frac{7}{2}O_2 + H_2O \rightarrow Fe^{2+} + 2SO_4{}^{2-} + 2\,H^+$$

Reaction 7.2 $$Fe^{2+} + \frac{1}{4}O_2 + H^+ \rightarrow Fe^{3+} + \frac{1}{2}H_2O$$

Reaction 7.3 $$FeS_2 + 14Fe^{3+} + 8H_2O \rightarrow 15Fe^{2+} + 2SO_4{}^{2-} + 16H^+$$

A common U mineral is uraninite (UO_2). The recovery of U from low-grade mineralization containing uraninite using traditional methods is challenging because the mineral has a low solubility (Lundgren & Silver, 1980). When a strong oxidizing agent is present, such as Fe^{3+}, the U in uraninite is oxidized to the hexavalent oxidation state, which forms soluble uranyl compounds (Reaction 7.4).

Reaction 7.4 $$UO_2 + 2Fe^{3+} \rightarrow UO_2^{2+} + 2Fe^{2+}$$

Rock forming silicate minerals are chemically weathered to clay minerals under near weak acidic to weak basic conditions and to amorphous silica under acidic conditions (Brantley, 2005). The release of $Al(OH)_{3-x}{}^{x+}$ species under the latter conditions often results in the precipitation of aluminum (Al)-hydroxides or Al-rich clay minerals such as imogolite ($Al_2SiO_3(OH)_4$) or allophone ($(Al_2)_3{\cdot}(SiO_2)_{1.3\text{-}2}{\cdot}H_2$) (Childs, et al., 1983). When acidic conditions are formed as a result of biogeochemical mineral dissolution of ferrous sulphide minerals, the concomitant dissolution of aluminosilicates, including potassium (K)-feldspars, takes places (Reaction 7.5). The formation of amorphous silica, by dehydration of H_4SiO_4, and Al-hydroxide is not a direct result of biogeochemical mineral dissolution, but rather due to the geochemical environmental conditions created by the bacterial oxidation process (Bigham & Nordstorm, 2000). The formation of secondary Al phases, including gibbsite, kaolinite, and Al-rich clays form as outlined in Reaction 7.6 and Reaction 7.7. The oxidation of Fe-sulphidic minerals in the presence of a K^+ source results in the precipitation of jarosite (Reaction 7.8) Ferric iron, liberate by the

biogeochemical dissolution process, and alkali metals, leached from the clay minerals (Reaction 7.5 to Reaction 7.7) according to Dutrizac and Jambor (2000)..

Reaction 7.5 $$KAlSi_3O_{8_{(s)}} + 4H^+ + 4H_2O \leftrightarrow Al^{3+} + 3H_4SiO_4 + K^+$$

Reaction 7.6 $$KAlSi_3O_{8_{(s)}} + H^+ + 7H_2O \leftrightarrow Al(OH)_{3_{(s)}} + 3H_4SiO_4 + K^+$$

Reaction 7.7 $$KAlSi_3O_{8_{(s)}} + H^+ + 4.5H_2O \leftrightarrow 0.5Al_2Si_2O_5(OH)_{4_{(s)}} + 2Si(OH)_4 + K^+$$

Reaction 7.8 $$3Fe^{3+} + K^+ + 2SO_4{}^{2-} + 6H_2O \leftrightarrow KFe_3(SO_4)_2(OH)_6 + H^+$$

Aluminum-rich phases have been found in uranium tailings of Elliot Lake mines as a result of highly acidic processing methods, which remove natural alkalinity of the mineralization (Feasby, 1997) . Tailings left exposed continued to generate acid through pyrite oxidation, thus mobilizing U, Fe, Th, and Al through the processes described above. Alumns, alunite, and aluminosilicate phases have been identified within sulphate-rich uranium tailings in Elliot Lake that contain high concentration dissolved Al species (Markos & Bush, 1982).

The purpose of the current investigation is to describe the retention mechanism of U in secondary precipitates formed on mineral surfaces during and after biogeochemical dissolution processes involving pyrite and uraninite. According worldwide best practice, when extractable resources are exhausted at a mining site, processed tailings, waste rock piles, and spent heap leach pads must be treated to control or remove all potential environmental liabilities, including radionuclide release to the environment. The results of this study will be useful to determine and guide management of the long term stability of U remaining in retired bio-heap leach piles. If the concentration of U in the waste pile is less that 40 mg kg^{-1} (approximately equal to 1 Bq g^{-1}) a Canadian Nuclear Safety Commission license would no longer be required and the material would no longer require institutional control, but rather be considered for permanent storage(International Atomic Energy Agency, 2004).

7.2 Experimental Methods

Fresh drill cores samples obtained from the Eco Ridge study site located approximately 11 km east of Elliot Lake, Ontario (Figure 7.1) were crushed to 2 to 4 cm in size and homogenized, with approximately 1 kg of this material being further crushed to 1 to 2 mm diameter and placed in leucite leaching columns (internal diameter of 1.27 cm) for a series of bioleaching trials executed by Williamson et al. (2014) to examine the viability of the biogeochemical mineral dissolution process.

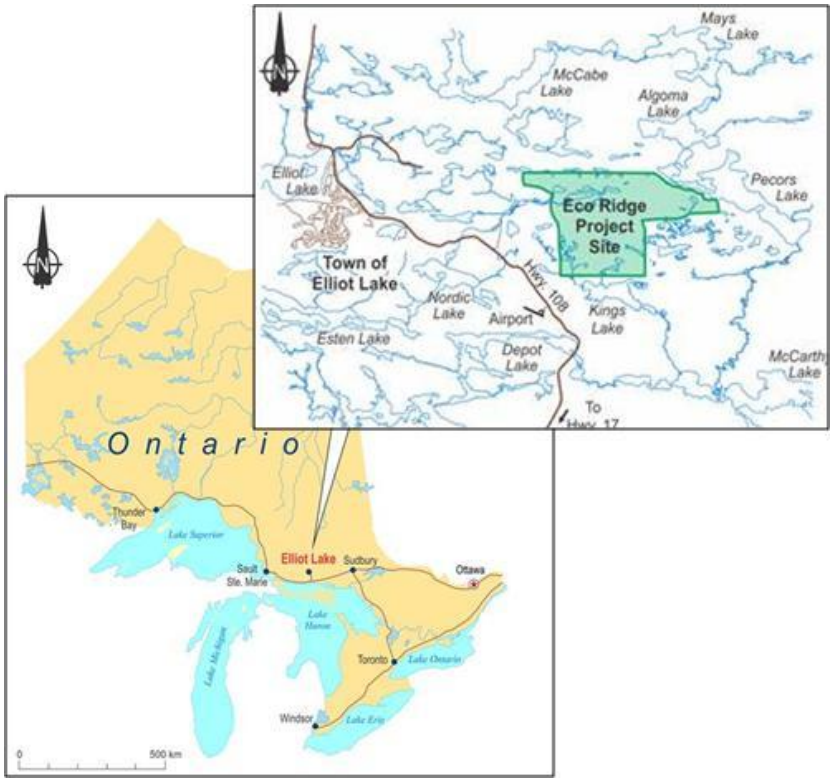

Figure 7.1 Location of Eco Ridge Mine Rare Earths and Uranium Project, east of Elliot Lake, Ontario (provided by PMR Ltd. 2013).

A local microbial population was cultured from water samples collected from the former tailings catchment area of the Stanrock Mine, Elliot Lake. After the crushed ore material was leached for 7 months in the presence of the microbe population, residue samples were collected from the columns, dried, homogenized, and divided for subsequent analysis and experimentation.

Sample Analysis & Analytical Parameters

The pH was measured with a Thermo Orion 370 PerpHecT Ion Selective Benchtop Meter equipped with a glass electrode (Orion 8165BNWP ROSS Sure-Flow Epoxy Bodied Combination pH Electrode) and calibrated with pH 4 and pH 7 standard buffer solutions. The oxidation potential (E_H), corrected to the standard hydrogen electrode, was measured using a platinum combination electrode (Accumet 13-620-115 Platinum Pin Indicating Half-Cell Electrode) coupled with the calomel electrode (Accumet 13-620-52 Glass Body Calomel Reference Electrode) and calibrated with an oxidation-reduction potential standard (Orion 967901 ORP Calibration Standard).

Chemical analyses

Inductively coupled plasma mass spectrometry (ICP-MS), tuned, optimized, and calibrated to operate under normal sensitivity mode, was used to analyze all leachate samples (Varian 810). The analysis was completed in an ISO 17025 accredited facility, Elliot Lake Research Field Station, at Laurentian University. The quality control program included the analysis of duplicates, certified reference materials (CRM), internal reference material (IRM), and water blanks. Internal standards (Re and Ru) were used to correct for mass bias, and to provide for continuous calibration verification (CCV). Prior to analysis, all experimental samples were filtered (0.45 µm) and diluted (1:10) with DDI. Samples collected from multi acid digests and leaching studies are reported as mg kg^{-1}, allowing the dissolution efficiency to be calculated by Equation 7.1.

Equation 7.1

$$\text{Dissolution Efficiency (\%)} = \frac{\text{Concentration dissolved } \left(\frac{\text{mg}}{\text{kg}}\right)}{\text{Solid phase concentration } \left(\frac{\text{mg}}{\text{kg}}\right)} \times 100\%$$

Total elemental concentration of the mineral material before and after leaching was measured by ICP-MS analysis of solutions obtained after acid digestion of the material. To ensure samples used represented an accurate sub-sample of the material, a riffle splitter was used to produce subsamples. After grinding to 74 µm using an agate ball mill, a 0.5 g sample was digested in an open 50 mL Teflon™ centrifuge tube using a programmable digestion block (Questron Q-Block 4200) according to the following method:

- 10 mL of HF/HCl (1:1) and evaporated dryness at 110 ℃ for 3.5 hours;
- 14 mL HCl/HNO_3 (1:1) and evaporated dryness at 110 ℃ for 4 hours; and
- 12.5 mL of $HF/HCl/HNO_3$ (1:4:20) and heated to 110 ℃ to reduce sample volume to 8 to 10 mL.

After digestion, ultrapure water was added to bring the total volume in each tube to 50 mL for subsequent analysis. The samples were then diluted (1:10) and analyzed by ICP-MS. All concentrations were calculated in mass per mass dry mineral basis.

Scanning Electron microscopy (SEM)

Electronoptical and microchemical examination of the mineral samples was completed using a JEOL 6400 instrument employing an operating voltage of 20 kV and a beam current of 1 nA using backscattered electron (BSE) and secondary electron microscopy. Both fresh and leached samples (2 mm top size) were mounted in epoxy resin prior to coarse polishing with 400, 600, and 1000 grit grinding powder (Buehler) in polishing oil on a smooth glass surface, with the final polish being completed with aluminum oxide powder (Buehler) suspended in oil on a polishing pad. Phase identification was accomplished using X-ray spectrometry (EDS) for quantitative chemical analysis (Oxford Instruments Analytical Limited). Data analysis and image manipulation was completed using INCA software (v. 4.15) by Oxford Instruments Analytical Limited.

Geochemical calculations

Phreeqc v.3.0.6 (Parkhurst & Appelo, 2013) was used to calculate saturation indices for mineral phases and dissolved species molality using the pH, E_H, and chemical composition of the leachate sample collected during the final leaching cycle. Phreeqc was coupled with the Minteq thermodynamic database(Allison, et al., 1991).

Laser-Ablation ICP-MS

Trace element distributions and concentrations in coatings on the surface of pyrite grains after biogeochemical dissolution were quantified by laser ablation inductively coupled plasma spectrometry (LA-ICP-MS) using a New Wave Nd:YAG 213 nm laser coupled to a Thermo X II series ICP-MS. Multiple areas of interest on each grain were analyzed using line scans with 19 µm spot sizes, a repetition rate of 5 Hz and an energy density of 7 J cm^{-2}. The sample ablation was done in a He atmosphere, with Ar being mixed as the carrier gas before introduction into the plasma. The data output line scans were recorded and used to generate region maps. The synthetic glass standard NIST610, which contains a nominal trace element abundance of about 400 mg kg^{-1}, was used as the external calibration standard. At the beginning of each analytical run, intermittently during acquisition, and at the end of each sample, the standard was ablated under the same operating conditions. Detection limits for elements depend on the experimental setting of the laser scan and are listed for a similar experimental setting in Durocher and Schindler (2011).

The zones for collection of line scans were selected to traverse the cross-section of coated grains, beginning with the outer epoxy (labeled E in Figure 7.2a) and traveling through the coating towards the underlying mineral (labeled M in Figure 7.2a), and through the coating to the mounting epoxy on the other side of the grain. The selection of integration areas for quantification was conducted based on chemical differences between coatings and underlying grains. The breadth of each integration area was determined by monitoring the inflection points of the Fe, Al and Si peaks, and the peak for U, which effectively defined the boundary between the coating and the underlying mineral.

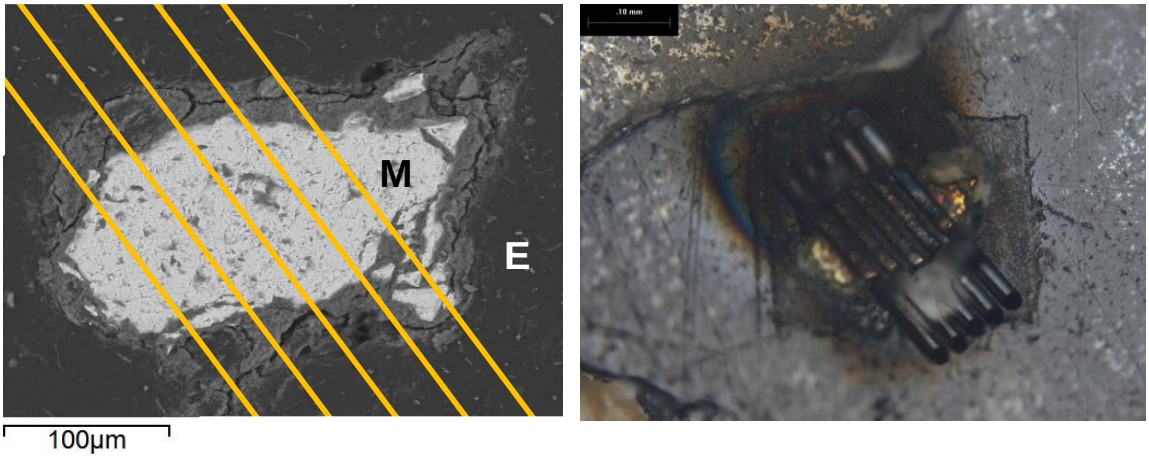

Figure 7.2 BSE image showing the placement of LA-ICP-MS line scans beginning with the outer epoxy (labeled E) and traveling through the coating towards the underlying mineral (labeled M) and through the coating to the epoxy on the other side of the grain (left) and the grain after LA-ICP-MS (right).

Laser Ablation ICP-MS data are commonly quantified by calibrating the counts per second (CPS) with respect to an internal standard as well as an external standard (e.g. NIST glasses). However, as the samples analyzed in this study were hydrous and heterogeneous, no single element was suitable as an internal standard and only the external standards were used. Elemental molar ratios were calculated from the counts and the known concentrations in the NIST glass, with elemental concentrations being calculated by normalizing molar totals to 100%, with the assumption that the samples are dominated by Fe, Si, Al, Ca, Na, and K (as observed by SEM-EDS). The mole-proportion of H_2O was estimated on the basis of the number of structurally bound H_2O groups associated with the Si, S, and Fe in phases identified in the coatings and potential amorphous phases commonly found in acidic systems. This procedure resulted in a semi-quantitative data set based on the uncertainty of the number of structurally bound H_2O groups per mole of Si, Fe, or S (±one H_2O group). This calculation resulted in an estimated error of <10% for the concentration of trace elements in an individual measurement.

7.3 Results

Mineral and chemical composition of sample before leaching

The content of elements of economic interest and environmental significance was determined by ICP-MS analysis after multi-acid digestion, summarized in Table 4.2. Representative samples of the whole ore were obtained following tumbling to homogenize, with use of a riffle splitter. The large standard

deviations obtained for the concentrations of some elements in the replicate samples suggest large variation in the distribution of heavy mineral grains within the ore material.

Table 7.1 Elemental composition of head grade quartz-pebble conglomerate ore ± standard deviations, in parenthesis (n=13).

Element	Concentration (mg kg^{-1})	
Economic Interest		
Sc	3	(0.5)
Y	50	(9)
La	300	(50)
Ce	590	(100)
Pr	53	(8)
Nd	180	(30)
Sm	30	(4)
Eu	1.79	(0.2)
Gd	30	(4)
Tb	2.7	(0.4)
Dy	11	(2)
Ho	1.8	(0.4)
Er	4.2	(0.9)
Tm	0.55	(0.1)
Yb	3.4	(0.7)
Lu	0.46	(0.09)
Th	340	(70)
U	310	(100)
Environmental Significance		
Ti	3400	(300)
Fe	23000	(9000)
Ni	20	(4)
Cu	78	(20)
Zn	24	(5)
As	13	(3)
Pb	68	(10)

The conglomerate beds at Eco Ridge are composed of 60 to 70% quartz, 10 to 20% orthoclase, 5 to 15% pyrite, 3 to 9% muscovite, and less than 1% U-, Thorium (Th)- and REE-bearing minerals, including Th-uraninite, monazite, and brannerite (Sylvester, 2007). The principal U, Th, and REEs bearing minerals

identified by electron probe micro-analysis (EMPA) and optical mineralogy studies of mineral material collected from the same geological region of the study site by Sylvester (2007) and Spasford et al. (2012) are listed in Table 7.2.

Table 7.2 Principal minerals carrying U, Th, and REEs is Elliot Lake area conglomerate identified by Sylvester (2007) and Sapsford (2012).

Mineral Phase	Chemical formula
Primary phases	
Th-enriched uraninite	UO_2
Monazite (Th rich)	(Ce, La, Y)PO_4
Thorite	(Th, U)SiO_4
Allanite	(Ca,REE)$Al_2Fe(SiO_4)(Si_2O_7)O(OH)$
Secondary alteration phases	
Coffinite	$U(SiO4)_{1-x}(OH)_{4x}$
Brannerite	UTi_2O_6
Uraninite	(Th, REE poor)UO_2
Florencite	(REE)$A1_3(PO_4)(OH)_6$
Xenotime	YPO_4
Uraniferous rutile or leucoxene	UO_2–Rutile
Silicified monazite	Mz-Silicate
Very fine-grained intergrowth of pitchblende, pyrite and aluminium-rich silicate phase	UO_2–Pyr–AlSi-mix
Uraniferous pyrite	UO_2–Pyrite

The BSE image and elemental distribution maps Figure 7.3a suggest that the bright grain, approximately 240 µm long and 100 µm wide, is a Th-enriched uraninite (Th-Urn) with a cerium phosphate (monazite) intergrowth, with other REE mineral phases suggested by the elemental distribution maps. Other primary mineral phases indicated by the relative elemental concentrations are quartz, pyrite, and feldspar. The phosphate minerals phases show evidence for weathering of the minerals in the samples prior to leaching (Figure 7.3b), with the formation of a Fe-(hydr)oxide secondary phase on the surface of the weathered phosphate phase.

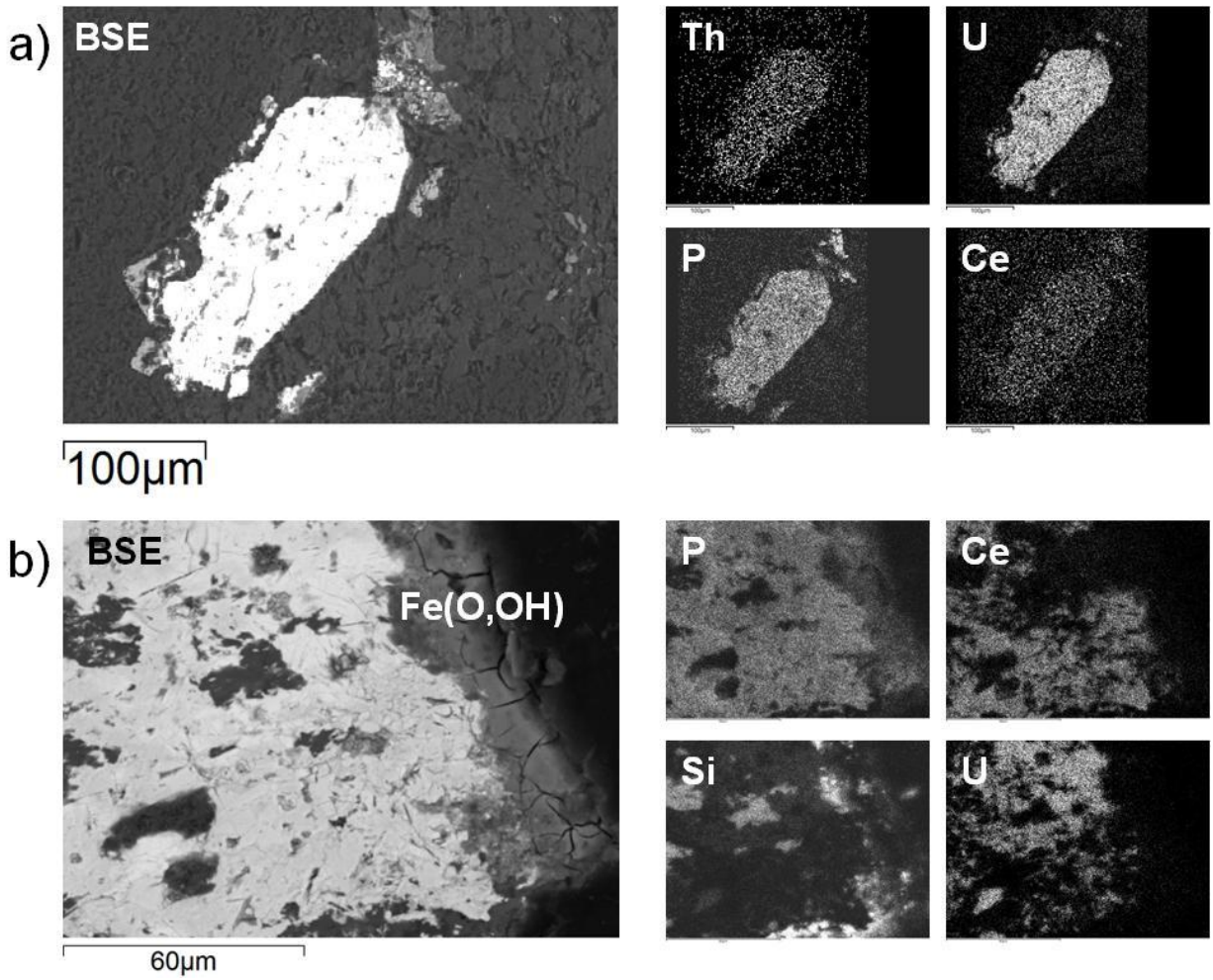

Figure 7.3 BSE images and EDS distribution maps indicating (a) thorium-enriched uraninite with cerium phosphate (monazite) intergrowth; and (b) formation of a Fe-(hydr)oxide secondary coating on the surface of the weathered phosphate phase .

The total S content of the mineralized material is 3.3% by, weight, occurring predominantly as pyrite, which is partially weathered to Fe-(hydr)oxides according to the corresponding alteration process under oxidizing conditions (Reaction 7.9).

Reaction 7.9 $$Fe^{3+} + 3H_2O \rightarrow Fe(OH)_3 + 3H^+$$

Mineral and chemical composition of a treated sample

Figure 7.4a-b show a BSE image and EDS maps for Fe, S, and Si showing an intergrowth feature of pyrite with quartz. The highly altered pyrite is partially replaced by an Fe(hydr)-oxide, especially along the quartz-pyrite interface. Al(hydr)oxide growth is suggested along the coating region, as indicated in the BSE image show in Figure 7.4c. Figure 7.4d shows the LA-ICP-MS transect beginning from the epoxy

traveling across the weathered pyrite phase into quartz, labeled A to B in Figure 7.4a. Line scan patterns for Fe and S clearly define sections associated with Fe(hydr)oxide coatings and pyrite, as well as a thin coating region. Elevated concentrations of P and trace elements exist in the Fe(hydr)oxide and thin coating region.

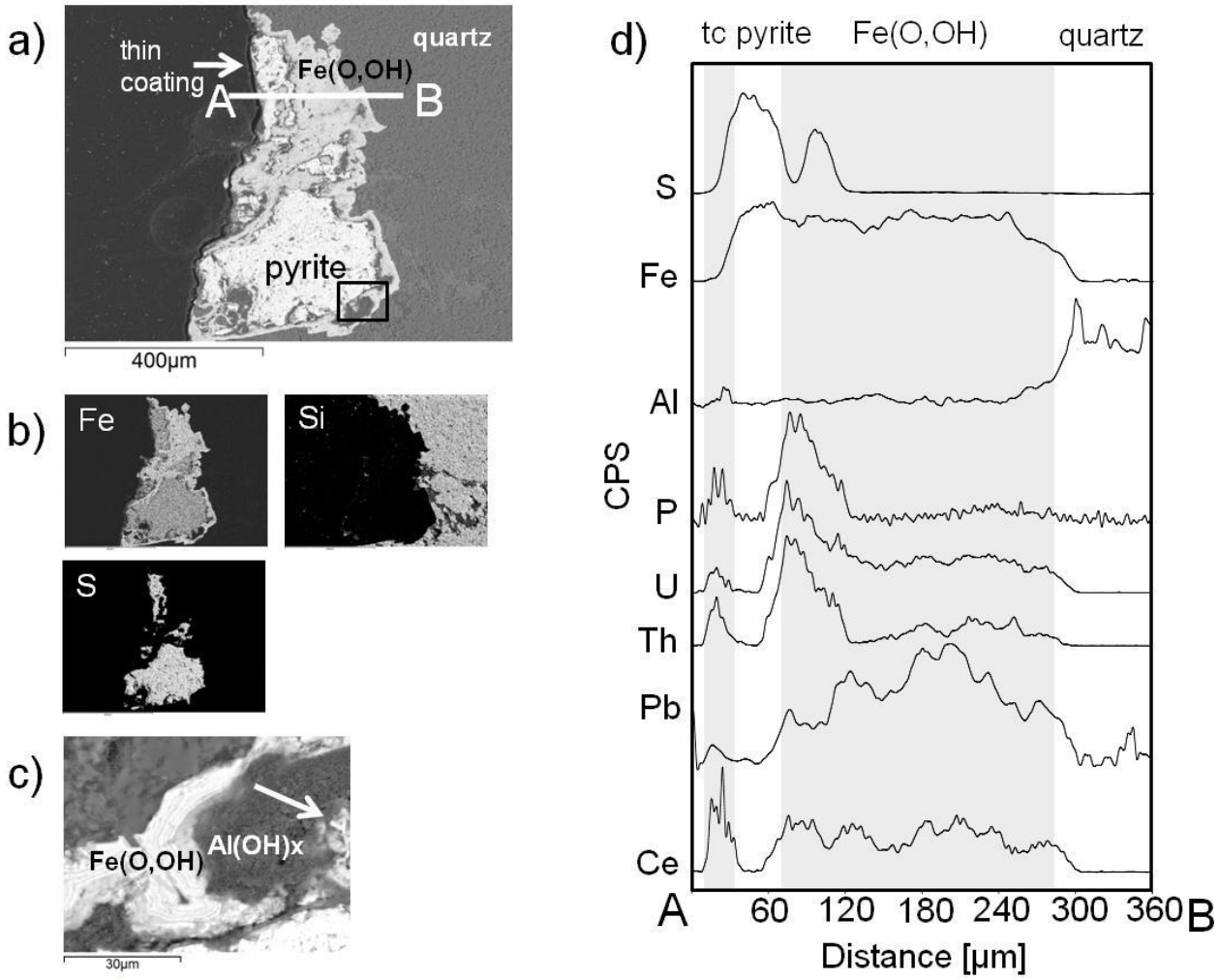

Figure 7.4 (a) BSE image of highly-altered pyrite and quartz with an Fe(hydr)oxide layer; (b) EDS distribution maps for Fe, Si, and S; (c) BSE Image of area indicated in 'a' showing Al(hydr)oxide inclusion in the coating; and (d) stacked plots of LA-ICP-MS line scans for S, Fe, Al, P, and selected trace elements across the A-B transect identified in 'a', with integration areas for thin coating (tc), pyrite, Fe-(hydr)oxide, and quartz indicated with shaded bars.

Chemical analyses of the bulk samples after treatment showed a decrease in concentrations of Al, Fe, and U of 5%, 43%, and 80%, respectively. Figure 7.5a-b show a BSE image and EDS maps for Fe, S, Al, and Si showing a highly weathered pyrite grain coated by Al(hydr)-oxide. The Al(hydr)-oxide coating occurs

with small amounts of Fe(hydr)oxide existing along the pyrite-coating interface, highlighted in the BSE image shown in Figure 7.5c. Figure 7.5d shows the LA-ICP-MS transect beginning from the epoxy, across weathered pyrite, ending with epoxy, labeled A to B in Figure 7.5a. Line scan patterns for Fe, S, and Al clearly indicated regions associated with Al(hydr)oxide coatings and pyrite, with elevated concentrations of P and trace elements exist in the Al(hydr)oxide coating region.

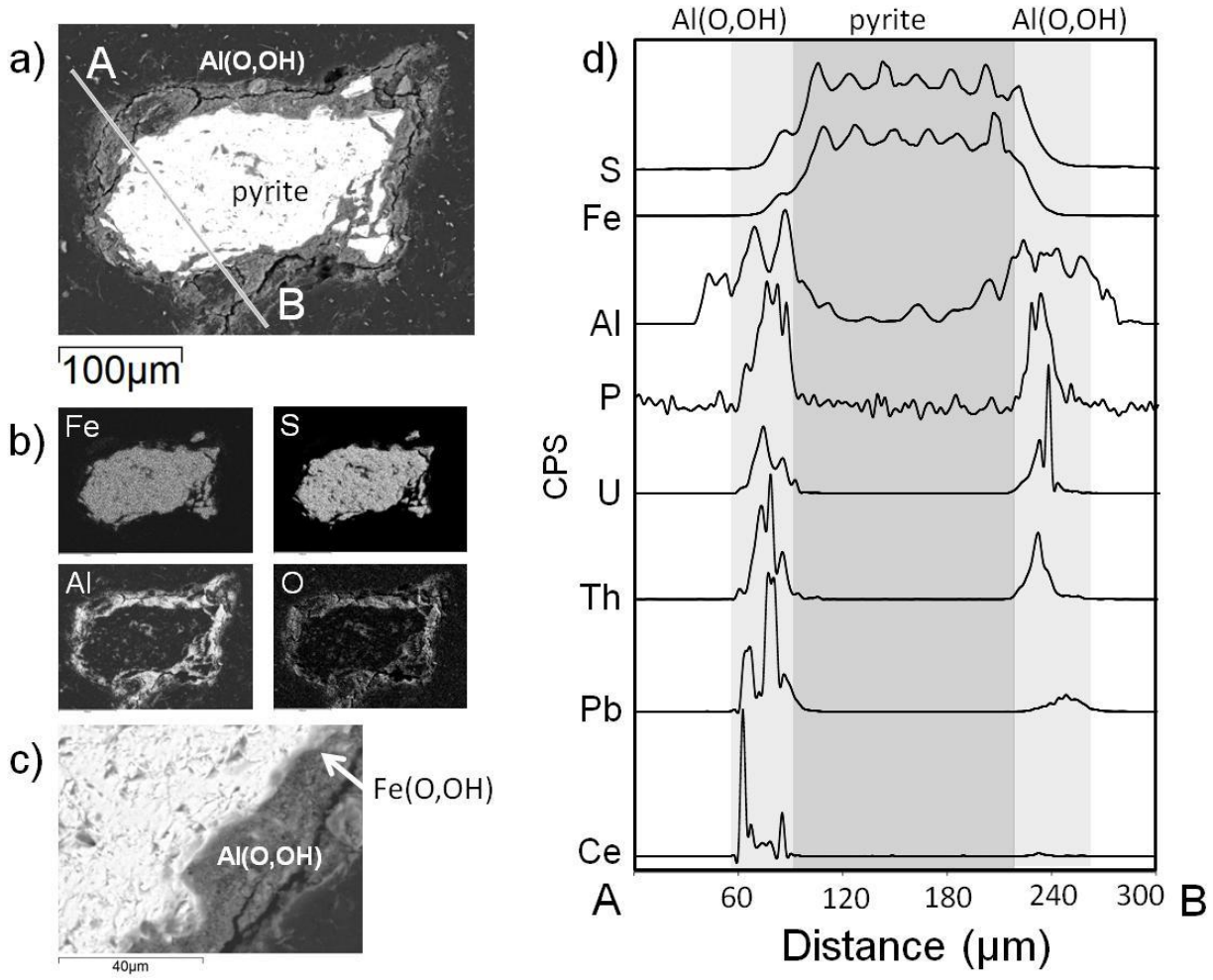

Figure 7.5 (a) BSE image of highly-altered pyrite with an Al(hydr)oxide layer; (b) EDS distribution maps for Fe, Si, Al, and S; (c) BSE Image of area indicated in 'a' showing Fe(hydr)oxide inclusion at the pyrite-coating interface; and (d) stacked plots of LA-ICP-MS line scans for S, Fe, Al, P, and selected trace elements across the A-B transect identified in 'a', with integration areas for pyrite, and Al(hydr)oxide indicated with shaded bars.

The ternary plot in Figure 7.4 indicates that the coating regions contain varying amounts of Al and Fe as well as Si, defining three distinct coatings regions: Al-Fe-Si-rich, Si-rich, and Fe-rich. This observation

suggests that natural weathering of pyrite produces Fe-(hydr)oxide coatings, consistent with the Fe-rich region, as observed in Figure 7.4. Under the acidic conditions promoting by the weathering of pyrite, rock forming silicate minerals are chemically weathered to form amorphous silica, the foundation for Si-rich coatings. Al becomes incorporated in to the coating with the mobilization of Al^{3+} species in acidic conditions possibly replacing Fe coatings, indicated by the large Al-Fe-Si rich region, as observed in Figure 7.4.

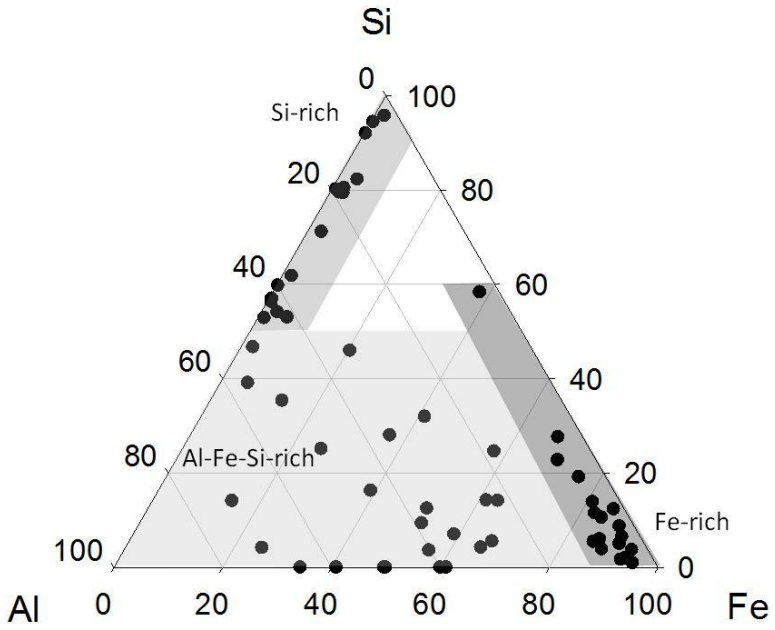

Figure 7.6 Ternary diagram of the normalized proportions of Si, Fe, and Al from LA-ICP-MS analysis in the coating regions; occurrences of different regions indicated by the shaded regions: Si-rich, Fe-rich, and Al-Fe-Si-rich.

Chemical composition of the leachate

The leachate solution was pH 2.1 ±0.1, with appreciable concentrations of Fe, Al, U, and S (see Appendix B). Geochemical calculations were completed with Phreeqc, using the leachate compositional chemistry for the sample collected on the final day of the biogeochemical mineral dissolution study was used to calculate the molarity of expected dissolved species and saturation indices (SI) for possible secondary phases (Table 7.3). The concentration of SO_4^{2-} is estimated based on the pH with H^+ as the major cation.

Table 7.3 Chemical composition of leachate samples collected on the final day of the biogeochemical mineral dissolution study.

Element	Chemical Composition	
pH	1.9	
pe	9.5	
Al	9	ppm
B	28	ppb
Cd	0	ppb
Cu	2	ppm
Fe	1057	ppm
Li	19	ppb
Mn	25	ppb
P	11	ppm
Pb	50	ppb
Sr	74	ppb
U	13	ppm
Zn	248	ppb
S^{6+}*	6.19×10^{-3}	mol kg^{-1}
Temp	25	ºC

The model predicted that soluble ionic species of Fe^{3+}, $Al^{3+,}$ UO_2^{2+}, and PO_4^{3-} are expected in the leachate (Table 7.4).

Table 7.4 Expected dissolved species, predicted by Phreeqc, for the sample described in Table 7.3.

Species	Molality (mol/kg)
Al^{+3}	2.63×10^{-4}
$AlSO_4^{+}$	9.54×10^{-5}
Fe^{+2}	1.70×10^{-2}
$FeH_2PO_4^{+2}$	5.41×10^{-5}
Fe^{+3}	1.05×10^{-5}
$FeOH^{+2}$	2.84×10^{-6}
FeH^2PO^{4+}	1.88×10^{-4}
H_3PO_4	6.48×10^{-5}
SO_4^{-2}	2.63×10^{-3}
HSO_4^{-}	1.71×10^{-3}
$FeSO_4$	1.70×10^{-3}
U^{+3}	1.80×10^{-40}
$U(SO_4)^2$	4.89×10^{-19}
UO_2^{+2}	4.03×10^{-5}
UO_2SO_4	1.09×10^{-5}
$UO_2(HPO_4)_2^{-2}$	2.86×10^{-6}

Interestingly, the saturation indices calculated using the Phreeqc model indicate undersaturation with respect to all Al, Fe, U, and P phases in the MinteqC database, with the exception of hematite, which is not expected because it does not precipitate directly from solutions at ambient temperature, and stengite, and iron-phosphate (Table 7.5).

Table 7.5 Expected mineral phases, predicted by Phreeqc, for the sample described in Table 7.3.

Mineral Phase		Saturation Index
Hematite	Fe_2O_3	4.26
Strengite	$FePO_4{:}2H_2O$	0.64
Goethite	FeOOH	-0.37
Jarosite-H	$(H_3O)Fe_3(SO_4)_2(OH)_6$	-1.01
Lepidocrocite	FeOOH	-1.24
Magnetite	Fe_3O_4	-1.75
$AlOHSO_4$		-1.99
Melanterite	$FeSO_4{:}7H_2O$	-2.55
Ferrihydrite	$Fe(OH)_3$	-4.76
Diaspore	AlOOH	-5.34
$(UO_2)_3(PO_4)_2$		-5.49
H-Autunite	$H_2(UO_2)_2(PO_4)_2$	-5.68
Maghemite	Fe_2O_3	-6.13
Schoepite	$UO_2(OH)_2{:}H_2O$	-6.32
Bassetite	$Fe(UO_2)_2(PO_4)_2$	-7.39
$UO_{3(C)}$		-8.64
$Al(OH)_{3(a)}$		-8.85
Vivianite	$Fe_3(PO_4)_2{:}8H_2O$	-10.58
$UO_{2(am)}$		-15.5
Al_2O_3		-19.92

7.4 Discussion

The chemical processes controlling the dissolution of U is well understood and is controlled by oxidation potential, which allows the transition from U^{4+} to U^{6+} to form a soluble uranyl compound when the oxidation potential increases. Under the conditions of this study, the chemical oxidizing potential is controlled by the Fe^{2+}/Fe^{3+} iron redox couple, whose dissolved concentration and ratio is directly related to the activity of the iron-oxidizing microbe community, which promoted the dissolution of 84% of the

total U from the sample, leaving 16% retained in the solid phase. The results of this study suggest that some amount of the retained U is held in the (hydr)oxide coatings present on weathered pyrite grains (Williamson, et al., 2014).

Studies at the Koongara U-ore deposit, Australia, document the occurrence of autunite group minerals in the pore spaces within goethite coatings in natural weathering conditions (Murakami, et al., 1997; Murakami, et al., 2005). The reaction mechanism proposed by Murakami et al. (1997) includes an initial formation of ferrihydrite, followed by the adsorption of phosphate species, and then by uranyl compounds to form a ternary complex. The uranyl-phosphate species are released as ferrihydrite matures to form goethite, allowing the precipitation of saleeite ($Mg(UO_2)_2(PO_4)_2 \cdot 10H_2O$) and meta-torbernite ($Cu(UO_2)_2(PO_4)_2 \cdot 8H_2O$) nano- to micro-crystals on the surface and within the pore spaces of Fe(hydr)oxide coatings. The results obtained in the current investigation suggest a similar, multi-step process controls the retention of U, initially released to solution by biogeochemical weathering processes, within weathering coatings on ferrous sulphide minerals.

Model for coating formation under acidic condition

From the results of this study, a model is proposed to describe for the formation of Al-rich coatings, with the incorporation of P, U, and trace elements in the coatings. Each step of the mechanism is described in detail, with reference to the results, in the following sections.

Formation of Fe(hydr)oxide coatings on weathered pyrite

The electronoptical observations of this study show weathered pyrite grains with secondary mineral phase development, providing. While Fe(hydr)oxide coatings phases were expected after biogeochemical dissolution, Al(hydr)oxide phases were also observed during the electronoptical observations of the mineral residue samples following the long term leaching experiments. Jarosite precipitation is expected under the leaching conditions, providing low-pH, sulphidic solutions with an expected influx of K+ resulting from the weathering of clay minerals. Modeling results indicate that the leaching solutions are

under-saturated with respect to jarosite (SI equal to -1.01), however areas of super-saturation may exist allowing the development of this secondary mineral phase.

The LA-ICP-MS analyses provide convincing evidence for some Fe(hydr)oxide regions within the coating zones. Thus Al is postulated to have replaced Fe in the coatings through a secondary series of mineral replacement reactions, with the release of Fe and precipitation of Al(hydr)oxide coatings on the weathered grains. Fe- and Al(hydr)oxides coatings are porous as a result of dissolution of ferrous sulphide minerals, with the secondary phase precipitation occurring in pore space occupied by fluids (Putnis, 2009). Mass transfer may occur through the porous coating network, promoting continued biogeochemical dissolution of pyrite, albeit at a leaching rate that decreases with time as the coating thickness increases (Hackl, et al., 1995).

Incorporation of phosphate species into the Fe(hydr)oxide coatings

Fe and Al oxides have a high capacity for adsorption and immobilization of P from percolating waters, with Fe- and Al-hydroxide coated quartz spheres having been used to treat waters high in P content (Arias, et al., 2006). Model calculations identified potential dissolve P species, H_3PO_4 and $H_2PO_4^-$, as well as dissolved Fe^{2+} and Fe^{3+} phosphate species, $FeH_2PO_4^+$ and $FeH_2PO_4^{2+}$ in the leachate solutions at end of the leaching experiments.

Parfitt (1989) explains the mechanism of adsorption for phosphates by ligand exchange with OH groups coordinated to Fe and Al. Arias et al. (2006) describe the sorption as occurring at coordination sites on the (hydr)oxide surfaces, allowing a direct linkage between the (hydr)oxide and the phosphate species. Dissolved $H_xPO_4^{-3+x}$ species existing in the leachate may become attracted to the Fe- and Al(hydr)oxide coatings. The extent of phosphate sorption is dependent on the nature and amount of reactive surface groups, and on the crystallinity of the (hydr)oxide phases; for instance, goethite allows little opportunity for diffusion of the phosphate species in the coating owing to the phase crystallinity (Parfitt, 1989). There

is always a competition effect between aqueous phosphate and silica species as the latter species has a higher affinity to either absorb on, or form complexes with, Fe-hydroxides (Stumm, 1992).

Formation of a ternary uranyl-phosphate adsorption complex

The LA-ICP-MS line scan indicated that Fe- and Al-(hydr)oxide coating regions on weathered pyrite grains are enriched in trace elements, including U, Th, REEs, and Pb, with respect to the underlying pyrite grain (Figure 7.2 and Figure 7.5). The composition of the coating region, both mineralogical and chemical, dictates the trace element composition of the coating. A plot of the concentration of P versus U shows two distinct correlation patterns for retention of U and P in the coating regions, Figure 7.7. Two correlation patterns may represent the retention of the trace elements in different coating regions, Fe- or Al-(hydr)oxide, suggesting different mechanisms by which trace elements are retained in the coatings, either nucleation or sorption.

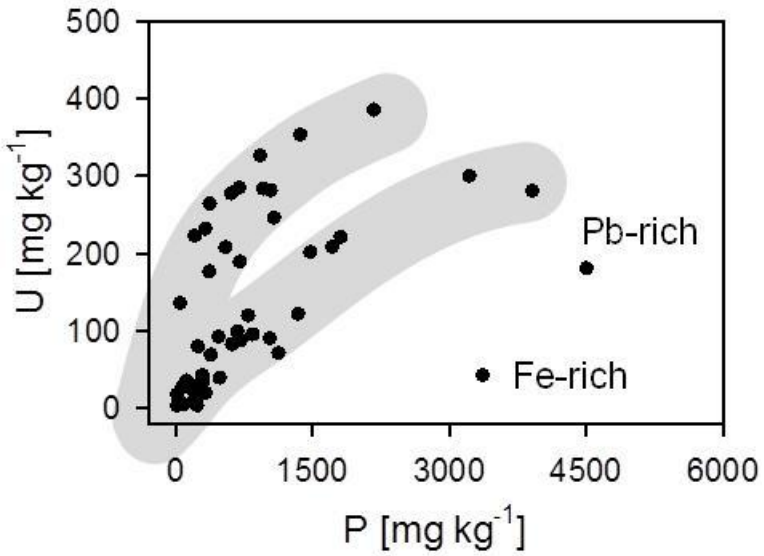

Figure 7.7 Correlations between P (mg kg^{-1}) versus U (mg kg^{-1}) in the examined coatings; different correlation patterns are indicated by the shaded areas.

An equimolar ratio between U and P is the common stoichiometry for U^{6+} phosphates of the autunite group (Fuller, et al., 2002). The current results suggest that U and P in the oxide coating regions are associated, possibly as a uranyl phosphate species incorporated into the coating or as precipitated phases at the water-oxide coating interface (Schindler & Ilton, 2013). Positively charged uranyl compounds,

UO_2^{2+}, are known to be attracted to negative phosphate, PO_4^{3-}, groups on the oxide coatings as described above, forming ternary uranyl-phosphate adsorption complexes as depicted in Figure 7.8 (Cheng, et al., 2004; Singh, et al., 2010; Del Nero, et al., 2011; Schindler & Ilton, 2013).

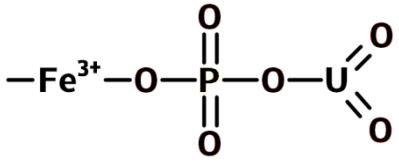

Figure 7.8 Ternary uranyl-phosphate adsorption complex with Fe(hydr)oxides.

Current research describes the use of phosphate compounds to remove of U^{+6} compounds from contaminated waters (Cheng, et al., 2004; Singh, et al., 2010; Sato., et al., 1997). Schindler and Ilton (2013) propose that the surface nucleation of autunite group minerals is promoted by adsorbed phosphate species to Fe(hydr)oxide. These authors further suggest that this process may be an important factor for the long-term fixation of U in a natural system, resulting in the nucleation of (meta)torbernite ($Cu(UO_2)_2(PO_4)_2{\cdot}8H_2O$) and saleeite ($Mg(UO_2)_2(PO_4)_2{\cdot}8H_2O$) intergrowths in the (hydr)oxide coating. The actual mechanism by which phosphate and uranyl compounds form a complex with the oxide coating network or a discrete uranyl-phosphate precipitate phase is dependent on both the pH of the system (Cheng, et al., 2004) and on the concentration of phosphate and U species (Schindler & Ilton, 2013). Cheng et al. (2004) reported an increase U^{6+} adsorption rate in low pH conditions in the presence of P, and an increased adsorption rate as P concentration increased, concluding that U^{6+} mobility is decreased in the presence of P owing to the formation of ternary uranyl-phosphate complexes forming in the presence of Fe-oxyhydroxides.

In the presence of Fe(hydr)oxide mineral coatings, the correlation observed between U and P may originate after sorption of the uranyl-phosphate species on the coating, or form by the precipitation of nanocrystals of uranyl-phosphate (Schindler & Ilton, 2013). Although the modeled solubility calculations in this study suggest undersaturation with respect to uranyl-phosphate phases, these phases may exist in more concentrated fluids in pore spaces within the coatings generating supersaturated zones with respect to these authigenic phases. Since the initial Fe(hydr)oxide coatings predicted to form under the study

conditions are porous, ternary U-phosphate adsorption complexes would be expected to occur throughout the coating, not just at the surface-water interface. These considerations are in accordance with the observations by Murakami et al. (1997, 2005), who showed that minerals of the autunite group formed in nano- to micrometer-size pore spaces, even the local groundwater was shown to be undersaturated with respect to these phases.

Mineral replacement reactions promoting the replacement of Fe(hydr)oxides with Al analogues

According to Murakami et al. (1997), the weathering of Fe(hydr)oxides breaks the ternary complex, releasing the uranyl-phosphate species. During the oxidation processes, Fe phases of poor crystallinity are formed and, depending on pH and temperature, crystallinity may increase. At low pH, the biogeochemical mineral dissolution conditions are such that the formation and crystallization of goethite would be expected following the dissolution- of a less-crystalline Fe(hydr)oxide phase such as ferrihydrite.

Increased crystallinity of the coating phases may also occur through replacement reactions in which Fe(hydr)oxides are replaced with Al phases. The low pH environment of the leaching experiments promotes the enhanced dissolution of silicate minerals, with the subsequent release of free Al ions into the pore solution. Marchs and Sangery (1982) report that U mine tailings, generated using traditional processing methods in the Elliot Lake region, commonly contained amorphous Si and amorphous Al (hydr)oxide phases, resulting from the breakdown of clay minerals during acid leaching. Fe(hydr)oxides in the environment are knows to incorporate various cations into their structures, suggesting that the pore solutions interact with previously formed Fe-hydroxides, which results in the replacement of the earlier formed Fe-hydroxides and the formation of aluminum-hydroxide coatings on the surface of the sulfides.

Dissolved Fe^{3+} and Al^{3+} ionic species have similar chemistry in mine tailing environments, with the solubility of Al species being controlled by the solubility of amorphous aluminium (hyrd)oxide released by the weathering of clay minerals (Dubrovsky, et al., 1984). The replacement of Fe(hydr)oxides with Al

analogs in soils has been confirmed by Norrish and Taylor (1961). From diffraction measurements of soil goethite phases, they concluded that Al is a common replacement for Fe, with the extent of replacement being dependent on the weathering conditions of the local soils. The modeling results in this study suggest the dissolution of silicate minerals in acidic conditions supplies the leachate with dissolved Al^{3+} species. The mechanism of the replacement of Fe in established (hydr)oxide coatings with Al in weathered soils may be applied to explain the formation of the Al rich surface coating on the leached pyrite grain (Figure 7.5), a process controlled by re-equilibrium reactions and influenced by the chemistry of the leachate (Putnis, 2009). Al-Si-Fe rich phases may develop with the precipitation of SiO_2-rich phases, such as allophone, which have also been observed in U tailings produced using traditional processing methods (Dubrovsky, et al., 1984).

Precipitation and nucleation of uranyl-phosphates

The release of uranyl-phosphate complexes during the maturation and transformation of less-crystalline Fe-hydroxide into a more crystalline form, or into Al-hydroxides, triggers the formation of uranyl-phosphates within the coating network. Solubility index calculations suggest H-autunite, bassetite, and torbernite are examples of uranyl-phosphate compounds that may be present among the Al(hydr)oxide coating phases. As ternary U-phosphate adsorption complexes were expected throughout the coating layer, the transformation to a higher crystalline state, whether goethite or Al-analogues, will release adsorbed uranyl-phosphate species resulting in nucleation of uranyl-phosphate nano-crystals throughout the coating network.

Alternative process

An alternative process may exist, initiated by the replacement of Fe(hydr)oxides with Al analogues, as described above, followed by the attraction and absorption of phosphate species to the Al(hydr)oxide coating. Under the acidic conditions that are sustained by the biogeochemical mineral dissolution process, Al-hydroxide coatings are positively charged, having a point of zero charge of approximately 9.6 (Burrell,

et al., 1999), thereby promoting the adsorption of negatively charged P species. Fe and Al oxides are known to provide a high capacity for adsorption and immobilization of P from waters, with Fe- and Al-hydroxide coated quartz spheres having been useful to treat waters high in P content (Arias, et al., 2006). From the sorption pathways proposed by Parfitt (1989), a higher phosphate content is expected in Al(hydr)oxide regions compared to Fe(hydr)oxide regions, explaining the two correlation patterns observed in Figure 7.7. Phosphate complexes are also predicted to form not only on the surface of the Fe- or Al(hydr)oxide, but, as Parfitt (1989) further describes, phosphate ions may penetrate the porous coatings. Ternary U-phosphate adsorption complexes on Al(hydr)oxide coatings have not been previously described, with the mechanism of U-phosphate precipitation under these conditions being currently unclear.

Model for the formation of Al-rich coatings

From the processes described above, the model in Figure 7.9 is proposed to describe for the formation of Al-rich coatings and the incorporation of P, U, and trace elements in the coatings

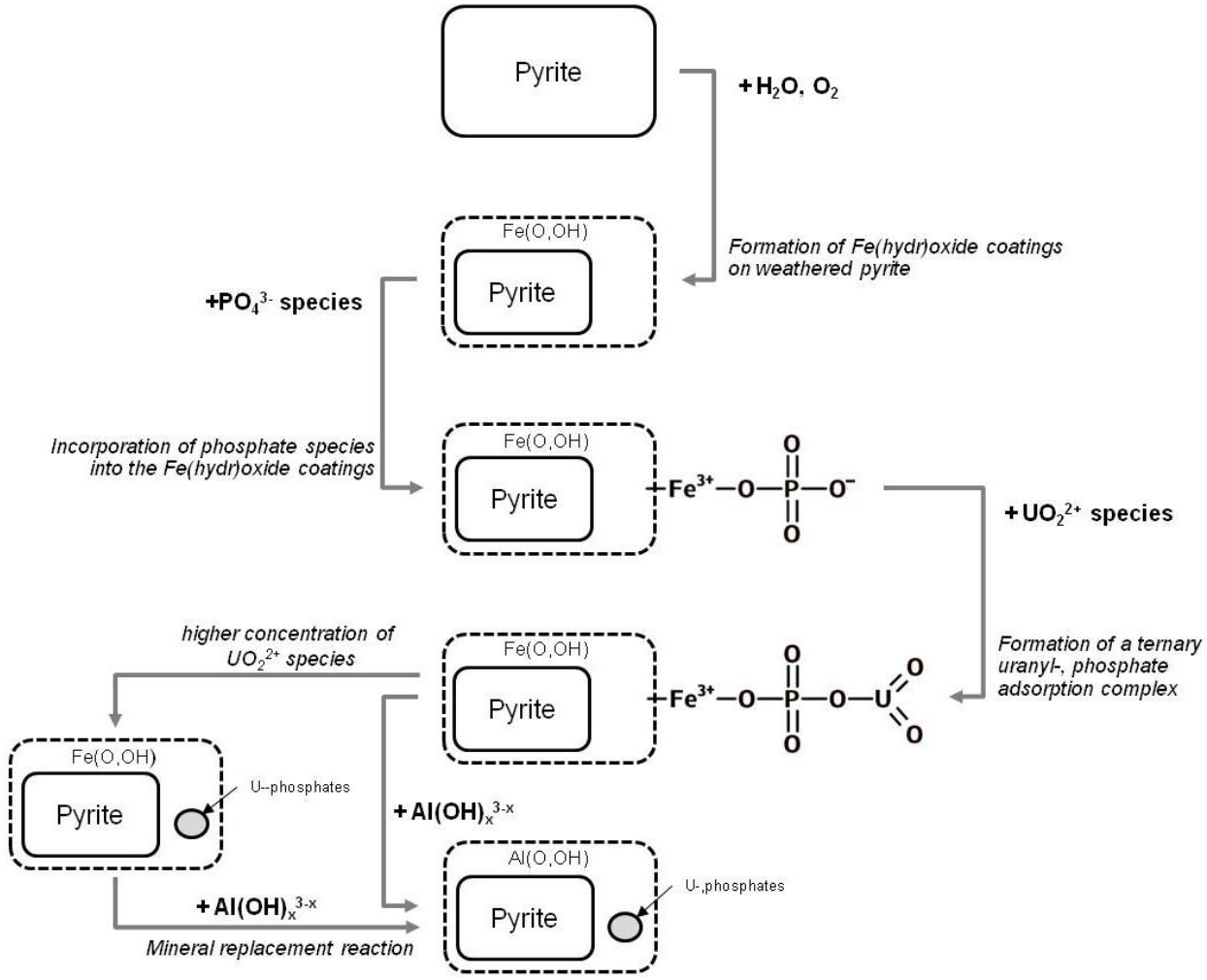

Figure 7.9 Model for the formation of Al-rich coatings and the incorporation of U, REEs, Th, and Pb species in the coatings; (1) formation of Fe(hydr)oxide coatings on weathered pyrite, (2) incorporation of phosphate species into the Fe(hydr)oxide coatings, (3) formation of a ternary uranyl-phosphate adsorption complex, (4) mineral replacement reaction, and (5) under higher concentration of UO_2^{2+} species.

Retention of metals and trace elements in the coatings.

An evaluation of the arithmetic and geometric means for the elemental composition of each region provides information on the ability of each coating region to regain trace elements (Table 7.6). The arithmetic mean is greatly influenced by higher values and providing greater indication nucleation. The geometric mean, on the other hand, indicates the typical value, thereby, the extreme values have a lesser impact on the mean value and tends to indicate adsorption. When the arithmetic and geometric means are very different, nucleation is indicated, while similar values suggest the process occurs by adsorption.

Table 7.6 Arithmetic mean (AM), standard deviation (STD), and geometric mean (GM) for the elemental composition of coating regions identified in Figure 7.4 and Figure 7.5; Data are expressed as mg kg^{-1}.

Element	Fe-rich, n= 17			Si-rich, n = 18			Al-Si-Fe-rich, n = 27		
	AM	STD	GM	AM	STD	GM	AM	STD	GM
Na	960	230	90	4000	960	160	700	140	230
Mg	90	20	20	850	210	180	1400	260	150
Al	14000	3300	13000	110000	26000	80000	120000	24000	110000
Si	28000	6800	18000	310000	76000	300000	45000	8600	1400
P	1400	340	870	360	90	230	1500	290	670
S	74000	18000	39000	5700	1400	1200	95000	18000	69000
K	2100	510	1200	15000	3700	4800	16000	3000	5600
Ca	390	90	330	2500	610	1900	4300	820	1100
Mn	30	10	20	40	10	20	70	10	20
Fe	450000	110000	440000	32000	7800	14000	220000	43000	190000
Co	150	40	130	10	0	0	90	20	30
Ni	70	20	60	60	20	30	50	10	20
Cu	660	160	540	110	30	40	110	20	40
Zn	430	100	240	520	130	60	30	10	0
Y	20	10	10	10	0	0	40	10	10
La	20	0	20	30	10	10	70	10	20
Ce	50	10	40	60	10	30	170	30	50
Pb	350	80	280	280	70	90	420	80	210
Th	150	40	100	180	40	70	170	30	90
U	360	90	220	90	20	40	380	70	100

Arithmetic mean, $AM = \frac{1}{n}(\sum_{i=1}^{n} x_i)$

Standard deviation, $STD = \sqrt{\frac{1}{N}\sum_{i=1}^{N}(x_i - \bar{x})^2}$

Geometric mean, $GM = (\prod_n x_i)^{1/n}$

An evaluation of the arithmetic-mean values for P each coating region indicates that the arithmetic mean in the Fe- and Al-Si-Fe-rich regions is much larger than the geometric mean, whereas the arithmetic mean and geometric mean values in the Si-region are quite similar. The mean concentration of metals (Co, Ni, Cu, and Zn) is much greater in the Fe-rich region than in the Al-Si-Fe-rich region, suggesting that when Al(hydr)oxide coatings replace Fe(hydr)oxide coatings, metals are released to the leaching liquid. The opposite is true for the U, Th, Pb, and the REEs (Y, La, Ce), in which an increase in the retention of these

elements is observed, indicating that as the Fe-coatings are replaced by Al-analogues, the retention of U, Th, Pb, and REEs bearing secondary phases is enhanced.

7.5 Conclusion

This study describes the following multi-step process for the retention of U in P phases in Al(hydr)oxide coatings on weathering pyrite after biogeochemical mineral dissolution:

- Formation of Fe(hydr)oxide coatings on weathered pyrite;
- Incorporation of phosphate species into the Fe(hydr)oxide coatings;
- Formation of a ternary uranyl-phosphate adsorption complex on the oxide coatings Mineral replacement reactions promoting the replacement of Fe(hydr)oxides with Al analogues; and
- Precipitation and subsequent nucleation of uranyl-phosphates, on the surface and throughout the coating network.

An alternative formation method may exist where Al(hydr)oxide coatings replace the Fe(hydr)oxide coatings prior to P adsorption. However, ternary U-phosphate adsorption complexes on Al(hydr)oxide coatings have not been previously described, and the controlling mechanism of U-phosphate precipitation under these geochemical conditions is unclear. The Al(hydr)oxide coatings observed in this study are consistent with previous results describing secondary Al phases in U tailings produced in the Elliot Lake region following the application of acidic extraction processes, yet the retention of U in the Al regions of the coatings has not previously been described.

The samples investigated in this study were collected from a biogeochemical mineral dissolution demonstration study (Williamson, et al., 2014) and the coatings that established may not provide ideal samples for a study dedicated to secondary phase analysis. Selected samples at collected at various time intervals of a biogeochemical dissolution study will, in future, provide evidence to support the proposed mechanism, or show that Al(hydr)oxides may develop prior to the incorporation of P into the coatings. Samples subjected to conditions that would promote a more controlled establishment of coatings may

provide samples more suitable for the investigation of the processes controlling coating establishment and U retention. For example, transmission electron microscopy (TEM) of thicker, more uniform coatings would be useful to prove or disprove the suggested methods of U retention by phosphates on Al(hydr)oxide coatings. When a coating mechanism is confirmed, prediction of the stability and long-term retention of U in the bio-heap leach waste piles can be assessed.

CHAPTER 8

8 Application Oxidation Resistance Testing of Passive Approaches to Prepare for Decommissioning

8.1 Introduction

The Environmental Code of Practice for Mines, in describing the industry-best practice pollution control procedures of the mine life cycle, advocates that processed tailings, waste rock piles, and spent leach pads must be treated to control or remove potential environmental liabilities (Environment Canada, 2009) such as acid production, mineral dissolution, and metal solubilization when extractable resources are exhausted at the site. Knowledge of the biogeochemical mineral dissolution process provides an understanding of techniques that may potentially be applied to disturb, interrupt, or stop the natural bioleaching process.

Decommissioning activities for bioleach heaps may be less arduous than those necessary for application to waste rock piles or tailings confinements as the acid rock drainage processes were optimized to enhance elemental recovery, potentially resulting in a more benign waste to be managed on closure. The bioleaching process, however, also produces stored acidity with precipitation of secondary mineral phases that may not be stable in all environmental conditions. Therefore the stored acidity in bioleaching heaps, must be neutralized, with removal or stabilization of secondary phases and prevention of ongoing oxidation of remaining sulphidic mineral for a successful site decommissioning (Zang & Evangelou, 1998). Passive approaches to prepare heap-leach pad for decommissioning have been investigated, which incorporate the extractive biogeochemical mineral dissolution processes to facilitate the site decommissioning.

In the absence of bacterial activity, biotic oxidation of iron (Fe) is suppressed (Kleinmann, 1987) allowing the slower, abiotic pyrite oxidation processes to dominate. As the activity of *Acidithiobacillus ferrooxidans*, the dominant bacterial species driving the bioleaching process, is suppressed by the presence of organic compounds. Inhibition of *A. ferrooxidans* and associated bacterial species has been achieved in laboratory studies by application of various organic substances (Leathen, et al., 1956; Silverman & Lundgren, 1959; Dugan & Lundgren, 1964; Duncan, et al., 1964; Tuttle & Dugan, 1976; Belzile, et al., 1997; Dugan, 1987a). The inhibitory effects of the organic compounds on *A. ferrooxidans* is possibly related to the relative lipid solubility of the compounds, which may promote molecule passage through the cell envelope, thus disrupting the cell membrane and suppressing the biochemical processes of the cell (Tuttle & Dugan, 1976). An assessment of organic acids and anion surfactants known to inhibit *A. ferrooxidans* concluded that anionic surfactants warrant the most promising option for investigation and application on a larger scale (Kleinmann & Erickson, 1983). The biotic oxidation of Fe has been observed to be retarded or eliminated in the presence of sodium lauryl sulphate (SLS), in both laboratory and field testing (Dugan, 1975; Kleinmann & Crerar, 1979; Kleinmann, 1980; Kleinmann & Erickson, 1982; Dugan & Apel, 1983; Onysko, et al., 1984). In the natural environment SLS is biodegradable, rapidly decomposing before having any significant effect on the discharging water. Surfactants are known to be more aggressive at low pH, so in the event of the release of SLS to receiving waters (natural streams, rivers, and lakes) the elevated pH of these waters (above 5.8) will neutralize the bactericidal properties of the surfactant (Kleinmann & Erickson, 1983).

A mineralogical approach to AMD prevention aims to halt the mineral dissolution and acid production process at source by either removing the reactive mineral from the system, or by rendering the reactive sites of the mineral inert. Passivation promotes the formation of a barrier phase between the reactive metal sulphide and the oxidizing environment, thereby preventing sulphide oxidation, thus hindering the biogeochemical mineral dissolution process (Evangelou, 1994; Evangelou & Zhang, 1995; Chen, et al., 1999). Leaching iron-sulphides in the presence of an oxidant, buffer, and compound such as di-hydrogen

orthophosphate or sodium metasilicate can produce inorganic secondary coatings or precipitates on surfaces of the reactive minerals (Evangelou, 2001; Harris & Lottermoser, 2006b).

Leaching pyrite with a phosphate solution in the presence of a strong oxidant promotes the formation of a ferric iron (Fe^{3+}) oxyhydroxide surface which will react with the dissolved orthophosphate ions to form an insoluble ferric-phosphate coating (Reaction 8.1), which protects the underlying pyrite mineral surface from further biogeochemically mediated oxidation (Evangelou, 1994). Stabilization of phosphate coatings encapsulating pyrite is then achieved by use of a buffer, such as sodium acetate (Fytas & Evangelou, 1998; Evangelou, 2001; Harris & Lottermoser, 2006a; Harris & Lottermoser, 2006b).

Reaction 8.1

$$FeS_2 + H_2PO_4^- + \tfrac{15}{2}H_2O_2 \rightarrow FePO_4 + 2SO_4^{2-} + 3H^+ + 7H_2O$$

The deposition of silicate coatings also takes place in the presence of a strong oxidant and a buffer to control the pH level. In the presence of metal hydroxides, silica will precipitate on the surface of the metal hydroxide. With the release of Fe^{3+} from pyrite minerals, a ferric-hydroxide-silica barrier (Reaction 8.2) may precipitate on mineral surface (Evangelou, 1996) . The authigenic ferric-hydroxide-silica coating would, in turn, suppress pyrite oxidation rates by preventing further oxidation of the pyrite mineral and acting as a sink for released free Fe^{3+} (Vandiviere & Evangelou, 1998). Evanglou (1996) has patented a technology to generate an oxidation-proof silica surface coating on iron-sulphide minerals; US Patent 5494703.

Reaction 8.2

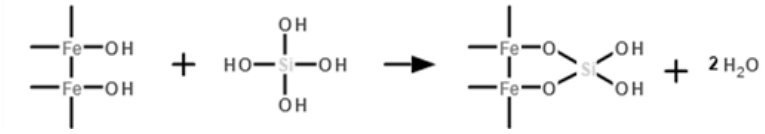

The extent of oxidation, or lack thereof, is determined by monitoring the solution chemical parameters associated with the oxidation of ferrous iron (Fe^{2+}) sulphide minerals, namely pH, E_H, dissolved Fe, and/or Fe^{3+} and Fe^{2+} concentrations. Previous studies have employed an oxidation resistance testing procedure by leaching treated and untreated samples with 0.01 M to 0.200 M hydrogen peroxide (H_2O_2)

(Evangelou, 1994; Georgopoulou, et al., 1995; Fytas, et al., 1999; Zang & Evangelou, 1998; Fytas, et al., 1999; Khummalai & Boonamnuayvitaya, 2005). Few studies, however, have incorporated an investigation of the subsequent resistance of the secondary mineral coatings to biological oxidation (Vandiviere & Evangelou, 1998; Khummalai & Boonamnuayvitaya, 2005).

In the current study, a series of experiments were conducted to investigate passive approaches to prepare for heap-leach decommissioning by applying a variety of organic compounds to achieve bacterial inhibition (Appendix C), as well as the application of variable concentrations of di-hydrogen orthophosphate or sodium metasilicate coating solutions to promote mineral passivation (Appendix D). The application of SLS and concentrated coating solutions using the solution delivery system optimized for bioleaching was examined using small columns and pre-leached mineral material (Appendix E). The objective of this current study is to demonstrate the application of pacification and inhibition treatments on previously leached mineral materials using column to represent the application at a pre-operational scale using the existing leachate delivery systems. The short-term capabilities of each treatment to resist further oxidation and subsequent mineral dissolution of the simulated waste rock after the application of the pacifying or inhibiting treatment is investigated by assessing resistance to both chemical and biological oxidation environments.

8.2 Experimental Methods

Material

Fresh drill core was collected from the study site, Eco Ridge Mine Rare Earths and Uranium Project site (Eco Ridge), owned by Pele Mountain Resources Incorporated (PMR), approximately 11 km east of Elliot Lake, Ontario (Figure 8.1). The ore minerals are hosted in a quartz-pebble conglomerate bed with a matrix of fine-grained quartz, feldspar and up to 15% pyrite (Sylvester, 2007). Uranium- (U), thorium- (Th), and rare earth element (REE)-bearing primary and secondary minerals exist in the matrix, being concentrated in halos around the quartz pebbles. A sub-sample of the material was crushed to 2 to 4 cm in size using a large mouth jaw crusher, a head size with 65% passing < 5 cm sieve and homogenized for a

series of bioleaching trials using acrylic leaching columns (11.5 cm internal diameter) to test the viability of the biogeochemical mineral dissolution process (See Chapters 5, 6, and 7). The previously leached mineral samples from the biogeochemical mineral dissolution studies were retained in the columns for the demonstration of passive approaches to prepare for decommissioning.

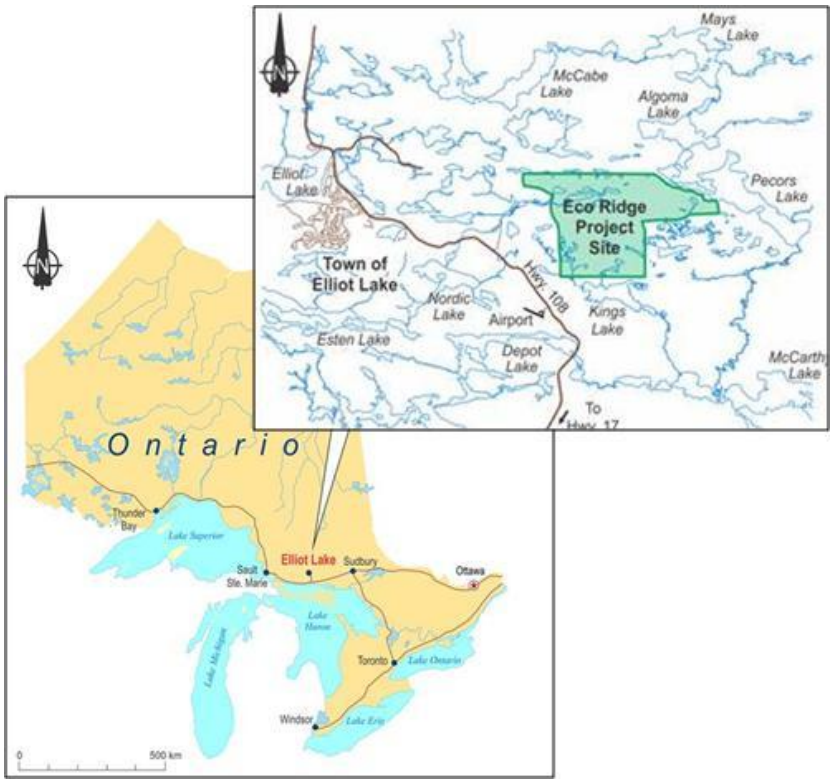

Figure 8.1 Location of Eco Ridge Mine Rare Earths and Uranium Project, east of Elliot Lake, Ontario (image provided by PMR Ltd. 2013).

Experimental Approach

Acrylic columns (11.5 cm internal diameter and 180 cm tall) were loaded from the bottom up with 500 mL of plastic beads (3 to 4 mm), 40 kg mineral material, and another 500 mL of beads. These columns remained intact after the biogeochemical mineral dissolution demonstration phase (Chapter 5), with only the reservoir contents being changed. These columns are expected to represent biogeochemically leached mineral material immediately prior to the decommissioning phase.

The passivation methods followed in this laboratory study are based on the studies documented by Evangaelou and Fytas (Evangelou, 1994; Fytas & Evangelou, 1998), with the inhibition methods

followed being similar to those described by Dugan and Apel (1983). Two pacifying coating treatments and one inhibition treatment were applied to the columns using the same delivery methods as the large column leaching phase using a closed-loop system with a peristaltic pump at a rate of 1 L hr^{-1} (Table 8.1). Coating treatments also included an oxidant (5 g L^{-1} hydrogen peroxide, H_2O_2) and a buffer (0.8 g L^{-1} sodium acetate, CH_3COONa) with the pH of all reservoirs adjusted between 5 and 6 with sodium hydroxide and hydrochloric acid.

Table 8.1 Large column inhibition and pacification treatments (n1=1, n2=3, n3=3, n4=3).

Treatment (g L^{-1})	**1**	**2**	**3**	**4**
None	x			
Passivation				
KH_2PO_4				
14		x		
Na_2SiO_3				
1.2			x	
Inhibition				
SLS				
0.010				x

Samples were collected from the reservoirs using sterile syringes every two days, filtered (0.45µm), and analyzed for pH, E_H, and dissolved elemental concentration by ICP-MS. Treatment application lasted for 10 days, after which the columns were left intact and allowed to air dry for one month.

Prior to initiation of the oxidation resistance investigations, the reservoirs were filled with 11 L of fresh DDI water and an oxidizing solution supplying either 0.20 M hydrogen peroxide (abiotic treatment) or inoculated with 10 mL of mature bacteria culture (biotic treatment). The peristaltic pump delivery rate was set at 1 L hr^{-1}. Samples were collected from the reservoirs using sterile syringes every two to fourteen days for 50 days, filtered (0.45µm), and analyzed for pH, E_H, and dissolved metal concentration by ICP-MS.

Sample Analysis & Analytical Parameters

The pH was measured with a Thermo Orion 370 PerpHecT Ion Selective Benchtop Meter equipped with a glass electrode (Orion 8165BNWP ROSS Sure-Flow Epoxy Bodied Combination pH Electrode) and calibrated with pH 4 and pH 7 standard buffer solutions. The oxidation potential (E_H), corrected to the standard hydrogen electrode, was measured using a platinum combination electrode (Accumet 13-620-115 Platinum Pin Indicating Half-Cell Electrode) coupled with the calomel electrode (Accumet 13-620-52 Glass Body Calomel Reference Electrode) and calibrated with an oxidation-reduction potential standard (Orion 967901 ORP Calibration Standard).

Inductively coupled plasma mass spectrometry (ICP-MS), tuned, optimized, and calibrated to operate under normal sensitivity mode, was used to analyze all leachate samples (Varian 810). The analysis was completed in an ISO 17025 accredited facility, Elliot Lake Research Field Station at Laurentian University. The quality control program included the analysis of duplicates, certified reference materials (CRM), internal reference material (IRM), and water blanks. Internal standards (Re and Ru) were used to correct for any mass bias and provide for continuous calibration verification (CCV). Prior to analysis, all experimental samples were filtered (0.45 µm) and diluted (1:10) with DDI.

Total elemental concentration of the mineral material before and after leaching was measured by ICP-MS analysis after acid digestion of the material. To ensure samples used represented an accurate sub-sample of the material, a riffle splitter was used to produce subsamples. After grinding to 74 µm using an agate ball mill, a 0.5 g sample was digested in an open 50 mL Teflon™ centrifuge tube using a programmable digestion block (Questron Q-Block 4200) according to the following steps:

- 10 mL of HF/HCl (1:1) and evaporated dryness at 110 ℃ for 3.5 hours;
- 14 mL HCl/HNO3 (1:1) and evaporated dryness at 110 ℃ for 4 hours; and
- 12.5 mL of HF/HCl/HNO3 (1:4:20) and heated to 110 ℃ to reduce sample volume to 8 to 10 mL.

After digestion, ultrapure water was added to bring the total volume in each tube to 50 mL for subsequent analysis. The samples were then diluted (1:10) and analyzed by ICP-MS. All concentrations were calculated in mass per mass dry mineral basis.

8.3 Results

Treatment application

The pH, E_H, and dissolved Fe concentration were monitored through the 10 day treatment application process (Figure 8.2) to assess the possibility of the leaching solution to support bio-oxidation processes. The pH of each treatment solution varied before application, with the observed decrease of pH during the ten day application phase probably reflecting the release of stored acidity in the previously leached mineral material (Figure 8.2a). The treatment solutions for all applications were initially highly oxidizing (0.82 ±0.02V), with the E_H of the columns receiving coating applications (Treatments 2 and 3) deceasing to 0.71V after 1 day of leaching and remaining below 0.80 V throughout the treatment application phase. The E_H of columns receiving inhibition treatment (Treatment 4) were similar to the control (Treatment 1), being 0.82 V after 10 days of application. The initial Fe concentration varied in each column, with all treatments having a decrease in dissolved Fe concentration during treatment application (Figure 8.2c), with the relative change in Fe concentration being lowest for the control (0.2 mg/L), followed by the inhibition treatment (0.5 mg/L) (Figure 8.2d). The columns receiving the passivation treatments Exhibited the most substantial Fe decrease, 1.1 mg L^{-1} and 1.4 mg L^{-1}, Treatments 3 and 4, respectively.

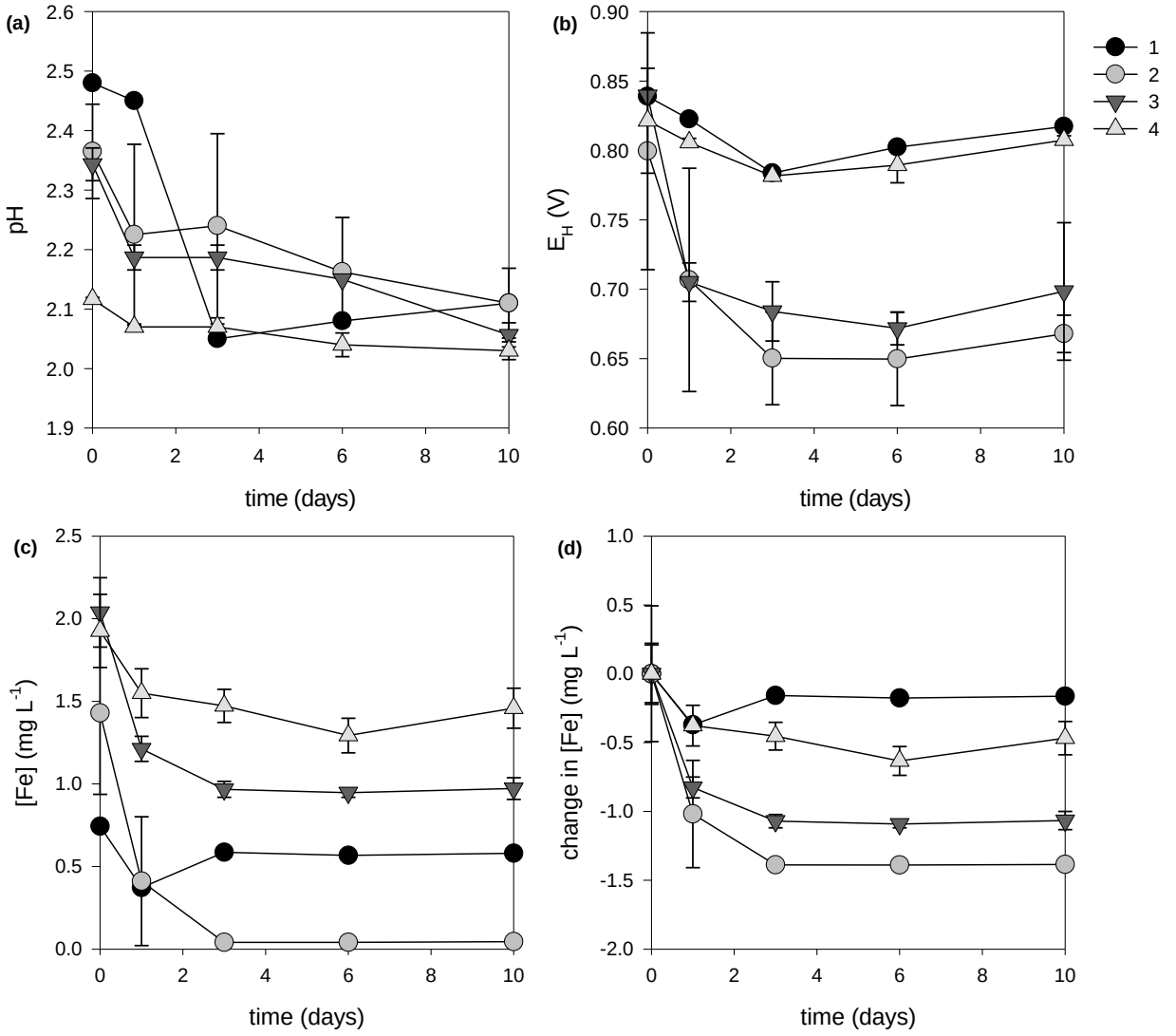

Figure 8.2 Time profiles for application of inhibition and passivation treatments during 10 days of application displaying the changes in: (a) pH, (b) oxidizing potential, (c) Fe concentration, and (d) change in Fe concentration.

Oxidation resistance testing

The same parameters, pH, E_H, and dissolved Fe concentration, were monitored after the application of the inhibition or passivation treatments to assess resistance to either chemical or biological oxidation (Figure 8.3). Biological oxidizing conditions (a) were promoted with the addition of mature culture broth and chemical oxidizing conditions (b) were induced with the addition of hydrogen peroxide (H_2O_2). Oxidizing conditions were not imposed on the control (Treatment 1). The pH of all treatments decreased under oxidizing conditions to 2.1 ±0.04, with the pH of the control after 50 days being 3 (Figure 8.3a). With the exception of one treatment (Treatment 2a), the E_H in the columns was 0.80 ±0.01 V (Figure 8.3b). After

10 days, the E_H for the column that was passivated with phosphate solution and chemically oxidized reached a low of +0.60 V and slowly increased to +0.74 V, being the only treatment that did not promote an increase in E_H potential to that expected for the Fe^{3+}/Fe^{2+} couple (~ 0.8 V). In 10 days, all treatments reported an increase in dissolved Fe concentration; either from iron dissolution occurring in the column itself or as a component of the broth culture in the biological oxidation treatment (Figure 8.3c). Four treatments (Treatments 3a, 3b, 4a, and 4b) developed a higher dissolved Fe concentration then the control after 50 days, with two treatments having a Fe concentration less than the control (Treatments 2a and 2b) (Figure 8.3d). No oxidation treatments were applied to the control, suggesting that those with Fe concentrations greater than the control have allowed the oxidation of Fe, whereas treatments with Fe concentrations lower then control have suppressed the Fe oxidation processes. The treatments to suppressed Fe oxidation were those predicted to form ferrous-phosphate passivation coatings, Treatment 2, under both chemical and biological oxidation conditions.

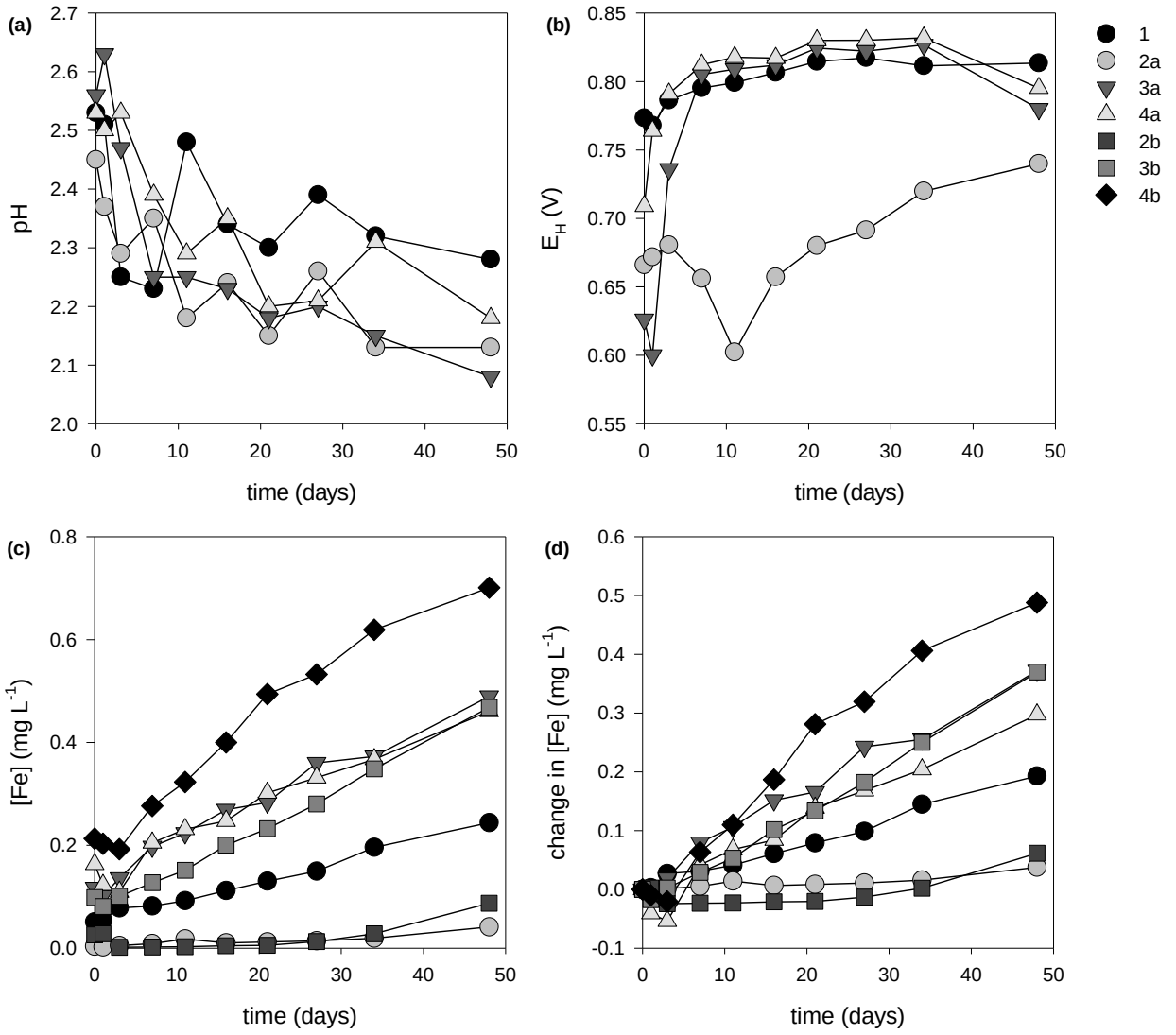

Figure 8.3 Time profiles during 50 days of oxidation resistance testing for inhibition and passivation treatments displaying the changes in: (a) pH, (b) oxidizing potential, (c) dissolved Fe concentration, and (d) change in dissolved Fe concentration; 'a' identifies biological oxidation and 'b' identifies chemical oxidation.

8.4 Discussion

During the application phase, the data obtained by the monitoring of pH, E_H, and dissolved Fe concentration identifies the treatments having an immediate effect on the potential for biogeochemical mineral dissolution to occur place in the experimental system. Inhibition by SLS did not affect the leachate chemistry, with the E_H and change of Fe concentration being similar to that observed for the untreated control (Figure 8.2). Both passivation treatments induced a decrease in E_H and a reduction in dissolved Fe concentration in the percolating solutions.

Analysis of the chemical process indicators, (pH, Eh, and dissolved Fe concentration), enabled the resistance of each treatment to chemical or biological oxidation to be assessed. Table 8.2 identifies the indicators suggestive of the establishment of an environment favorable for oxidation of ferrous sulphide minerals, with the values observed for the control treatment providing a baseline indicative of non-oxidative conditions during the experimental phase.

Table 8.2 Assessment of the indicators of (bio)geochemical oxidation of ferrous sulphide minerals after 7 weeks after the introduction of oxidative conditions.

Parameter	Indicator	None	Biological oxidation			Chemical oxidation		
		1	2	3	4	2	3	4
pH	> 2	2.3	2.1	2.1	2.2	2.1	2.1	2.1
Eh (V)	increasing	0.81	0.74	0.78	0.80	0.79	0.82	0.81
Δ[Fe] (mg L^{-1})	increasing	0.19	0.04	0.37	0.30	0.06	0.37	0.49

Under biological and chemical oxidation conditions, application of a treatment promoting the development of a phosphate-containing coating (Treatment 2) maintained a low E_H, inducing minimal Fe dissolution. Evangelou (1994) also indicated that the leaching of pyrite with a phosphate solution in the presence of a strong oxidant promoted the formation of a Fe^{3+}-rich surface coating which reacted with phosphate to form the insoluble ferric-phosphate coatings to protect the pyrite below the authigenic coating from further oxidation (Reaction 8.1). The decrease of Fe concentration in the leachate solution during the application phase is expected because the dissolved Fe^{3+} becomes incorporated in into the Fe phosphate coating.

The amorphous silica coating (Treatment 3) did not resist oxidation under either treatment, indicated by both the E_H being ~0.8 V and the dissolved Fe concentration being greater than measured in the control system. Although the formation of Fe^{3+} hydroxide-silica barriers has been suggested as a promising approach for the abatement of the oxidation of pyrite tailings or mine waste material (Fytas, et al., 1999; Kargbo & Chatterjee, 2005), evidence in this current study suggests the protection is only minimal.

The results documented here demonstrate that biooxidation is suppressed in the presence of SLS (Treatment 4), with 61% more Fe dissolution being induced under the chemical oxidizing conditions than

with the biogeochemical oxidation induced by presence of the microbe community. The application of SLS as an inhibitory compound may offer an initial control on the bio-oxidation processes and as prior study assessing the application of metals, organic acids, and anion surfactants known to inhibit *A. ferrooxidans*, concluded that, after eliminating substances that may be environmental or health liabilities, anionic surfactants warrant the most promising path for investigation and have potential for application on a larger scale (Kleinmann & Erickson, 1983).

8.5 Conclusion

The results of this study demonstrate the application of passivation and inhibition treatments to previously leached mineral material using large columns and pumped percolating leachate delivery system. Upon application of SLS, there were minimal observable changes in leachate chemistry compared with the control. The inhibition ability of the compound on biological processes was evident during the following oxidation resistance testing. In the presence of the biological oxidizer, the release of Fe to solution was suppressed compared to that that occurred in chemically oxidizing conditions and the control under biological oxidizing conditions, indicating that SLS inhibited, to some degree, the activity of the iron-oxidizing bacteria.

The application of both passivation treatments resulting with a decrease in E_H and a reduction in dissolved Fe concentration in the percolating solutions during the ten days of treatment application. The decrease of dissolved Fe concentration is expected to take place as a consequence of the coating process, in which free Fe is incorporated into the insoluble ferric-phosphate coating when leached with the phosphate solution (Evangelou, 1994). The oxidation-resistance testing experiments indicated that the ferric-phosphate coatings are much more resistant to chemical and biological oxidation than the amorphous silica-network coatings, maintaining an E_H lower than both the control and biological oxidation treatments during the 50 days stability assessment period. The silica coatings, on the other hand, had similar impact on Fe dissolution to the inhibition treatment under biological oxidizing conditions, offering no additional protection under chemical oxidation processes.

The study demonstrated that the passivation approach most resistant to biotic and abiotic oxidizing conditions involved leaching with a phosphate solution promoting the formation of a Fe^{3+}-rich coating on the pyritic mineral surface. The leachate delivery system used during the biogeochemical mineral dissolution phase is suitable to also deliver the coating solutions, indicating that infrastructural changes may not be required to initiate the application of the passivation treatment on the operational-scale. The combination of a phosphate solution and inhibition compound may provide additional oxidation resistance, controlling the pre-existing bacterial populations.

This short term study has provided preliminary details describing passive approaches to prepare for decommissioning. In this short amount of time, the pH for all treatments remained unaffected and well below MMER discharge guidelines and the oxidizing potential for most treatments, with the exception of the phosphate passivation treatment, reached levels that may be controls by the Fe^{2+}/Fe^{3+} redox couple, mediated by biotic oxidation. It is not expected that any treatment assessed in this report could provide protection against AMD generation along, but rather provide passive options that may be used to prepared retired heap leach pads for decommissioning by other methods. For instance, soil and vegetation cover applied after passivation and/or inhibition would limit oxygen and water diffusion through the waste pile while natural organic acids in the soils may continued to inhibit *A. ferrooxidans* and related populations.

CHAPTER 9

9 Radionuclide Release from Simulated Waste Material after Biogeochemical Leaching

Williamson, A. L., Caron, F. & Spiers, G., 2014. Radionuclide release from simulated waste material after biogeochemical leaching of uraniferous mineral samples. Journal of Environmental Radioactivity, Volume X, pp. Y-Z. http://dx.doi.org/10.1016/j.jenvrad.2014.03.004

Journal of Environmental Radioactivity xxx (2014) 1–7

Contents lists available at ScienceDirect

Journal of Environmental Radioactivity

journal homepage: www.elsevier.com/locate/jenvrad

Radionuclide release from simulated waste material after biogeochemical leaching of uraniferous mineral samples

Aimee Lynn Williamson [a,b,*], François Caron [a], Graeme Spiers [a]

[a] Dept. of Chemistry & Biochemistry, Laurentian University, 935 Ramsey Lake Rd., Sudbury, ON, Canada P3E 2C6
[b] MIRARCO, Laurentian University, 935 Ramsey Lake Rd., Sudbury, ON, Canada P3E 2C6

ARTICLE INFO

Article history:
Received 29 October 2013
Received in revised form
4 March 2014
Accepted 9 March 2014
Available online xxx

Keywords:
Bioleaching
Waste
Uranium
Remediation
^{235}U
^{226}Ra

ABSTRACT

Biogeochemical mineral dissolution is a promising method for the released of metals in low-grade host mineralization that contain sulphidic minerals. The application of biogeochemical mineral dissolution to engineered leach heap piles in the Elliot Lake region may be considered as a promising passive technology for the economic recovery of low grade Uranium-bearing ores. In the current investigation, the decrease of radiological activity of uraniferous mineral material after biogeochemical mineral dissolution is quantified by gamma spectroscopy and compared to the results from digestion/ICP-MS analysis of the ore materials to determine if gamma spectroscopy is a simple, viable alternative quantification method for heavy nuclides. The potential release of Uranium (U) and Radium-226 (^{226}Ra) to the aqueous environment from samples that have been treated to represent various stages of leaching and passive closure processes are assessed. Dissolution of U from the solid phase has occurred during biogeochemical mineral dissolution in the presence of *Acidithiobacillus ferrooxidans*, with gamma spectroscopy indicating an 84% decrease in Uranium-235 (^{235}U) content, a value in accordance with the data obtained by dissolution chemistry. Gamma spectroscopy data indicate that only 30% of the ^{226}Ra was removed during the biogeochemical mineral dissolution. Chemical inhibition and passivation treatments of waste materials following the biogeochemical mineral dissolution offer greater protection against residual U and ^{226}Ra leaching. Pacified samples resist the release of ^{226}Ra contained in the mineral phase and may offer more protection to the aqueous environment for the long term, compared to untreated or inhibited residues, and should be taken into account for future decommissioning.

1. Introduction

The potential for biogeochemical dissolution of strategic metals from low-grade host ores containing low levels of sulphidic minerals is a potentially cost-effective extractive method for recovery by hydrometallurgical techniques (Boseker, 1997; Rawlings, 2002). Under the appropriate geochemical conditions, iron oxidizing bacteria may dissolve the ferrous-sulphide minerals with a concomitant release of acidity which may, in turn, dissolve uranium (U)-bearing minerals to release U for recovery from solution (Nemati et al., 1997).

The oxidation of pyrite, with subsequent solubilization of U, occurs through a series of reactions (Fig. 1). In the presence of atmospheric oxygen and water, ferrous-sulphide minerals are oxidized, liberating ferrous iron and sulfuric acid to the environment (Reaction 1). The released ferrous iron is oxidized by molecular oxygen (Reaction 2) to release ferric iron which, in turn, promotes the oxidization of additional ferrous-sulphide minerals (Reaction 3). The oxidation and reduction of iron is a cyclic, self-propagating process (Kleinmann et al., 1981). The relatively slow chemical oxidation of iron is the rate determining step. In the presence of iron-oxidizing bacterial cultures, however, this oxidative dissolution rate can be increased by up to six orders of magnitude (Evangelou and Zhang, 1995; Johnson, 2010; Marchand and Silverstein, 2003; Singer and Stumm, 1970).

Acidithiobacillus ferrooxidans is the most notable bacterial species that drives the bioleaching process, being capable of oxidizing iron and sulfur compounds (Evangelou and Zhang, 1995; Fisher, 1966; Marchand and Silverstein, 2003; Nemati et al., 1997; Singer and Stumm, 1970). This bacterium is an aerobic mesophile which thrives in acidic conditions. When the rate of the reaction is increased significantly, acidity begins to accumulate, thus

* Corresponding author. Dept. of Chemistry & Biochemistry, Laurentian University, 935 Ramsey Lake Rd., Sudbury, ON, Canada P3E 2C6. Tel.:+1 7056751151.
E-mail addresses: al_williamson@laurentian.ca (A.L. Williamson), fcaron@laurentian.ca (F. Caron), gspiers@laurentian.ca (G. Spiers).

http://dx.doi.org/10.1016/j.jenvrad.2014.03.004
0265-931X/

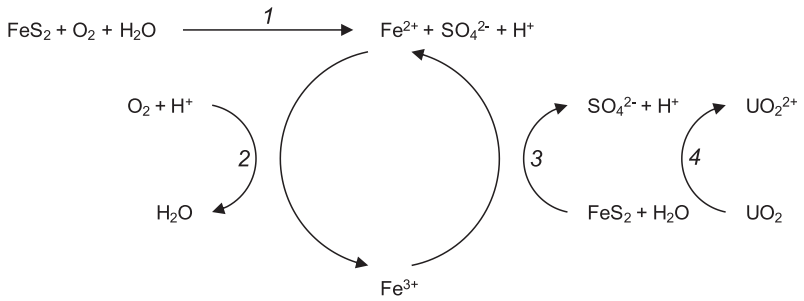

Reaction 1 $$FeS_2 + \frac{7}{2}O_2 + H_2O \rightarrow Fe^{2+} + 2SO_4{}^{2-} + 2\,H^+$$

Reaction 2 $$Fe^{2+} + \frac{1}{4}O_2 + H^+ \rightarrow Fe^{3+} + \frac{1}{2}H_2O$$

Reaction 3 $$FeS_2 + 14Fe^{3+} + 8H_2O \rightarrow 15Fe^{2+} + 2SO_4{}^{2-} + 16H^+$$

Reaction 4 $$UO_2 + 2Fe^{3+} \rightarrow UO_2^{2+} + 2Fe^{2+}$$

Fig. 1. Schematic diagram illustrating the biogeochemical mineral dissolution processes for pyrite and the relationship with U (Evangelou and Zhang, 1995; Fernandes and Franklin, 2001; Kleinmann and Erickson, 1983; Kleinmann, 1987; McIlwaine and Ridd, 2004).

increasing the oxidizing potential of the environment greatly (Baker and Banfield, 2003; Johnson, 2010), causing the concentration of dissolved iron to increase at a much faster rate than with chemical oxidation alone.

Uranium, in the insoluble mineral uraninite, is in the tetravalent oxidation state, making recovery from the mineral host challenging (Lundgren and Silver, 1980). The presence of a strong oxidizing agent, such as ferric iron, promotes the oxidation of the U hosted in the uraninite mineral, with the resulting hexavalent U forming a soluble uranyl compound (Fig. 1, Reaction 4).

Biogeochemical mineral dissolution for the solubilization of U, previously investigated at mine sites in the Elliot Lake area (Campbell et al., 1987, 1985; McCready, 1986; McCready and Gould, 1990; Olson et al., 2003), is the focus of renewed economic in the extraction of U and associated rare earth elements in the former U-mining camp. The application of biogeochemical mineral dissolution techniques to engineered heap leach piles in the Elliot Lake region is a promising passive technology for the recovery of U from low grade mineralization which may compete with higher-grade deposits. Worldwide mining best practice requires that, when extractable resources are exhausted at a mining site, processed tailings, waste rock piles, and spent heap leach pads be treated to control or remove potential environmental liabilities such as radionuclide release to the environment.

1.1. Objective

The objectives of the current work, focused on potential management of radioactive contaminants, are: 1) to assess and monitor the decrease of radiological activity of uraniferous mineral material and the potential release of U and Radium-226 (^{226}Ra) to the aqueous environment following biogeochemical mineral dissolution to provide models to guide decommissioning efforts; and 2) to determine whether gamma spectroscopy is a viable analytical measurement alternative to costly and tedious acid digestion of the mineral phases with ICP-MS solution analysis for heavy nuclides, in particular U. Gamma analysis, not requiring the use of hazardous chemicals that produce waste and disposal issues, requires minimal sample preparation, thus offering potential operational advantages to multi-step digestion procedures.

2. Materials and methods

2.1. Sample collection & preparation

Samples were obtained from the Eco Ridge Project Site located approximately 10 km east of Elliot Lake, Ontario (Fig. 2). Fresh drill cores samples were crushed to 2–4 cm in size and homogenized. Approximately 1 kg of this material was further crushed to a 2 mm in size and placed in leucite leaching columns (internal diameter of 1.27 cm), for a series of bioleaching trials to examine the viability of the biogeochemical mineral dissolution process (Munoz et al., 1993). The columns were leached with a solution inoculated with *A. ferrooxidans* (Ferroni et al., 1986; Leduc and Ferroni, 1994; Leduc et al., 1997) for 7 months, after which residue samples collected from the column were dried, homogenized, and divided for subsequent analysis and experimentation.

Experiments designed to interrupt the biogeochemical mineral dissolution process in preparation for simulated heap closure were completed with the residue sub-samples. Passivation studies were conducted in which coatings were precipitated from solution on the mineral surface to encapsulate the host minerals with an oxygen-impermeable barrier to provide long-term protection from chemical and microbiological oxidative attack (Harris and Lottermoser, 2006). Leaching columns, charged with 60 g of residue, were leached with a coating solution containing an oxidant (0.15 M hydrogen peroxide, H_2O_2), a buffer (0.10 M sodium acetate, CH_3COONa), and either 0.1 M potassium dihydrogen phosphate, KH_2PO_4, or 0.01 M sodium metasilicate, Na_2SiO_2, to induce the formation of ferric phosphate or ferric hydroxide-silica networks on the mineral surface (Evangelou, 2001). Inhibition studies (Onysko et al., 1984) were carried out in parallel to the passivation studies. The residue material was leached with a solution containing 0.010 g L^{-1} sodium lauryl sulfate, an organic surfactant

Please cite this article in press as: Williamson, A.L., et al., Radionuclide release from simulated waste material after biogeochemical leaching of uraniferous mineral samples, Journal of Environmental Radioactivity (2014), http://dx.doi.org/10.1016/j.jenvrad.2014.03.004

Fig. 2. Location of study site, east of Elliot Lake, Ontario (image provided).

known to inhibit biotic iron oxidation by *A. ferrooxidans* at concentrations as low at 5 mg L^{-1}. After 12 days of passivation and inhibition treatments, the samples were dried, homogenized, and divided for further testing or analysis, with five mineral samples selected for further extraction testing representing various fresh material, untreated leached material, and leached material that had be subjected to inhibition or passivation treatments (Table 1).

2.2. Leachate extraction testing and gamma measurements

Extraction tests, based on Standard Practice for Shake Extraction of Solid Waste with Water ASTM D3987–12 (ASTM International, 2013), required the addition of a 5-g sample to an Erlenmeyer flask, filled with 200 mL of de-ionized water, and shaken on a bench top shaker for 72 h at 30 °C. The resulting leachate was collected by vacuum filtration through a 0.45-μm filter. The leachate samples were evaporated on a polyethylene sheet in a dish placed on a low-heat plate under IR lamps overnight (Caron and Mankarios, 2004; Caron et al., 2007). The sheet was folded and pressed into a disk (2 cm by 0.5 cm) which was then laid into a 4.5 cm × 4.5 cm clear polystyrene jar (Qorpak) for gamma spectroscopic analysis. The dried residual solid materials were weighed (approx. 8 g) and also placed in a polystyrene jar for analysis.

Table 1
Mineral sample origin and previous treatments.

Sample		Solid material	Extraction test
1	Fresh	X	X
2	Leached	X	X
3	Leached, pacified (KH_2PO_4)		X
4	Leached, pacified (Na_2SiO_3)		X
5	Leached, inhibited (SLS)		X

SLS, sodium lauryl sulfate.

2.3. Solid phase digestion & ICP-MS analysis

Sub-samples of the mineral material before and after leaching were ground to 74 μm (>200 mesh) for acid digestion in an open 50 mL Teflon™ tube using a programmable digestion block. The digestion involved addition of 10 mL of HF/HCl (1:1) to 0.5 g of ground mineral material, heating to 110 °C for 3.5 h to evaporate to dryness, with further addition of 14 mL HCl/HNO_3 (1:1), heating to 110 °C for 4 h to evaporate to dryness. The final digestion step involved addition of 0.5 mL of $HF/HCl/HNO_3$ (1:4:20), heating to 110° C with reduction of solution volume to 8–10 mL prior to bringing to a final volume of 50 mL with ultrapure water. The solutions, further diluted (1:10), were then analyzed by ICP-MS (Varian 810). Each sample solution was analyzed read three times, with 30 mass scans per replicate. The quality control program included analysis of duplicates, Certified Reference Materials

Please cite this article in press as: Williamson, A.L., et al., Radionuclide release from simulated waste material after biogeochemical leaching of uraniferous mineral samples, Journal of Environmental Radioactivity (2014), http://dx.doi.org/10.1016/j.jenvrad.2014.03.004

(CRM's), Internal Reference Materials (IRM's), procedural and calibration blanks, with continuous calibration verification and use of internal standards (Re and Ru) to correct for any mass bias. The ICP-MS analysis was completed in an ISO 17025 accredited facility (Elliot Lake Research Field Station of Laurentian University), with final concentrations calculated as mass/mass (dry soil basis).

2.4. Gamma counting

Uranium (^{235}U) and ^{226}Ra were analyzed by gamma spectrometry using a Canberra Model GC1020 HP germanium detector housed in a Canberra lead castle controlled by a DSA-1000 digital processor and Genie 2000 software. The jars containing the solid samples and the pressed polyethylene sheets were placed directly on the detector and counted for 12 and 24 h respectively. Detector calibration and efficiencies (Table 2) were calculated by interpolation for the pressed polyethylene sheet using a NIST traceable multi-gamma standard (QCY-48, AEA Technologies). The detector efficiencies for equivalent masses for the solid material were obtained directly using a tailings standard (UTS-2, CANMET, Ottawa, ON) (Table 2). A background reading, counted for 24 h, was used for spectral correction in the regions of the peaks of interest.

The gamma spectra for U containing samples are complex, with Uranium-235 having two prominent peaks at 143.8 keV (10.5% intensity) and 185.6 keV (54.0% intensity), respectively. The ^{235}U peak, overlapping the ^{226}Ra peak at 186.2 keV (3.3% intensity), can be employed to correct for ^{235}U contribution to the composite peak at ~186 keV. The calculated contribution from ^{235}U at 185.6 keV is 5.14 times the peak intensity at 143.8 keV with deconvolution for the 186 keV peak allowing quantification of the ^{235}U and ^{226}Ra intensity contribution. The UTS-2 listed values were used to estimate the amounts of ^{235}U and ^{226}Ra, based on the source report (NUTP-2E). The above ratio of 5.14 was used to remove the ^{235}U counts at 186 keV in samples, based on the number of disintegrations expected for ^{235}U at 143 keV. The total number of disintegrations for ^{235}U and ^{226}Ra at 186 keV was calculated using Equations (1) and (2) respectively, where C is the number of observed counts at indicated energy and ε is the detector efficiency that the indicated energy.

$$C_{\mathrm{U-235@186}} = \frac{C_{\mathrm{U-235@143}}}{\varepsilon_{143}} \times 5.14 \times \varepsilon_{186} \quad (1)$$

$$C_{\mathrm{Ra-226@186}} = C_{\mathrm{total@186}} - C_{\mathrm{U-235@186}} \quad (2)$$

The specific activity, A_{Ei}, of each radionuclide i was calculated (Equation (3)), where E is the energy, C_{Ei} net peak area of a peak at energy E, ε_E is the detection efficiency at energy E, t is the analysis time, and γ is the number of gammas per disintegration of this nuclide at energy E (Tzortzis et al., 2003).

$$A_{Ei} = \frac{C_{Ei}}{\varepsilon_E \cdot t \cdot \gamma} \quad (3)$$

Using these corrections, the comparison can be made for the crushed sample cores before and after leaching. The comparison between total U concentration (by digestion-ICP-MS analysis) and ^{235}U activity concentration (by gamma counting) is relative; hence back-calculating to total U is unnecessary.

Table 2
Detector efficiency.

Sample type	Energy	
	143 keV	186 keV
Pressed polyethylene film	8.4%	7.3%
Solid material	38%	8.9%

3. Results & discussion

3.1. Solid material

The concentrations of heavy nuclides, particularly U, were obtained by ICP-MS analysis, after the multi-acid digestion of crushed mineral samples (Fig. 3). Gamma spectroscopy was investigated to determine whether it was a suitable alternate technique for these nuclides. The latter technique may be advantageous, saving on tedious contamination, preparation, and digestion techniques, albeit at the expense of longer individual sample counting times.

Biogeochemical mineral dissolution decreased the U content of the mineral material by 84%, from approximately 940 to 150 mg U kg^{-1} of material (Fig. 3a). After the biogeochemical mineral dissolution process, there was an 84% decrease of measurable activity for ^{235}U (Fig. 3b). These results confirm the release of U nuclides from the solid phase is driven by the biogeochemical mineral dissolution of ferrous sulphide minerals (pyrite) in acidic and oxidizing conditions, as explained by Reaction 4.

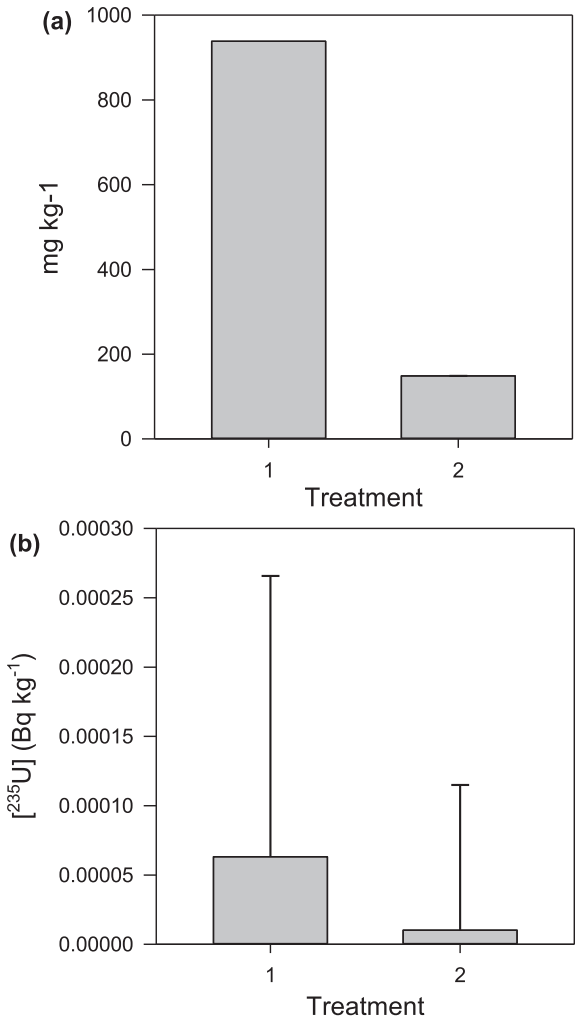

Fig. 3. Total U concentration (mg g^{-1}) (a) and ^{235}U activity concentration (Bq kg^{-1}) in fresh (1) and biogeochemically leached (2) solid material.

Please cite this article in press as: Williamson, A.L., et al., Radionuclide release from simulated waste material after biogeochemical leaching of uraniferous mineral samples, Journal of Environmental Radioactivity (2014), http://dx.doi.org/10.1016/j.jenvrad.2014.03.004

The activity concentration of ^{226}Ra in the solid material decreased from 3.0×10^{-3} to 2.1×10^{-3} Bq kg^{-1} after the biogeochemical mineral dissolution experiments (Fig. 4). Radium-226 may not dissolve during the leaching process, but instead form insoluble radium sulphates. According to Lind et al. (1918), the solubility of pure radium sulfate in acidic conditions at 25 °C is 2.1×10^{-12} g L^{-1}, suggesting that any dissolved Ra should precipitate under the high sulfuric acid concentrations generated by the biogeochemical mineral dissolution processes. The management of the ^{226}Ra in this potential waste material will need to be considered in site decommissioning planning, should this extraction procedure be commercially implemented.

3.2. Leachate

Conventional leachate extraction testing was used to estimate the potential for residual radionuclides to be leached by percolating solutions from a processed heap leach pad to the surrounding aqueous environment. The samples subjected to this extraction experiment represented both untreated and treated samples, thus representing the various materials that may be present in residual heap at closure for decommissioning (Fig. 5).

The activity concentrations of ^{235}U observed in the previously leached and pacified samples (sample 2, 3, and 4) was approximately 90% less than that of the fresh sample (sample 1), being 0.12–0.14 Bq L^{-1} compared to 1.33 Bq L^{-1} (Fig. 5a). These results indicate that pacification offered no additional protection for the continued leaching of residual U from the previously biogeochemically extracted material. However, samples previously treated with an inhibitor (sample 5) demonstrated the more resistance to continued U dissolution during the extraction testing with an activity of only 0.01 Bq L^{-1} being measured in the leachate solution (Fig. 5a).

The Canadian Nuclear Safety Commission (CNSC) requires all licence holders of U mine and milling operations to meet the discharge criteria defined in the Metal Mining Effluent Regulations (MMER) under the Fisheries Act, which applies the ALARA principle (as low as reasonably achievable) with respect to total U concentration in treated effluents (Canadian Nuclear Safety Comimission, 2012). The optimization screening objective (OSO) recognized by the CNSC for total dissolved U concentration in treated effluent is 0.1 mg L^{-1} (Canadian Nuclear Safety Commission and Environment Canada, 2012). Adherence to these regulations prevents any unreasonable risk to the environment, and ensures that operators will not have any violation of licence conditions with effluent concentrations. Exceedance of the OSO by facilities with U concentrations greater than the OSO requires facilities optimization and/or upgrade of effluent treatment process. The OSO is considerably lower than established regulatory limits for the maximum monthly average U concentration permissible in the United States, 2 mg L^{-1} (Enviromental Protection Agency, 2000) and Saskatchewan, 2.5 mg L^{-1} (Government of Saskatchewan, 1996)). The fresh sample in this study (sample 1) had a U concentration 23 times greater than the OSO limit for U, whereas the leached samples had total U concentrations 2 times greater than the OSO limit, with the exception of one sample (Table 3).

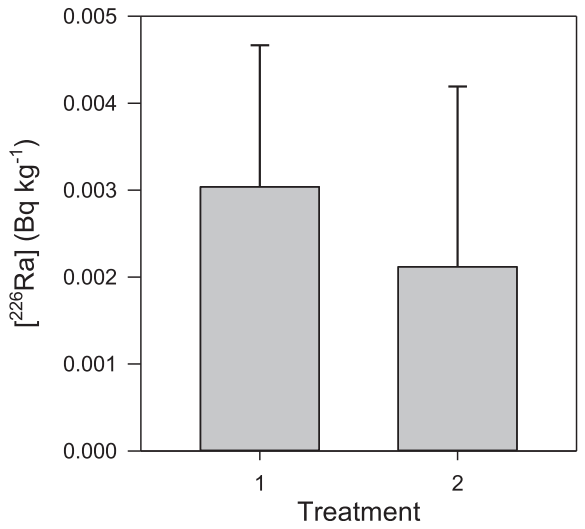

Fig. 4. Activity concentration (Bq kg^{-1}) of radium-226 in fresh (1) and biogeochemically leached (2) solid material.

The effect of the treatments on the release of ^{226}Ra was quite different (Fig. 5b). The activity of the pacified treatments (samples 3 and 4) was below the detection limit, 0.1 Bq L^{-1}. The leachate from the fresh and inhibition treated samples (samples 1 and 5) were 0.37 and 0.43 Bq L^{-1}, respectively. The previously leached sample, not prepared for closure (sample 2) by passivation or inhibition, had the highest amount of ^{226}Ra leaching, 2.04 Bq L^{-1}. These results suggest that both the passivation and inhibition applications have the ability to limit ^{226}Ra leaching from materials that have been treated in preparation for closure of heap leach operations.

The comparison of the ^{226}Ra activity concentrations from the extraction testing and the MAC criteria is show in Table 3. The Mining Metals Effluent Regulations define the maximum authorized concentration of ^{226}Ra as 1.11 Bq L^{-1} for grab samples and 0.37 Bq L^{-1} for a monthly mean (Government of Canada, 2002). The leachate from the fresh sample (sample 1) had a ^{226}Ra activity concentration equal to the monthly mean MAC, whereas the sample previously treated with an inhibiting compound (sample 5) had an activity concentration slightly greater than the monthly mean MAC, but lower than the grab sample allowance. The activity concentration was greater than the monthly mean and the grab sample MAC for the previously leached sample that did not receive additional treatments in preparation for decommissioning (Sample 2), 2.04 Bq L^{-1}.

All samples examined in this study were above the MAC respect to total U concentration with one exception, sample 5 (Table 3). The fresh material (sample 1) released U to solution as a consequence of the geochemical mineral dissolution process, driven either abiotically or in the presence of microbes. Only low quantities of U were leached from the remaining samples which had been previously been exposed to ideal leaching conditions; this also ensured minimal amounts of U remaining in the crushed mineral samples. The treatment of samples with the passivation coating solutions offered no additional protection against the further release of U to solution, whereas the inhibition treated sample released undetectable amounts of U. The outcomes of this study indicate the requirement for effluent treatment for previously leached samples having U concentrations greater than the OSO in accordance with the CNSC recommendations.

The only sample that does not meet the MAC criteria for ^{226}Ra activity concentration in this study is the previously leached sample that was not prepared for passive closure. The amount of ^{226}Ra present in the leachate for this sample was four times greater than the MAC value. The fresh material (sample 1), was slightly below the MAC value. Pardue and Guo (1998) reported that the biogeochemical control of ^{226}Ra solubility in sediments is related to coprecipitation of metal sulfates, with potential remobilization occurring under anaerobic, sulfate-reducing conditions. The results in this study suggest 30% of the ^{226}Ra was removed during biogeochemical mineral dissolution, with subsequent extraction tests showing that, in the absence of passivation treatment, that activity concentration of ^{226}Ra leaching from the solid phase

Please cite this article in press as: Williamson, A.L., et al., Radionuclide release from simulated waste material after biogeochemical leaching of uraniferous mineral samples, Journal of Environmental Radioactivity (2014), http://dx.doi.org/10.1016/j.jenvrad.2014.03.004

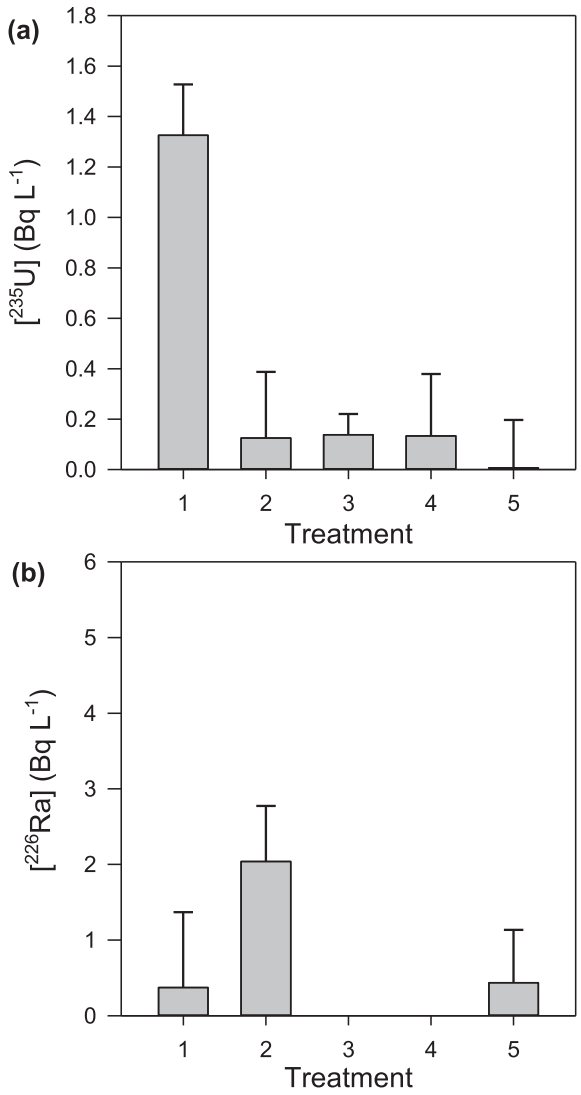

Fig. 5. Activity (Bq L^{-1}) of (a) uranium-235 and (b) radium-226 in extraction test leachate for fresh (1), biogeochemically leached (2), KH_2PO_4 pacified (3), Na_2SiO_3 pacified (4), and SLS inhibited (5) solid material.

residue was four times greater than the MAC defined levels. Pacified samples offered the greatest protection against ^{226}Ra leaching and the inhibition treatment is slightly below the MAC criteria.

4. Conclusion

Dissolution of U from the solid phase crushed ore materials was driven by biogeochemical mineral dissolution in the presence of *A. ferrooxidans*. Gamma spectroscopy indicated an 84% decrease in ^{235}U content in the residual ore materials, a value in agreement with results obtained by digestion and ICP-MS quantification of U in the digested solutions. This study demonstrates that gamma spectroscopy is a viable alternative to the time and labor intensive acid digestion and ICP-MS analysis of U content of the solid mineral phase. This measurement alternative is simpler in terms of manipulations, chemical operations and expensive equipment requirements, and thus may be suitable advantageous for small monitoring facilities, albeit at the expense of longer counting times.

After biogeochemical mineral dissolution, most ^{226}Ra remained in the waste mineralized rock, and thus ^{226}Ra presence will need to be taken into consideration in planning for site decommissioning. The inhibition treatments offer greater protection against U leaching than the passivation treatment, with the reverse being observed in controlling the potential of ^{226}Ra leaching from the biogeochemically treated mineral residue. As only 30% of ^{226}Ra was removed during biogeochemical mineral dissolution phase, the potential for radionuclide release will continue to exist during the site decommissioning phase. Samples treated with a passivation coating tend to resist the release of ^{226}Ra contained in the mineral phase, thus potentially offering more protection to the aqueous environment for the long term.

Leachate from fresh mineral material exceeded the OSO recommended concentration for U content, whereas the biogeochemical mineral dissolution process in a simulated heap under the laboratory test conditions reduced the total U concentration in the crushed ore materials. Treatment of this effluent would likely be required based on CNSC recommendations. The results obtained in this study indicate the need to understand the mechanisms of ^{226}Ra retention and dissolution during biogeochemical mineral dissolution to advise the decommissioning planning process, and to enable accurate prediction of the rate of ^{226}Ra release into the leachate and into the aqueous environment.

Table 3
Comparison of the maximum effluent concentrations for total U and ^{226}Radium from extraction testing samples.

Sample	Total uranium (mg/L)	Radium-226 (Bq/L)
1	2.33[a]	0.37
2	0.22[a]	2.04[a]
3	0.24[a]	0.00
4	0.23[a]	0.00
5	0.01	0.43[a]
Limit	0.1 (OSO)	0.37 (MMER)

OSO, optimization screening objective.
MMER, Metal Mining Effluent Regulations.
[a] Greater than limit.

Acknowledgments

The authors wish to thank the following: Al Shefsky, Fergus Kerr, and Roger Payne of Pele Mountain Resources Limited, Toronto, Ontario, for supplying the mineral drill core samples; Chris Colaneri for conducting the preliminary gamma spectroscopy investigations of the mineral material; and Troy Maki of Elliot Lake Research Field Station of LU for assistance with analytical aspects. The research was supported by Pele Mountain Resources Inc., The Ontario Research Fund (grant number RE01-030 to Kaiser, Spiers, and Dunn), and Natural Science and Engineering Research Council (NSERC IPS-2 to Williamson). This work was presented in the Environmental Radiochemistry Symposium at the 96th Canadian Chemistry Conference and Exhibition in Quebec City, Quebec, May 26–30, 2013.

References

ASTM International, 2013. Standard Practice for Shake Extraction of Solid Waste with Water. ASTM International.
Baker, B.J., Banfield, J.F., 2003. Microbial Communities in Acid Mine Drainage, vol. 44, pp. 139–152.
Boseker, K., 1997. Bioleaching: metal solubilization by microorganisms. FEMS Microbiol. Rev. 20, 591–604.
Campbell, M.C., Parsons, H.W., Jongejan, A., Sanmugasunderam, V., Silver, M., 1985. Biotechnology for the Mineral Industry. Can. Metall. Q. 24, 115–120.
Campbell, M.C., Wadden, D., Marchbank, A., McCready, R.G.L., Ferroni, G., 1987. In-place leaching of uranium at Denison Mines Limited. Development of Projects for the production of Uranium Concentrates, Vienna, pp. 151–165.
Canadian Nuclear Safety Commission, 2012a. Management of Uranium Mine Waste Rock and Mill Tailings. Canadian Nuclear Safety Commission.
Canadian Nuclear Safety Commission and Environment Canada, 2012b. Annual Report on Uranium Management Activities. Canadian Nuclear Safety Commission, Ottawa, p. 2010.

Caron, F., Laurin, S., Simister, C., Jacques, C., Mankarios, G., 2007. Potential use of ultrafiltration for groundwater remediation and aqueous speciation of 60-Co and 137-Cs from A Contaminated area. Water, Air, Soil. Pollut. 178.
Caron, F., Mankarios, G., 2004. Pre-assessment of the speciation of 60-Co, 125-Sb,137-Cs and 241-Am in a contaminated aquifer. J. Environ. Radioact. 77, 29–46.
Environmental Protection Agency, 2000. Section 440.32-Effluent Limitations Representing the Degree of Effluent Reduction Attainable by the Application. US Government.
Evangelou, V.P., 2001. Pyrite microencapsulation technologies: principles and potential field applications. Ecol. Eng. 17, 165–178.
Evangelou, V.P., Zhang, Y.L., 1995. A review: pyrite oxidation mechanisms and acid mine drainage prevention. Crit. Rev. Environ. Sci. Technol. 25 (2), 141–199.
Fernandes, H.M., Franklin, M.R., 2001. Assessment of acid rock drainage pollutants release in the uranium mining site of Poços de Caldas–Brazil. J. Environ. Radioact. 54 (1), 5–25.
Ferroni, G.D., Leduc, L.G., Todd, M., 1986. Isolation and temperature characterization of physchrotropic strains of thiobacillus ferrooxidans from the environment of a uranium mine. J. General. Appl. Microbiol. 32, 169–175.
Fisher, J.R., 1966. Bacterial Leaching of Eliot Lake Uranium Ore. The Canadian Mining and Metallurgical Bulletin, May.
Government of Saskatchewan, 1996. The Mineral Industry Environmental Protection Regulations, 1996. Ministry of Environment.
Government of Canada, 2002. Metal Mining Effluent Regulations SOR/2002-222. Minister of Justice.
Harris, D.L., Lottermoser, B.G., 2006. Phosphate stabilization of polyminerallic mine wastes. Mineral. Mag. 70, 1–13.
Johnson, D.B., 2010. The biogeochemistry of biomining. In: Barton, L.L., Mandl, M., Loy, A. (Eds.), Geomicrobiology: Molecular and Environmental Perspective. Springer, New York.
Kleinmann, R.L.P., 1987. Bacterial Oxidation of Acid-forming Materials. Planning, Rehabilitation and Treatment of Disturbed Lands Billings Symposium, Billings, Montana, pp. 34–46.
Kleinmann, R.L.P., Crerar, D.A., Pacelli, R.R., 1981. Biogeochemistry of acid mine drainage and a method to control acid formation. Mining Eng. (March), 300–305.
Kleinmann, R.L.P., Erickson, P.M., 1983. Control of Acid Drainage from coal refuse Using anionic Surfactants. United States Department of the Interior.
Leduc, L.G., Ferroni, G.D., 1994. The chemolithotrophic bacterium *Thiobacillus ferrooxidans*. FEMS Microbiol. Rev. 14, 103–120.
Leduc, L.G., Ferroni, G.D., Trevors, J.T., 1997. Resistance to heavy metals in different strains of *Thiobacillus ferrooxidans*. FEMS Microbiol. Lett. 14, 103–120.
Lind, S.C., Underwood, J.E., Whittemore, C.F., 1918. The solubility of pure radium sulfate. Am. Chem. J. 40, 465–472.
Lundgren, D.G., Silver, M., 1980. Ore leaching by bacteria. Annu. Rev. Microbiol. 34, 263–286.
Marchand, E.A., Silverstein, J., 2003. The role of enhanced heterotrophic bacterial growth on iron oxidation by *Acidithiobacillus ferrooxidans*. Geomicrobiol. J. 20, 231–244.
Munoz, J.A., Gonzalea, F., Ballester, A., Blazquez, M.L., 1993. Bioleaching of a Spanish uranium ore. FEMS Microbiol. Rev. 11, 109–120.
McCready, R.G.L., 1986. Process in the bacterial leaching of Metals in Canada. In: Norris, P.R., Kelly, D.P. (Eds.), Fundamental and Applied Biohydrometallurgy: Proceedings of the Sixth International Symposium on. Elsevier, Vancouver.
McCready, R.G.L., Gould, W.D., 1990. Bioleaching of uranium. In: Ehrlich, H.L., Brierley, C.L. (Eds.), Microbial Mineral Recovery. McGraw-Hill, New York.
McIlwaine, L.M., Ridd, M., 2004. Assessment of leachate from blended waste rock material and Pasminco Century Mine – Initial results from a two-year study. In: AUSIMM New Leader's Conference, Ballarat, Australia.
Nemati, M., Harrison, S.T.L., Hansford, G.S., Webb, C., 1997. Biological oxidation of ferrous sulfate by *Thiobacillus ferrooxidans*: a review on the kinetic aspects. Biogeochem. Eng. J. 1, 171–190.
Olson, G.J., Brierley, J.A., Brierley, C.L., 2003. Bioleaching review part B: progress in bioleaching: applications of microbial processes by the minerals industries. Appl. Microbiol. Biotechnol. 63 (3), 249–257.
Onysko, S.J., Kleinmann, R.L.P., Erickson, P.M., 1984. Ferrous iron oxidation by Thiobacillus ferrooxidans: inhibition with benzoic acid, sorbic acid and sodium laurly sulfate. Appl. Environ. Microbiol. 48, 229–231.
Pardue, J.H., Guo, T.Z., 1998. Biogeochemistry of Ra-226 in contaminated bottom sediments and oilfield waste pits. J. Environ. Radioact. 39, 239–253.
Rawlings, D.E., 2002. Heavy metal mining using microbes. Annu. Rev. Microbiol. 56, 65–91.
Singer, P.C., Stumm, W., 1970. Acidic mine drainage: the rate-determining step. Science 167, 1121–1123.
Tzortzis, M., Haralabos, T., Christofides, S., Christodoulides, G., 2003. Gamma-ray measurements of naturally occurring radioactive samples from Cyprus characteristic geological rocks. Radiat. Meas. 37, 221–229.

Please cite this article in press as: Williamson, A.L., et al., Radionuclide release from simulated waste material after biogeochemical leaching of uraniferous mineral samples, Journal of Environmental Radioactivity (2014), http://dx.doi.org/10.1016/j.jenvrad.2014.03.004

CHAPTER 10

10 Summary

The overarching goal of this thesis was to simulate biologically mediated heap-leach conditions in the laboratory in anticipation of the potential application of passive recovery methods being applied at Pele Mountain Resources' (PMR) Eco Ridge Mine Rare Earth and Uranium Project site, located near Elliot Lake, Ontario. Monitoring of the mineralogical and geochemical dynamics of the extraction process provide detailed information on metal release dynamics and an investigation of passive, minimal maintenance, approaches to decommissioning of heap-leach pads aid in decommissioning preparations.

The review of the published research focused on the biogeochemical dissolution of pyrite with co-release of uranium (U) from the ores with subsequent implementation of passive approaches to prepare for decommissioning to assess the current state of knowledge in these two areas. Biogeochemical mineral dissolution experiments with the application of passive approaches to subsequently prepare for decommissioning were designed. The goal of the combined dissolution and decommissioning experiments was to provide an understanding of metal release by the biogeochemical mineral dissolution process using native microbial populations, with potential application of passive approaches to prepare for decommissioning to determine the overall suitability of the process and application methods to the development heap-leach pads at in the Elliot Lake region.

The chemical analyses of effluents collected throughout the experimentation, coupled with mineralogical and geochemical analyses of the feed and residual mineral material has enabled an understanding of the chemical controls of the overall biogeochemical mineral dissolution process for iron, U, and thorium (Th), together with the preferential leaching release patterns for rare earth elements (REEs), to be

obtained. A mechanism describing U retention in secondary coatings has been proposed, with a passive approach to closure using inhibition and encapsulation methods being demonstrated, along with a determination of the potential for ongoing radionuclide release from a simulated heap upon decommissioning.

The application of biogeochemical mineral dissolution has been demonstrated to assess the chemical controls on U and Th dissolution. Large columns stocked with ore of the expected on-site top-size has demonstrated the importance of chemical, mineralogical, and microbiological optimization for the success of a biogeochemical mineral dissolution process for the recovery of U, Th, and REE from heap-leaching pads. The studies suggest that the leaching environment may be optimized to promote microbial activity in the absence of direct inoculation of a mature culture and, with suitable leaching environmental conditions, U, Th, and some REE may potentially be completely leached from the mineral feed materials with minimal preprocessing.

A solid phase investigation to identify the REE-bearing mineral phases was completed to provide an understanding of the mineralogical and chemical controls on dissolution of REE. The leaching experiments highlight preferential release of heavy REEs, with the associated solid phase investigation enabling the identification of REE-bearing mineral phases and the mineralogical and chemical controls on REE dissolution. Under the environmental conditions established by the biogeochemical mineral dissolution process, it is expected that REE-bearing mineral phases associate with uraninite-based mineral phases will be available to the leaching liquid. Heavy REEs-bearing mineral phases are found to be associated with pyrite, the mineral driving the biogeochemical mineral dissolution process. The dissolution of pyrite thus contributes to the release of heavy REE-bearing minerals to the dissolved phase, with the associated production of acidity and sulphate. The light REEs are present in monazite and rutile mineral phases. The accumulation of sulphate in solution contributes to a decrease of pH, driving the dissolution of monazite to release the associated light REE's into the dissolved phase. The mobilization of light REE-bearing minerals associated with rutile are not expected to contribute greatly to the solution

under the experimental biogeochemical conditions because rutile is stable in these bioleaching conditions. This study confirms that the natural chemical process provided by the biogeochemical mineral dissolution environment is sufficient to promote the dissolution of U and most REE's in the conglomerate ore. Thus the design of a leaching protocol to further optimize the economic dissolution of REE's to support the return to U mining to the Elliot Lake region may be feasible.

The retention mechanism of U as phosphate phases in secondary precipitates formed on mineral surfaces during and after biogeochemical mineral dissolution has been described as a multi-step process. It is suggested that Al(hydr)oxide coatings on weathering pyrite after biogeochemical mineral dissolution retain uranyl-phosphate phases following a five step process: formation of Fe(hydr)oxide coatings on weathered pyrite; incorporation of phosphate species into the Fe(hydr)oxide coatings; formation of a ternary uranyl-phosphate adsorption complex on the oxide coatings Mineral replacement reactions promoting the replacement of Fe(hydr)oxides with Al analogues; and precipitation, and subsequent nucleation of uranyl-phosphates, on the surface and throughout the coating network. An alternative method may exist where Al(hydr)oxide coatings replace the Fe(hydr)oxide coatings prior to P adsorption. However, ternary U-phosphate adsorption complexes on Al(hydr)oxide coatings have not been previously described, and the mechanism of U-phosphate precipitation under these geochemical conditions is unclear.

The application of pacification and inhibition treatments to previously leached mineral materials was demonstrated and an assessment of the short-term capabilities of each treatment to resist further oxidation and subsequent mineral dissolution from the simulated waste rock was completed. Encapsulation and inhibition treatments using large columns stocked with pre-leached material demonstrated the application process and provided an assessment of the potential longevity of the decommissioning treatment. The study demonstrated that the passivation method most resistant to biotic and abiotic oxidizing conditions required leaching with a phosphate solution, which is thought to promote the formation of a ferric iron–rich coating on the pyritic mineral surface with no need for modification of the solution application

system. The combination of the phosphate solution with a biological inhibition compound may provide additional oxidation resistance through control of the existing bacterial populations. This short term study has provided preliminary details describing passive approaches to prepare for decommissioning. It is not expected that any treatment assessed in this report could provide protection against AMD generation for the long term, but rather allow passive applications to prepare retired heap leach pads for decommissioning by other methods. For instance, soil and v-egetation cover applied after passivation and/or inhibition would limit oxygen and water diffusion through the waste pile while natural organic acids in the soils may continued to inhibit *A. ferrooxidans* and related populations.

An assessment on the decrease of radiological activity of uraniferous mineral material has been determined and the potential release of U and ^{226}Ra to the aqueous solution following biogeochemical mineral dissolution was assesses, which will provide models to guide decommissioning efforts. This study found that, after completion of the biogeochemical mineral dissolution phase of the investigation, most of the ^{226}Ra remained in the mineralized waste rock, thus requiring the ^{226}Ra presence to be taken into consideration in any long term planning for site decommissioning. The passive mineral encapsulation treatments resisted the release of ^{226}Ra from the solid phase, potentially providing long term protection to the aqueous environment. An improved understanding of the mechanisms controlling ^{226}Ra retention and dissolution during biogeochemical mineral dissolution would be beneficial to guide the long-term planning of the decommissioning process. Low quantities of U were leached from samples which had been previously been exposed to ideal leaching conditions and it was shown that the treatment of samples with passive mineral encapsulation treatments offered no additional protection against the further release of U to solution, whereas the inhibition treated sample released undetectable amounts of U. Further development of the chemical and mineralogical encapsulation processes may enable the materials remaining in the leach piles to successfully prevent any release of residual U and decay daughter products to environmental media.

The proposed U and REE mine at EcoRidge could employ a sustainable heap-leach method for the extraction of U and REEs from the low-grade host mineralization. The investigations conducted as part of this thesis have determined that biogeochemical mineral dissolution, mediated by an indigenous microbe population, successfully releases U, Th, and select REE's from the ore from the EcoRidge site, with the possibility of improving the REE dissolution processes. The dissolution of sulphide-bearing minerals throughout the operational phase will allow a spent heap-pad to be less reactive, thus posing minimal environmental threat from release of both U and acidity, as the decommissioning phases are implemented. The encapsulation of reactive minerals shows promise for limiting the ongoing biogeochemical mineral dissolution process, especially if used in association with a bacterial inhibition process, and may effectively inhibit the biogeochemical processes in the residual heap well into the closure phase.

The research laboratory demonstrations in this study have shown that biogeochemical mineral dissolution, followed by waste material encapsulation, can be successfully applied to heap-leach pads enabling the economic recovery of U, Th, and selected REEs to solution for subsequent metallurgical collection. The studies strongly support the concept of sustainable development for the operation of Pele Mountain Resources' Eco Ridge Mine Rare Earth and Uranium Project site in the Elliot Lake region.

REFERENCES

Agate, A. D., 1996. Recent advances in microbial mining. *World Journal of Microbiology & Biotechnology,* Volume 12, pp. 487-495.

Ahonen, L. & Tuovinen, O. H., 1989. Microbial oxidation of ferrous iron at low temperatures. *Applied and Environmental Microbiology,* Volume 55, pp. 312-316.

Ahonen, L. & Tuovinen, O. H., 1995. Bacterial leaching of complex sulfide ore samples in bench-scale column reactors. *Hydrometallurgy,* Volume 37, pp. 1-21.

Alexander, B., Leach, S. & Ingledew, W. J., 1987. The relationship between chemiosmosis parameters and sensitivity to anions and organic acids in the acidophile Thiobacillus ferrooxidans. *Journal of General Microbiology,* Volume 133, pp. 1171-1179.

Allison, J. D., Brown, D. S. & Novo-Grandac, K. J., 1991. *MINTEQA2, a geochemical assessment data base and test cases for environmental systems.* Report EPA/600/3-91/-21 ed. Athens: US EPA.

Arias, M. et al., 2006. Retention of phosphorous by iron and aluminium-oxides-coated quartz particles. *Journal of Colloid and Interface Science,* Volume 295, pp. 65-70.

ASTM International, 2013. *Standard Practice for Shake Extraction of Solid Waste with Water.* West Conshohocken: ASTM International.

Baker, B. J. & Banfield, J. F., 2003. Microbial communities in acid mine drainage. Volume 44, pp. 139-152.

Banfield, J. F. & Eggleton, R. A., 1990. Analytical transmission electron microscope studies of plagioclase, muscovite, and K-feldspar weathering. *Clays and Clay Minerals,* Volume 38, pp. 77-89.

Banks, D. et al., 1997. Mine-waste chemistry: the good, the bad and the ugly. *Environmental Geology,* 32(2), pp. 157-174.

Bartlett, R. W., 1998. *Solution Mining: Leaching and Fluid Recovery of Materials.* 2nd Edition ed. Amsterdam: Gordon and Breach Science Publishers.

Belzile, N., Maki, S., Chen, Y. W. & Goldsack, D., 1997. Inhibition of pyrite oxidation by surface treatment. *The Science of the Total Environment,* Volume 196, pp. 177-186.

Berthelot, D., Leduc, L. G. & Ferroni, G. D., 1997. Iron-oxidizing autotrophs and acidophilic heterotrophs from uranium mine environments. *Geomicrobiology Journal,* Volume 14, pp. 317-324.

Bessho, M., Wajima, T., Ida, T. & Nishiyama, T., 2011. Experimental study on prevention of acid mine drainage by silica coating on pyrite waste rocks with amorphous silica solution. *Environmental Earth Sciences,* Volume 64, pp. 311-318.

Bigham, J. M. & Nordstorm, D. K., 2000. Iron and Aluminum Hydroxysulfates from Acid Sulfate Waters. *Reviews in Mineralogy and Geochemistry,* Volume 40, pp. 351-403.

Blowes, D. W. & Jambor, J. L., 1990. 'The pore-water geochemistry and the mineralogy of the vadose zone of sulfide tailings, Waite Amulet, Quebec, Canada. *Applied Geochemistry,* Volume 5, pp. 327-346.

Boorman, R. S. & Watson, D. M., 1976. Chemical processes in abandoned sulfide tailings dumps and environmental implication of northeastern New Brunswick. *Canadian Institute of Mining and Metallurgy Bulletin,* Volume 69, pp. 86-96.

Boseker, K., 1997. Bioleaching: Metal solubilization by microorganisms. *FEMS Microbiology Reviews,* Volume 20, pp. 591-604.

Bouffard, S. C. & Dixon, D. G., 2002. On the rate-limiting steps of pyritic refractory gold ore heap leaching: results from small and large column tests. *Minerals Engineering,* Volume 15, pp. 859-870.

Brahmaprakash, G. P. et al., 1988. Development of Thiobacillus ferrooxidans ATCC 19859 strains tolerant to copper and zinc. *Bulletin of Material Science,* Volume 10, pp. 461-465.

Brantley, S. L., 2005. Reaction kinetics of primary rock-forming minerals under ambient conditions. *Treatise on Geochemistry,* Volume 5, p. 644.

Brierley, J. A. & Brierley, C. L., 2001. Present and future commercial applications of biohydrometallurgy. *Hydrometallurgy,* Volume 59, pp. 233-239.

Bryner, L. C. & Jameson, A. K., 1958. Microorganisms in Leaching Sulfide Minerals. *Applied and Environmental Microbiology,* Volume 6, pp. 281-287.

Burrell, L. S., Lindblad, E. B., White, J. L. & Hem, S. L., 1999. Stability of aluminium-containing adjuvants to autoclaving. *Vaccine,* Volume 17, pp. 2599-2603.

Callahan, J., 1987. A nontoxic heavy liquid and inexpensive filter for separation of mineral grains. *Journal of Sedimentary Petrology,* Volume 57, pp. 765-766.

Campbell, M. C. et al., 1985. Biotechnology for the Mineral Industry. *Canadian Metallurgical Quarterly,* Volume 24, pp. 115-120.

Campbell, M. C. et al., 1987. *In-place leaching of uranium at Denison Mines Limited*. Vienna, International Atomic Energy Agency, pp. 151-165.

Canadian Nuclear Safety Commission and Environment Canada, 2012. *2010 Annual Report on Uranium Management Activities.* Ottawa: Canadian Nuclear Safety Commission.

Canadian Nuclear Safety Commission, 2012. *Management of Uranium Mine Waste Rock and Mill Tailings.* Ottawa: Canadian Nuclear Safety Commission.

Caron, F. et al., 2007. Potential Use of Ultrafiltration for Groundwater Remediation and Aqueous Speciation of 60-Co and 137-Cs from A Contaminated Area. *Water, Air, & Soil Pollution,* Volume 178.

Caron, F. & Mankarios, G., 2004. Pre-assessment of the speciation of 60-Co, 125-Sb,137-Cs and 241-Am in a contaminated aquifer. *Journal of Environmental Radioactivity,* Volume 77, p. 29–46.

Carver, R. E., 1971. *Procedures in sedimentary petrology.* New York: Wiley-Interscience.

Cheng, T., Barnett, M. O., Roden, E. & Zhuang, J., 2004. Effects of Phosphate on UraniumIVI) Adsorption to Goethite-Coated Sand. *Enviromental Science and Technology,* Volume 38, pp. 6056-6065.

Chen, Y. S. R., Butler, J. N. & Stumm, W., 1973. Kinetic study of phosphate reaction with aluminum oxide and kaolinite. *Environmental Science & Technology,* Volume 7, p. 327–332.

Chen, Y. W., Belzile, N. & Goldsack, D. E., 1999. *Passivation of pyrite oxidation by organic compounds.* Sudbury, Laurentian University, pp. 1063-1071.

Childs, C. W., Parfitt, R. L. & Lee, R., 1983. Movement of aluminium as an inorganic complex in some podzolised soils, New Zealand. *Geoderma,* Volume 29, pp. 139-155.

Cochrane, L. B., Hwozdyk, L. R. & Hayden, A. S., 2007. Preliminary Assessment on the Elliot Lake Project, Ontario, Canada. In: Toronto: Scott Wilson Roscoe Postle Associates Inc.

Colmer, A. R., 1962. Relation of the iron oxidizer Thiobacillus ferrooxidans, to thiosulfate. *Journal of Bacteriology,* Volume 83, pp. 761-765.

Colmer, A. R. & Hinkle, M. E., 1947. The role of microorganisms in acid mine drainage: A preliminary report. *Science,* Volume 106, pp. 253-256.

Colmer, A. R., Temple, K. L. & Hinkle, M. E., 1950. An iron-oxidizing bacterium from the acid drainage of some bituminous coal mines. *Journal of Bacteriology,* Volume 59, pp. 317-328.

Cox, J. J., Ciuculescu, T., Altman, K. & Hwozdyk, L., 2012. *Technical Report on the Eco Ridge Mine Project, Elliot Lake, Ontario, Canada: NI 43-101 Report.* Toronto: Roscoe Postle Associates Inc..

Das, T., Ayyappan, S. & Chaudhury, G. R., 1999. Factors affecting bioleaching kinetics of sulfide ores using acidophilic micro-organisms. *BioMetals,* 12(1), pp. 1-10.

Del Nero, M., Galindo, C., Barillon, R. & Made, B., 2011. TRLFS Evidence for Precipiotation of Uranyl Phosphate on the Surface of Alumina: Environmental Implications. *Environmental Science and Technology,* Volume 45, pp. 3982-3988.

Drobner, E., Huber, H. & Stettter, K. O., 1990. Thiobacillus ferrooxidans, a facultative hydrogen oxidizer. *Applied and Environmental Microbiology,* Volume 56, pp. 2922-2923.

Dubrovsky, N. M., Morin, K. A., Cherry, J. A. & Smyth, D. J. A., 1984. Uranium tailings acidification and subsurface contaminant migration in a sand aquifer. *Water Pollution Research Journal of Canada* , Volume 19, pp. 55-89.

Dugan, P. R., 1975. Bacterial Ecology of strip mine areas and its relationships to production of acid mine drainage. *The Ohio Journal of Science,* Volume 75, pp. 226-278.

Dugan, P. R., 1987a. Prevention of formation of acid drainage from high-sulfur coal refuse by inhibition of iron- and sulfur-oxidizing microorganisms. I. Preliminary experiments in controlled shaken flasks. *Biotechnology and Bioengineering,* Volume 29, pp. 41-48.

Dugan, P. R., 1987b. Prevention of formation of acid drainage from high-sulfur coal refuse by inhibition of iron- and sulfur- oxidizing microorganisms: II Inhibition in "run of mine" refuse under simulated field conditions. *Biotechnology and Bioengineering,* Volume 29, pp. 49-54.

Dugan, P. R. & Apel, W. A., 1983. Bacteria and acidic drainage from coal refuse: inhibition by sodium lauryl sulfate and sodium benzoate. *Applied and Environmental Microbiology,* Volume 46, pp. 279-282.

Dugan, P. R. & Lundgren, D. G., 1964. Acid production by Ferrobacillus ferrooxidans and its relation to water pollution. *Developments in Industrial Microbiology,* Volume 5, pp. 250-257.

Dugan, P. R., Macmillan, C. B. & Pfister, R. M., 1970a. Aerobic heterotrophic bacteria indigenous to pH 2.8 acid mine water: microscopic examination of acid streamers. *Journal of Bacteriology,* Volume 101, pp. 973-981.

Dugan, P. R., Macmillan, C. B. & Pfister, R. M., 1970b. Aerobic heterotrophic bacteria indigenous to pH 2.8 mine water: predominant slime-producing bacteria in acid streamers. *Journal of Bacteriology,* Volume 101, pp. 982-988.

Duncan, D. W., Trussell, P. C. & Walden, C. C., 1964. Leaching of chalcopyrite with Thiobacillus ferrooxidans: Effect of surfactants and shaking. *Applied Microbiology and Biotechnology,* Volume 12, pp. 122-126.

Dutrizac, J. E. & Jambor, J. L., 2000. Jarosites and Their Application in Hydrometallurgy. *Reviews in Mineralogy and Geochemistry,* Volume 40, pp. 405-452.

Du, X. & Graedel, T. E., 2013. Uncovering the end uses of the rare earth elements. *Science of the Total Environment,* Volume 461-462, pp. 781-784.

Ehrlich, H. L., 2001. Past, present and future of biohydrometallurgy. *Hydrometallurgy,* Volume 59, pp. 127-134.

Elsetinow, A. R., Borda, M. J., Schoonen, M. A. A. & Strongin, D. R., 2003. Suppression of pyrite oxidation in acidic aqueous environments using lipids having two hydrophobic tails. *Advances in Environmental Research,* Volume 7, pp. 696-974.

Environment Canada, 2009. *Environmental Code of Practice for Metal Mines.* Ottawa: Minister of the Environment.

Evangelou, V. P., 1994. *Potential Microencapsulation of pyrite by artificial inducement of FePO4 coatings.* Pittsburg, United States Department of the Interior, Bureau of Mines.

Evangelou, V. P., 1996. Oxidation proof silicate surface coatings on iron sulfides. *US Patent Number 5494703,* 2 February.

Evangelou, V. P., 2001. Pyrite microencapsulation technologies: principles and potential field applications. *Ecological Engineering,* Volume 17, pp. 165-178.

Evangelou, V. P. & Zhang, Y. L., 1995. A review: Pyrite oxidation mechanisms and acid mine drainage prevention. *Critical Reviews in Environmental Science and Technology,* 25(2), pp. 141-199.

Feasby, D. G., 1997. *Environmental restoration of uranium minesin Canada: Progress overy 52 years.* Vienna, International Atomic Energy Agency.

Fernandes, H. M. & Franklin, M. R., 2001. Assessment of acid rock drainage pollutants release in the uranium mining site of Poços de Caldas--Brazil. *Journal of Environmental Radioactivity,* Volume 54, pp. 5-25.

Ferroni, G. D., Leduc, L. G. & Todd, M., 1986. Isolation and temperature characterization of psychotropic strains of thiobacillus ferrooxidans from the environment of a uranium mine. *Journal of General and Applied Microbiology,* Volume 32, pp. 169-175.

Ferroni, G. D., Leduc, L. G. & Todd, M., 1986. Isolation and temperature characterization of psychotropic strains of thiobacillus ferrooxidans from the environment of a uranium mine. *Journal of General and Applied Microbiology,* Volume 32, pp. 169-175.

Fuller, C. C., Bargarr, J. R., Davis, J. A. & Piana, M. J., 2002. Mechanisms of Uranium Interaction with Hydroxyapatite: Implications for Groundwater Remediation. *Environmental Science and Technology,* Volume 36, pp. 158-165.

Fuller, C. C., Rargar, J. R., Davis, J. A. & Piana, M. J., 2002. Mechanisms of Uranium Interaction wiht Hydroxyapatite: Implications for Groundwater Remediation. *Enviromental Science and Technology,* Volume 36, pp. 158-165.

Fytas, K., Bousquet, P. & Evangelou, B., 1999. *Application of silicate coatings on pyrite to prevent acid mine drainage.* Sudbury, Sudbury Mining and the Environment '99.

Fytas, K. & Evangelou, B., 1998. Phosphate coating on pyrite to prevent acid mine drainage. *International Journal of Surface Mining, Reclamation and Environment,* Volume 12, pp. 101-104.

Garcia, O. J., 1993. Bacterial leaching of uranium ore from Figueira—PR, Brazil, at laboratory and pilot scale. *FEMS Microbiology Reviews,* 11(1-3), pp. 237-242.

Georgopoulou, Z. J., Fytas, K., Soto, H. & Evangelou, B., 1995. *Pyrrhotite coating to prevent oxidation.* Sudbury, Sudbury Mining & the Environment '95.

Government of Canada, 1985. *Fisheries Act R.S.C., 1985, c. F-14.* Ottawa: Minister of Justice.

Government of Canada, 2002. *Metal Mining Effluent Regulations SOR/2002-222.* Ottawa: Minister of Justice.

Guay, R., Silver, M. & Torma, A. E., 1976. Microbiological leaching of a low-grade uranium ore by Thiobacillus ferrooxidans. *Applied Microbiology and Biotechnology,* Volume 3, pp. 157-167.

Hackl, R. P., Dreisinger, D. B., Peters, E. & King, J. A., 1995. Passivation of chalcopyrite during oxidative leaching in sulphate media. *Hydrometallurgy,* Volume 39, pp. 25-48.

Harris, D. L. & Lottermoser, B. G., 2006a. Evaluation of phosphate fertilizers for ameliorating acid mine waste. *Applied Geochemistry,* Volume 21, pp. 1216-1225.

Harris, D. L. & Lottermoser, B. G., 2006b. Phosphate stabilization of polyminerallic mine wastes. *Mineralogical Magazine,* Volume 70, pp. 1-13.

Harrison, V. F., Gow, W. A. & Ivarson, K. C., 1965. Leaching of uranium from Elliot Lake ore in the presence of bacteria. *Canadian Mining Journal,* Volume 87, pp. 64-67.

Hayes-Labruto, L., Schillebeeckx, S. J. D., Workman, M. & Shad, N., 2013. Contrasting perspectives on China's rare earth polices: Reframing the debate through a stakeholder lens. *Energy Policy,* Volume 63, pp. 55-68.

Hotchkiss, R. D., 1946. The Nature of the Bactericidal Action of Surface Active Agents. *Annals of the New York Academy of Sciences,* Volume 46, pp. 479-493.

Huber, H. & Setter, K. O., 1975. Thiobacillus cuprinus sp. nov., a Novel Facultatively Organotrophic Metal-Mobilizing Bacterium. *Applied and Environmental Microbiology,* Volume 39, pp. 1349-1354.

Hugo, W. B., 1965. Some aspects of the action of cationic surface-active agents on microbial cells with special reference to their actions on enzymes. In: *SCI monograph.* London: Society of Chemical Industry, pp. 67-82.

Huminicki, D. M. C. & Rimstidt, J. D., 2009. Iron oxyhydroxide coating of pyrite for acid mine drainage control. *Applied Geochemistry,* Volume 24, pp. 1626-1634.

Imai, K., Sugio, T. & Tsuchida, T., 1975. Effect of heavy metal ions on the growth and iron-oxidizing activity of Thiobacillus ferrooxidans. *Agricultural and Biological Chemistry,* Volume 39, pp. 1349-1354.

Ingledew, W. J. & Houston, A., 1986. The organization of the respiratory chain of Thiobacillus ferrooxidans. *Biotechnology and Applied Biochemistry,* Volume 8, pp. 242-248.

International Atomic Energy Agency, 2004. *IAEA Safety Standards SeriesApplication of the Concepts of Exclusion, Exemption and Clearance,* Vienna: IAEA.

Johnson, D. B., 2006. Biohydrometallurgy and the environment: Intimate and important interplay. *Hydrometallurgy,* Volume 83, pp. 153-166.

Johnson, D. B., 2010. The Biogeochemistry of Biomining. In: *Geomicrobiology: Molecular and Environmental Perspective.* New York: Springer, pp. 401-426.

Jordens, A., Cheng, Y. P. & Waters, K. E., 2013. A review of the beneficiation of rare earth element bearing minerals. *Minerals Engineering,* Volume 41, pp. 97-114.

Jurjovec, J., Ptacek, C. J. & Blowes, D. W., 2002. Acid neutralization mechanisms and metal release in mine tailings: a laboratory column experiment. *Geochimica et Cosmochimica Acta,* 66(9), pp. 1511-1523.

Karamanev, D. G. & Nikolov, L. N., 1988. Influence of some physicochemical parameters on bacterial activity of biofilm: ferrous iron oxidation by Thiobacillus ferrooxidans. *Biotechnology and Bioengineering,* Volume 31, pp. 295-299.

Kargbo, D. M. & Chatterjee, S., 2005. Stability of silicate coatings on pyrite surface in a low pH environment. *Journal of Environmental Engineering,* Volume 131, pp. 1340-1349.

Khummalai, N. & Boonamnuayvitaya, V., 2005. Suppression of arsenopyrite surface oxidation by sol-gel coatings. *Journal of Bioscience and Bioengineering,* Volume 99, pp. 277-284.

Kim, E. & Osseo-Asare, K., 2012. Aqueous stability of thorium and rare earth metals in monazite hydrometallurgy: Eh-pH diagrams for the systems Th-, Ce-, La-, Nd- (PO4)-(SO4)-H2O at 25oC. *Hydrometallurgy,* Volume 113-114, pp. 67-78.

Kim, S. D., Kilbane, J. J. & Cha, D. K., 1999. Prevention of acid mine drainage by sulfate reducing bacteria: organic substrate addition to mine waste piles. *Environmental Engineering Science,* Volume 16, pp. 139-145.

Kleinmann, R. L., 1980. Bactericidal control of acid problems in surface mines and coal refuse. In: D. H. Graves, ed. *University of Kentucky Symposium on Surface Mining, Hydrology, Sedimentology and Reclamation.* Lexington: University of Kentucky, pp. 333-337.

Kleinmann, R. L. & Crerar, D. A., 1979. Thiobacillus ferrooxidans and the formation of acidity in simulated coal mine environments. *Geomicrobiology Journal,* Volume 1, pp. 373-388.

Kleinmann, R. L. & Erickson, P. M., 1982. Full-scale field trials of bactericidal treatment to control acid mine drainage. In: D. H. Graves, ed. *University of Kentucky Symposium on Surface Mining, Hydrology, Sedimentation and Reclamation.* Lexington: University of Kentucky, pp. 617-622.

Kleinmann, R. L. P., 1987. *Bacterial Oxidation of Acid-Forming Materials.* Billings, Montana, Montana State University, pp. 34-46.

Kleinmann, R. L. P., Crerar, D. A. & Pacelli, R. R., 1981. Biogeochemistry of acid mine drainage and a method to control acid formation. *Mining Engineering,* March, pp. 300-305.

Kleinmann, R. L. P. & Erickson, P. M., 1983. *Control of Acid Drainage from Coal Refuse Using Anionic Surfactants.* Pittsburg: United States Department of the Interior.

Kleinmann, R. L. P. & Rastogi, V., 1996. *Reducing acid mine drainage liabilities using bactericides & other control technologies.* Princeton: American Society for Surface Mining and Reclamation.

Kusano, T. et al., 1992. Electrotransformation of Thiobacillus ferrooxidans with plasmid containing a mer determinant. *The Journal of Bacteriology,* Volume 174, pp. 6617-6623.

Lacey, D. T. & Lawson, F., 1970. Kinetics of the liquid-phase oxidation of acid ferrous sulfate by the bacterium Thiobacillus ferrooxidans. *Biotechnology and Bioengineering,* Volume 12, pp. 29-50.

Leathen, W. W., Kinsel, N. A. & Braley, S. A., 1956. Ferrobacillus ferrooxidans: A chemosynthetic autotrophic bacterium. *Journal of Bacteriology,* Volume 72, pp. 700-704.

Leduc, L. G. & Ferroni, G. D., 1994. The chemolithotrophic bacterium Thiobacillus ferrooxidans. *FEMS Microbiology Reviews,* Volume 14, pp. 103-120.

Leduc, L. G. & Ferroni, G. D., 2002. Quantification of bacterial populations indigenous to acid mine drainage systems. *Water, Air, and Soil Pollution,* Volume 135, pp. 1-21.

Leduc, L. G., Ferroni, G. D. & Trevors, J. T., 1997. Resistance to heavy metals in different strains of Thiobacillus ferrooxidans. *FEMS Microbiology Letters,* Volume 14, pp. 103-120.

Li, M. G., Catalan, L. J. J. & Payant, S., 1998. Characterization of Products From Mining and Metallurgy. In: W. Petruk, ed. *Waste Characterization and Treatment.* Littleton: Society for Mining, Metallurgy and Exploration Inc., pp. 109-125.

Li, M. G., Jacob, C. & Comeau, G., 1996. *Decommissioning of sulphuric acid-leached heap by rinsing.* Fort Collins, Colorado State University, pp. 295-305.

Lundgren, D. G. & Silver, M., 1980. Ore leaching by bacteria. *Annual Review of Microbiology,* Volume 34, pp. 263-286.

Lundgren, D. G., Vestal, J. R. & Tabita, F. R., 1974. The Iron Oxidizing Bacteria. In: J. B. Neilands, ed. *Microbial Iron Metabolism.* New York: Academic, pp. 457-473.

Lyalikova, N. N., 1958. A study of chemosynthesis in Thiobacillus ferrooxidans. *Microbiologiya,* Volume 27, pp. 556-559.

MacDonald, D. G. & Clark, R. H., 1970. The oxidation of aqueous ferrous sulphate. *The Canadian Journal of Chemical Engineering,* Volume 48, pp. 669-676.

Marchand, E. A. & Silverstein, J., 2003. The role of enhanced heterotrophic bacterial growth on iron oxidation by Acidithiobacillus ferrooxidans. *Geomicrobiology Journal,* Volume 20, pp. 231-244.

Markos, G. & Bush, K. J., 1982. *Geochemical processes in uranium mill tailings and their relationship to contamination.* Vienna, International Atomic Energy Agency.

Martin, P. A. W., Dugan, P. R. & Tuovinen, O. H., 1983. Uranium resistance of Thiobacillus ferrooxidans. *European Journal of Applied Microbiology and Biotechnology,* Volume 18, pp. 392-395.

Mawhiney, A. & Pitblado, J., 1999. *Town Blues: Elliot Lake, Collapse and Revival in a Single-Industry Community.* Toronto: Dundurn Group.

McCready, R. G. L., 1986. Process in the Bacterial Leaching of Metals in Canada. In: P. R. Norris & D. P. Kelly, eds. *Fundamental and applied biohydrometallurgy: Proceedings of the Sixth International Symposium on.* Vancouver: Elsevier, pp. 177-195.

McCready, R. G. L., 1988. Process in the Bacterial Leaching of Metals in Canada. In: P. R. Norris & D. P. Kelly, eds. *Proceedings of the International Symposium on Hydrometallurgy.* Kew Surrey: University of Warwick, pp. 177-195.

McCready, R. G. L. & Gould, W. D., 1990. Bioleaching of Uranium. In: H. L. Ehrlich & C. L. Brierley, eds. *Microbial Mineral Recovery.* New York: McGraw-Hill, pp. 107-125.

McCready, R., Wadden, D. & Marchbank, A., 1986. Nutrient requirements for the in-place leaching of uranium by Thiobacillus ferrooxidans. *Hydrometallurgy,* Volume 17, pp. 61-71.

McIlwaine, L. M. & Ridd, M., 2004. *Assessment of leachate from blended waste rock material and Pasminco Century Mine - Initial results from a two-year study.* Ballarat, Australia, The Australasian Institute of Mining and Metallurgy.

Morrow, J. R. & Webster, G. D., 1989. A cryogenic density Separation technique for conodont and heavy mineral separations. *Journal of Paleontology,* Volume 63, pp. 953-955.

Mousavi, S. M., Yaghmaei, S., Salimi, F. & Jafari, A., 2006. Influence of process variables on biooxidation of ferrous sulfate by an indigenous Acidithiobacillus ferrooxidans. Part I: Flask experiments. *Fuel ,* Volume 85, pp. 2555-2560.

Munoz, J. A., Blazquez, M. L., Ballesterr, A. & Gonzalez, F., 1995. A study of the bioleaching of a Spanish uranium ore. Part III: Column experiments. *Hydrometallurgy,* Volume 38, pp. 79-97.

Munoz, J. A., Gonzalez, F., Ballester, A. & Blazquez, M. L., 1993. Bioleaching of a Spanish uranium ore. *FEMS Microbiology Reviews,* Volume 11, pp. 109-120.

Murakami, T., Ohnuki, T., Isobe, H. & Sato, T., 1997. Mobility of uranium during weathering. *American Mineralogist,* Volume 82, pp. 888-899.

Murakami, T., Sato, T., Ohnuki, T. & Isobe, H., 2005. Field evidence for uranium nanocrystallization and its implications for uranium transport. *Chemical Geology,* Volume 221, pp. 117-126.

Nemati, M., Harrison, S. T. L., Hansford, G. S. & Webb, C., 1997. Biological oxidation of ferrous sulfate by Thiobacillus ferrooxidans: a review on the kinetic aspects. *Biogeochemical Engineering Journal,* Volume 1, pp. 171-190.

Norris, P. R. & Kelly, D. P., 1978. Toxic metals in leaching systems. In: L. E. Murr, A. E. Torma & J. A. Brierley, eds. *Metallurgical Applications of Bacterial Leaching and Related Microbiological Phenomean.* New York: Academic Press, pp. 83-102.

Office of Radiation and Indoor Air, 2003. *EPA Assessment of Risks from Radon in Homes.* Washington: United States Environmental Protection Agency.

Okereke, A. & Stevens, S. E. J., 1991. Kinetics of ferrous iron oxidation by Thiobacillus ferrooxidans. *Applied and Environmental Microbiology,* Volume 57, pp. 1052-1056.

Olson, G. J., Brierley, J. A. & Brierley, C. L., 2003. Bioleaching review part B: Progress in bioleaching: applications of microbial processes by the minerals industries. *Applied Microbiology and Biotechnology,* 63(3), pp. 249-257.

Onysko, S. J., Kleinmann, R. L. P. & Erickson, P. M., 1984. Ferrous iron oxidation by Thiobacillus ferrooxidans: Inhibition with benzoic acid, sorbic acid and sodium laurly sulfate. *Applied and Environmental Microbiology,* Volume 48, pp. 229-231.

Parfitt, R. L., 1989. Phosphate reactions with natural allophane, ferrihydrite and goethite. *Journal of Soil Science,* Volume 40, pp. 359-369.

Parkhurst, D. L. & Appelo, C. A. J., 2013. *Description of input and examples for PHREEQC version 3—A computer program for speciation, batch-reaction, one-dimensional transport, and inverse geochemical calculations: U.S. Geological Survey Techniques and Methods.* Denver: U.S. Geological Survey.

Parkhurst, D. L. & Appelo, C. A. J., 2013. *Description of input and examples for PHREEQC version 3—A computer program for speciation, batch-reaction, one-dimensional transport, and inverse geochemical calculations: U.S. Geological Survey Techniques and Methods.* s.l.:U.S. Geological Survey.

Petersen, J. & Dixon, D. G., 2002. Thermophilic heap leaching of a chalcopyrite concentrate. *Materials Engineering,* 15(11), pp. 777-785.

Postle, J. et al., 2000. *CIM Standards on Mineral Resources and Reserves: Definitions and Guidelines*. Westmount: Canadian Institute of Mining, Metallurgy, and Petroleum.

Powell, A. R. & Parr, S. W., 1919. A study of the forms in which sulphur occurs in coal. *University of Illinois Engineering Experiment Station*.

Putnis, A., 2009. Mineral Replacement Reactions. *REviews in Mineralogy & Geochemistry,* Volume 70, pp. 87-124.

Rawlings, D. E., 2002. Heavy Metal Mining Using Microbes. *Annual Review of Microbiology,* Volume 56, pp. 65-91.

Rawlings, D. E., 2004. Microbially assisted dissolution of minerals and its use in the mining industry. *Pure Applied Chemistry,* 76(4), pp. 847-859.

Rohwerder, T., Gehrke, T., Kinzler, K. & Sand, W., 2003. Bioleaching review part A: Progress in bioleaching: fundamentals and mechanisms of bacterial metal sulfide oxidation. *Applied Microbiology and Biotechnology ,* Volume 63, pp. 239-248.

Sahin, M., Ayranic, K., Kousn, E. & Ayranci, E., 2009. Density, sound velocity and viscosity properties of aqueous sodium metatungstate solutions and an application of these solutions in heavy mineral separations. *Chemical Geology,* Volume 264, pp. 96-100.

Sand, W., Rohde, K., Sobotke, B. & Zenneck, C., 1992. Evaluation of Leptospirillum ferrooxidans for Leaching. *Applied and Environmental Microbiology,* Volume 58, pp. 85-92.

Sapsford, D. J. et al., 2012. Factors influencing the release rate of uranium, thorium, yttrium and rare earth elements from a low grade ore. *Minerals Engineering,* Volume 39, pp. 165-172.

Sasaki, K., Tsunekawa, M., Tanaka, S. & Konno, H., 1996. Supression of microbial mediated dissolution of pyrite by originally isolated fulvic acids and related compounds. *Colloids and Surfaces; A: Physiochemical and Engineering Aspects,* Volume 119, pp. 241-253.

Sato., T. et al., 1997. Iron Nodules Schavening Uranium from Groundwater. *Environmental Science and Technology,* Volume 31, pp. 2854-2858.

Schindler, M. & Ilton, E. S., 2013. Uranium mineralogy and geochemistry on the nano- to micrometre scale: redox, dissolution and precipitation process at the mineral-water interface. In: P. C. Burns & G. E. Sigmon, eds. *Uranium: Cradle to Grave.* s.l.:s.n.

Seidel, H. et al., 2000. Bioleaching of heavy metal-contaminated sediments vby indigenous Thiobacillus sppL metal solubilization and sulfur oxidation in the presence of surfactants. *Applied Microbiology and Biotechnology,* Volume 54, pp. 854-857.

Shafa, F. & Salton, M. R. J., 1960. Disaggregation of Bacterial Cell Walls by Anionic Detergents. *Journal of General Microbiology,* Volume 23, pp. 137-141.

Silverman, M. P. & Ehrlich, H. L., 1964. Microbial formation and degradation of minerals. *Advances in Applied Microbiology,* Volume 6, pp. 153-206.

Silverman, M. P. & Lundgren, D. G., 1959. Studies on the chemoautotrophic iron bacterium Ferroobacillus ferrooxidans: II. Manometric studies. *The Journal of Bacteriology,* Volume 78, pp. 326-331.

Simms, P. H., Yanful, E. K., St. Arnaud, L. & Aube, B., 2000. A laboratory evaluation of metal release and transport in flooded pre-oxidized mine tailings. *Applied Geochemistry,* 15(9), pp. 1245-1263.

Singer, P. C. & Stumm, W., 1970. Acidic mine drainage: the rate-determining step. *Science,* Volume 167, pp. 1121-1123.

Singh, A., Ulrich, K. U. & Giammar, D. E., 2010. Impact of phosphatre on U(VI) immobilization in the presence of goethite). *Geochimica et Cosmochimica Acta,* Volume 74, pp. 6324-6343.

Singh, G. & Bhatnagar, M., 1988. Inhibition of bacterial activity in acid mine drainage. *International Journal of Mine Water,* Volume 7, pp. 13-26.

Smith, J. R., Luthy, G. R. & Middleton, A. C., 1959. Microbial ferrous iron oxidation in acidic solution. *Journal of the Water Pollution Control Federation,* Volume 78, pp. 326-331.

Stott, M. B., Watling, H. R., Franzmann, P. D. & Sutton, D., 2000. The role of iron-hydroxy precipitates in the passivation of chalcopyrite during bioleaching. *Minerals Engineering,* Volume 13, pp. 1117-1127.

Stumm, W., 1992. *Chemistry of the solid-water interface : processes at the mineral-water and particle-water interface in natural systems.* New York: Wiley.

Suzuki, I., 2001. Microbial leaching of metals from sulfide minerals. *Biotechnology Advance,* Volume 19, pp. 119-132.

Sylvester, P. J., 2007. *Mineralogy of Conglomerate Beds, Elliot Lake Uranium Deposit, Ontario, Canada.* St. John's: Memorial University.

Takeno, N., 2005. *Atlas of Eh-pH diagrams, Intercomparison of thermodynamic databases.* Naoto: Geological Survey of Japa.

Temple, K. L. & Colmer, A. R., 1951. The autotrophic oxidation of iron by a new bacterium: Thiobacillus ferrooxidans. *Journal of Bacteriology,* Volume 62, pp. 605-611.

Torma, A. E., 1977. The role of Thiobacillus ferrooxidans in hydrometallurgical processes. *Advances in Biochemical Engineering,* Volume 6, pp. 1-37.

Trevors, J. T., 1996. Sterilization and inhibition of microbial activity in soil. *Journal of Microbiological Methods,* Volume 26, pp. 53-59.

Tuovinen, O. H. & Kelly, D. P., 1973. Studies on the growth of Thiobacillus ferrooxidans: I. Use of membrane filters and ferrous iron agar to determine viable numbers, and comparison with 14CO2 fixation and iron oxidation as measures of growth. *Archives of Microbiology,* Volume 88, pp. 295-298.

Tuovinen, O. H. & Kelly, D. P., 1974. Studies on the growth of Thiobaillus ferrooxidans. II. Toxicity of uranium to growing cultures and tolerance conferred by mutation, other metal cations and EDTA. *Archives of Microbiology,* Volume 95, pp. 153-164.

Tuovinen, O. H., Niemela, S. I. & Gyllenberg, H. G., 1971. Tolerance of Thiobacillus ferrooxidans to some metals. *Antonie van Leeuwenhoek Journal of Microbiology,* Volume 37, pp. 489-496.

Tuttle, J. H. & Dugan, P. R., 1976. Inhibition of growth, iron, and sulfur oxidation in Thiobacillus ferrooxidans by simple organic compounds. *Canadian Journal of Microbiology,* Volume 22, pp. 719-730.

Tuttle, J. H., Dugan, P. R. & Apel, W. A., 1977. Leakage of cellular material from Thiobacillus ferrooxidans in presence of organic acids. *Applied and Environmental Microbiology,* Volume 33, pp. 439-469.

Tuttle, J. H., Randles, C. I. & Dugan, P. R., 1968. Activity of microorganisms in acid mine water. I. Influence of acid water on aerobic heterotrophs of a normal stream. *Journal of Bacteriology,* Volume 95, p. 1495–1503.

Vandiviere, M. M. & Evangelou, V. P., 1998. Comparative testing between conventional and microencapsulation approaches in controlling pyrite oxidation. *Journal of Geochemical Exploration,* Volume 64, pp. 161-176.

Wadden, D. & Gallant, A., 1985. The in-place leaching of uranium at Denison mines. *Canadian Metallurgical Quarterly,* Volume 24, pp. 127-134.

Wakao, N., Mishina, M., Sakurai, Y. & Shiota, H., 1983. Bacterial pyrite oxidation II. The effect of various organic substrates on release of iron from pyrite by Thiobacillus ferrooxidans. *Journal of General and Applied Microbiology,* Volume 29, pp. 177-185.

Wakeman, K., Auvinen, H. & Johnson, D. B., 2008. Microbiological and geochemical dynamics in simulated-heap leaching of a polymetallic sulfide ore. *Biotechnology and Bioengineering,* 101(4), pp. 739-750.

Wang, Z. Z., 2001. *Anion Analysis by Ion Chromatography.* Sudbury: Elliot Lake Research Field Station.

Williamson, A. L., Caron, F. & Spiers, G., 2014. Radionuclide release form simulated waste material after biogeochemical leaching of uraniferous mineral samples. *Journal of Environmental Radioactivity,* Volume In Press.

Wolf, H., 1981. *Ore size, a major factor affecting the in-situ uranium acid leaching.* Denver, Society of Mining Engineers and Society of Petroleum Engineers.

Wubbeke, J., 2013. Rare earth elements in China: Policies and narratives of reinventing an industry. *Resources Policy,* Volume 38, pp. 384-394.

Yanful, E. K. & St. Arnaud, L. C., 1992. Migration of acidic pore waters at the Waite Amulet tailings site near Rouyn-Noranda, Quebec. *Canadian Geotechnical Journal,* Volume 29, pp. 466-476.

Zang, Y. L. & Evangelou, V. P., 1998. Formation of ferric hydroxide-silica coatings on pyrite and its oxidation behaviour. *Soil Science,* Volume 163, pp. 53-62.

Zhou, Q. G. et al., 2007. Isolation of a strain of Acidithiobacillus caldus and its role in bioleaching of chalcopyrite. *World Journal of Microbiology and Biotechnology,* Volume 23, pp. 1217-1225.

Zimmerley, S. R., 1958. *Cyclic leaching process employing oxidizing bacteria.* United States, Patent No. 2829964.

APPENDIX A

A Bioleaching: Microcosm Study

A.1 Introduction

Chemolithotrophic microorganisms accelerate the dissolution of sulphidic minerals, releasing sulphide to solution with a concomitant release of protons, which encourages the dissolution of other minerals (Lundgren & Silver, 1980; Leduc & Ferroni, 1994; Suzuki, 2001). The dissolution of other minerals releases elements of economic importance and environmental significance from the host mineralization or mine wastes materials. The success of bioleaching, when applied as an extraction method, relies on important interactions between the microbial population and the mineralogy. Iron-sulphide minerals are of fundamental importance to the bioleaching process.

Bench-top or microcosm experimentation is useful to investigate the interactions between the microbial population and the mineralized material, either using established optimum leaching conditions or altered conditions to determine threshold values (Guay, et al., 1976; Munoz, et al., 1993). The influence of individual parameters can be controlled or manipulated in small laboratory experiments to determine the overall affect of the parameter on the leaching process. Experiments of this scale require minimal materials and can generally produce results over a short timeframe and assess many parameters in controlled environments, compared with more elaborate investigations. When basic parameters are established using bench-top experiments, leaching columns can then be used to gain greater insight of the leaching process using methods that would be more representative of a full-scale model.

The goals of this study include:

- Assessment of the biogeochemical mineral dissolution-mediated release of U and REEs from ore samples originating from the Quirke Syncline;
- Comparison of laboratory controlled conditions and potential industrial application conditions, including variance of inoculum type, material sterilization, and leaching solution composition; and
- Assessment of the overall acid generating potential of residue or waste material from ore subjected to bioleaching.

The findings from this experiment will provide an evaluation of the potential economic benefits and environmental effects of biogeochemical mineral dissolution, both important parameters to assess the potential for commercial success of bioleaching along the Quirke Syncline and guide the development of leaching column experiments. The contents of this appendix have been compiled from a paper published in conference proceedings and a report submitted to Pele Mountain Resources:

- Williamson, A. L., Payne, R., Kerr, F., Hall, S., & Spiers, G. A. (2010). Microbes: Uranium Miners, Money Makers, Problem Solvers. In E. K. Lam, J. W. Rowson, & E. Ozberk (Ed.), Uranium 2010: The Future is U, pp. 531-543. Saskatoon: The Metallurgical Society of the Canadian Institute of Mining, Metallurgy, and Petroleum.
- Reported submitted to Pele Mountain Resources, July 2011 titled "Leaching for closure: Geochemical Monitoring of a Biological Extraction Process"

A.2 Experimental Methods

Fresh drill core was collected from the study site, Eco Ridge Mine Rare Earths and Uranium Project site (Eco Ridge), owned by Pele Mountain Resources Incorporated (PMR), approximately 11 km east of Elliot Lake, Ontario. The drill core was crushed to 2 to 4 cm and homogenized in a large tumbler. Approximately 15 kg was sub-sampled and crushed with a small crusher to 1 to 2 mm , with a final sub-

sample, approximately 5 kg, being ground to 74µm using an agate ball mill. The representative sub-samples were collected using a riffle splitter.

Two culture sources have been investigated:

- Pure strain: *Acidithiobacillus ferrooxidans* (D7) stored at Laurentian University (Ferroni, et al., 1986; Leduc & Ferroni, 1994; Leduc, et al., 1997); and
- Environmental culture: population representative of that expected at Eco Ridge cultured from water samples collected from the former tailings catchment area of Stanrock Mine.

Homogenized mineral material was sterilized by heating 7.5 gram samples in 250 mL Erlenmeyer flasks to 200°C for 24 hours in a laboratory oven to allow for complete microbial control during the experiment(Trevors, 1996). Each sample flask was closed using aluminium caps to prevent contamination of the sample. After sterilization, 150 mL of sterile nutrient solution, TK solution A, was added to each flask (Tuovinen & Kelly, 1973). TK solution B is not added to extraction flasks because the Fe source is already present in the mineral material. The ore-solution mixture was inoculated with 5 mL of prepared *A. ferrooxidans* broth culture, estimated to contain $2.4x10^7$ cells mL^{-1}. The flasks were agitated using an enclosed bench-top shaker at a rate of 150 RPM at 30°C under ambient lighting conditions for 10 weeks.

Treatments were designed to compare controlled conditions with possible industrial application conditions. Variances of inoculum type, material sterilization, and leaching solution composition have been investigated. The D7 strain of *A. ferrooxidans* represented controlled conditions and an environmentally sourced population isolated from the Stanrock Dam in Elliot Lake represented industrial application conditions. Material mineralization was either sterilized or not and various compositions of nutrient solutions were compared with DDI water. Inoculum type, material sterilization, and solution parameters were replicated in triplicate flasks to assess the effect of the parameters on the release of U, REEs, and other elements, which may affect decommissioning conditions from the mineralized material (Table A.1). After the 24 hours of agitation the extraction flasks were inoculated with 5 mL of the

specified inoculum from prepared broth cultures. Non-inoculated controls are compared with each inoculated treatment depending on material treatment and solution selected.

Table A.1 Extraction flask leaching treatments (n=3).

Parameter	1[a]	2	3[b]	4[a]	5[a]	6[a]	7[b]	8[b]
Inoculum								
Distilled deionized water	x	x	x					
Pure culture, A. ferrooxidans				x	x	x		
Environmental consortium								
Headwater source							x	
Dam seepage source								x
Mineral Sample								
Sterilized	x			x	x	x		
Not sterilized		x	x				x	x
Leaching Solution								
Nutrient media								
Acidic (pH = 3.5)	x	x		x				
Neutral (pH = 6.8)					x			
Solution B added (Fe^{2+} supplement)						x		
Distilled deionized water			x				x	x

[a] laboratory control conditions

[b] industrial application conditions

A sample (10 mL) was removed every two to fifteen days, with frequency decreasing over time, filtered (0.45µm), and analyzed for pH, oxidation potential, and dissolved elemental concentrations by ICP-MS. Sterile nutrient solution or water was added bi-weekly to compensate for volume loss from sampling and evaporation. The mass of the flasks was recorded before and after sampling, with solution addition to allow for compensation of dilution. The extraction flask experiment was continued for approximately 80 days, a stage at which the cumulative elemental release rate from the mineralization had reached an experimental maximum. Residue samples were collected from each flask for subsequent chemical and mineralogical analysis and passive closure demonstrations.

A.3 Results & Discussion

At the end of the experiment, the pH of microcosms treated with the pure strain and the environmental culture is lower than those of the n`on-inoculated microcosms. The pH decrease in the microcosms treated with pure strain and environmental culture decreased at a similar rate to the same equilibrium level of 1.90 ±0.07 (Figure A.1). The pH of the pure strain treatments reduced at a rate equal to fresh cultures obtained from Elliot Lake mine waters (Figure A.1).

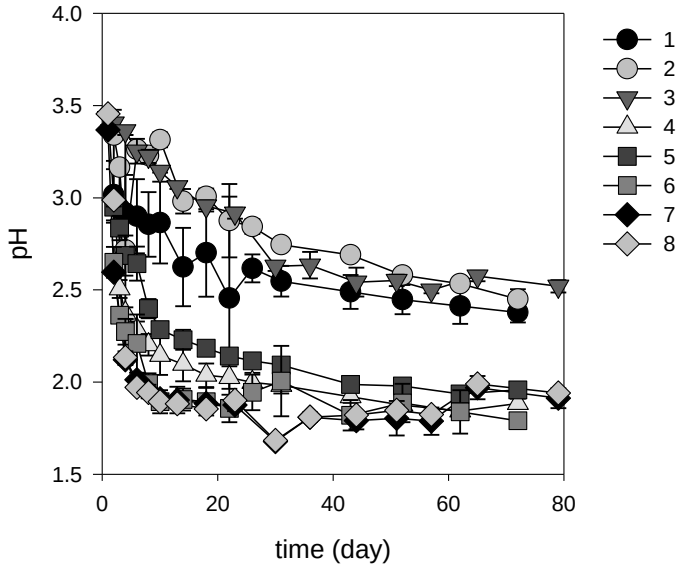

Figure A.1 Time profiles for microcosm leaching treatments (Table A.1) during 80 days of leaching displaying the changes in pH.

The oxidation-reduction potential (E_H) of the inoculated flasks was higher than those of the non-inoculated flasks (Figure A.2), indicative of the oxidation of Fe^{2+} to Fe^{3+}. The rate of E_H increase in the inoculated microcosms suggests presence of *A. ferrooxidans*, or other Fe oxidizing bacterial, because the reactions would proceed very slowly if not biocatalyzed, as reported in the non-inoculated flasks. The E_H measurements and rates of change in all inoculated microcosms were similar and stabilized around 0.78 ±0.01 V, suggesting the pure strain and environmental culture are equally efficient in catalyzing the oxidation of pyrite, with minimal apparent effects from the addition of nutrients (Figure A.2). A Pourbaix diagram for the Fe-H_2O system under standard conditions indicated that in acidic conditions (pH less than 2.5) the transition between Fe^{2+} and Fe^{3+}takes place at 0.80 V(Takeno, 2005).

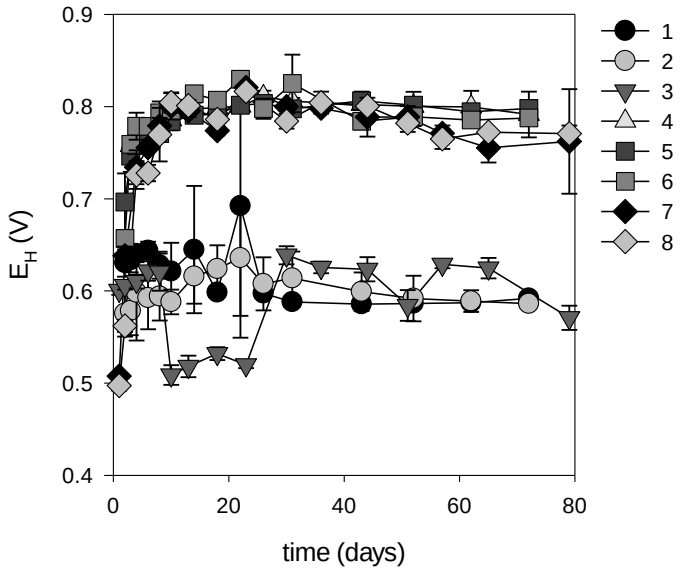

Figure A.2 Time profiles for microcosm leaching treatments (Table A.1) during 80 days of leaching displaying the changes in oxidizing potential parameters resulting.

The pH and E_H results for the simulations suggests that Elliot Lake mine water cultures effectively oxidize the pyrite in the uraniferous mineralization and would thus be suitable to further demonstrate the bioleaching application. The addition of nutrients had no obvious affect on acid generation, confirming the environmental water alone contains sufficient nutrients for a viable microbial consortium for use as an elemental extraction solution.

Dissolution of insoluble tetravalent U minerals, such as uraninite (UO_2), occurs when the mineral is in close association with ferrous-sulphide minerals because the biogeochemical mineral dissolution of the sulphide liberates Fe^{3+}, which subsequently oxidizes uraninite (Lundgren & Silver, 1980). The release of U in inoculated microcosms was greater compared with those that were not inoculated (Figure A.3). After leaching, the inoculated laboratory conditions showed a U dissolution efficiency compared with inoculated industry application conditions, 84±9% and 69±5% respectively. The inoculated industry application conditions showed a much greater recover then all non-inoculated treatments, 22±2%.

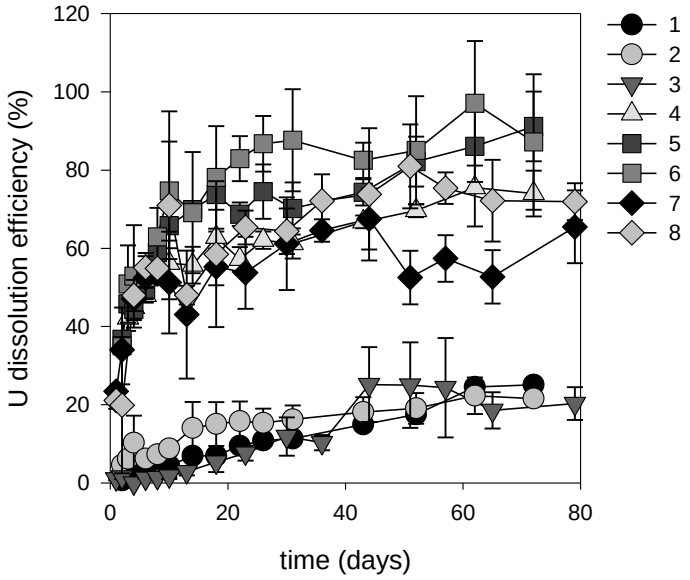

Figure A.3 Time profiles for microcosm leaching treatments (Table A.1) during 80 days of leaching displaying the changes in U dissolution efficiency.

These results suggest that Pele Mountain Resources can rely on local sources for the supply of viable microbial communities to promote biogeochemical mineral dissolution of sulphidic minerals and subsequent dissolution of U mineral, offering economical and convenient benefits. Furthermore, all inoculated treatments proved very effective in the recovery of U from the mineralization, with maxim dissolution ranging from 68% to 97% (Figure A.4). The distribution of U in the system shows greater amounts held in the mineralized residue of the non-inoculated treatments, up to 78%.

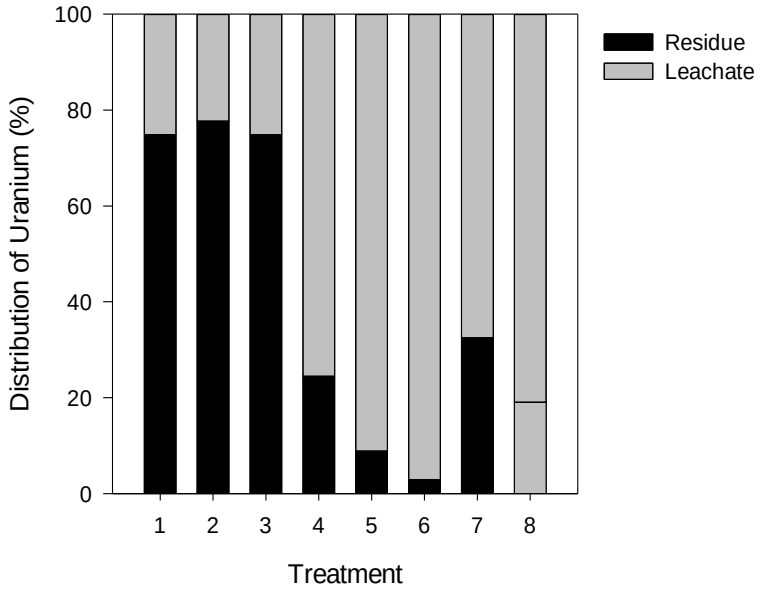

Figure A.4 Distribution of U for microcosm leaching treatments (Table A.1) after 80 days of leaching.

Inoculation of the microcosms allowed for recovery of REEs through the biogeochemical mineral dissolution process, potentially further improving the economics of biomining the Quirke Syncline conglomerate. Higher recoveries were achieved for heavy REEs than for light REEs (Figure A.5).

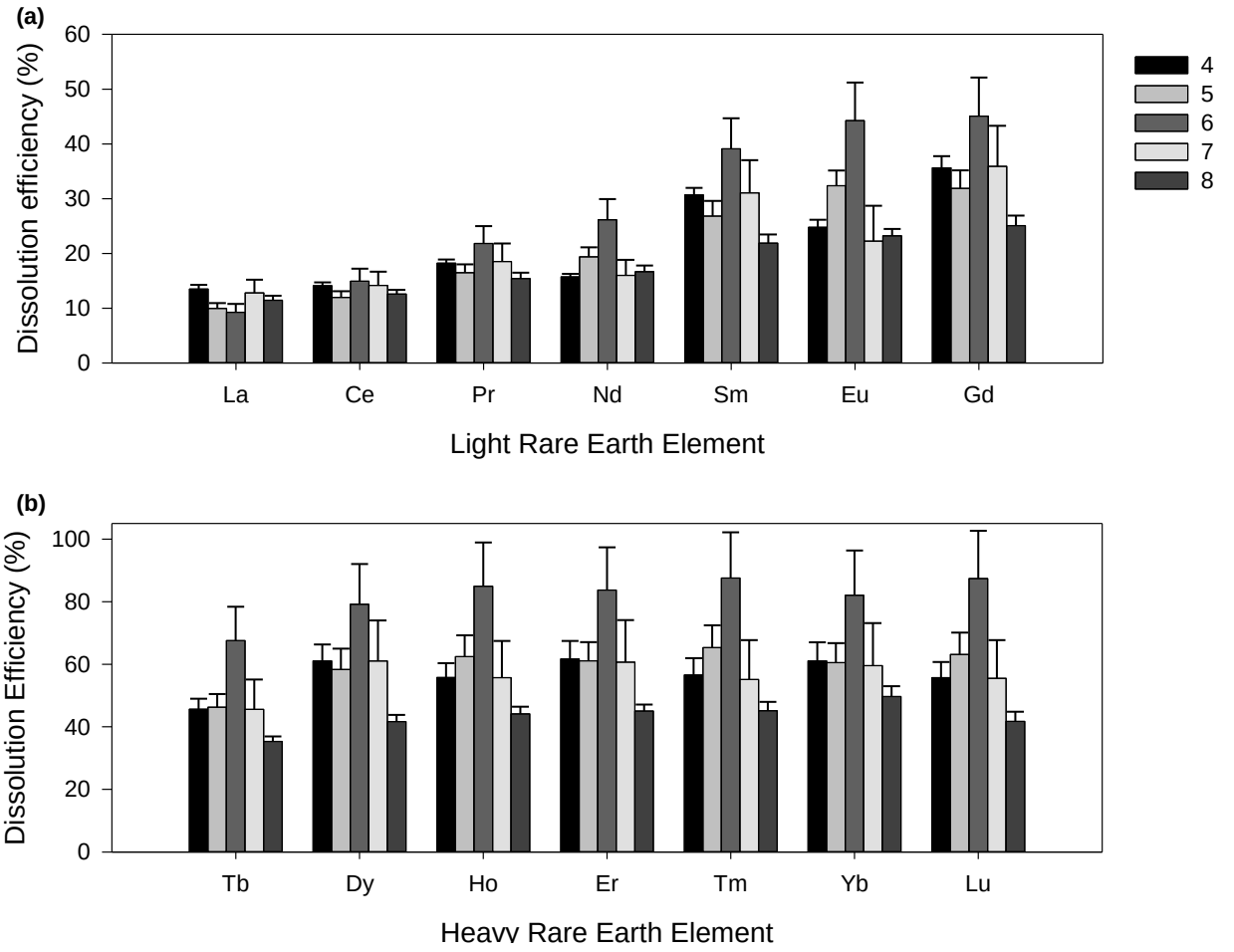

Figure A.5 Dissolution efficiency for microcosm leaching treatments (Table A.1) after 80 days of leaching for: (a) light REEs and (b) heavy REEs.

Treatment 6, the addition of f Fe^{2+}, consistently produced a higher recovery of REE's from the uraniferous mineralization. However, manual addition of Fe^{2+} to the leachate in the industrial setting may further complicate the decommissioning plan for Pele Mountain Resources because added Fe^{2+} may limit the amount of pyrite, which will dissolve and amount of sulfur released during production increase acid generation at the closing phase. The oxidation of Fe^{2+} in effluent solutions may also increase the oxide mineral precipitation in the environmental media, potentially causing secondary aesthetics issues.

The heavy REEs are released most efficiently and are assumed to be associated with minerals that are easily dissolved in the biogeochemical mineral dissolution conditions. The light REEs are not released as easily to solution and are possibly contained in the minor accessory minerals. Detailed mineralogical studies are required to confirm the predicted mineral associations.

The results show that the dissolution of the Fe is achieved by the inoculated microcosms (Figure A.6). The treatments achieving complete Fe removal from the mineralization suggest complete dissolution of pyrite, which is the only sulfur containing mineral in the Quirke Syncline conglomerate beds that is of industrial process interest because the extraction approach has the potential to mitigate AMD production in mine waste rock. A decline in Fe dissolution, most evident for the environmental culture inoculations, suggests the precipitation of Fe on the mineral surface as Fe hydroxides or Fe oxyhydroxide phases; mineralogical studies are required to confirm. Treatment 6 reports an Fe dissolution greater than 100% because Fe was added to the nutrient solution to encourage biogeochemical mineral dissolution.

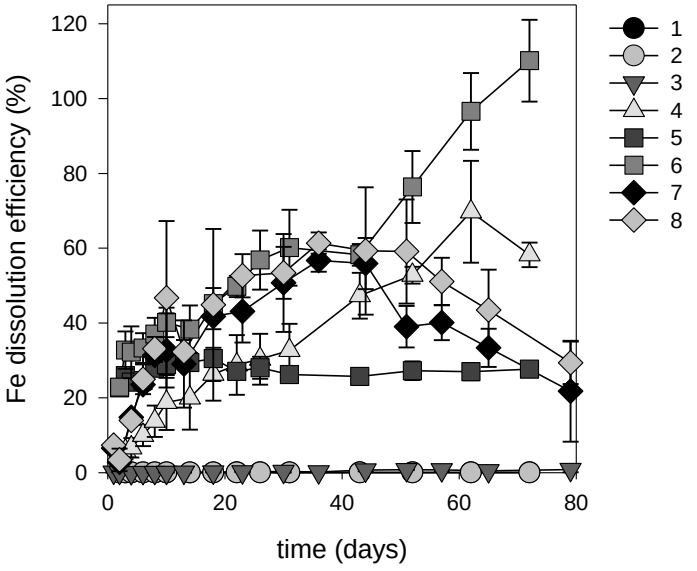

Figure A.6 Time profiles for microcosm leaching treatments (Table A.1) during 80 days of leaching displaying the changes in Fe dissolution efficiency.

The distribution of Fe in the system shows greater amounts held in the mineralized residue of the non-inoculated treatments while the Fe content of the inoculated treatments is unchanged compared with the material prior to leaching (Figure A.7). Iron distribution is not quantified for Treatment 6 because Fe was added to the nutrient solution of this treatment.

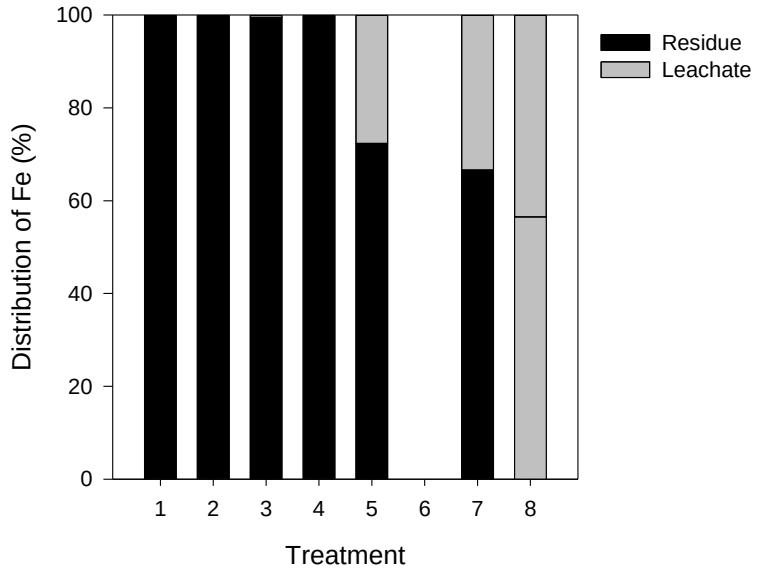

Figure A.7 Distribution of Fe for microcosm leaching treatments (Table A.1) after 80 days of leaching.

Total sulfur concentrations of the spent mineralized material confirm that the majority of the sulfur was released to solution through the bioleaching extraction process (Figure A.8). Material that was not leached reported a total suphur content of 3.3% by weight. The sulphur content decreased by 88% after leaching in the presence of both the pure strain and environmental culture, whereas the sulphur content of the non-inoculated sample decreased by 27%.

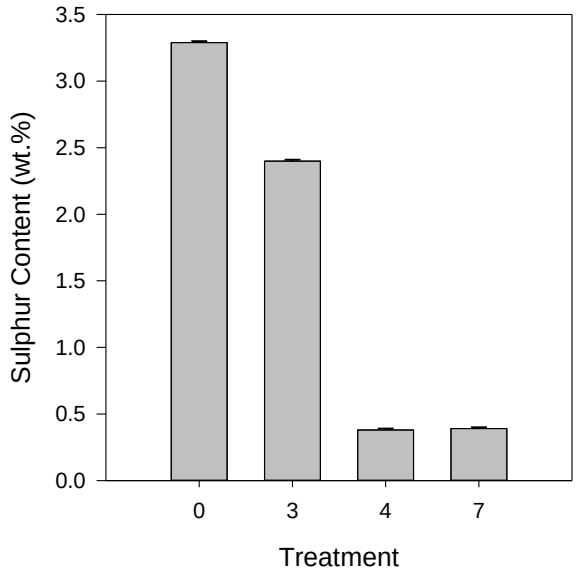

Figure A.8 Total S concentration in residues from microcosm leaching treatments (Table A.1) after 80 days of leaching.

These results may have an enormous affect on the decommissioning plan for Pele Mountain Resources because the removal of sulphidic minerals in the extraction process means the potential for acid generation is minimized on closure of the leaching beds. Acid mine drainage is the major post-mine closure issue for the mining industry, having a negative environmental affect with the release of acidity and dissolved potentially toxic metals and radionuclides to surface and groundwater.

Samples collected from fresh material and residue material from microcosm treatment 4 were selected for initial XRD and SEM-EDS examination and analysis for comparison between fresh and leached material. XRD was used to identify the dominant mineral components of the fresh and biogeochemically leached samples. A sub-sample of each sample type was placed on carbon tape, carbon coated, and analyzed on a Zeiss EVO-50 Scanning Electron Microprobe, where electron backscatter images and secondary electron images were collected. Quantitative and semi-quantitative values were obtained using Oxford Energy Dispersive Spectrometer (EDS) and INCA software.

XRD analysis of fresh material indicated four dominant mineral phases in the untreated sample: quartz, feldspars, mica, and pyrite present (Figure A.9a). Residue material collected from treatment 4 appeared similar to the fresh material, with one critical exception. Diffraction peaks indicating presence of pyritic phases were absent after leaching, signifying a pyrite content of less than 2% (Figure A.9b), indicating that the biogeochemical leaching process has the potential to remove this mineral from the system. The lack of pyrite in the leached sample confirms the suggestions from chemical analysis results presented earlier and that the sulfur and Fe associated with pyritic minerals has been removed from the solid material through the biogeochemical mineral dissolution process.

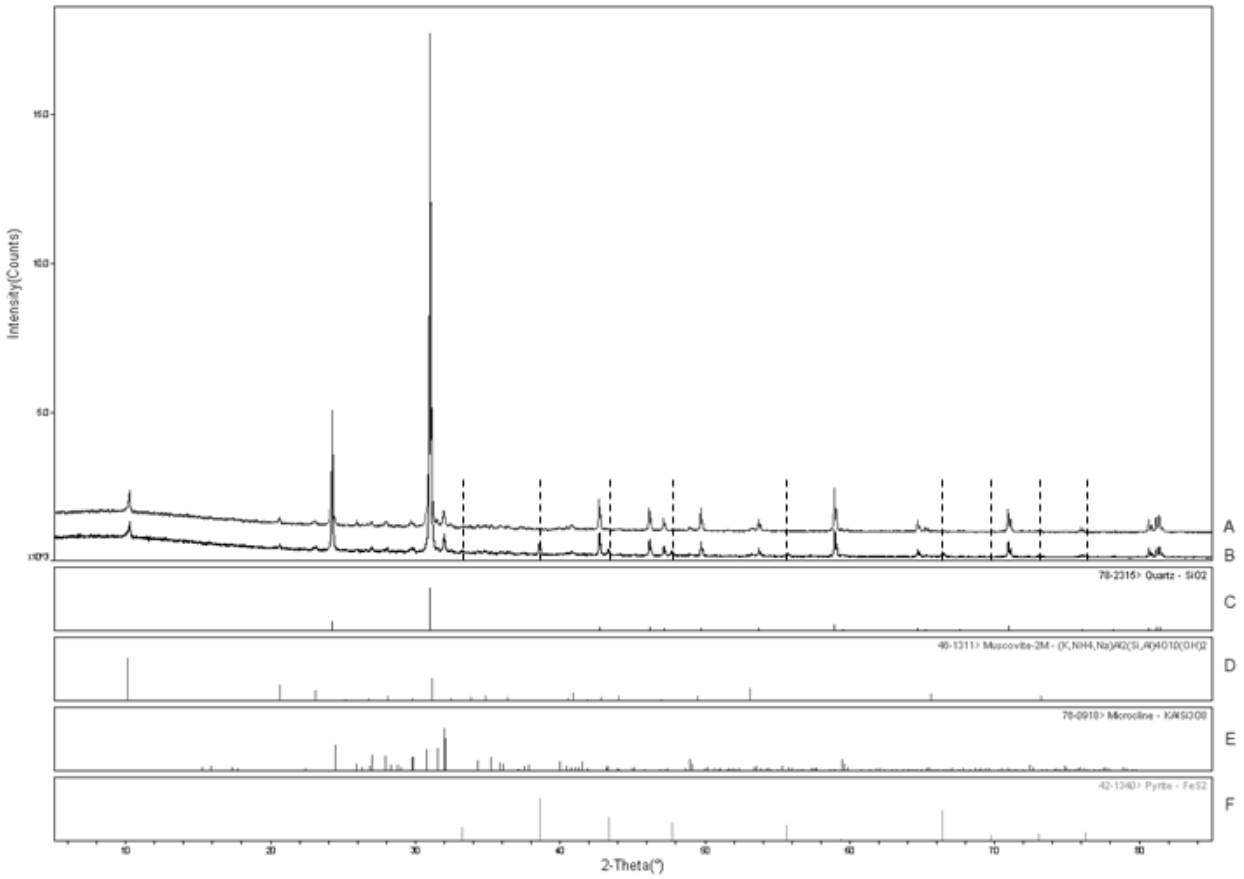

Figure A.9 Powder x-ray diffraction pattern of the quartz-pebble conglomerate material (74 µm): (A) treatment 4 reside material and (B) fresh, unaltered material; XRD data baselines for (C) quartz, (D) muscovite, (E) orthoclase and (F) pyrite; locations of peaks corresponding to pyrite listed in the JCPDS database for samples are indicated by dashed lines in the sample scans.

SEM images illustrating the morphology of the pyrite grains in the fresh and residue materials are presented in Figure A.10. The surfaces of the fresh pyrite grain appear smooth with minimal indication of surface dissolution or corrosion features. These latter features are found on the very minor number of pyritic grains surviving the biogeochemical dissolution process as cracks, dissolution pits, and fractures on the grain surface. Detailed electronoptical examination of the fresh ground rock material indicated the presence of numerous pyrite grains, with the location of a single grain in the leached sample being very difficult, even in backscatter imaging mode, further confirmation of the removal of pyritic minerals by the biogeochemical dissolution process.

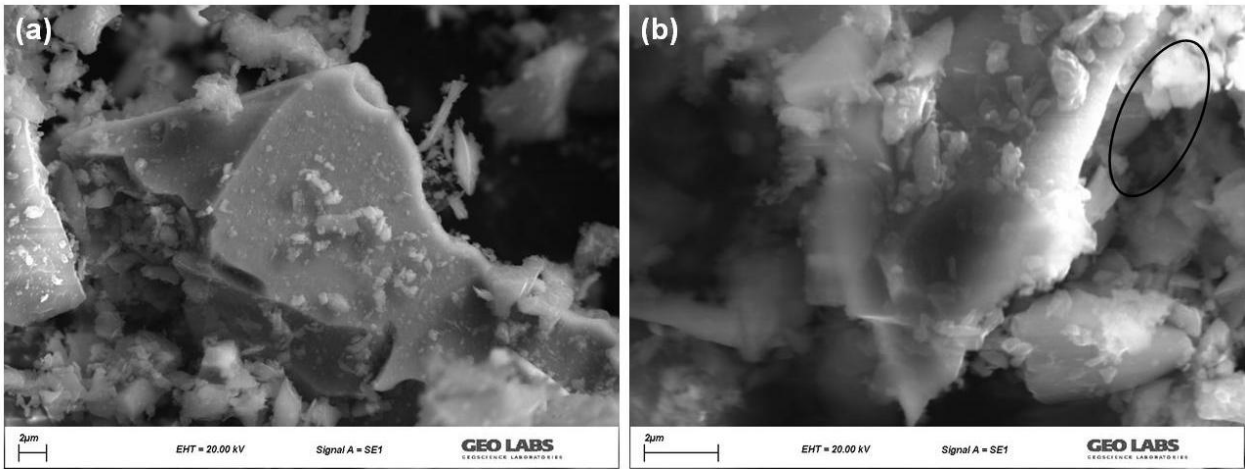

Figure A.10 SEM images of: (a) pyrite grain from fresh, unaltered material and (b) a corroded pyritic grain from treatment 4 residue after 80 days of treatment; surface imperfections are highlighted

The identification of minerals other than quartz, feldspar and pyrite in this preliminary electronoptical observation stage was limited by the dominance for these three mineral types (Figure A.11).

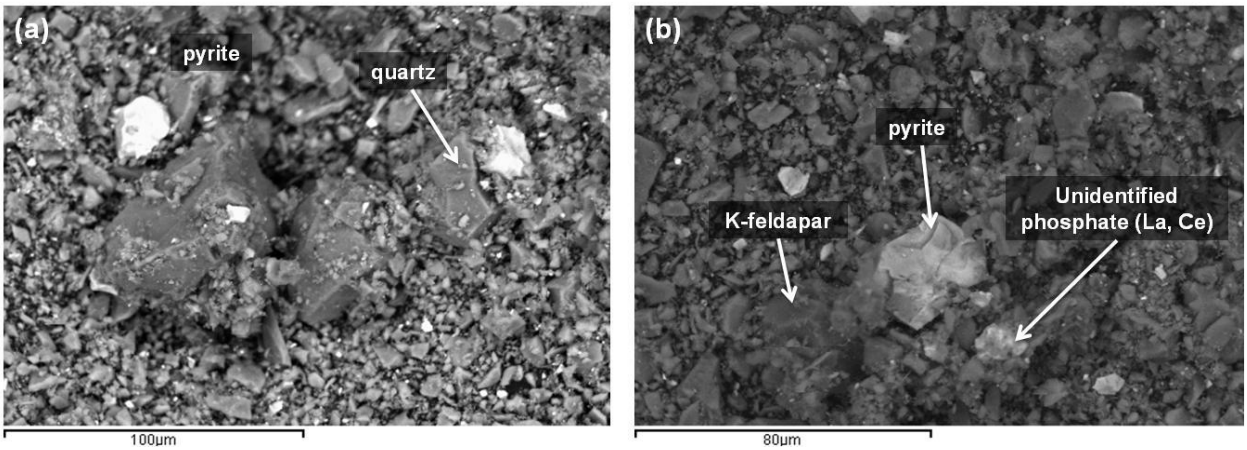

Figure A.11 SEM images of mineral grains in the fresh material suggesting: (a) pyrite and quartz and (b) pyrite, potassium feldspar, unidentified phosphate mineral grain containing lanthanum and cerium.

Numerous very small mineral grains containing a variety of REE were observed, with distinct elemental groupings being associated with the individual grains, with the light and heavy REE groupings being in different mineral phases (Figure A.12). The suggested mineral phases include zircon (Figure A.12a), potassium feldspar, quartz, and an unidentified mineral grain that contains La, Nd, and Ce (Figure A.12b), potassium feldspar and an unidentified mineral grain containing Dy, Gd, and Os (Figure A.12c), and an unidentified mineral grain that contains U and Ti, an unidentified mineral grain that contains La, Nd, and

Ce, and an unidentified mineral grain that contains Fe and Cr (Figure A.12d). Accurate mineral identification of these individual phases was not completed as part of this preliminary examination.

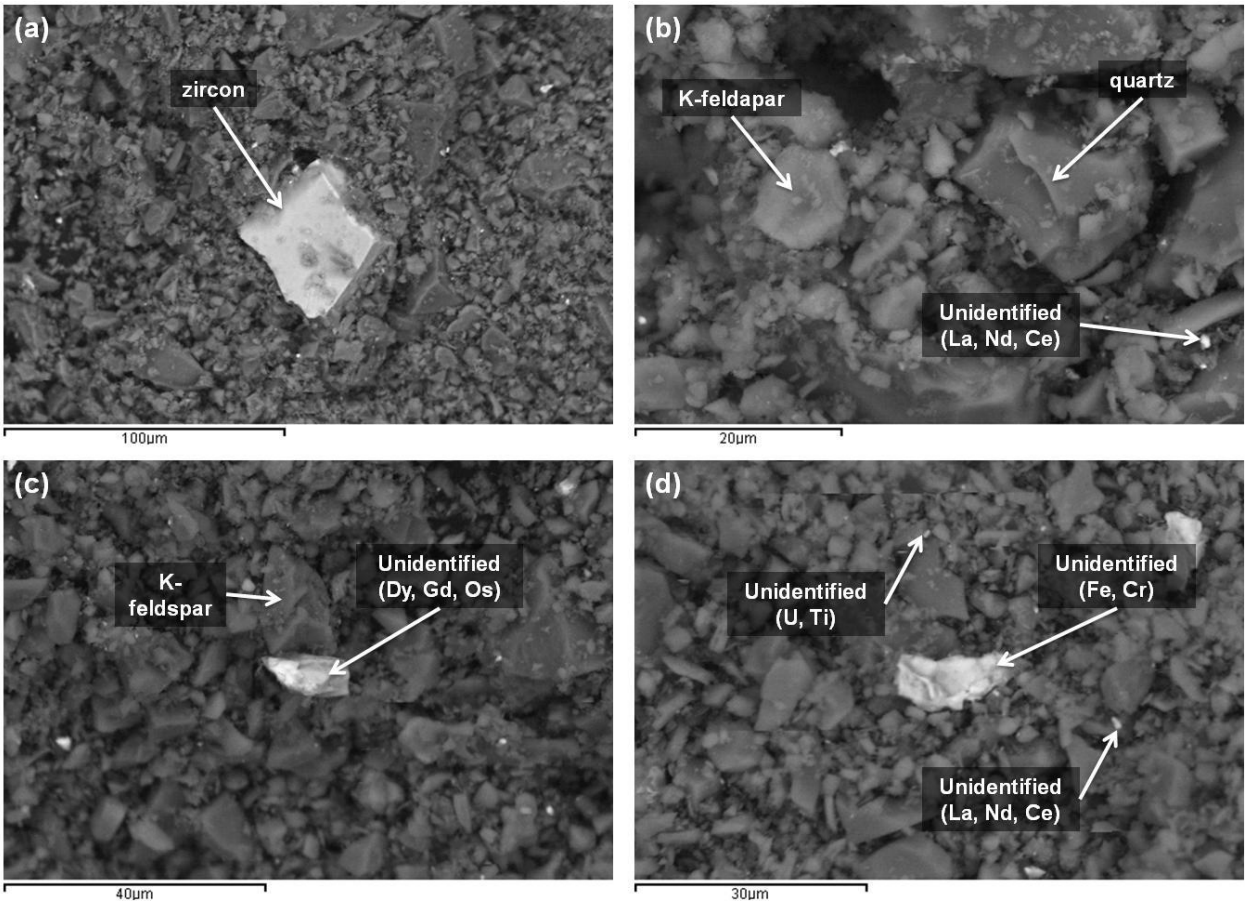

Figure A.12 SEM images of mineral grains in the leached material suggesting: (a) zircon, (b) k-feldspar, quartz, unidentified Ce-, Nd-, and La-, bearing mineral phase, (c) K-feldspar, unidentified Dy-, Gd-, Oz-bearing mineral phase, and (d) unidentified U- and Ti- bearing mineral phase, unidentified Fe- and Cr-bearing mineral phase, unidentified Ce-, Nd-, and La-, bearing mineral phase.

Although some key conclusions can be drawn from the limited mineralogical analysis performed to date, more selective grain preconcentration techniques are necessary to provide accurate diffraction identification of critical mineral phases of interest. The dominance of quartz, for example, in the raw samples limits the possibility of identification of phases at less than 1 to 2 % abundance in the sample. The same preconcentration techniques will also provide greater detail in both the morphological and chemical determinations.

A.4 Conclusion

The following conclusions have been draw from this study:

- Inoculated treatments produced superior release of U and REEs, compared with non-inoculated treatments, mediated by biogeochemical mineral dissolution conditions providing economic benefits to the application;
- Industrial application conditions of biogeochemical mineral dissolution methods may produce similar U and rare earth element recoveries to those obtained under aseptic laboratory conditions; and
- The Fe release curves for inoculated treatments showed the complete removal of Fe during the experimental stages, indicative of complete dissolution of pyritic minerals, which is supported by XRD scans, suggesting the possible elimination of the risk of acid mine drainage from the waste materials.

The results presented would indicate that metal recoveries using bioleaching is a practical, low cost, method of recovery for a broad range valuable metals. The dissolution of Fe has significant affect on the decommissioning of waste products on mine sites with the possible elimination of a major environmental issue in the minerals industry, namely a reduction in acid generating potential always associated with Fe sulphides.

Experimental work continues with small leaching columns, of which the leaching parameters (inoculation, leaching liquid composition, and pH) are guided by the results of this phase of experimentation. Leach column testing will be used to confirm the REE, U and Fe release obtained with shake flask testing.

APPENDIX B

B Bioleaching: Small Column Study

B.1 Introduction

The success of bioleaching for the recovery of metals from mineralized material depends on the characteristics of the host mineralization, microbial population, and environmental conditions. Many of these parameters can be optimized using bench-top studies, however studies of this scale do not address the leaching solution application method. Wetting protocol, usually trickle and flood application methods, is a parameter that can be easily investigated using column experiments. Experimental methods have used the trickle leaching approach far more commonly to simulate surface heap leaching in laboratory studies because the application method is much more feasible to apply to a full scale heap than a flooding application.

The assessment of biogeochemical mineral dissolution with leaching columns can provide details of particular leaching characteristics that may be controlled at the field level (Wadden & Gallant, 1985; Munoz, et al., 1993; Nemati, et al., 1997). After basic leaching parameters are established using bench-top experiments, leaching columns are used to provide greater insight to the leaching process by using methods that may be applied at a larger scale. The effect of individual application methods can be tested in leaching column experiments to determine the overall affect on the leaching process. Experiments of this scale require minimal materials and can generally produce results to assess many parameters in a short amount of time under controlled environments, compared with more elaborate investigations.

The objectives of this study include:

- Confirmation for the suitability of an environmental microbial culture, collected from the study site, for the bioleaching application by comparing in parallel experiments against the D7 strain *A. ferrooxidans*; and
- Comparison of two leachate application methods, continuous irrigation and periodic flooding, applied to small column experiments to determine the leaching methods that will be technically and logistically feasible to apply to larger column experiments, which will be more complex to carry out.

The findings from this experiment will provide an evaluation of the potential methods of application for the leaching solution that will guide the development of large leaching column experiments and describe one factor related to the potential commercial success of bioleaching along the Quirke Syncline. The contents of this appendix have been compiled from a report submitted to Pele Mountain Resources:

- Reported submitted to Pele Mountain Resources, July 2011 titled "Leaching for closure: Geochemical Monitoring of a Biological Extraction Process"

B.2 Experimental Methods

Fresh drill core was collected from the study site, Eco Ridge Mine Rare Earths and Uranium Project site (Eco Ridge), owned by Pele Mountain Resources Incorporated (PMR), approximately 11 km east of Elliot Lake, Ontario. The drill core was crushed to 2 to 4 cm and homogenized in a large tumbler. Approximately 15 kg was sub-sampled and crushed with a small crusher to 1 to 2 mm. The representative sub-samples were collected using a riffle splitter.

Two culture sources have been investigated:

- Pure strain: *Acidithiobacillus ferrooxidans* (D7) stored at Laurentian University (Ferroni, et al., 1986; Leduc & Ferroni, 1994; Leduc, et al., 1997); and

- Environmental culture: population representative of that expected at Eco Ridge cultured from water samples collected from the former tailings catchment area of Stanrock Mine.

Lucite columns (1.27 cm internal diameter and 90 cm tall) were loaded from the bottom up with 2.5 mL of plastic beads (3 to 4 mm), 90 grams of mineral material, and another 2.5 mL of beads. The beads aid in the flow distribution through the column. The bottom of each column was covered with nylon mesh (0.5mm) to retain the charge before being connected to a reservoir filled with 760 mL of DDI water. Fresh air was supplied with an air pump at the base of each column to ensure aerobic conditions were maintained throughout the columns during the experimental period (Nemati, et al., 1997).

Treatments were designed to compare methods of leachate application that may be applicable at a pilot or field scales. Solutions were supplied using a closed-loop system by continuous irrigation (Munoz, et al., 1993) or flooding (Wadden & Gallant, 1985) (Table B.1). The continuous irrigation simulations were fed with solution from a reservoir by peristaltic pump at 0.5 L hr^{-1}. The top-flooded columns were supplied 200 mL of solution by peristaltic pump, with the drainage valve closed and 50 mL of solution supplied to fully flood the mineralized material interstices in the column. The flood solution was released after 24 hours, with another 200 mL of solution being flushed through the column. After the first 24 hours of leachate application reservoirs were inoculated with 10 mL of the specified culture from prepared broth cultures.

Table B.1 Small column leaching treatments (n=2)

Parameter	1	2	3	4	5	6
Inoculum						
water	x			x		
pure culture, *A. ferrooxidans*		x			x	
environmental consortium			x			x
Leaching solution						
recycled	x	x	x	x	x	x
Wetting Type						
continuous percolating	x	x	x			
periodic flooding				x	x	x

Leachate samples were collected using sterile syringes every two to fourteen days and filtered (0.45µm). The experiment was continued until the elemental cumulative release from the mineralized material reached a stead state, approximately 7 months. The research columns were disassembled and the residue material was stored for use in future decommissioning simulations. A subsample from each column was retained for subsequent chemical and mineralogical analysis.

B.3 Results & Discussion

All treatments allowed a decrease of leachate pH through 7 months of leaching (Figure B.1). The rate of acid generation in the first three months was the slowest in the non-inoculated treatments (1 and 4), which all columns stabilized to pH 2.1 ±0.1. After four months the leachate solution in the reservoirs was replaced with fresh water to prevent an increase of concentrations of elements toxic to the microbial populations; indicated by the abrupt change in pH at this time.

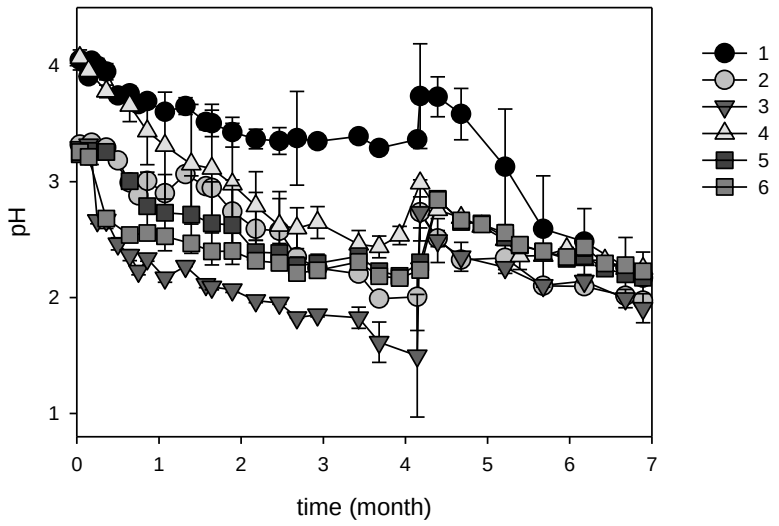

Figure B.1 Time profiles for small column leaching treatments (Table B.1) during 7 months of leaching displaying the changes in pH.

During the last half of the experiment, both water-inoculated treatments (1 and 4) reached pH conditions favorable for *A. ferrooxidans* at a rate similar to treatments receiving the pure strain and environmental consortium. The activity of *A. ferrooxidans* increases the reaction rate of mircobiogeochemical oxidation of Fe six orders of magnitude (Singer & Stumm, 1970; Marchand & Silverstein, 2003; Johnson, 2010). Thus, in the non-inoculated treatments, pyritic minerals will be chemically oxidized at a slower reaction than biotic oxidation. The mineralized material was not sterilized prior to loading into the small columns and indigenous *A. ferrooxidans* colonies (or related bacteria) existing in microfissures may have been introduced into the system as a component of the mineralization loading into the columns, establishing a population after an initial slow growth stage.

The oxidation-reduction potential (E_H) of leachate sampled from all treatments was between 0.74 and 0.82 V after seven months, with the fastest initial rate of increased in the treatments inoculated with the environmental consortium isolated from Elliot Lake mine waters, regardless of irrigation method (3 and 6) (Figure B.2). This result confirms that inoculation allow the microbial activity to increase the oxidation potential more rapidly, with pure strain and natural microorganism consortia eventually promoting similar redox environments.

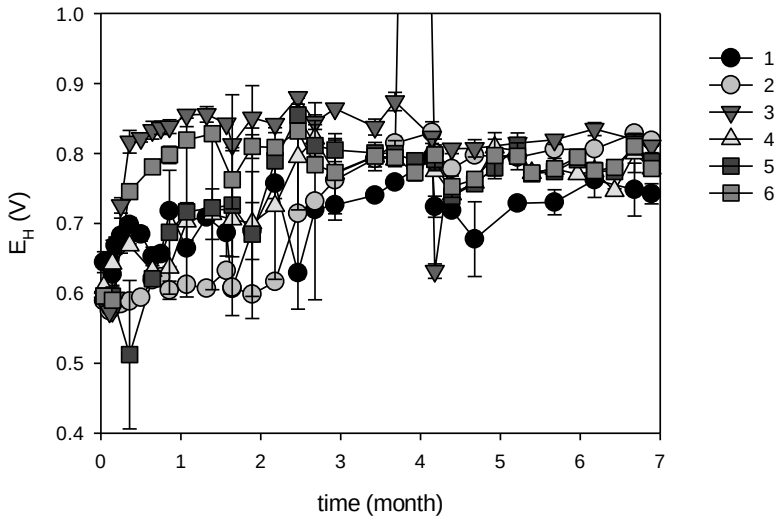

Figure B.2 Time profiles for small column leaching treatments (Table B.1) during 7 months of leaching displaying the changes in oxidizing potential.

The pure strain inoculated treatments (treatments 2 and 5) experienced a slow growth stage at the beginning of the experiment with respect to increasing solution E_H, but similar E_H conditions to the consortia treatments were reached by approximately four months (Figure B.2). Other studies have demonstrated that consortia of microorganisms tend to show superior leaching kinetics compared with pure strains because they have synergistic metabolic physiologies (Johnson, 2010), which may explain the slow growth stage for treatments inoculated with the pure strain in the present study that does not exist for treatments inoculated with environmental culture.

The release of U for all columns was similar after the 7 month experiment. The non inoculated columns saw 94 and 73% of the total U content released for the irrigated and flooded columns, respectively, while the U release to solution from the inoculated columns ranged from 71% to 100% (Figure B.3). Although the release of U from the non-inoculated columns comparable with the inoculated columns after 7 months, the leaching rate profile between inoculated and non-inoculated columns differ greatly (Figure B.3). A large range exists for both non-inoculated treatments (1 and 4); half of the columns showed signs of self-inoculated while the other half did not, thus the results span dissolution from non-inoculated and self-inoculated columns.

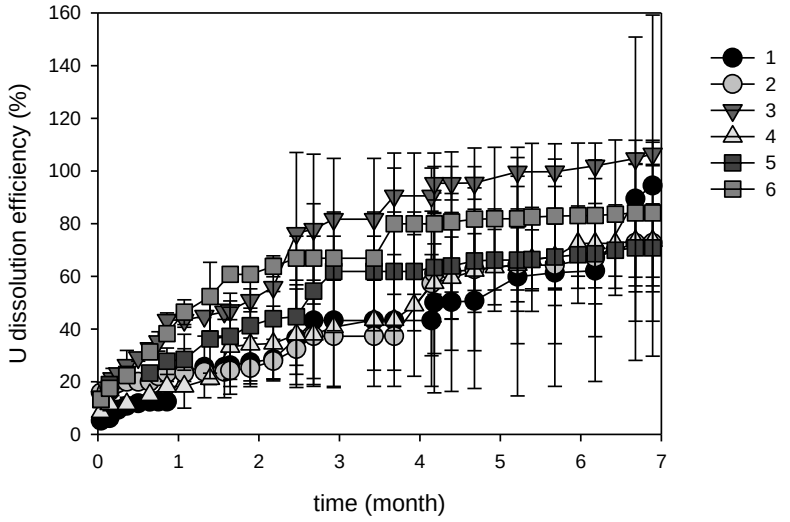

Figure B.3 Time profiles for small column leaching treatments (Table B.1) during 7 months of leaching displaying changes in U dissolution efficiency.

For both wetting techniques, the treatments inoculated with the environmental culture (3 and 6) had a higher dissolution efficiency achieved sooner, compared with the pure strain inoculated samples (2 and 5). These results suggest that a consortium of microorganisms may have superior leaching kinetics because of synergistic leaching efforts.

The study indicates that periodic flooding and continuous can be effective as wetting methods to promote and sustain biogeochemical mineral dissolution conditions that drive the dissolution of minerals containing U for metallurgical extraction. The distribution of U between the leachate and residue is summarized in Figure B.4. The final distribution of U between the leachate and residue show that inoculation with the environmental cultured and continuous irrigation leaching conditions promoted the greatest U leaching, treatment 3. The other inoculated columns (treatments 2, 5, and 6) show the potential for almost 80% U dissolution and the results from the non-inoculated columns (1 and 4) reflected self-inoculation and subsequent dissolution.

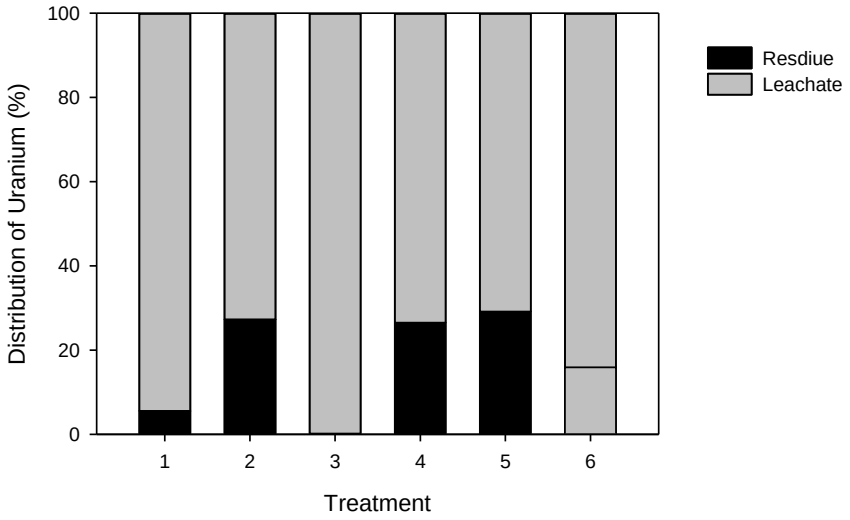

Figure B.4 Distribution of U for small column leaching treatments (Table B.1) after 7 months of leaching.

Small columns inoculated with the environmental culture, regardless of irrigation method (treatment 3s and 6), allowed greater dissolution of REEs from the mineralization compared with pure strain inoculation (Figure B.5). The environmental culture promoted the extraction of REE, which present additional economic advantages for the biogeochemical mineral dissolution process by allowing between 29% and 54% dissolution for heavy REEs (Figure B.5a). Release of light rare earths to solution by associated mineral biogeochemical leaching is less efficient; approximately 6 to 23% (Figure B.5b).

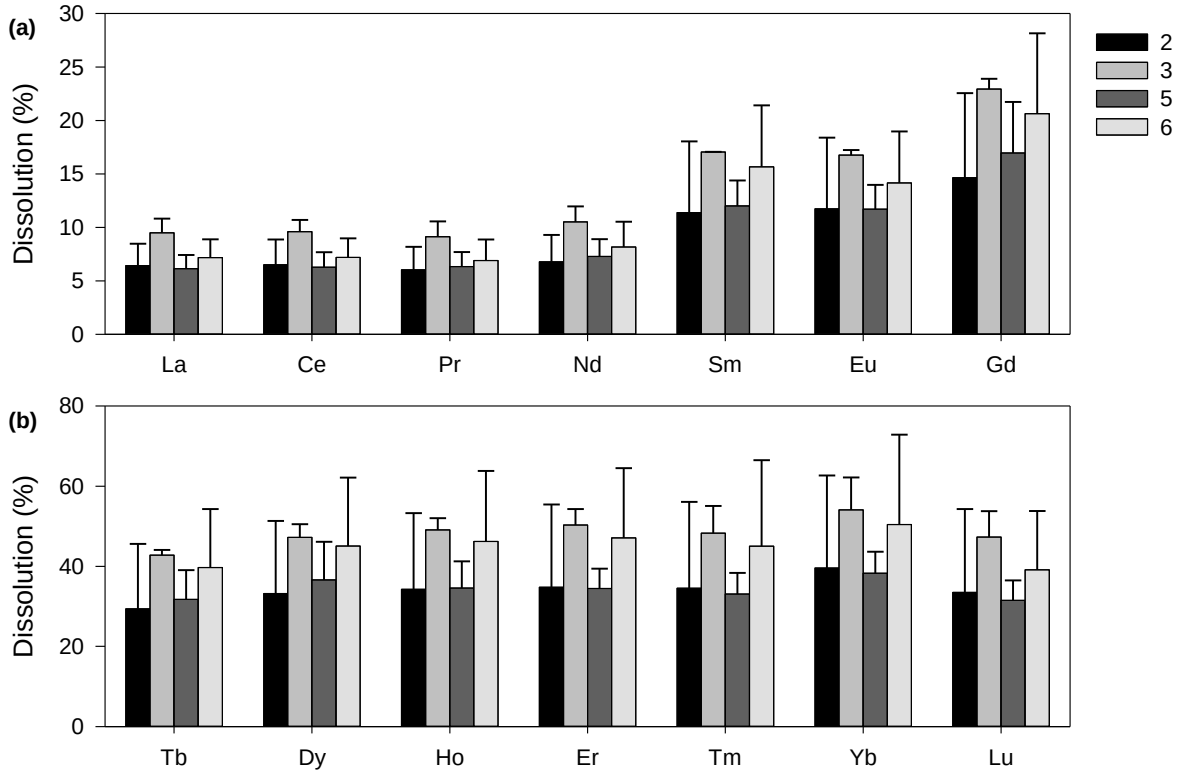

Figure B.5 Dissolution efficiency for small column leaching treatments (Table B.1) after 7 months of leaching of leaching for: (a) light REEs and (b) heavy REEs.

The dissolution trends of the heavy and light REEs are consistent with those reported in the microcosm experiments (Appendix A); heavy REEs were readily released and light REEs remained held in the mineralization. The column leaching is not as effective as the microcosm approach, probably related to a decreased surface area. Detailed chemistry of feed and residue material provides a complete understand elemental-mineralogical association. The details for the mineralogical analysis are presented in Chapter 6.

The dissolution of Fe varies greatly from the inoculated and non-inoculated columns (Figure B.6). The results show that the greatest dissolution of Fe is achieved by the inoculated columns that received continuous irrigation wetting and the most efficient dissolution took place in columns inoculated with the environmental culture, 53% (treatment 3). The environmental culture inoculated columns with flooding application reported 17% Fe dissolution.

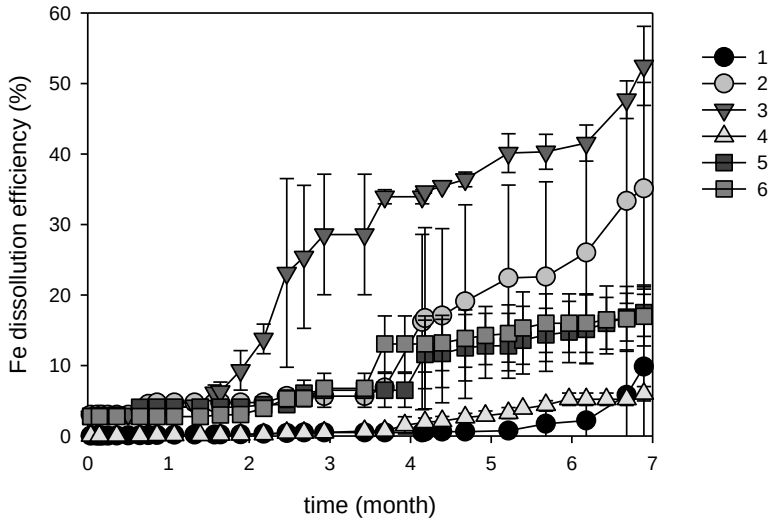

Figure B.6 Time profiles for small column leaching treatments (Table B.1) during 7 months of leaching displaying changes in Fe dissolution efficiency; note: maybe separate treatments 1 and 4 to show not-inoculated and self-inoculated b/c show very large error

The distribution of Fe in the system shows greater amounts held in the mineralized residue from the non-inoculated treatments (1 and 4) while the Fe content of the inoculated treatments vary, with the greatest total release is from the irrigation treatments (2 and 3) (Figure B.7). Iron release in the small column experiment was less than reported in the microcosm experiment (Appendix A), and the decrease is probably related to a decrease in mineral surface area and exposure of the ferrous sulphide minerals to the leaching environment.

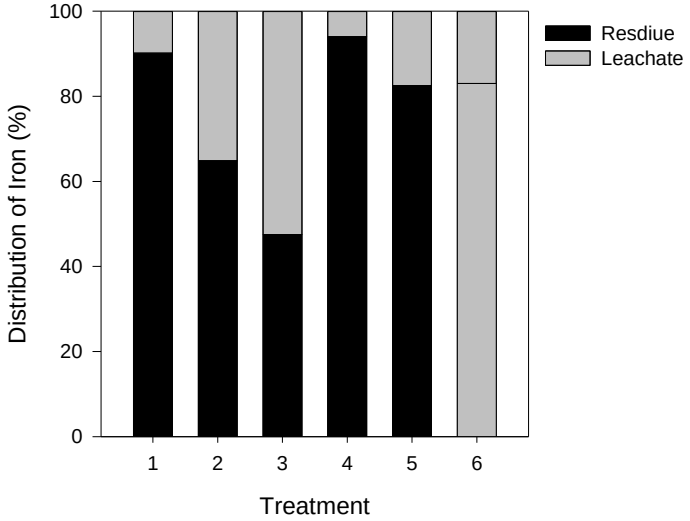

Figure B.7 Distribution of Fe for small column leaching treatments (Table B.1) after 7 months of leaching.

Total sulfur concentrations of the spent mineralized material confirm that sulfur is released to solution through the bioleaching extraction process (Figure B.8). Prior to leaching, a total suphur content of 3.3% by weight was reported for the mineralized material. The sulphur content decreased by 72% under biogeochemical mineral dissolution with *A. ferrooxidans* via continuous irrigation and 64 to 66% when inoculated with the environmental culture for either wetting technique. Surprisingly, the lowest sulphur removal was from the flooded columns inoculated with *A. ferrooxidans* reporting 38%.

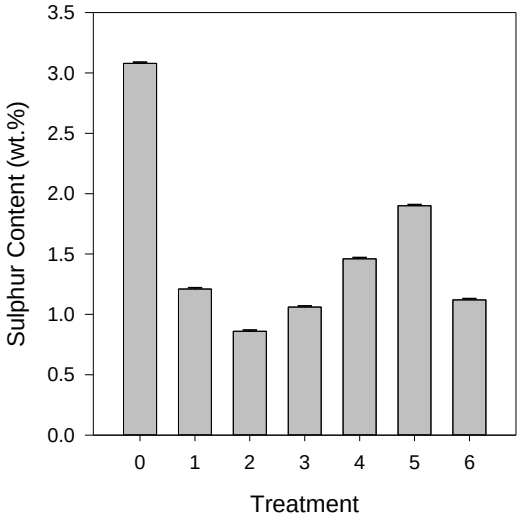

Figure B.8 Total S concentration in residues from small column leaching treatments (Table B.1) after 80 days of leaching.

A mineralogical study on the selective biogeochemical release of critical metals, including U and REEs from the uraniferous mineralization is completed in Chapter 6. Detailed mineralogical analysis of fresh and leached material has been completed to further investigate the biogeochemical mineral dissolution process, focusing on secondary phase production. The results of this study are provided in Chapter 7.

B.4 Conclusion

The following conclusions have been draw from this study:

- Small column biogeochemical mineral dissolution experiments confirm the preliminary findings of the microcosm experiments and indicate that particle size of the mineralized material sample is a critical control on elemental release to solution by biogeochemical methods;

- Inoculation of solutions with the appropriate bacterial culture is vital to drive the complex biogeochemistry of the leaching processes of the sulphidic and Fe containing minerals in the mineralization to facilitate the dissolution of U and REE's; and
- Both the continuous irrigation and periodic flooding released similar amounts of U from the crushed material, thus practical considerations may dictate the leaching methodology chosen for further studies

The results from the small column biogeochemical mineral dissolution experiments guide processes to be optimized in larger leaching columns, suggesting the large columns be inoculated with the environmental consortium and leached by continuous percolation.

APPENDIX C

C Inhibition: Microcosm Study

C.1 Introduction

In the absence of bacterial activity, biotic oxidation of Fe no longer takes place (Kleinmann, 1987). With the termination of this process, the spontaneous cycle of bacterial oxidation of Fe^{2+} coupled with pyrite oxidation by Fe^{3+} discontinuous when existing Fe^{3+} is exhausted and the slow process of abiotic oxidation of pyrite begins to take over. *Acidithiobacillus ferrooxidans* is negatively affected by the presence of organic compounds in its habitual area and many accounts confirming the inhibition of *A. ferrooxidans* and related bacteria by organic substances have been reported (Leathen, et al., 1956; Silverman & Lundgren, 1959; Dugan & Lundgren, 1964; Duncan, et al., 1964; Kleinmann & Erickson, 1983; Dugan, 1987a). Many of the compounds that prove to be inhibitory to the genus *ferrooxidans* are innocuous to other heterotrophic microorganisms (Tuttle & Dugan, 1976) allowing these compounds may to applied with an aim of limiting *A. ferrooxidans* activity yet not produced detrimental effects to other microbial populations.

The goals of this study include:

- Demonstrate the direct application of various organic compounds known to inhibit the activity of *A. ferrooxidans* to partly oxidized pyrite-containing minerals to determine the success or failure of a compound to inhibit biogeochemical mineral dissolution; and
- Determine the ability of the treatment to maintain inhibition conditions after the introduction of factors that promote biogeochemical mineral dissolution.

C.2 Experimental Methods

Five grams of homogenized residue material from the small column leaching phase were added to 250 mL Erlenmeyer flasks along with 125 mL of DDI water and inoculated with 5 mL of prepared environmental culture broth.

The flasks were agitated using an enclosed bench-top shaker at a rate of 150 RPM at 30°C under ambient lighting conditions for 4 weeks to reach biogeochemical equilibrium and an environment appropriate to further assess decommissioning options (Dugan & Apel, 1983). Once biogeochemical equilibrium was reached, various combinations of organic compounds known to inhibit the activity of *A. ferrooxidans* were added to the flasks (Table C.1).

Table C.1 Extraction flask inhibition treatments (n=3).

Inhibitor Concentration (mg L^{-1})		**1**	**2**	**3**	**4**	**5**	**6**	**7**	**8**	**9**
None		x								
Sodium Benzoate (SB)	10		x	x	x	x				
Sodium Lauryl Sulphate (SLS)	5		x	x			x	x		
Sorbic Acid (SA)	10			x	x		x		x	
Calcium-Magnesium Lime (lime)	0.15									x

After 4 four weeks from the time of treatment application, the contents of each flask was split three ways, with conditions known to promote bacterial activity and/or acid production being introduced. The flasks were either supplemented with an active bacterial culture and/or a Fe^{2+} solution to investigate the performance of the applied decommissioning treatment under conditions that promoted acid production.

Sample aliquots of 3 mL were collected from the flask using sterile pipette tips at predetermined intervals. The resistance testing was continued for 30 days. The mass of the flasks was recorded before sampling to monitor volume lost by sampling and evaporation.

C.3 Results

Initial Inhibitory Effects

A state of biogeochemical equilibrium was achieved in the flasks after 40 days and conditions present were optimum for biogeochemical mineral dissolution: pH was 2.2±0.1, E_H was 0.80±0.2V, and the Fe^{2+} concentration was 190±25 mg g^{-1} (Figure C.1). The inhibitory compounds were added directly to the flaks and monitored for 40 days while an assessment of inhibitory effects was based on the solution pH, E_H, Fe^{2+} concentration, and relative microbe population density.

Biotic oxidation dominates when pH is below 2.5. The pH of all other treatments remained constant at 2.2±0.1, with the exception of the lime addition sample (treatment 9). As expected, the addition of Ca-Mg lime increased the pH of the system increased to almost 7 in 4 hours of application and ferric hydroxide precipitates are formed.

When bio-oxidation continues the oxidation potential of the solution increases and eventually stabilizes. A high or increasing E_H is representative of oxidation conditions and low or decreasing pH is representative of reducing conditions, which is not favorable for bio-oxidation to continue. Prior to treatment application, the E_H for the suite of flasks was 0.80±0.02 V. After five days, a clear trend emerged from the flasks supplemented with organic compounds; the E_H of all flasks supplemented with sodium laurly sulphate (treatments 3, 5, 7, and 8) decreased to 0.54 V. These results suggest that sodium laurly sulphate, used alone or in combination with the organic acids, is capable of decreasing microbial activity, thus promoting reducing conditions. The addition of sodium benzonate or sorbic acid alone (treatments 2 and 4) produce strongly oxidizing effects and the E_H is higher than the control sample (treatment1). When used in combination the sorbic acid and sodium benzoate solution (treatment 6) is similar to the control (treatment 1) and lime addition (9).

When bio-oxidation progresses, there is a continuous oxidation-reduction cycle from Fe^{2+} to Fe^{3+}. In the absence of Fe oxidizing bacteria, Fe^{2+} will begin to accumulate because chemical oxidation, a much slower process, takes over. An accumulation of Fe^{2+} suggests that it is not being oxidized to Fe^{3+}, and is

therefore indicative of little or no biological Fe oxidation. The treatments that report an accumulation then stable concentration of Fe^{2+} (667±7 ppb) are the flasks supplemented with SLS (treatments 3, 5, 7, and 8). The concentration of the flasks treated with organic acids (treatments 2, 4, and 6) show a concentration in range with the control (393±93 ppb). The concentration of Fe^{2+} in the lime treated flask (treatment 9) is much lower (295 ppb), but a large quantity of Fe-hydroxide precipitates have formed, thus removing Fe from the aqueous phase.

Relative microbe population density is a measure of the existence of an Fe-oxidizing microbe culture assesses the likelihood of bio-oxidation to take place. This parameter provides a comparison of the population directly before the addition if the inhibitory compounds. The population for almost all treatments remands unchanged after application, but there is an increase in population for treatment 5,6, and 8 by the end of the testing phase. An increase in population may suggest that the inhibiting compound is no longer effective.

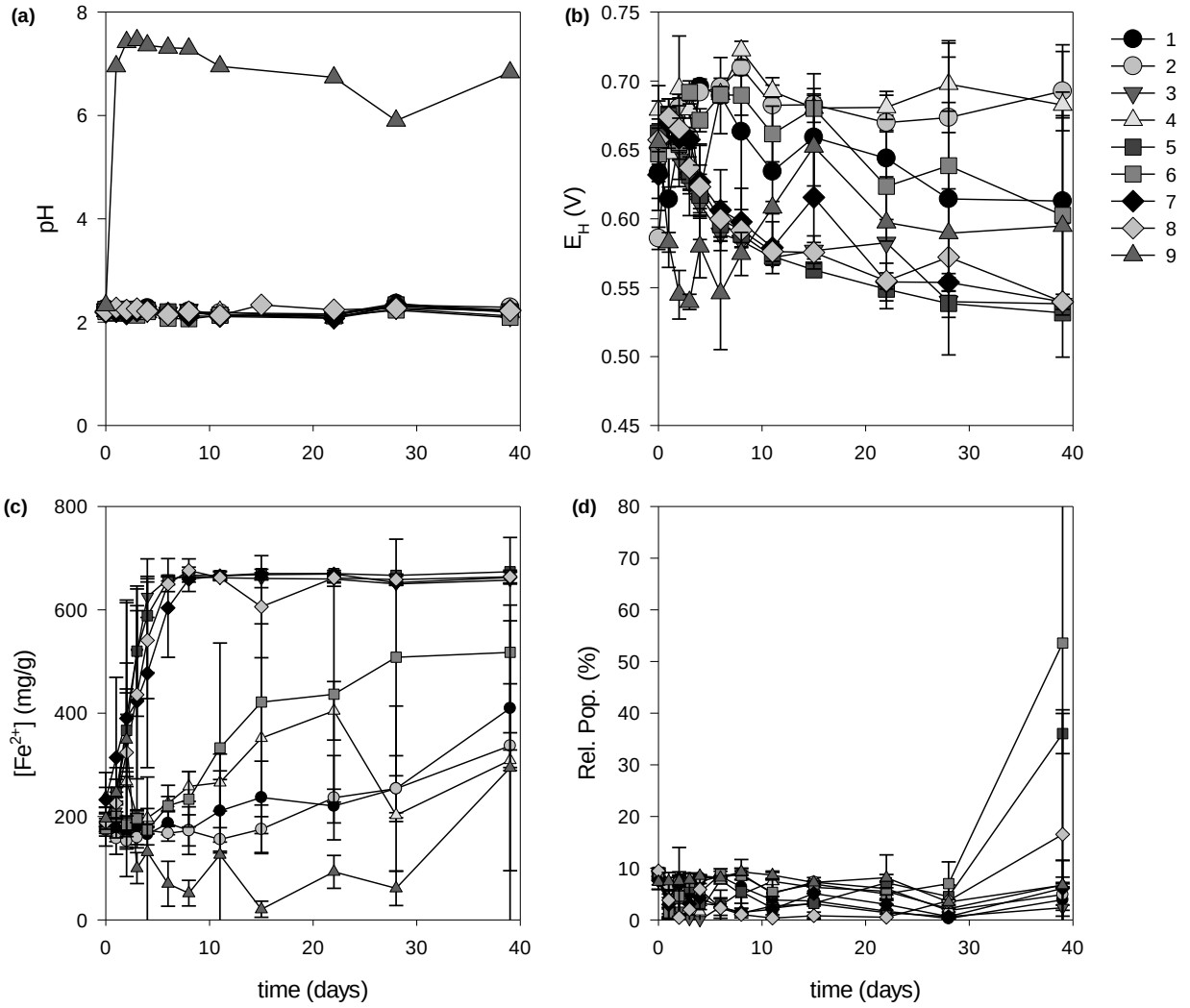

Figure C.1 Time profiles for microcosm inhibition treatments (Table C.1) during 40 days of application displaying the changes in: (a) pH, (b) oxidizing potential, (c) Fe^{2+} concentration, and (d) relative population density.

The treatments that showed the greatest potential to inhibit bio-oxidation conditions were SLS alone (treatment 3) and SLS applied with sorbic acid (7). Although the other SLS-combination applications (treatment 5 and 8) decreased oxidizing conditions and increased Fe^{2+} concentration, the relative population density increased after 20 days.

Resistance Study

The ability of each treatment to allow biogeochemical mineral dissolution conditions to be established after treatment application was determined by introducing a mature environmental culture or Fe^{2+} solution to the flasks. The oxidants were added alone or in combination, the latter would to provide the mature

culture with readily available Fe^{2+} that may be oxidized. Both the culture and Fe solution were acidic, approximately pH 2. pH, E_H, Fe^{2+} concentration, and relative microbe population were monitored for 10 days (Figure C.)

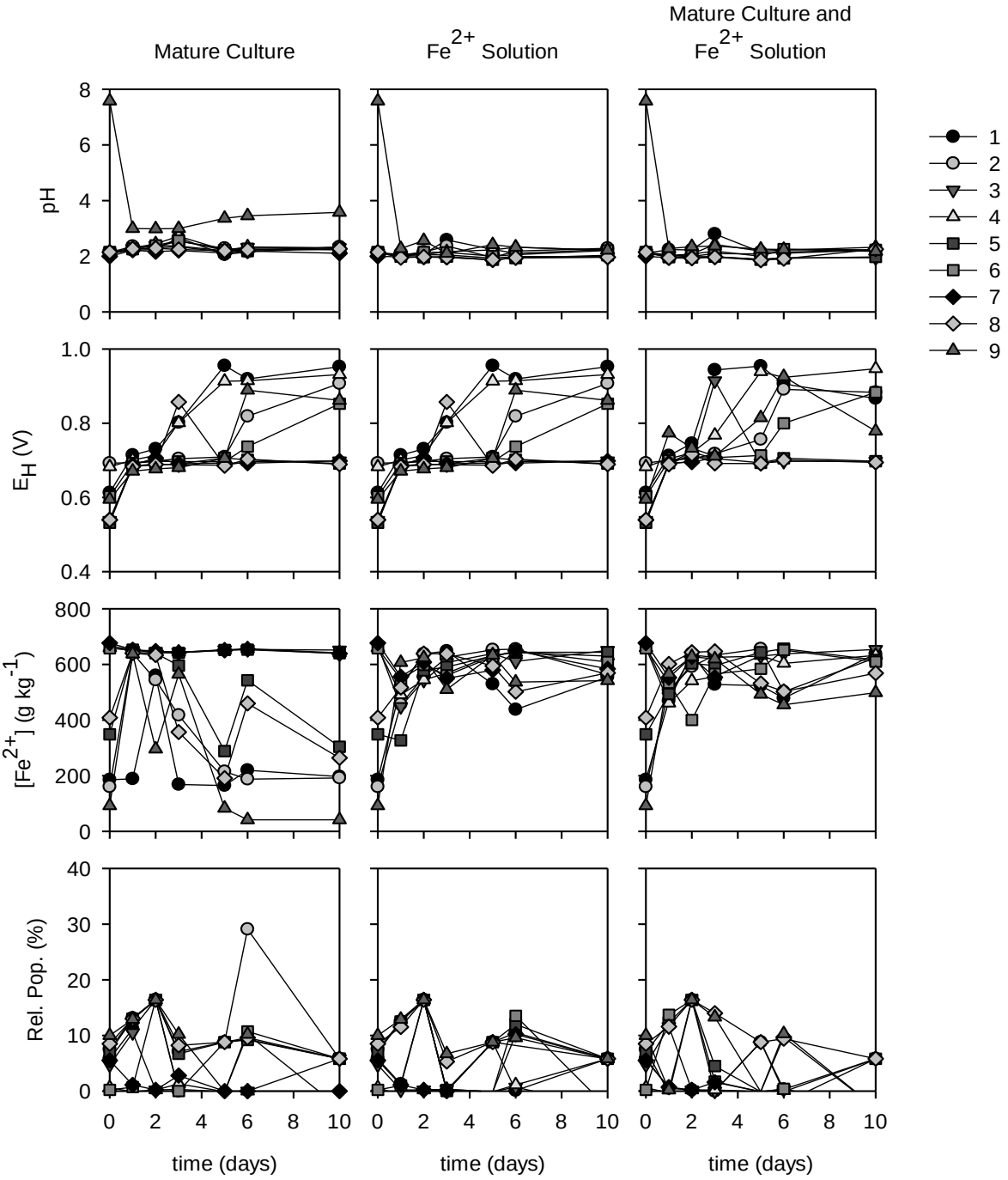

Figure C.2 Time profiles for microcosm inhibition treatments (Table C.1) during 10 days of oxidation resistance testing displaying the changes in pH, oxidizing potential, Fe^{2+} concentration, and relative population density in the presence of a mature culture and/or Fe^{2+} solution.

The pH remained stable with the exception of the lime-treated flasks (sample 9), which decreased in range with the rest of the samples. The oxidizing potential for all flasks increased initially with the addition of mature culture and Fe^{2+}. Flaks that were treated with SLS (treatments 3, 5, 7 and 8) stabilized around 0.70 V while the oxidizing potential of other treatments increased, up to as high as 0.95 V for the sorbic acid treatment in the presence of the mature culture and Fe^{2+} solution. The flasks that reported an increased in oxidizing potential showed a decrease in Fe^{2+} concentration in the presence of the mature culture, suggesting that oxidizing conditions are present and Fe^{2+} is effectively begin oxidized. The relative population density fluctuated between 20% and 0% for all treatments. The results suggest that only the flasks treated with SLS may effectively inhibit bacterial activity and bio-oxidation for a short amount of time. Treatments lacking SLS did not show any resistance to either oxidizing condition.

C.4 Conclusion

The following conclusions have been draw from this study:

- Lime addition is beneficial to achieve neutral conditions and remove dissolved Fe by precipitation, but the system does not respond well when a mature culture iron oxidizing culture is introduced, resulting in the return of and acid generating conditions;
- Sodium benzoate and sorbic acid applications slow the bio-oxidation process upon application, but reported low resistance to deter bio-oxidation processes when a mature culture is introduced; and
- Sodium laurly sulphate treatments, either alone or in combination with an organic acid, reported immediate inhibitory effects and the system remained resistant in the presence of a mature culture for the duration of the study.

The results presented suggest sodium laurly sulphate may be beneficial to inhibit bacterial activity when applied to pre-leached mineral material. A decrease in bacterial activity will result in a reduction of biogeochemical mineral dissolution, which is important for the decommissioning of waste products on

mine sites with the possible elimination of a major environmental issue in the minerals industry. Experimental work will continued using small leaching column to assess the application method of promising inhibitory compounds.

APPENDIX D

D Passivation: Microcosm Study

D.1 Introduction

A mineralogical approach to AMD prevention aims to stop mineral dissolution and acid production at the source with the removal or protection of the reactive mineral from the system or by rendering the reactive mineral inert. Chelating and precipitation methods to produce coatings on the surface of the reactive mineral, effectively blocking oxygen transport to the mineral surface to protect the reactive mineral from further oxidation (Evangelou, 1994). Pacification considers the hypothesis that oxidation inhibition of a reactive mineral, such as pyrite, can only by mitigated for the long-term by a surface coating directly on the reactive mineral (Evangelou, 2001). Whereas some approaches to decommissioning and closure aim to prevent oxidation of the reactive metal sulphide by installing a soil or water cover in attempt to block oxygen diffusion to the entire area, pacification aims to treat each grain individually with the application of a pacifying coating directly on the mineral surface (Belzile, et al., 1997). Reactive metal sulphides may be pacified by a forming a thin coating on the surface of the minerals preventing oxygen diffusion and subsequent mineral dissolution (Evangelou & Zhang, 1995; Chen, et al., 1999). Encapsulation of the sulphide mineral with an oxygen-impermeable coatings, either naturally produced or induced can provide long-term protection from chemical and microbiological oxidation (Harris & Lottermoser, 2006b).

The objectives of this study include:

- Formation of pacifying coatings on polymineralic material of primary ferrous sulphides and secondary minerals that developed as products of the biogeochemical mineral dissolution process, including secondary sulphides, oxides, hydroxide, and sulphates; and

- Assess the resistance of the coating to biological and chemical oxidation using a strong chemical oxidation and a mature culture capable of Fe oxidation.

D.2 Experimental Methods

Passivation studies follow the methodology developed in the early works of Evangaelou and Fytas (Evangelou, 1994; Fytas & Evangelou, 1998). In these studies, the mineral samples are washed with a strong acid, followed by DDI water, to remove any existing coatings. For the purpose of this study, the samples were not washed to remove existing coatings, as a strong acid wash would not be feasible at the field scale. Instead, the study was designed to test the application of pacification coatings on mineral grains with moderate secondary mineral formation present because these conditions better mimic oxidized, or weathered, mine waste material.

Ten grams of homogenized mineral material that had been subjected to oxidation under atmospheric conditions was added to 150 mL of the coating solution in a 250 mL Erlenmeyer flask.

The coating solution is composed of an oxidant (5 g L^{-1} hydrogen peroxide, H_2O_2), a buffer (0.8 g L^{-1} sodium acetate, CH_3COONa), and an inorganic compound, either sodium silicate (Na_2SiO_3) or phosphate (KH_2PO_4) (Table D.1). The pH of the solution was adjusted to between 5 and 6 using sodium hydroxide (NaOH) and hydrochloric acid (HCl). The flasks were agitated using an enclosed bench-top shaker at a rate of 240 RPM and 25°C under ambient lighting conditions for 24 hours.

Table D.1 Extraction flask pacification treatments (n=1).

Coating treatment* (g L^{-1})	1	2	3	4	5	6	7
None	x						
KH_2PO_4							
0.14		x					
1.4			x				
14				x			
Na_2SiO_3							
0.12					x		
0.61						x	
1.2							x

*All treatments also contain 5 g L^{-1} hydrogen peroxide (H_2O_2) and 0.8 g L^{-1} sodium acetate (CH_3COONa)

After 24 hours, the residual material was air dried, with subsamples from each treatment being collected for oxidation resistance testing to evaluate the coating's effectiveness at preventing further abiotic and biotic oxidation and/or acid generation. Approximately 3 grams of dried sample from each treatment was added to a 250 mL Erlenmeyer flask along with the either oxidizer or DDI water alone. The flasks were shaken on a bench top shaker at 240 RPM and 25°C under ambient lighting conditions. The oxidation resistance testing was carried out over 6 days with frequent sampling.

D.3 Results

The pH, oxidizing potential (E_H), and Fe concentration were monitored during oxidation resistance testing (Figure D.1). These parameters were selected because they provide indication of geochemical mineral dissolution driven by Fe-oxidizing bacterial; for instance, pH decreases, oxidizing potential increases, and stabilizes, and Fe concentration increases throughout the biogeochemical mineral dissolution process.

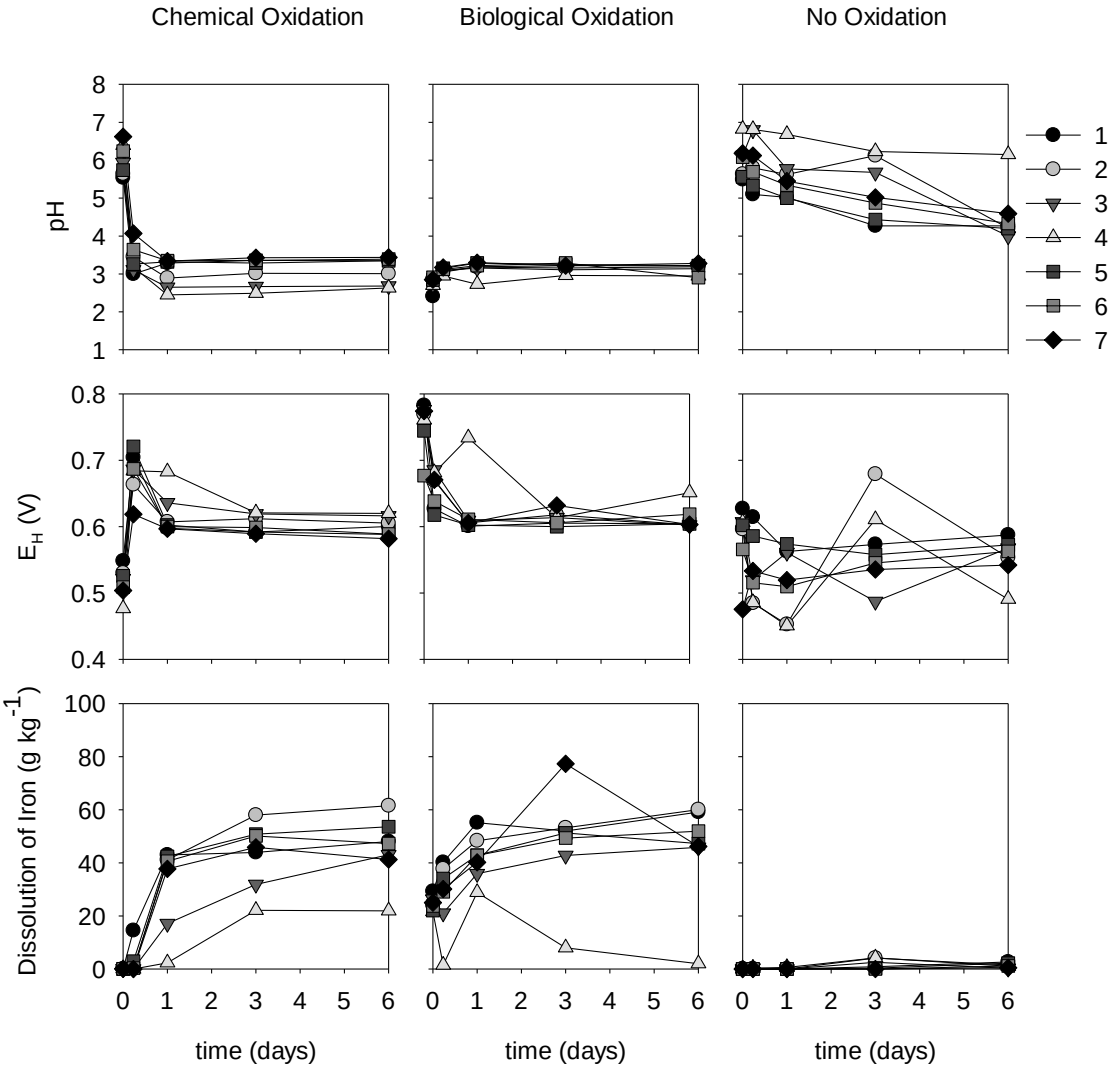

Figure D.1 Time profiles for microcosm passivation treatments (Table D.1) during 6 days of oxidation resistance testing displaying the changes in pH, oxidizing potential, dissolution of Fe^{2+} in the presence of a mature culture and/or Fe^{2+} solution.

When no oxidant was present, the pH of all treatments stabilized at 4.3 ±0.2, with the exception of the flask treated with the most concentration phosphate coating solution (treatment 4), which stabilized at pH 6.2 The pH did not decrease under this treatments, suggesting that the reactive minerals have been protected from oxidation. The leachate pH under chemical and biologic oxidation was 3.1 ±0.3 and 3.1 ±0.1, respectively. The lower pH in the oxidized samples suggests that acid production is taking place in the presence of both oxidants.

The oxidizing potential stabilized at 0.56 ±0.02 V in the absence of an oxidant, with the exception of the most concentrated phosphate coating solution (treatment 4), which stabilized 0.49 V, indicating that

oxidizing conditions are not present. There was fluctuation though the testing phase with potential reaching as high as 0.68 V (treatment 2) and as low as 0.45 V (treatment 2 and 4). The E_H of the systems in the presence of an oxidant were much more consistent, stabilizing at 0.60 ±0.01V and 0.61±0.02V for the chemical and biological oxidizers, respectively.

The dissolution of Fe arises in the biological or chemical mineral dissolution of ferrous sulphides. In the absence of an oxidant, the release of Fe is negligible, less than 3 ppb. Chemical oxidation was permitted to take place in the control, silica pacified treatments, and the two lowest concentration of the phosphate solutions (treatment 1, 2, 3, 5, 6, and 7) releasing 49 ±7 ppb for the suite of treatments. The most concentrated phosphate solution (treatment 4) allowed half that amount of Fe to become dissolved, 22 ppb. This trend was followed under biological oxidation. Although there was an initial input of 25 ±3 ppb of Fe to the systems as a component of the bacterial broth culture, the most concentrated phosphate pacified treatment (treatment 4) saw a reduction in Fe concentration to 2 ppb. This result indicates that the Fe introduced to the system is available to become incorporated in to a ferric-phosphate network and provide additional oxidative protection. The other treatments, including the control, allowed the release of Fe, 52 ±6 ppb, which is 27 ±4 ppb more than the initial input.

D.4 Conclusion

The following conclusions have been draw from this study:

- Oxidation resistance tests suggests that ferric hydroxide phosphate coatings may be established on fine grained pyrite-containing mineral samples that be been exposed to air and allowed to oxidized and form secondary mineral precipitates and/or coatings; and
- Investigation of the resistance of coatings to biological oxidation draws conclusions similar to chemical oxidation, although to a lesser extent because the biological oxidation takes more time to establish and whereas chemical oxidation by hydrogen peroxide is a fast reaction.

The results presented suggest pacification by phosphate coating solution may be established with the application of a coating solution containing 14 g L^{-1} monopotassium phosphate to effectively limit further oxidation of the mineral material. When biotic or abiotc geochemicall mineral dissolution is hindered, AMD production is limited. This concept can support the intentions of waste product decommissioning activities on mine sites and addresses environmental issues in the minerals industry. Experimental work will continued using small leaching column to assess the application method of promising inhibitory compounds

APPENDIX E

E Inhibition & Passivation: Small Column Study

E.1 Introduction

An understanding of the biogeochemical mineral dissolution process provides insight to approaches that may be used to disturbed, interrupt, or stop the bioleaching process. The application of bacterial inhibitors decreases the biogeochemical mineral dissolution reaction rate and limit acid production and subsequent metal dissolution. Passivation promotes the formation of a barrier phase between the metal sulphide and the oxidizing environment, thereby preventing oxidation of the sulphide and hindering the biogeochemical mineral dissolution process.

Following bench-top experiments to test the ability of compounds to inhibit bacterial activity or form oxidation-barrier phases, leaching columns are used to investigate the application of the selected bacterial inhibitors and pacifying coatings. In microcosm testing, sodium laurly sulphate effectively inhibited the activity of Fe oxidizing bacteria present in microbe populations existing at the study site when used alone or in combination with other organic acids (Appendix C). An investigation into the deposition of pacifying coatings or networks at the microcosm scale revealed the phosphate pacifying coating or the deposition silica networks on the mineral surface may be established on fine grained pyrite-containing to prevent further oxidation of the mineral surface (Appendix D).

Drawing from the results of the previous studies using partly oxidized mine ferrous-sulphide minerals, a larger grain size and experimental leaching columns are used to simulate the application of pacifying and inhibiting solutions to simulated waste material. The objects of this study include:

- Demonstration of a continuous irrigation application method to apply solutions that may be used to inhibit bacterial activity or provide oxidation resistance to previous leached materials as an approach to decommissioning option; and
- Assessment of the abilities of each application to resist oxidation by chemical or biological oxidations to identify applications with the greatest potential for decommissioning applications, which will be assessed at a larger scale.

The mineral material used in this study has been subjected to biogeochemical mineral dissolution (Appendix B). As such, the ferrous sulphate content of the material is expected to be lower than fresh materials and secondary mineralization and oxidation coatings are expected to be present. This material is expected to simulate waste material ready for closure treatment.

E.2 Experimental Methods

Lucite columns (1.27 cm internal diameter and 90 cm tall) were loaded from the bottom up with 2.5 mL of plastic beads (3 to 4 mm), 60 grams of previously leached mineral material from the small column leaching phase, and another 2.5 mL of beads. The beads aid in the flow distribution through the column. The bottom of each column was covered with nylon mesh (0.5 mm) to retain the biogeochemically weathered mineral charge before being connected to a reservoir filled with 500 mL of the inhibitor or coating treatment. Fresh air was supplied with an air pump at the base of each column to ensure aerobic conditions were maintained throughout the columns (Nemati, et al., 1997).

The passivation methods followed in this laboratory study are based on the publications of Evangaelou and Fytas (Evangelou, 1994; Fytas & Evangelou, 1998), with the inhibition methods followed being similar to those described by Dugan and Apel (1983). The inhibition or coating solution was supplied to the columns using the same delivery methods as the continuously irrigated small columns using a closed-loop system with a peristaltic pump at a rate of 0.5 L hr^{-1} (Table E.1). Coating treatments also included an

oxidant (5 L^{-1} hydrogen peroxide, H_2O_2) and a buffer (0.8 g L^{-1} sodium acetate, CH_3COONa) with the pH of all reservoirs adjusted to between 5 and 6 with sodium hydroxide and hydrochloric acid.

Table E.1 Small column inhibition and pacification treatments (n=3).

Treatment (g L^{-1})	**1**	**2**	**3**	**4**	**5**	**6**
None	x					
Passivation						
KH_2PO_4						
1.4		x				
14			x			
Na_2SiO_3						
0.61				x		
1.2					x	
Inhibition						
SLS						*x*
0.010						

*coating solution also include 5 g L-1 hydrogen peroxide (H2O2) and 0.8 g L-1 sodium acetate (CH3COONa)

Samples were collected from the reservoirs using sterile syringes every two days, filtered (0.45µm). Treatment application lasted for 12 days, after which the columns were deconstructed and the residues were aid dried.

The residual material from each treatment was split three ways and subjected to abiotic and biotic oxidation resistance testing by supplying 0.20 M hydrogen peroxide or bacteria culture, respectively. The flasks were agitated using an enclosed bench-top shaker at a rate of 240 RPM and 25°C under ambient lighting conditions. The oxidation resistance testing was carried out over 12 days with frequent sampling.

E.3 Results & Discussion

The pH, oxidizing potential (E_H), and total dissolved Fe concentration were monitored during oxidation resistance testing (Figure E.1). These parameters were selected because they are indicators of geochemical mineral dissolution driven by Fe-oxidizing bacteria, where pH decreases, oxidizing potential increases and stabilizes, and Fe concentration increases.

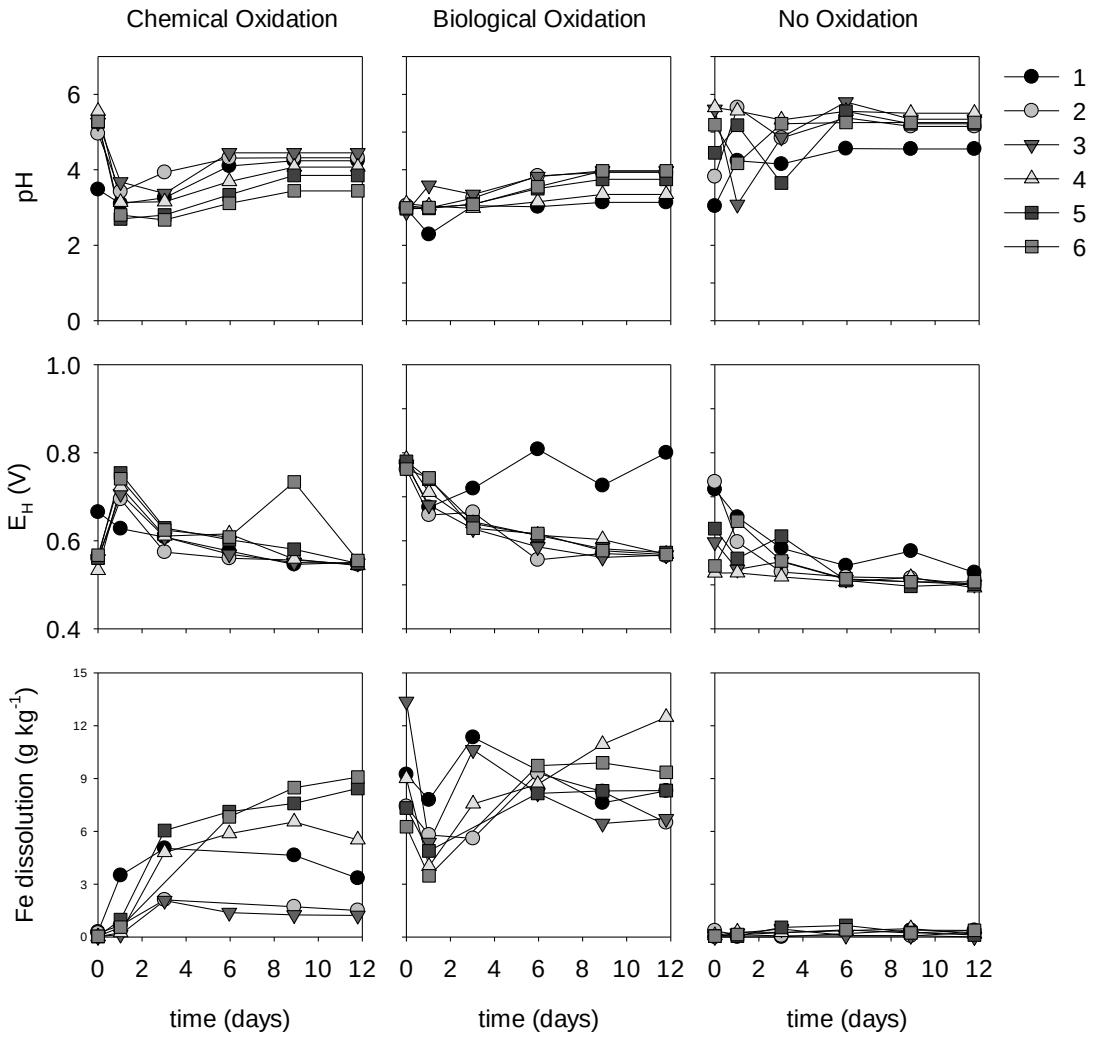

Figure E.1 Time profiles for small column inhibition and passivation treatments (Table E.1) during 12 days of oxidation resistance testing displaying the changes in pH, oxidizing potential, dissolution of Fe in the presence of a chemical or biological oxidation conditions.

The pH of all flasks stabilized at 5.3 ±0.1 when no oxidant was present (water), with the exception of the flask that did not receive an inhibition or pacifying treatment, which stabilized at pH 4.6. The lower pH in the controlled conditions demonstrates the acidic nature of the mineral material. In the presence of chemical or biological oxidizers, the pH of all flasks was less than when no oxidizer was present, 4.1 ±0.4 and 3.7 ±0.4 respectively, suggesting that acid production has taken place in the presence of both oxidants.

The oxidizing potential, E_H, for all treatments in all oxidizing conditions stabilized at 0.54±0.03 V, with the exception of one treatment; the treatment that did not received inhibiting or pacifying treatments

(treatment 1) under biological oxidation. The initial E_H for all inoculated treatments was 0.77±0.1 V at the time of inoculation, after which the potential for all treated flasks (treatments 2 to 6) decreased to 0.57±0.00 V after 12 days while the control flask (treatment 1) increased to 0.80 V. This value is in range of the oxidizing potential reported for active leaching experiments at both the microcosm and small column scale (Appendix A and Appendix B). This result indicates that the inoculated cultures are capable of prompting and retaining oxidizing conditions, but this activity is suppressed with the experimental treatments, and biological oxidation does not influence the oxidizing potential.

The dissolution of Fe takes place in the biological or chemical oxidative mineral dissolution of ferrous sulphides. In the absence of an oxidant, the release of Fe is negligible. Under chemical oxidation, Fe released to solution for all treatments. Inhibition offers no protection to chemical Fe oxidation and the highest dissolution takes place, 9 ppm (treatment 9). Treatments excepted to form silica network provide a slight suppression of Fe release, 5.5 to 8.4 ppm, with Fe release increasing as coating concentration decreases (treatments 2 and 3). Treatments expected to form ferric-phosphate coatings on the mineral surface effectively limit Fe dissolution to less than 1.5 ppm after twelve days (treatments 4 and 5). In the presence of a mature culture containing Fe-oxidizing bacteria, an initial input of Fe was introduced because Fe is supplied as a nutrient component in the broth culture. The trend of Fe dissolution by biologic oxidizers is similar to chemical oxidation, but the quantity of Fe is influenced by the initial addition of Fe with the broth culture. Release of Fe is lowest for the phosphate-pacification treatments (treatments 2 and 3) and silica-pacification treatments were higher (treatments 4 and 5). When taking initial Fe concentration into consideration, sodium laurly inhibition (treatment 6) preformed better under biological oxidation compared with chemical oxidation, indicating that bacterial inhibition by sodium laurly sulphate is effective. These results indicated that only the phosphate treatments resisted the dissolution of Fe from the mineral phases. Silica-pacification treatments may have poor results because the components of the coating solution may have preferentially formed as discrete precipitate phase rather than a coating network on the surface of the miner.

Chemical (IR) and mineralogical (SEM-EDS) analysis was conducted to assess the establishment of ferric hydroxide-phosphate coatings or silica network on the mineral surface. IR analysis of the mineral phase was inconclusive and did not confirm the presence of the coatings or networks (Figure E.2).

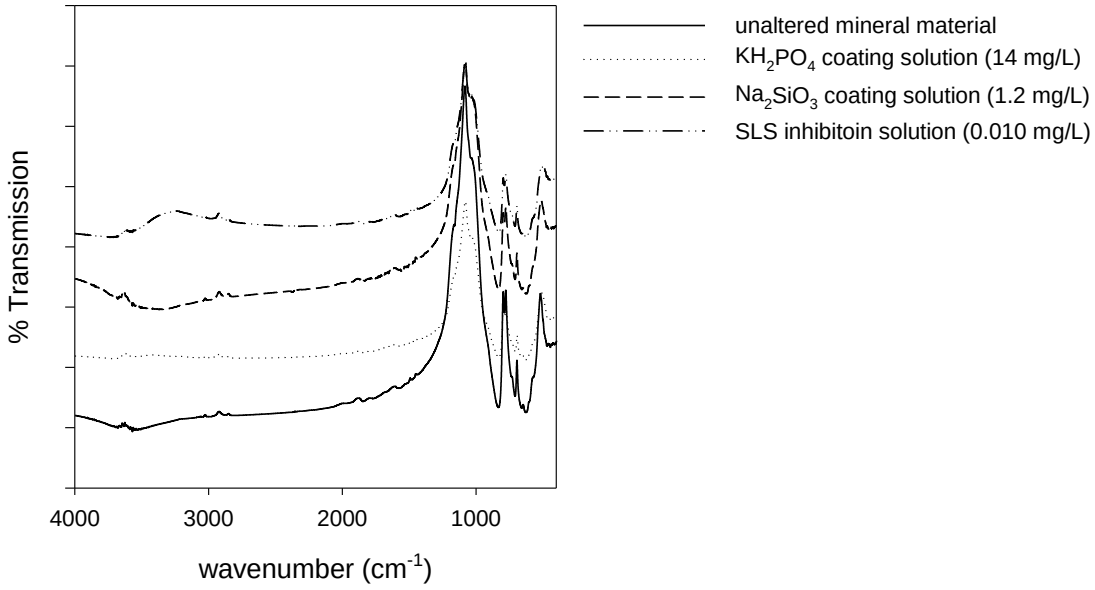

Figure E.2 IR analysis of selected mineral samples after small column inhibition and passivation treatment application (Table E.1); off-set

All samples produced a very strong signal characteristic of quartz with a strong with broad band at 1084 cm^{-1}. The broad band in this region masks the area of interest that would provide details on other structures and/or functional groups, such as the presence of Si-O networks or Fe-PO_4 phases. Other regions worth noting and the significance are present in Table E.2.

Table E.2 Prominent IR regions in mineral samples.

Remarks	Regions
Quartz	doublet at 780 and 798 cm^{-1}
	peak at 697 cm^{-1}
	strong band at 1084 cm^{-1}
Organics	2800 to 3000 cm^{-1}
Carbonates	1500 cm^{-1}

Analysis by SEM-EDS did not reveal any topographical features or chemical confirmation for the existence of ferric hydroxide-phosphate phases or silica networks on the mineral surface. It is though that

sample preparation methods, including epoxy mounting followed by grinding and polishing, may have removed surface features of interest.

E.4 Conclusion

The following conclusions have been draw from this study:

- Bacterial inhibition by sodium laurly sulphate is effective to limit biological oxidation, but chemical oxidation is not inhibited because the grains are left unprotected and available for oxidation;
- Silica network formation is a less reliable or robust coatings option because the treatment did not withstand oxidation resistance testing and dissolved Fe concentration continue to increase, indicating that an effective protective layer was not formed and Fe dissolution continued; and
- Phosphate coatings that are expected to be established on the polyminerallic mine waste protect mineral grains from chemical and biological oxidation and dissolved Fe concentration stabilized after a few days, suggesting that Fe oxidation is no longer taking place.

The application concentrated of phosphate coating solutions at a large scale will be tested using the continuous irrigation application method. This method will be beneficial in practice because infrastructure designed for the delivering of leaching solutions during the active stage can be used to distribute the coating solution, incurring minimal costs to change solution delivery systems

APPENDIX F

F Data Tables

Data tables corresponding to figures presented in Results and Discussion sections in the chapters and appendices are available in electronic format upon request: Al_Williamson@laurentian.ca or GSpiers@laurentian.ca.